รายงานวิจัยฉบับสมบูรณ์

โครงการ **The effects of statins on cardiac and renal functions in streptozotocin-induced diabetic rats: drug transporter focusing**

โดย ผศ.ดร. อนุสรณ์ ลังกาพินธ์ และคณะ

มิถุนายน พ.ศ. 2560

สัญญาเลขที่ RSA5780029

รายงานวิจัยฉบับสมบูรณ์

โครงการ The effects of statins on cardiac and renal functions in streptozotocin-induced diabetic rats: drug transporter focusing

ผศ.ดร. อนุสรณ์ ลังกาพินธ์ มหาวิทยาลัยเชียงใหม่

สนับสนุนโดยสำนักงานกองทุนสนับสนุนการวิจัย

และมหาวิทยาลัยเชียงใหม่

กิตติกรรมประกาศ

งานวิจัยนี้ สนับสนุนโดยทุนอุดหนุนการวิจัยจากสำนักงานกองทุนสนับสนุนการวิจัย ผู้วิจัยขอขอบคุณสำหรับทุนสนับสนุนการวิจัยทั้งหมดตลอดโครงการ และขอขอบคุณคณะแพทยศาสตร์ และมหาวิทยาลัยเชียงใหม่ที่ให้ทุนสนับสนุนบางส่วนในการวิจัยครั้งนี้ นอกจากนี้ ผู้วิจัยขอขอบคุณภาควิชาสรีรวิทยา คณะแพทยศาสตร์ มหาวิทยาลัยเชียงใหม่ สำหรับการเอื้อเฟื้อสถานที่ทำการวิจัย

สุดท้ายนี้ผู้วิจัยขอขอบพระคุณอย่างสูง ต่อ ศ.ดร. วรนุช ฉัตรสุทธิพงษ์ และศ.ดร. นิพนธ์ ฉัตรทิพากร อาจารย์ที่ปรึกษาโครงการที่คอยให้คำปรึกษา คำแนะนำและให้กำลังใจในการทำวิจัยตลอดโครงการ

ผศ. ดร. อนุสรณ์ ลังกาพินธ์

บทคัดย่อ

รหัสโครงการ : RSA5780029

ชื่อโครงการ : ผลของสเตตินต่อการทำงานของหัวใจและไตในหนูขาวที่ถูกเหนี่ยวนำให้เป็นเบาหวานโดยสเตรปโตโซโทซิน: โดยมุ่งเน้นการศึกษาโปรตีนขนส่งยา

ชื่อนักวิจัย : ผู้ช่วยศาสตราจารย์ ดร. อนุสรณ์ ลังกาพินธ์ มหาวิทยาลัยเชียงใหม่

E-mail Address : onanusorn@yahoo.com

ระยะเวลาโครงการ : 3 ปี

ในภาวะเบาหวานมักพบภาวะเครียดออกซิเดชั่นการจากมีน้ำตาลในเลือดสูง ยาอทอร์วาสเตติน หรือยาในกลุ่มยับยั้งการทำงานของ hydroxy-3-methylglutaryl-coenzyme A (HMG-CoA) reductase มีการใช้งานอย่างแพร่หลายเพื่อลดระดับไขมันในกระแสเลือดและฤทธิ์อย่างอื่นในผู้ป่วยเบาหวาน วัตถุประสงค์การทดลองครั้งนี้ เพื่อศึกษาฤทธิ์ป้องกันของยาสเตตินและอินซูลินต่อการทำงานของไตและโปรตีนขนส่งสารอินทรีย์ประจุลบชนิดที่ 3 ที่ไต และหัวใจ ที่เกี่ยวข้องกับการปรับภาวะเครียดออกซิเดชั่นและการทำงานของตับอ่อนในภาวะเบาหวานชนิดที่ 1 ที่ถูกกระตุ้นด้วยการฉีดสเตรปโตโซโตซิน (50 mg/kg BW) หลักจากนั้นให้การรักษาด้วยยาอทอร์วาสเตตินและอินซูลินโดยการรักษาเพียงอย่างใดอย่างหนึ่งหรือใช้ร่วมกันเป็นเวลา 4 สัปดาห์ จากผลการศึกษาพบว่า ภาวะเบาหวานมีการสูญเสียการทำงานของไตและโปรตีนขนส่งที่หัวใจร่วมกับการเพิ่มขึ้นของระดับมาลอนไดอัลดีไฮด์ที่เพิ่มสูงขึ้นบริเวณเนื้อไตส่วนนอก การแสดงออกของโปรตีน Nrf2 และ HO-1 ร่วมกับการลดลงของระดับการแสดงออกของโปรตีน SOD การรักษาด้วยอินซูลินและอินซูลินร่วมกับยาอทอร์วาสเตตินส่งผลให้การทำงานของไตดีขึ้นโดยเกี่ยวข้องกับการลดลงของภาวะน้ำตาลในเลือดสูงและภาวะเครียดต่อออกซิเดชั่น ผลการทดลองครั้งนี้ชี้ให้เห็นว่าการให้การรักษาด้วยยาอทอร์วาสเตตินร่วมกับอินซูลินระดับต่ำสามารถเห็นผลในการป้องกันการทำงานของไตและหัวใจและนำไปสู่การปรับการทำงานของเบต้าเซลล์ของตับอ่อนในหนูที่ถูกเหนี่ยวนำให้เกิดภาวะเบาหวานโดยสเตรปโตโซโทซิน การปรับปรุงนี้เกิดจากการปรับภาวะเครียดออกซิเดชั่น การอักเสบ และการตายของเซลล์ตับอ่อน นอกจากนี้การลดปริมาณการฉีดอินซูลินสามารถป้องกันการเกิดผลข้างเคียงที่ไม่พึงประสงค์ในการรักษาระยะยาวโดยเฉพาะอย่างยิ่งในภาวะเบาหวานชนิดที่ 1 ดังนั้นการใช้ยาอทอร์วาสเตตินร่วมกับอินซูลินแสดงให้เห็นถึงประสิทธิภาพที่เป็นประโยชน์อย่างมากในการคงไว้ซึ่งการทำงานของไต หัวใจ และตับอ่อนในภาวะเบาหวานชนิดที่ 1 ดังนั้นจึงควรมีการศึกษาถึงประโยชน์เหล่านี้เพิ่มเติมในมนุษย์ด้วย

คำหลัก : ภาวะเบาหวาน; โปรตีนขนส่งสารอินทรีย์ประจุลบชนิดที่ 3 ที่ไต; โปรตีนขนส่งสารอินทรีย์ประจุลบที่หัวใจ; อทอร์วาสเตติน; ภาวะเครียดออกซิเดชั่น

Abstract

Project Code : RSA5780029

Project Title : The effects of statins on cardiac and renal functions in streptozotocin-induced diabetic rats: drug transporter focusing

Investigator : Assist. Prof. Dr. Anusorn Lungkaphin Chiang Mai University

E-mail Address : onanusorn@yahoo.com

Project Period : 3 years

Hyperglycemia-induced oxidative stress is usually found in diabetic condition. 3-hydroxy-3-methylglutaryl coenzyme-A (HMG-CoA) reductase inhibitors, statins, are widely used as cholesterol-lowering medication with several “pleiotropic” effects in diabetic patients. This study aims to evaluate whether the protective effects of atorvastatin and insulin on renal function and renal organic anion transporter 3 (Oat3) function and cardiac Oat function involve the modulation of oxidative stress and pancreatic function in type 1 diabetic rats. Type 1 diabetes was induced by intraperitoneal injection of streptozotocin (50 mg/kg BW). Atorvastatin and insulin as single or combined treatment were given for 4 weeks after diabetic condition had been confirmed. Diabetic rats demonstrated renal function and renal Oat3 and cardiac Oat function impairment with an increased MDA level and decreased SOD protein expression concomitant with stimulation of renal Nrf2 and HO-1 protein expression. Insulin plus atorvastatin (combined) treatment effectively restored renal function as well as renal Oat3 and cardiac Oat function which correlated with the decrease in hyperglycemia and oxidative stress. Moreover, pancreatic inflammation and apoptosis in diabetic rats were ameliorated by the combined drugs treatment. The results obtained from this study indicate that combined atorvastatin and low dose insulin treatment exhibit renoprotective effects and lead to the reversal of pancreatic β-cell function in streptozotocin-induced diabetes in rats. These improvements occurred via the modulation of oxidative stress, pancreatic inflammation and apoptotic pathways. Moreover, the reduced insulin injection dosage could prevent the adverse effect of insulin in prolonged treatment especially in Type 1 diabetes. Since the use of atorvastatin and insulin showed great potential benefits in the preservation of renal cardiac and pancreatic function in rats with diabetes type 1, further study is recommended to investigate whether these benefits could also be conferred in humans.

Keywords : Diabetes Mellitus; Renal Oat3; Cardiac Oat; Atorvastatin; Oxidative stress

Introduction

Type 1 diabetes (T1D) is an autoimmune disease characterized by low plasma insulin due to a destruction of the pancreatic β-cells which synthesize insulin[1] leading to the development of hyperglycemia. Diabetic nephropathy (DN) is a devastating complication of type 1 diabetes, which is the leading cause of end-stage renal disease (ESRD) and a major cause of morbidity and mortality in T1D patients[2]. Although the pathogenesis of DN is still not fully understood it has been suggested that long-term hyperglycemia activates reactive oxygen species (ROS) production by increasing advanced glycation end products (AGE). Subsequently, AGE activates the polyol pathway resulting in the activation of Nicotinamide adenine dinucleotide phosphate (NADPH) oxidase causing cell damage and dysfunction[3-5]. These conditions can lead to diabetic nephropathy and diabetic-induced complications in several organs including the pancreas. DN is characterized by various ultrastructural changes of nephrons including basement membrane thickening, glomerular and tubular hypertrophy, glomerulosclerosis and tubulointerstitial fibrosis[6]. This pathology markedly affects the secretory and excretory capacities of transporters in renal proximal tubules.

The organic anion transporter 3 (Oat3) is an important renal transporter which is localized in the basolateral membrane of the renal proximal tubule. It plays an essential role in renal excretion of a variety of drug metabolites, endogenous substances, and environmental toxins. Our previous study has demonstrated that a decrease in function and expression of renal Oat3 and cardiac Oat in diabetic rats were associated with an increased oxidative stress level from hyperglycemia[7]. Moreover, we found that an impairment of renal Oat3 transport function and expression in diabetic rats was restored by insulin treatment[7,8].

Atorvastatin, an 3-hydroxy-3-methylglutaryl coenzyme-A (HMG-CoA) reductase inhibitor, is widely used to treat hypercholesterolemia and dyslipidemia in diabetic patients. A recent study demonstrated the pleiotropic effects of statins in attenuating oxidative stress, inflammation, apoptosis and thrombosis[9]. In addition, cardioprotective effects of statins in an angiotensin II (Ang II)-induced cardiac hypertrophy and fibrosis mice model[10] and the renoprotective effects of statins in gentamicin-induced nephropathy in rats through the attenuation of oxidative stress leading to improving renal Oat3 and renal function[11] have been reported by our team. We also

demonstrated that renal inflammation, endoplasmic reticulum (ES) stress and apoptosis were ameliorated by atorvastatin in gentamicin-induced nephrotoxicity in rats[12]. In contrast-induced nephropathy, rosuvastatin was found to modulate nitric oxide synthesis, inflammation, oxidative stress and apoptosis in diabetic male rats[13]. Taken together, either insulin or atorvastatin can improve renal function and cardiac Oat function in diabetic rats but their combined effect has not been investigated. In addition, we were very interested in the effect of the combined treatment on pancreatic function and whether it was effective in the modulation of insulin secretion in diabetic condition. Therefore, in this study we have evaluated the renoprotective and cardioprotective effects of atorvastatin plus low dose insulin treatment on renal function and the function of the important renal transport protein, renal Oat3, and cardiac Oat function in modulation of the oxidative stress pathway, and its effect on the inflammation and apoptosis of the pancreas in streptozotocin (STZ)-induced diabetic rats.

Materials and methods

Animals.

Male Wistar rats (200-250 g) were obtained from the National Animal Center, Salaya Campus, Mahidol University, Thailand. The animal facilities and protocols involved in the study were approved by the Laboratory Animal Care and Use Committees at the Faculty of Medicine, Chiang Mai University, Chiang Mai, Thailand (Permit No: 12/2557). All methods were performed in accordance with the relevant guidelines and regulations. All experimental rats were housed under controlled temperatures of 25±1°C and lighting in a 12 h-light/dark cycle with food and water *ad libitum*. After seven days of acclimatization, thirty-six rats were randomly divided into control (12 rats) and diabetic (24 rats) groups. The control group was divided into 2 groups, control (C), and control plus atorvastatin (CS) (six rats per group). Rats in the diabetic group were intraperitoneally (i.p.) injected with 50 mg/kg BW of streptozotocin in 10 mM citrate buffer pH 4.5 while the control rats received the equivalent dose of citrate buffer solution as a vehicle. After 7 days, rats with fasting blood glucose $\geq$ 250 mg/dl were included in the diabetic group and assigned into four sub-groups (six rats per group): diabetic (DM), diabetic plus insulin (DMI), diabetic plus atorvastatin (DMS), and diabetic plus insulin and atorvastatin (DMIS). Insulin (4 units/day) was injected subcutaneously while 10 mg/kg/day of atorvastatin dissolved in saline was administered orally for 4 weeks. All rats had free access to water and food and body weight was recorded daily. At the end of the experimental period, a 24-hr urine sample was collected using a metabolic cage. Rats were killed after being anesthetized using isoflurane inhalation. Blood samples were collected. Plasma and serum were separated and then stored at -20°C until use. The kidneys were removed immediately, decapsulated and weighed to facilitate further use for the determination of renal Oat3 transporter function, malondialdehyde (MDA) concentration, hematoxylin and eosin (H&E) staining, and western blot analysis. Pancreatic tissue was collected and kept at -80°C for further western blot analysis.

Biochemical parameters.

The plasma glucose, triglyceride, cholesterol and urine glucose levels were determined by the enzymatic colorimetric method using a commercial kit (ErbaLachemas.r.o., Brno, CZ). Plasma insulin concentration was evaluated by the Sandwich ELIZA method using a commercial

kit (Rat/Mouse Insulin ELISA kit, Merck Millipore, MA, USA). Renal function was estimated by the determination of serum and urine creatinine, serum blood urea nitrogen (BUN) levels and estimated glomerular filtration rate (eGFR). Serum and urine creatinine and serum blood urea nitrogen (BUN) levels were measured using an automatic biochemical analyzer at the Clinical Laboratory, Maharaj Nakorn Chiang Mai Hospital, Chiang Mai, Thailand. eGFR was calculated using the following equation :-

$$\text{eGFR} = (\text{urine creatinine} \times \text{urine flow rate}) / \text{serum creatinine} \quad (1)$$

Determination of renal and cardiac Oat function.

The decapsulated kidneys or cardiac tissues were placed into freshly-oxygenated ice-cold modified Cross and Taggart saline buffer (contain: 95 mM NaCl, 80 mM mannitol, 5 mM KCl, 0.74 mM $CaCl_2$, and 9.5 mM Na_2HPO_4, pH 7.4). Thin renal cortical slices or cardiac tissues ($\leq$ 0.5 mm; 5-15 mg, wet weight) were cut using a Stadie-Riggs microtome and incubated in 1 ml of buffer containing 50 nM [^{3}H] estrone sulfate (ES), a prototypical organic anion that is preferentially transported by Oat3[35,36], to enable an uptake study for 30 mins at room temperature. At the end of the uptake period, the slices were washed in 0.1 M $MgCl_2$, blotted on filter paper, weighed and dissolved in 0.4 ml of 1 M NaOH, and neutralized with 0.6 ml of 1 N HCl. Five renal cortical slices were used for each rat (5-6 rats per group). The radioactivity was measured using a liquid scintillation analyzer (Perkin Elmer, MA, USA). The transport of ES was calculated as tissue to medium (T/M) ratio.

$$\text{T/M ratio} = \text{dpm/g tissue} \div \text{dpm/ml medium} \quad (2)$$

Determination of renal oxidative stress and pancreatic apoptosis.

Determination of MDA in renal cortical tissue

The renal cortical tissue was cut and suspended in Cell Lytic MT mammalian tissue lysis/extraction reagent (Sigma Aldrich, MO, USA) containing a 1% complete protease inhibitor cocktail (Roche Applied Science, IN, USA). After being homogenized and centrifuged at 1,600 g for 10 min at 4°C, the supernatants were collected. The MDA concentration as an indicator of renal oxidative stress condition was determined by using a commercial thiobarbituric acid reactive substance (TBARS) assay kit from Cayman Chemical (Ann Arbor, MI, USA) in line with the manufacturer's protocol.

Western blot Analysis

The renal cortical or pancreatic tissues were homogenized in Cell Lytic MT mammalian tissue lysis/extraction reagent (Sigma Aldrich, MO, USA) containing a 1% complete protease inhibitor cocktail (Roche Applied Science, IN, USA) and centrifuged at 5,000 g for 10 minutes. The supernatant was collected and served as the whole cell lysate fraction and the pellet served as the nuclear fraction. The remaining supernatant was centrifuged at 100,000 g for 2 hrs, then the collected pellet served as the membrane fraction. Protein concentration was measured using a colorimetric Bradford protein assay commercially available kit (Bio-Rad, PA, USA). Total cell lysates, nuclear and membrane fractions from the renal cortex were subjected to 10% SDS-polyacrylamide gel electrophoresis (SDS-PAGE). Proteins were transferred onto PVDF membrane (Millipore, MA, USA) and were allowed to react with primary antibodies overnight at 4 °C. Antibodies against Nrf-2, IL-6, IFN-γ and PKC-α were obtained from Santa-cruz Biotechnology (CA, USA). Antibodies against GCLC and HO-1 were obtained from Abcambiochemicals (MA, USA). Antibodies against SOD2, Bcl-2, β-actin and Lamin B were obtained from Cell signaling Technology (MA, USA). Antibodies against Oat3 were obtained from Cosmo Bio Co. Ltd., (Tokyo, Japan) and antibodies against Bax, cleaved caspase-3, Na^+-K^+-ATPase from Merck Millipore (MA, USA). Membranes were developed using an ECL enhanced chemiluminescence agent (BioRad Laboratory Ltd., HemelHemstead, UK) and exposed using the ChemiDoc™ Touch Imaging system (BioRad Laboratory Ltd., HemelHemstead, UK). Relative molecular mass of the labeled protein bands was estimated using a Page Ruler Prestained Protein Ladder (Fermentas, MA, USA), and the density was determined by the software ImageJ (National Institutes of Health, Bethesda, MD, USA). Density of the protein bands was expressed in arbitrary units relative to the respective β-actin.

Histopathological study

To determine the changes in kidney morphology, kidneys were cut along the transverse axis then fixed in 10% neutral buffered formalin and embedded in paraffin. Paraffin-embedded specimens were cut into 2 µm-thick sections, mounted on glass slides and stained with hematoxylin and eosin (H&E) for histological assessment. The samples were observed by an observer blinded to animal treatment groups to determine the presence of glomerular and tubular changes or damage. Five slices of kidney section from each group of experiments were

examined and scored under light microscope (Olympus Co., Tokyo, Japan) and evaluated the severity of renal injury score (0-4) by estimating the percentage of tubules in cortex or outer medullar and glomerulus that exhibited increases capsular space of glomerular capsule, peritubular leukocyte infiltration, tubular dilatation, and interstitial fibrosis. The histopathological evaluation was performed as follows: 0-none; 1-<5%; 2-5-25%; 3-25-75% and 4->75%[37,38].

Statistical analysis

All data were expressed as mean ± standard error (SEM). A one-way ANOVA was used to compare the data from the various treatments followed by Fisher's Least significant difference test (LSD). A *p* value of less than 0.05 was considered to be statistically significant.

Results

Effects of pharmacological intervention on metabolic parameters in STZ-induced diabetic rats

As shown in Table 1, type 1 diabetic rats showed a significant decrease in body weight and plasma insulin level when compared with those of the control and control plus atorvastatin rats ($p<0.05$). Plasma glucose, cholesterol, triglyceride, urine glucose and urine volume were significantly increased in diabetic rats when compared with control or control plus atorvastatin-treated rats ($p<0.05$). Treatment with insulin as a single entity or combined with atorvastatin correlated with significantly increased body weight compared with diabetic rats ($p<0.05$). Similarly, the rats that received the combined drug treatment (atorvastatin plus insulin) had significantly higher body weight than those receiving only a single treatment of either insulin or atorvastatin-treated rats ($p<0.05$). Rats on insulin or atorvastatin treatment alone and combined drugs treatment showed significantly decreased fasting blood glucose levels when compared with those of diabetic rats ($p<0.05$). However, the fasting blood glucose in the combined drug treatment was lowest and significantly different from that of insulin or atorvastatin-treated rats ($p<0.05$). Co-administration of insulin and atorvastatin had a marked effect on the restoration of plasma insulin which nearly returned to normal levels and was significantly different when compared to that of diabetic, insulin or atorvastatin-treated rats ($p<0.05$). Also, rats having the combined drug treatment showed a significantly lower plasma cholesterol level when compared to diabetic and atorvastatin-treated rats ($p<0.05$). In addition, rats receiving insulin or atorvastatin alone or the combined therapy showed significantly lowered urine glucose concentration when compared to that of diabetic rats ($p<0.05$). Rats having insulin as a single or combined treatment with atorvastatin showed a significantly decreased 24-hr urine volume in comparison with that of diabetic rats ($p<0.05$). Surprisingly, atorvastatin treatment significantly increased 24-hr urine volume with respect to diabetic, insulin-treated and combined-treated rats ($p<0.05$).

Table 1 Effects of pharmacological interventions on metabolic parameters

	Control	DM	DMI	DMS	DMIS	CS
Body weight (g)	396.67±17.21	245±14.50*	302.5±17.69*$^{\dagger\#}$	219±6.11*	344.17±14.17*$^{\dagger\ddagger\#}$	400±12.18$^{\dagger\ddagger\#}$
Fasting blood glucose (mg/dl)	154.85±13.93	565.57±37.03*	467.04±40.30*†	422.94±31.92*†	254.92±32.82*$^{\dagger\ddagger\#}$	131.08±5.45$^{\dagger\ddagger\#}$
Plasma insulin (U/ml)	2.47±0.43	0.57±0.24*	0.85±0.19*	0.65±0.20*	2.20±0.71$^{\dagger\ddagger\#}$	3.23±0.48$^{\dagger\ddagger\#}$
Plasma cholesterol (mg/dl)	74.71±3.99	102.92±5.97*	91.88±1.55*	95.01±4.89*	81.13±1.67$^{\dagger\#}$	70.87±4.62$^{\dagger\ddagger\#}$
Plasma triglyceride (mg/dl)	75.27±6.98	166.65±28.62*	163.18±16.23*	154.62±26.57*	122.22±12.35	78.51±8.09$^{\dagger\ddagger\#}$
Urine glucose (mg/dl)	115.84±5.84	8834.1±375.5*	6350.6±831.9*†	6136.9±802.7*†	6056.9±426.5*†	110.41±3.08$^{\dagger\ddagger\#}$
Urine volume (ml/24h.)	18.83±0.83	216.33±14.70*	133.67±15.75*$^{\dagger\#}$	251.67±6.60*†	135.50±8.43*$^{\dagger\#}$	18.67±1.61$^{\dagger\ddagger\#}$

Data presented are means ± SEM. n=6 rats per group. C - control group; DM - diabetic group; DMI - diabetic plus insulin group; DMS - diabetic plus atorvastatin group; DMIS - diabetic and insulin plus atorvastatin group; CS - control plus atorvastatin group. *$p < 0.05$ vs. control and control plus atorvastatin groups, $^{\dagger}p < 0.05$ vs. diabetic group, $^{\ddagger}p < 0.05$ vs. diabetic plus insulin group, $^{\#}p < 0.05$ vs. diabetic plus atorvastatin group

Effects of pharmacological intervention on kidney weight, kidney weight to body weight ratio, and renal function in STZ-induced diabetic rats

Type 1 diabetic rats showed significant increases in kidney weight (KW) and kidney weight to body weight (KW/BW) ratio compared with the control and control plus atorvastatin rats ($p<0.05$) (Table 2). Although, the KW/BW ratio of both insulin and combined drug treatment rats ($p<0.05$) was significantly lower than that of diabetic rats. The greater reduction in KW/BW ratio was observed in the combined drug treatment (insulin plus atorvastatin) group ($p<0.05$).

Significant increases in serum blood urea nitrogen (BUN) and creatinine levels, along with a decrease in urine creatinine level and estimated glomerular filtration rate (eGFR) in diabetic rats, compared with that of the control or control plus atorvastatin rats ($p<0.05$) were observed which indicated an impairment in renal function in rats with the diabetic condition (Table 2). The greatest reduction in BUN was found in the combined drug treatment group. Of note, the decreased serum BUN and creatinine levels, in this group showed a strong correlation with an improved eGFR. The results suggested that combined drug treatment produced the greatest effect in improving kidney function in the diabetic rats.

Table 2 Effects of pharmacological interventions on renal functions

	Control	DM	DMI	DMS	DMIS	CS
Kidney weight (g)	1.10±0.02	1.34±0.06*	1.38±0.06*	1.25±0.03*	1.29±0.04*	1.05±0.03$^{\dagger\ddagger\#}$
Kidney weight / Body weight ratio (10^{-3})	2.79±0.01	5.55±0.38*	4.66±0.36*$^{\dagger\#}$	5.81±0.28*	3.79±0.21*$^{\dagger\ddagger\#}$	2.64±0.10$^{\dagger\ddagger\#}$
BUN (mg/dl/g BW)	0.05±0.01	0.22±0.03*	0.10±0.01*$^{\dagger\#}$	0.19±0.01*	0.06±0.01$^{\dagger\#}$	0.05±0.01$^{\dagger\ddagger\#}$
Creatinine (10^{-3}mg/dl/g BW)	1.15±0.04	2.13±0.15*	1.82±0.22*	1.74±0.12*†	1.08±0.06$^{\dagger\ddagger\#}$	0.99±0.07$^{\dagger\ddagger\#}$
Urine creatinine (mg/dl)	56.64±7.42	6.37±0.92*	14.45±3.95*	5.88±0.57*	29.36±9.61*$^{\dagger\#}$	54.57±7.59$^{\dagger\ddagger\#}$
eGFR (% of control)	100±1.29	52.69±4.43*	67.11±2.67*$^{\dagger\#}$	50.58±1.41*	75.77±3.30*$^{\dagger\ddagger\#}$	92.31±2.81$^{\dagger\ddagger\#}$

Data presented are means ± SEM. n=6 rats per group. C - control group; DM - diabetic group; DMI - diabetic plus insulin group; DMS - diabetic plus atorvastatin group; DMIS - diabetic and insulin plus atorvastatin group; CS - control plus atorvastatin group. eGFR, estimated glomerular filtration rate calculated as follow :- eGFR= (urine creatinine x urine flow rate) / serum creatinine. *$p < 0.05$ vs. control and control plus atorvastatin groups, $^{\dagger}p < 0.05$ vs. diabetic group, $^{\ddagger}p < 0.05$ vs. diabetic plus insulin group, $^{\#}p < 0.05$ vs. diabetic plus atorvastatin group

Effects of atorvastatin on kidney histological change in STZ-induced diabetic rats

As shown in Figure 1A, moderate glomerular lesions were found in diabetic rats when compared with control and control plus atorvastatin rats. Glomerular capillaries were attached to the Bowman's capsule, their wide and irregular morphology leading to increased capsule space in the diabetic group. In the kidneys from the diabetic rats, tubulointerstitial damage was found with epithelial cell atrophy. Furthermore, a small amount of focal interstitial fibrosis with neutrophil accumulation was observed. These results were supported by the significant increase in renal injury score when compared with control ($p<0.05$) (Figure 1B). Atorvastatin plus insulin (combined) treatment led to a decrease in these morphological changes as indicated by a significant improve in renal injury score when compared with diabetic group ($p<0.05$). Moreover, the combined treatment found to have a significant different in renal injury score when compared to insulin or atorvastatin treatment alone ($p<0.05$).

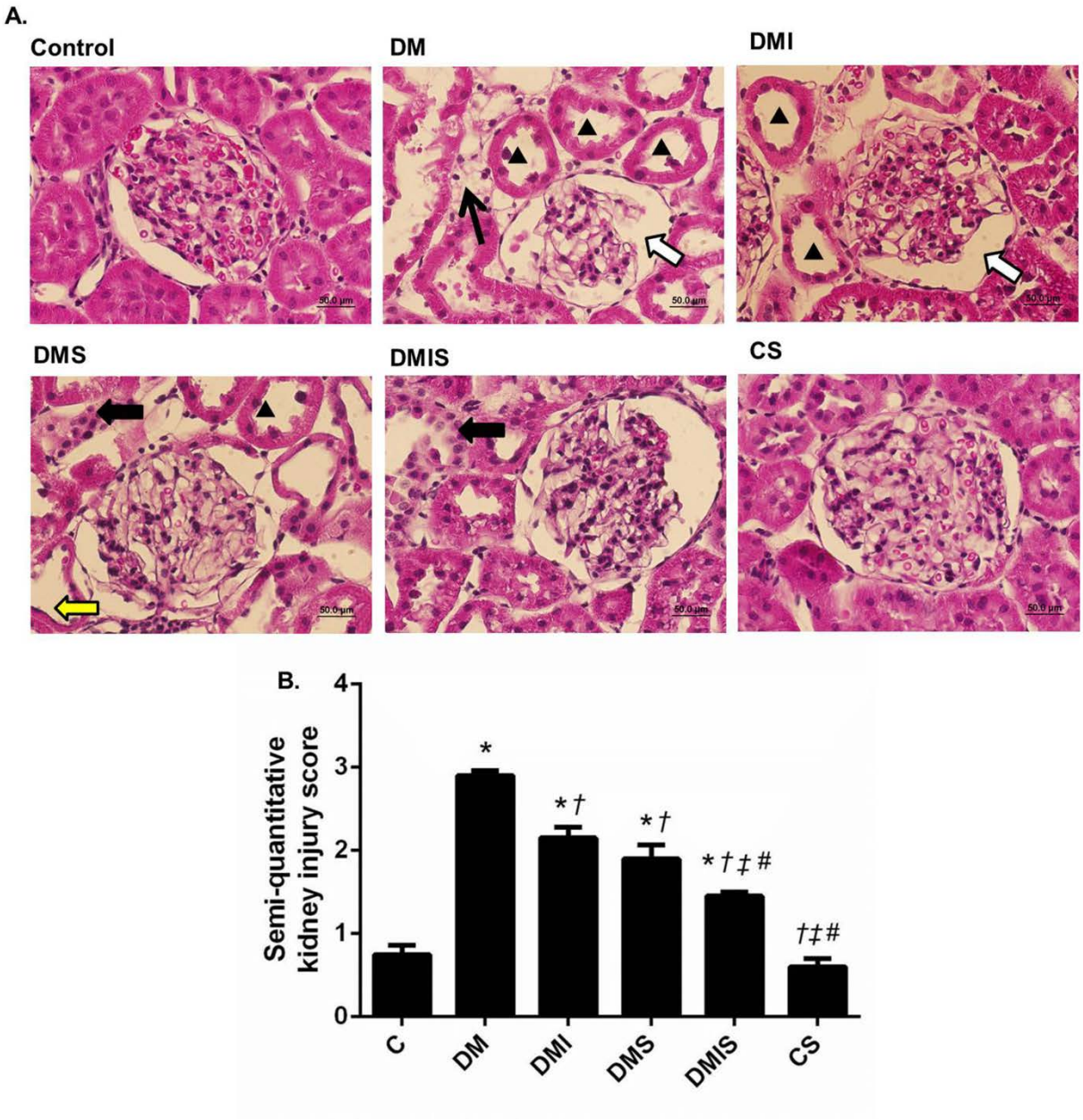

Figure 1. A. Photomicrographs of histological sections of kidney stained with hematoxylin and eosin (H&E) (x40); images of glomeruli and renal tubules from control, diabetic (DM), diabetic plus insulin (DMI), diabetic plus atorvastatin (DMS), diabetic and insulin plus atorvastatin (DMIS) groups, and control plus atorvastatin (CS) are indicated. ( ) shows dilatation of renal tubular; (arrow) represents interstitial fibrosis; (white arrow) represents capsular space of the glomerular capsule; (black arrow) represents neutrophil accumulation; (yellow arrow) represents tubular atrophy. B. Quantitative analysis of diabetic injury kidney was

determined by semi-quantitative kidney injury scoring (0-4); Bar graphs presented show mean ± SEM. n=5 rats per group. C - control group; DM - diabetic group; DMI - diabetic plus insulin group; DMIS - diabetic and insulin plus atorvastatin group; DMS - diabetic plus atorvastatin group; CS - control plus atorvastatin. *$p < 0.05$ vs. control group and control plus atorvastatin groups, $^{\dagger}p < 0.05$ vs. diabetic group, $^{\ddagger}p < 0.05$ vs. diabetic plus insulin group, and $^{\#}p < 0.05$ vs. diabetic plus atorvastatin group.

Effects of pharmacological intervention on renal Oat3 function and expression in STZ-induced diabetic rats

An impairment in renal Oat3 function in diabetic rats was indicated by a significant decrease in [^{3}H]estrone sulfate (ES) uptake when compared with the control or control plus atorvastatin rats ($p<0.05$) (Figure 2A). Insulin as a single or combined treatment with atorvastatin led to significantly elevated [^{3}H]ES uptake in comparison with diabetic rats ($p<0.05$). Although, atorvastatin treatment led to a tendency to increase [^{3}H]ES uptake it was still significantly lower than that of the control group. As presented in Figure 2B and 2C, the expression of renal Oat3 in the whole cell lysate of cortical tissues was comparable among the experimental groups while renal Oat3 expression in the membrane fraction was significantly decreased in diabetic rats ($p<0.05$). All drug treatment groups indicated a tendency to increase [^{3}H]ES uptake. However, a significant increase in renal Oat3 expression in the membrane fraction was only observed in the combined drug treatment rats ($p<0.05$) but there was an increasing trend noted in insulin-treated rats. These findings indicated that the decreased Oat3 function associated with the down-regulation of Oat3 in the membrane of renal tubular cells in cases of diabetes mellitus may well be improved by insulin or insulin plus atorvastatin treatment.

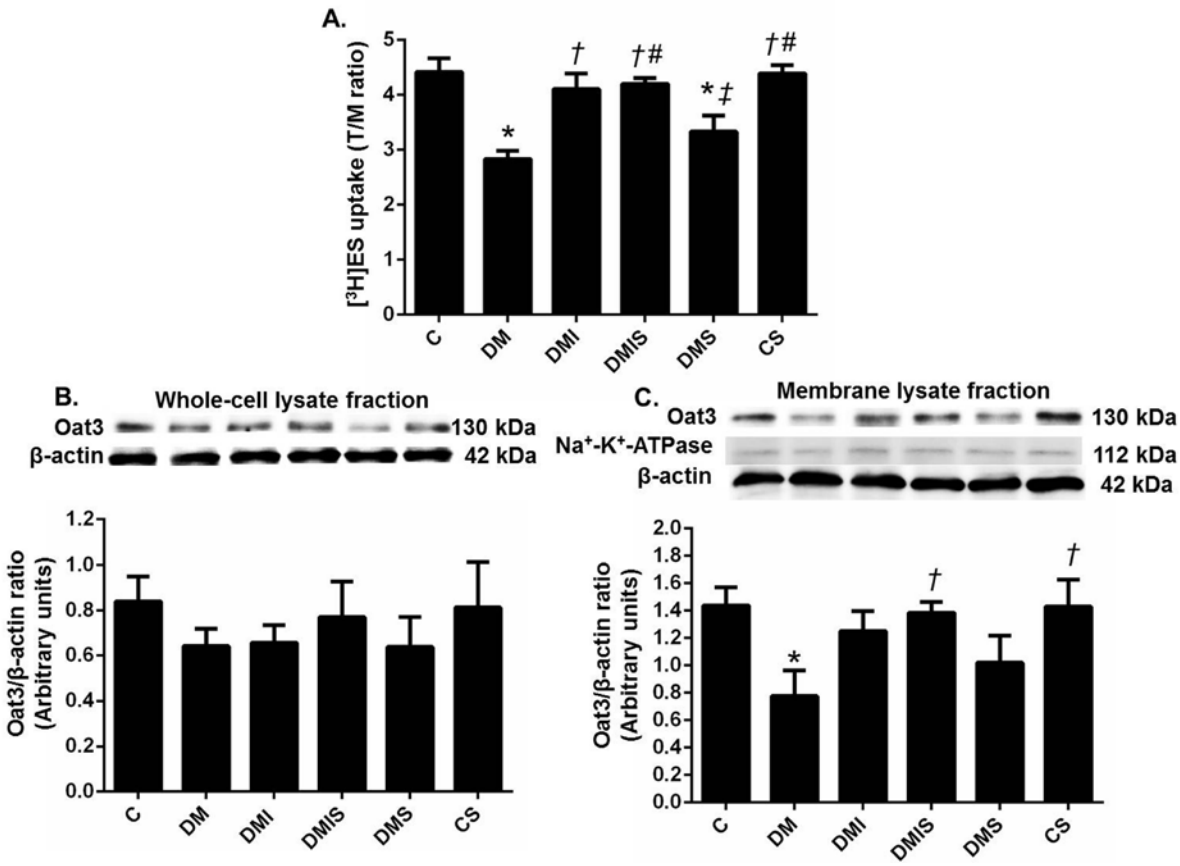

Figure 2. Effects of pharmacological intervention on renal cortical Oat3 function and expression. [^{3}H]ES uptake calculated from tissue/medium ratio (A). Western blot analysis of Oat3 expression in whole cell lysate fraction normalized by β-actin (B) and in membrane lysate fraction (cropped blots) normalized by β-actin (C). Na^{+}-K^{+} ATPase was used as a marker for the membrane fraction. Bar graphs presented show mean ± SEM. n=6 rats per group. C - control group; DM - diabetic group; DMI - diabetic plus insulin group; DMIS - diabetic and insulin plus atorvastatin group; DMS - diabetic plus atorvastatin group; CS - control plus atorvastatin. *$p < 0.05$ vs. control group and control plus atorvastatin groups, $^{\dagger}p < 0.05$ vs. diabetic group, $^{\ddagger}p < 0.05$ vs. diabetic plus insulin group, and $^{\#}p < 0.05$ vs. diabetic plus atorvastatin group.

Effects of pharmacological intervention on oxidative stress status in STZ-induced diabetic rats

As shown in Figure 3, significant increases in malondialdehyde (MDA) level and protein kinase C alpha (PKC-α) expression along with an apparent decrease in superoxide dismutase (SOD) expression were observed in the renal cortical tissues of diabetic rats compared with that of the control rats ($p<0.05$) reflecting an increase in oxidative stress in diabetes. Insulin as a single or combined treatment with atorvastatin led to a significantly decreased renal cortical MDA level when compared with diabetic rats ($p<0.05$) and this value was approaching the control level. The atorvastatin treatment alone seemed to have no effect on cortical MDA. Interestingly, diabetic rats on the combined drug treatment showed a significant increase in the expression of SOD ($p<0.05$) with compared to diabetic rats and the ones with insulin or atorvastatin treatment alone. Moreover, rats on the combined drug treatment showed a significant decrease in the expression of PKC-α when compared with the diabetic rats ($p<0.05$). The results from this study suggested that atorvastatin plus insulin treatment could markedly decrease oxidative stress in the diabetic condition.

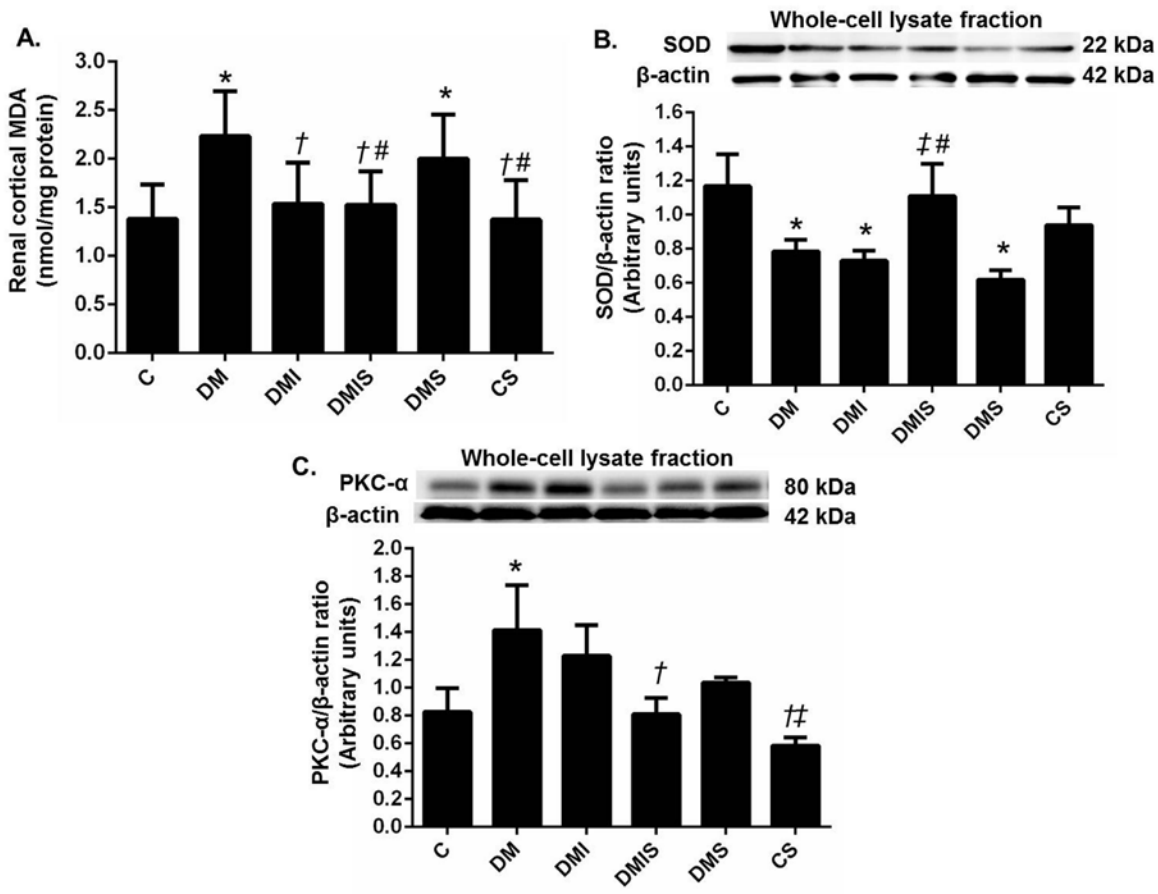

Figure 3. Effects of pharmacological intervention on renal cortical MDA level (A), renal cortical expression of SOD (B) and PKC-α (C). Western blot analysis of SOD and PKC-α expression in the whole cell lysate fraction of renal cortical tissues (cropped blots) normalized by β-actin. Bar graphs presented show mean ± SEM. n=6 rats per group. C - control group; DM - diabetic group; DMI - diabetic plus insulin group; DMIS - diabetic plus insulin and atorvastatin group; DMS - diabetic plus atorvastatin group; CS - control plus atorvastatin.*$p < 0.05$ vs. control group and control plus atorvastatin groups, $^{\dagger}p < 0.05$ vs. diabetic group, $^{\ddagger}p < 0.05$ vs. diabetic plus insulin group, and $^{\#}p < 0.05$ vs. diabetic plus atorvastatin group.

Effects of pharmacological intervention on the oxidative stress pathway in STZ-induced diabetic rats

To further study the mechanism by which combined drug treatment led to decreased hyperglycemia-induced oxidative stress, the expression of proteins involved in the oxidative stress pathway, including nuclear factor erythroid 2-related factor 2 (Nrf2), glutamate-cysteine ligase catalytic subunit (GCLC), and heme oxygenase-1 (HO-1) were investigated in the renal cortical tissues. Diabetic rats showed a significant increase in the expression of Nrf2 in both the nuclear and whole cell lysate fractions of renal cortical tissues compared with the control and control plus atorvastatin rats ($p<0.05$) (Figure 4). These results indicated, not only was there an increase in Nfr2 protein synthesis in the cell, but there was also increased translocation of Nrf2 from the cytoplasm to nucleus occurring in the diabetic rats. Interestingly, the combined drug treatment significantly reversed the expression of Nrf2 in both the whole cell lysate and the nuclear fraction when compared with that of diabetic rats ($p<0.05$). Rats on atorvastatin alone had significantly attenuated Nrf2 expression in whole cell lysate fractions but there was no significant effect on Nrf2 in the nuclear fraction compared with diabetic rats ($p<0.05$). Of note, Nrf2 induced a significant increase in antioxidant enzyme HO-1 in diabetic rats compared to that of control or control plus atorvastatin rats ($p<0.05$) whereas there was no change of GCLC expression among the experimental groups. All types of drug treatment showed a significant lowering of the expression of HO-1 in comparison with that of the diabetic rats ($p<0.05$). The results indicated that combined drug treatment inactivated Nrf2 translocation to nucleus which was related to the reduced HO-1 expression.

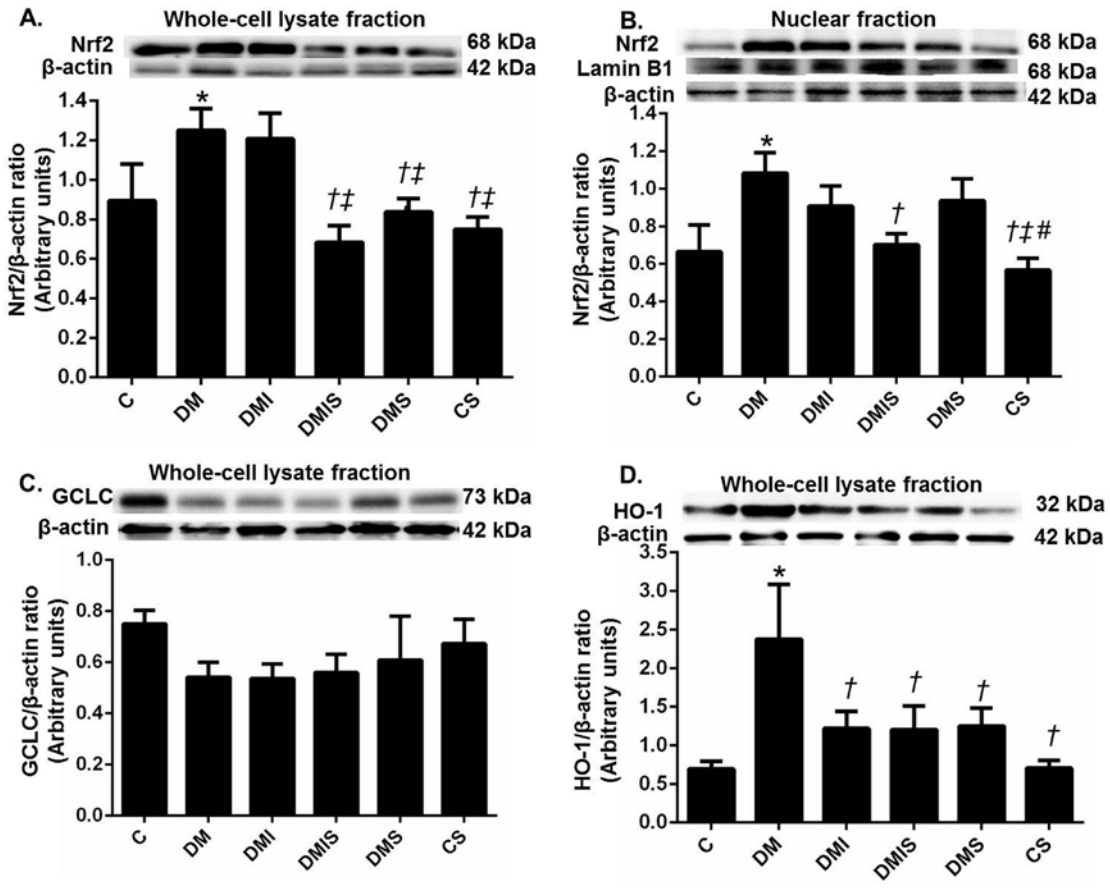

Figure 4. Effects of pharmacological intervention on the renal cortical expression of Nrf-2, GCLC and HO-1. Western blot analysis of Nrf2 expression in nuclear (A), Nrf2 in whole cell lysate fractions (B), GCLC (C), and HO-1 (D) of renal cortical tissues (whole cell lysate fraction) (cropped blots) normalized to β-actin. Lamin B1 was used as a marker for the nuclear fraction. Bar graphs presented show mean ± SEM. n=6 rats per group. C - control group; DM - diabetic group; DMI - diabetic plus insulin group; DMIS - diabetic and insulin plus atorvastatin group; DMS - diabetic plus atorvastatin group; CS - control plus atorvastatin. *$p < 0.05$ vs. control group and control plus atorvastatin groups, $^{\dagger}p < 0.05$ vs. diabetic group, $^{\ddagger}p < 0.05$ vs. diabetic plus insulin group, and $^{\#}p < 0.05$ vs. diabetic plus atorvastatin group.

Effects of pharmacological intervention on the pancreatic apoptotic pathway in STZ-induced diabetic rats

Atorvastatin has been shown to inhibit the apoptosis of myocardial cells in cases of heart failure following myocardial infarction in rats[14]. As plasma insulin levels were found to decrease in diabetic type 1 rats and the combined drug treatment led to the restoration of these levels to within normal limits, it is likely that pancreas function recovered after the treatment. To verify this hypothesis the expression of apoptotic proteins in pancreatic tissue was investigated. As shown in Figure 5, diabetic rats showed a significant increase in B-cell lymphoma 2 (Bcl-2) associated X (Bax) protein and cleaved caspase-3 expression, and marked reduction of Bcl-2 expression in pancreatic tissue when compared with that of the control or control plus atorvastatin rats ($p<0.05$). The combined drug treatment led to a significant reduction of Bax and cleaved caspase-3 expression and apparently enhanced the expression of Bcl-2 in comparison with diabetic rats ($p<0.05$) whereas insulin or atorvastatin treatment alone had no effects on these parameters. These results suggested that combined drug treatment protected against pancreatic apoptosis which helps preserve the pancreas tissue and function in diabetic rats.

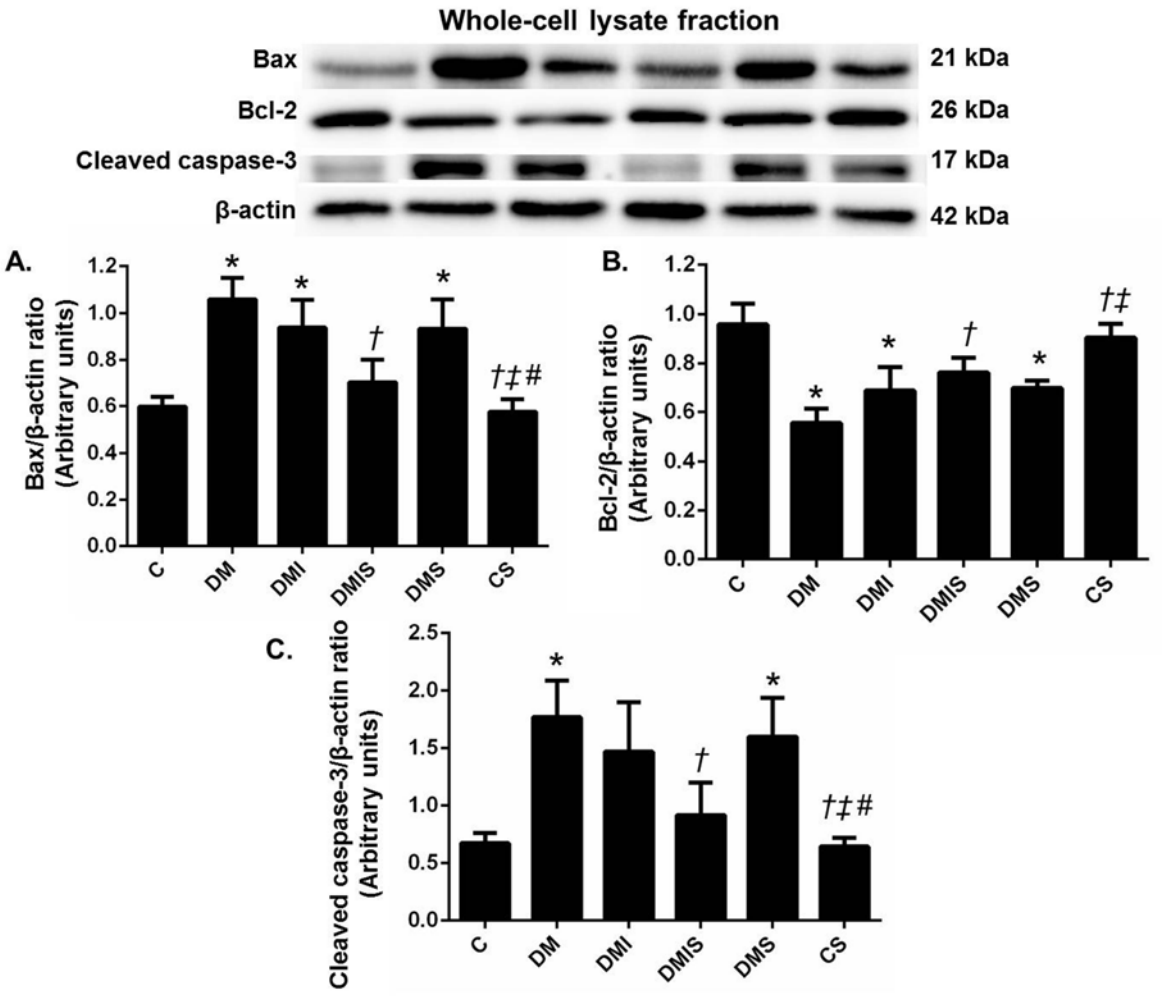

Figure 5. Effects of pharmacological intervention on the expression of Bax, Bcl-2, and cleaved caspase-3 in pancreatic tissues. Western blot analysis showing the expressions of Bax (A), Bcl-2 (B), and cleaved caspase-3 (C) in pancreatic tissues (cropped blots) normalized to β-actin. Bar graphs presented show mean ± SEM. n=6 rats per group. C - control group; DM - diabetic group; DMI - diabetic plus insulin group; DMIS - diabetic and insulin plus atorvastatin group; DMS - diabetic plus atorvastatin group; CS - control plus atorvastatin.*$p < 0.05$ vs. control group and control plus atorvastatin groups, $^{\dagger}p < 0.05$ vs. diabetic group, $^{\ddagger}p < 0.05$ vs. diabetic plus insulin group, and $^{\#}p < 0.05$ vs. diabetic plus atorvastatin group.

Effects of pharmacological intervention on pancreatic inflammation pathways in STZ-induced diabetic rats

It has been reported that chronic hyperglycemia can cause β-cell degranulation and reduction[15]. It has been shown that statins have anti-inflammatory effects in asymmetrical dimethylarginine-induced inflammatory endothelial cells[16]. We, therefore, went on to investigate the effect of atorvastatin treatment on the inflammation of pancreatic tissues. As shown in Figure 6, there was significantly increased interferon gamma (IFN-γ) and interleukin-6 (IL-6) protein expression in diabetic rats when compared with that of the control and control plus atorvastatin rats ($p<0.05$). The single treatment with either insulin or atorvastatin tended to lower levels of inflammatory proteins but the significant difference in IFN-γ was only observed in insulin-treated rats ($p<0.05$) whereas the combined drug treatment led to the significant decreases seen in both IFN-γ and IL-6 protein expression when compared with diabetic rats ($p<0.05$).

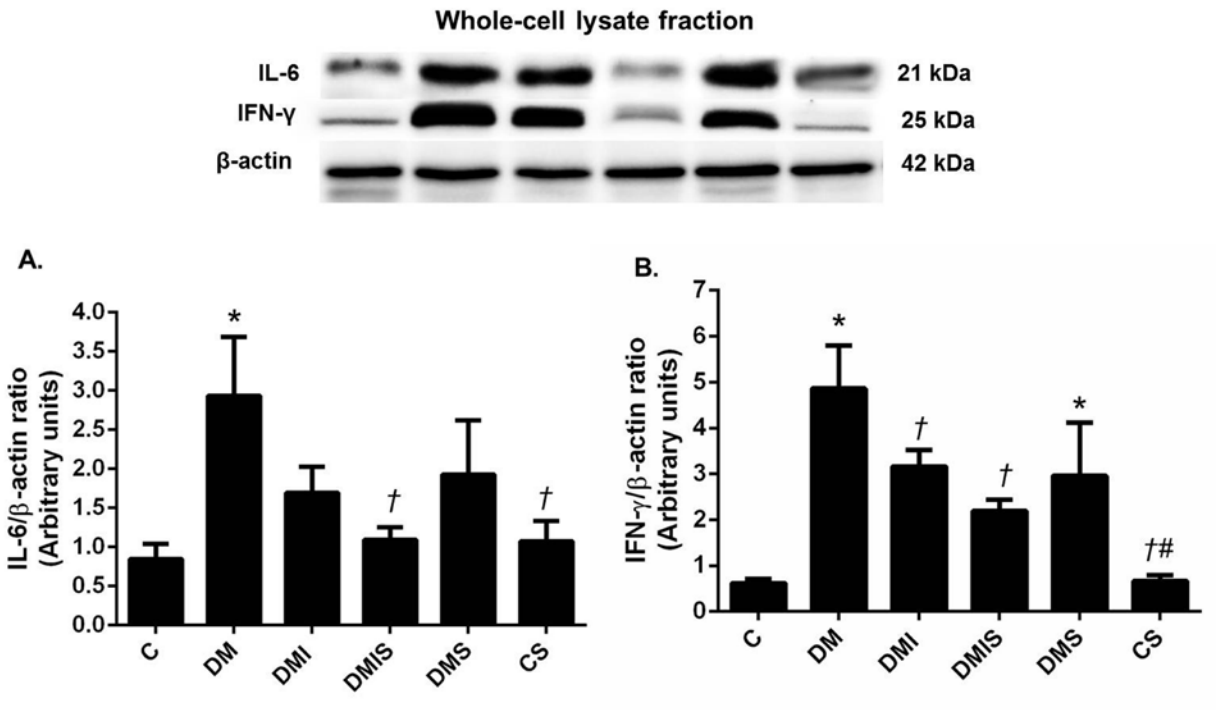

Figure 6. Effects of pharmacological intervention on the expression of IL-6, and IFN-γ in pancreatic tissues. Western blot analysis showing the expression of IL-6 (A), and IFN-γ (B) in pancreatic tissues (cropped blots) normalized to β-actin. Bar graphs presented show mean ± SEM. n=6 rats per group. C - control group; DM - diabetic group; DMI - diabetic plus insulin group; DMIS - diabetic and insulin plus atorvastatin group; DMS - diabetic plus atorvastatin group; CS - control plus atorvastatin. *$p < 0.05$ vs. control group and control plus atorvastatin groups, $^{\dagger}p < 0.05$ vs. diabetic group, $^{\ddagger}p < 0.05$ vs. diabetic plus insulin group, and $^{\#}p < 0.05$ vs. diabetic plus atorvastatin group.

Effects of pharmacological intervention on cardiac Oat function in STZ-induced diabetic rats

An impairment in cardiac Oat function in diabetic rats was indicated by a decrease in [^{3}H]estrone sulfate (ES) uptake when compared with the control or control plus atorvastatin rats (Figure 7). Insulin as a single or combined treatment with atorvastatin led to elevated [^{3}H]ES uptake in comparison with diabetic rats. These findings indicated that the decreased cardiacOat function was also observed in cases of diabetes mellitus. This alteration may be improved by insulin or insulin plus atorvastatin treatment.

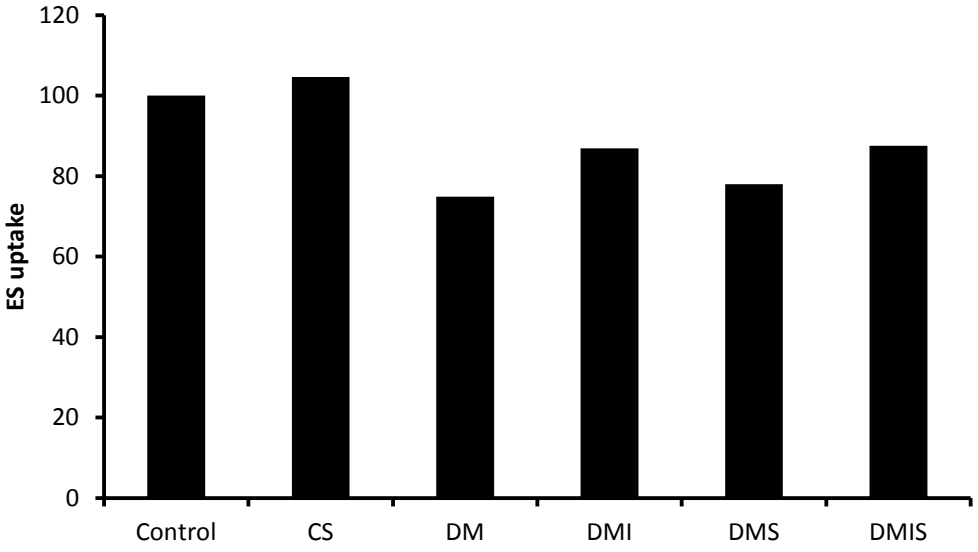

Figure 7. Effects of pharmacological intervention on cardiac Oat function. [^{3}H]ES uptake calculated from tissue/medium ratio. Bar graphs presented show mean ± SEM. n=6 rats per group. C - control group; DM - diabetic group; DMI - diabetic plus insulin group; DMIS - diabetic and insulin plus atorvastatin group; DMS - diabetic plus atorvastatin group; CS - control plus atorvastatin.

Discussion

The STZ-induced diabetes type 1 in the rats in this study was characterized by body weight loss, hyperglycemia, decreased plasma insulin level, renal dysfunction and renal histological changes which were shown to have a correlation with an increase in renal oxidative stress. In addition, hyperglycemia-induced oxidative stress was found to activate the oxidative defense mechanisms through the Nrf2 pathway to protect cytotoxicity. This was consistent with findings from our previous study[7] which reported that the increased ROS generation in diabetes activated the PKC signaling pathway resulting in the downregulation of renal Oat3 and expression in the renal tissues and cardiac Oat function. Of note, hyperglycemia also increased pancreatic expression of IL-6 and IFN-γ, indicators of inflammation, leading to pancreatic apoptosis as shown by the increase in Bax, cleaved caspase-3 protein expression and the Bax/Bcl-2 ratio. Interestingly, atorvastatin plus insulin (combined) treatment led to amelioration of the inflammation and destruction of pancreatic cells leading to an increase in insulin secretion which subsequently improved conditions of hyperglycemia. Thus, combined drug treatment could exert additive effects in preserving both renal and pancreatic and also cardiac Oat functions via modulation of oxidative stress, inflammation and apoptotic pathways.

Long-term hyperglycemia leads to an increase in reactive oxygen species and reactive nitrogen species (ROS&RNS) leading to increased oxidative stress[17]. The condition of increased oxidative stress in the diabetic rats in this study was confirmed by the elevation of renal MDA, the stimulation of HO-1 expression and the reduction of antioxidant enzyme expression, SOD2. Antioxidant mechanisms are usually activated when oxidative stress occurs. The Nrf2-Kelch-like ECH-associated protein 1 (Keap1) pathway is the major regulator of cytoprotective responses and regulates the expression of antioxidant proteins which protect against oxidative damage triggered by injury and inflammation[18,19]. In the presence of ROS, cysteine residues in Keap1 are oxidized leading to a conformational change of Keap1, which prevents its binding to Nrf2. After that, Nrf2 passes by translocation into the nucleus to promote the translation of oxidative-stress-inducible genes, including HO-1[20]. In this study, an increased oxidative stress, induced by hyperglycemia in diabetic rats, led to activated Nrf2 expression and translocation, which subsequently promoted the expression of HO-1 proteins. It is now widely accepted that induction of HO-1 expression represents an adaptive response that increases cellular defense to

oxidative injury. It has been reported that HO-1 is increased in livers of obese versus lean individuals and of diabetic versus nondiabetic subjects[21]. These results are supported by the previous study that found high-glucose-induced upregulation of Nrf2 and HO-1 gene expression[22]. This is in agreement with our previous reports showing the increased expression of renal Nrf2, NAD(P)H quinone dehydrogenase 1 (NQO1) and HO-1 due to oxidative stress in gentamicin-induced nephrotoxicity in rats[11,23].

An increased expression of PKC-α in diabetic rats was also consistent with the previous report that PKC-α was activated in hyperglycemia[7]. Moreover, the decreased renal Oat3 function and expression and cardiac Oat function in the present study when PKC-α was activated due to oxidative stress were similar to that observed previously in diabetic[7,8] and gentamicin-induced nephrotoxicity in rats[11,23].

In this study, increased pancreatic apoptosis was found to be significantly related to the decreased plasma insulin levels in diabetic rats. Hyperglycemia may negatively affect β-cell mass by inducing apoptosis without a compensatory increase in β-cell proliferation and neogenesis. It has been reported that chronic hyperglycemia can cause β-cell degranulation and reduction[15]. The increased pancreatic expression of IL-6, and IFN-γ, indicating inflammation in diabetic rats in the present study, was found to be correlated with the findings of an *in vitro* study demonstrating that the exposure of β-cells to high glucose induced interleukin 1 beta (IL-1β) which activated nuclear factor-kappa B (NF-kB) and Fas signaling and consequently triggered apoptosis[24,25]. Moreover, both IL-1β and IFN-γ also activated NF-kB and appeared to increase inducible nitric oxide synthase (iNOS) expression resulting in the stimulation of ER stress conditions and mononuclear cell activation and infiltration leading to β-cell death[26].

Atorvastatin is a lipid-lowering agent in statins or the HMG-CoA reductase inhibitor group which inhibit the HMG-CoA reductase enzyme, the catalyst of the rate-limiting step of the mevalonate pathway[27]. It has been reported as having pleiotropic effects including anti-apoptosis[28,29], anti-inflammation[30], antioxidant[11,31] and anti-thrombotic effects[32]. Although the direct effect of atorvastatin in reducing plasma levels of cholesterol was not observed in this study, the beneficial effects of the restoration of plasma insulin, reduced blood glucose,

improved renal function, as well as decreased pancreatic inflammation and apoptosis were demonstrated in the diabetic rats that had undergone the combined treatment (atorvastatin with a low dose of insulin). It initiated a greater effect than that observed in the rats undergoing insulin or atorvastatin treatment alone. These pleiotropic effects of atorvastatin which led to the adjustment of glucose homeostasis and renoprotection observed in this study might be due to the additive effect of atorvastatin and insulin in controlling metabolic parameters and subsequently protect kidney dysfunction in diabetes. This proposed mechanism is supported by the previous study reporting that atorvastatin can increase β-cell function by increasing β-cell proliferation and decreasing ER stress conditions[33]. The increased insulin secretion and the attenuation of apoptosis of pancreatic tissue seen in rats on the combined treatment in this study reflected an improvement in β-cell function. The dosage of insulin used in this study had no effect on the lowering of plasma glucose to normal levels as indicated in the group on insulin treatment alone. Thus, the effective reduction of the hyperglycemic condition in the group on the combined drug treatment corroborated the pleiotropic effects of atorvastatin in the reduction of oxidative stress leading to the improvement of renal and pancreatic functions seen in this study. We found that only combined treatment had the significant effect on Nrf-2 expression while insulin, atorvastatin and combined treatment had similar effect on HO-1 expression. The results indicated that combined drug treatment inactivated Nrf2 translocation to nucleus which was related to the reduced HO-1 expression. However, the reduced HO-1 expression in insulin or atorvastatin treatment alone might be involved the other regulated mechanisms such as inflammation or insulin. Insulin has been reported to stimulate HO-1 expression in skeletal myoblast[34]. The decreased HO-1 expression might be related to the low level of plasma insulin in insulin or atorvastatin treatment alone. Thus, the combined drug treatment produced highly effective effects in the control of glucose homeostasis and the prevention of organ dysfunction when compared to of the insulin or atorvastatin treatment alone.

In conclusion, the results obtained from this study indicate that combined atorvastatin and low dose insulin treatment exhibit renoprotective and cardioprotective effects and lead to the reversal of pancreatic β-cell function in streptozotocin-induced diabetes in rats. These improvements occurred via the modulation of oxidative stress, pancreatic inflammation and apoptotic pathways. Moreover, the reduced insulin injection dosage could prevent the adverse effect of insulin in prolonged treatment especially in Type 1 diabetes. Since the use of

atorvastatin and insulin showed great potential benefits in the preservation of renal, cardiac and pancreatic function in rats with diabetes type 1, further study is recommended to investigate whether these benefits could also be conferred in humans.

References

1. Diagnosis and Classification of Diabetes Mellitus. *Diabetes Care* **37**, S81-S90 (2014).
2. Reutens, A. T. &Atkins, R. C. Epidemiology of diabetic nephropathy. *Contrib Nephrol* **170**, 1-7 (2011).
3. Duran-Salgado, M. B. & Rubio-Guerra, A. F. Diabetic nephropathy and inflammation. *World J Diabetes* **5**, 393-398 (2014).
4. Ramasamy, R., Yan, S. F. & Schmidt, A. M. Receptor for AGE (RAGE): signaling mechanisms in the pathogenesis of diabetes and its complications. *Ann N Y Acad Sci* **1243**, 88-102 (2011).
5. Tang, S. C. &Lai, K. N. The pathogenic role of the renal proximal tubular cell in diabetic nephropathy. *Nephrol Dial Transplant* **27**, 3049-3056 (2012).
6. Jefferson, J. A., Shankland, S. J.& Pichler, R. H. Proteinuria in diabetic kidney disease: a mechanistic viewpoint. *Kidney Int* **74**, 22-36 (2008).
7. Phatchawan, A., Chutima, S., Varanuj, C. & Anusorn, L. Decreased renal organic anion transporter 3 expression in type 1 diabetic rats. *Am J Med Sci* **347**, 221-227 (2014).
8. Lungkaphin, A., Arjinajarn, P., Pongchaidecha, A., Srimaroeng, C., Chatsudthipong, L., et al. Impaired insulin signaling affects renal organic anion transporter 3 (Oat3) function in streptozotocin-induced diabetic rats. *PLoS One* **9**, e96236 (2014).
9. Satoh, M., Takahashi, Y., Tabuchi, T., Minami, Y., Tamada, M., et al. Cellular and molecular mechanisms of statins: an update on pleiotropic effects. *Clin Sci (Lond)* **129**, 93-105 (2015).
10. Kudo, S., Satoh, K., Nogi, M., Suzuki, K., Sunamura, S., et al. SmgGDS as a Crucial Mediator of the Inhibitory Effects of Statins on Cardiac Hypertrophy and Fibrosis: Novel Mechanism of the Pleiotropic Effects of Statins. *Hypertension* **67**, 878-889 (2016).
11. Jaikumkao, K., Pongchaidecha, A., Chattipakorn, N., Chatsudthipong, V., Promsan, S., et al. Atorvastatin improves renal organic anion transporter 3 and renal function in gentamicin-induced nephrotoxicity in rats. *Exp Physiol* **101**, 743-753 (2016).
12. Jaikumkao, K., Pongchaidecha, A., Thongnak, L. O., Wanchai, K., Arjinajarn, P., et al. Amelioration of Renal Inflammation, Endoplasmic Reticulum Stress and Apoptosis

Underlies the Protective Effect of Low Dosage of Atorvastatin in Gentamicin-Induced Nephrotoxicity. *PLoS One* **11**, e0164528 (2016).

13. Deng, J., Wu, G., Yang, C., Li, Y., Jing, Q., et al. Rosuvastatin attenuates contrast-induced nephropathy through modulation of nitric oxide, inflammatory responses, oxidative stress and apoptosis in diabetic male rats. *J Transl Med* **13**, 53 (2015).
14. Song, X. J., Yang, C. Y., Liu, B., Wei, Q., Korkor, M. T., et al. Atorvastatin inhibits myocardial cell apoptosis in a rat model with post-myocardial infarction heart failure by downregulating ER stress response. *Int J Med Sci* **8**, 564-572 (2011).
15. Kaiser, N., Leibowitz, G. & Nesher, R. Glucotoxicity and beta-cell failure in type 2 diabetes mellitus. *J Pediatr Endocrinol Metab* **16**, 5-22 (2003).
16. Jiang, J. L., Wang, S., Li, N. S., Zhang, X. H., Deng, H. W., et al. The inhibitory effect of simvastatin on the ADMA-induced inflammatory reaction is mediated by MAPK pathways in endothelial cells. *Biochem Cell Biol* **85**, 66-77 (2007).
17. Busik, J. V., Mohr, S. & Grant, M. B. Hyperglycemia-induced reactive oxygen species toxicity to endothelial cells is dependent on paracrine mediators. *Diabetes* **57**, 1952-1965 (2008).
18. Baird, L.& Dinkova-Kostova, A. T. The cytoprotective role of the Keap1-Nrf2 pathway. *Arch Toxicol* **85**, 241-272 (2011).
19. Motohashi, H. & Yamamoto, M. Nrf2-Keap1 defines a physiologically important stress response mechanism. *Trends Mol Med* **10**, 549-557 (2004).
20. Ishii, T., Itoh, K., Takahashi, S., Sato, H., Yanagawa, T., et al. Transcription factor Nrf2 coordinately regulates a group of oxidative stress-inducible genes in macrophages. *J Biol Chem* **275**, 16023-16029 (2000).
21. Jais, A., Einwallner, E., Sharif, O., Gossens, K., Lu, T. T., et al. Heme oxygenase-1 drives metaflammation and insulin resistance in mouse and man. *Cell* **158**, 25-40 (2014).
22. Ungvari, Z., Bailey-Downs, L., Gautam, T., Jimenez, R., Losonczy, G., et al. Adaptive induction of NF-E2-related factor-2-driven antioxidant genes in endothelial cells in response to hyperglycemia. *Am J Physiol Heart Circ Physiol* **300**, H1133-1140 (2011).
23. Promsan, S., Jaikumkao, K., Pongchaidecha, A., Chattipakorn, N., Chatsudthipong, V., et al. Pinocembrin attenuates gentamicin-induced nephrotoxicity in rats. *Can J Physiol Pharmacol* **94**, 808-818 (2016).

24. Donath, M. Y.& Halban, P. A. Decreased beta-cell mass in diabetes: significance, mechanisms and therapeutic implications. *Diabetologia* **47**, 581-589 (2004).

25. Donath, M. Y., Storling, J., Maedler, K. & Mandrup-Poulsen, T. Inflammatory mediators and islet beta-cell failure: a link between type 1 and type 2 diabetes. *J Mol Med (Berl)* **81**, 455-470 (2003).

26. Cnop, M., Welsh, N., Jonas, J. C., Jorns, A., Lenzen, S., et al. Mechanisms of pancreatic beta-cell death in type 1 and type 2 diabetes: many differences, few similarities. *Diabetes* **54 Suppl 2**, S97-107 (2005).

27. Chogtu, B., Magazine, R. & Bairy, K. L. Statin use and risk of diabetes mellitus. *World J Diabetes* **6**, 352-357 (2015).

28. Buranrat, B., Senggunprai, L., Prawan, A. & Kukongviriyapan, V. Simvastatin and atorvastatin as inhibitors of proliferation and inducers of apoptosis in human cholangiocarcinoma cells. *Life Sci* **153**, 41-49 (2016).

29. Wang, H., Yin, Y., Wang, P., Xiong, C., Huang, L., et al. Current situation and future usage of anticancer drug databases. *Apoptosis* **21**, 778-794 (2016).

30. He, X., Li, L., Tan, H., Chen, J. & Zhou, Y. Atorvastatin attenuates contrast-induced nephropathy by modulating inflammatory responses through the regulation of JNK/p38/Hsp27 expression. *J Pharmacol Sci* **131**, 18-27 (2016).

31. Tian, S., Zhao, W., Yang, D., Yu, Y., Zou, J., et al. Atorvastatin inhibits miR-143 expression: A protective mechanism against oxidative stress in cardiomyocytes. *Int J Cardiol* **211**, 115-118 (2016).

32. Violi, F., Carnevale, R., Pastori, D. & Pignatelli, P. Antioxidant and antiplatelet effects of atorvastatin by Nox2 inhibition. *Trends Cardiovasc Med* **24**, 142-148 (2014).

33. Chen, Z. Y., Liu, S. N., Li, C. N., Sun, S. J., Liu, Q., et al. Atorvastatin helps preserve pancreatic beta cell function in obese C57BL/6 J mice and the effect is related to increased pancreas proliferation and amelioration of endoplasmic-reticulum stress. *Lipids Health Dis* **13**, 98 (2014).

34. Aggeli, I. K., Theofilatos, D., Beis, I. & Gaitanaki, C. Insulin-induced oxidative stress up-regulates heme oxygenase-1 via diverse signaling cascades in the C2 skeletal myoblast cell line. *Endocrinology* **152**, 1274-1283 (2011).

35. Sweet, D. H., Miller, D. S., Pritchard, J. B., Fujiwara, Y., Beier, D. R., et al. Impaired organic anion transport in kidney and choroid plexus of organic anion transporter 3 (Oat3 (Slc22a8)) knockout mice. *J Biol Chem* **277**, 26934-26943 (2002).

36. Aslamkhan, A. G., Thompson, D. M., Perry, J. L., Bleasby, K., Wolff, N. A., et al. The flounder organic anion transporter fOat has sequence, function, and substrate specificity similarity to both mammalian Oat1 and Oat3. *Am J Physiol Regul Integr Comp Physiol* **291**, R1773-1780 (2006).

37. Ma, L., Fei, J., Chen, Y., Zhao, B., Yang, Z. T., et al. Vitamin C Attenuates Hemorrhagic Shock-induced Dendritic Cell-specific Intercellular Adhesion Molecule 3-grabbing Nonintegrin Expression in Tubular Epithelial Cells and Renal Injury in Rats. *Chin Med J (Engl)* **129**, 1731-1736 (2016).

38. Zhao, B., Fei, J., Chen, Y., Ying, Y. L., Ma, L., et al. Vitamin C treatment attenuates hemorrhagic shock related multi-organ injuries through the induction of heme oxygenase-1. *BMC Complement Altern Med* **14**, 442 (2014).

เอกสารแนบหมายเลข 3

Output จากโครงการวิจัยที่ได้รับทุนจาก สกว.

1. ผลงานตีพิมพ์ในวารสารวิชาการนานาชาติ (ระบุชื่อผู้แต่ง ชื่อเรื่อง ชื่อวารสาร ปี เล่มที่ เลขที่ และหน้า)

1.1 Laongdao Thongnak, Anchalee Pongchaidecha, Krit Jaikumkao, Varanuj Chatsudthipong, Nipon Chattipakorn and **Anusorn Lungkaphin**. The additive effects of atorvastatin and insulin on renal function and renal organic anion transporter 3 function in diabetic rats. Scientific Reports 2017 Accepted

1.2 Wanchai K, Pongchaidecha A, Chatsudthipong V, Chattipakorn SC, Chattipakorn N, **Lungkaphin A.** Role of Gastrointestinal Microbiota on Kidney Injury and the Obese Condition. Am J Med Sci. 2017 Jan;353(1):59-69.

1.3 Jaikumkao K, Pongchaidecha A, Thongnak LO, Wanchai K, Arjinajarn P, Chatsudthipong V, Chattipakorn N, **Lungkaphin A.** Amelioration of Renal Inflammation, Endoplasmic Reticulum Stress and Apoptosis Underlies the Protective Effect of Low Dosage of Atorvastatin in Gentamicin-Induced Nephrotoxicity. PLoS One. 2016 Oct 11;11(10):e0164528.

1.4 Jaikumkao K, Pongchaidecha A, Chattipakorn N, Chatsudthipong V, Promsan S, Arjinajarn P, **Lungkaphin A**Atorvastatin improves renal organic anion transporter 3 and renal function in gentamicin-induced nephrotoxicity in rats. Experimental Physiology 2016; 101(6):743-53.

1.5 **Anusorn Lungkaphin**, Anchalee Pongchaidecha, Siripong Palee, Phatchawan Arjinajarn, Wilart Pompimon, and Nipon Chattipakorn. Pinocembrin reduces cardiac arrhythmia and infarct size in rats subjected to acute myocardial ischemia/reperfusion Appl. Physiol. Nutr. Metab. 2015; 1-7.

1.6 Arjinajarn P, Chueakula N, Pongchaidecha A, Jaikumkao K, Chatsudthipong V, Mahatheeranont S, Norkaew O, Chattipakorn N, **Lungkaphin A**. Anthocyanin-rich Riceberry bran extract attenuates gentamicin-induced hepatotoxicity by reducing oxidative stress, inflammation and apoptosis in rats. Biomed Pharmacother. 2017 May 27;92:412-420.

1.7 Arjinajarn P, Pongchaidecha A, Chueakula N, Jaikumkao K, Chatsudthipong V, Mahatheeranont S, Norkaew O, Chattipakorn N, **Lungkaphin A.** Riceberry bran extract prevents renal dysfunction and impaired renal organic anion transporter 3 (Oat3) function by modulating the PKC/Nrf2 pathway in gentamicin-induced nephrotoxicity in rats. Phytomedicine. 2016 Dec 15;23(14):1753-1763.

1.8 Promsan S, Jaikumkao K, Pongchaidecha A, Chattipakorn N, Chatsudthipong V, Arjinajarn P, Pompimon W, **LungkaphinA.** Pinocembrin attenuates gentamicin-induced nephrotoxicity in rats. Can J Physiol Pharmacol. 2016 Aug;94(8):808-18.

2. การนำผลงานวิจัยไปใช้ประโยชน์

- เชิงวิชาการ (มีการพัฒนาการเรียนการสอน/สร้างนักวิจัยใหม่)

โดยมีการนำองค์ความรู้จากผลงานวิจัยที่ตีพิมพ์ผลงานตีพิมพ์ในวารสารระดับนานาชาติไปใช้เป็นประโยชน์ด้านวิชาการ การเรียนรู้ การเรียนการสอน ในระดับปริญญาตรี และระดับบัณฑิตศึกษาทั้งปริญญาโทและเอก ในภาควิชาสรีรวิทยา คณะแพทยศาสตร์ มหาวิทยาลัยเชียงใหม่ และผู้สนใจด้านวิชาการ และมีการนำผลงานวิจัยไปทำการวิจัยต่อยอดเพื่อศึกษาถึงกลไกการเกิดภาวะความผิดปกติของการทำงานของไตและหัวใจในภาวะเบาหวาน หรือในภาวะดื้อต่อฮอร์โมนอินซูลิน และศึกษาถึงกลไกการออกฤทธิ์ของยาและสารอื่นๆ ในการต้านต่อการเกิดภาวะแทรกซ้อนของไตและหัวใจที่เกิดจากภาวะเบาหวาน เพื่อประโยชน์ในการนำสารสกัดหรือสมุนไพรที่มีฤทธิ์ต้านต่อการเกิดภาวะเครียดออกซิเดชั่นและการอักเสบ เช่น การศึกษาการใช้โพรไบโอติกหรือพรีไบโอติกในภาวะเบาหวานเพื่อการพัฒนาไปสู่การเกิดนวัตกรรมการผลิตผลิตภัณฑ์ที่สามารถใช้เสริมกับยารักษาเบาหวานในการลดภาวะแทรกซ้อนดังกล่าวต่อไป และได้มีความร่วมมือกับนักวิจัยจาก คณะเภสัชศาสตร์และคณะวิทยาศาสตร์ มหาวิทยาลัยเชียงใหม่ และคณะวิทยาศาสตร์ มหาวิทยาลัยมหิดล เพื่อศึกษาต่อยอดในการศึกษาและสร้างสรรผลิตภัณฑ์ที่มีฤทธิ์ในการรักษาภาวะเบาหวานต่อไป นอกจากนี้ยังได้ผลิตบัณฑิตนักวิจัยรุ่นใหม่ระดับปริญญาโท นางสาวลอองดาว ทองนาค และนายกฤช ใจคุ้มเก่า จากโครงการวิจัยนี้ซึ่งขณะนี้กำลังศึกษาในระดับปริญญาเอก

3. อื่นๆ (เช่น ผลงานตีพิมพ์ในวารสารวิชาการในประเทศ การเสนอผลงานในที่ประชุมวิชาการ หนังสือ การจดสิทธิบัตร)

3.1 Laongdao Thongnak, Anchalee Pongchaidecha and **Anusorn Lungkaphin**. The Protective Effect of Atorvastatin on Renal Function in Streptozotocin-induced

Diabetic Rats. Presentation at the International Graduate Research Conference 2015: 11 December 2015; Chaing Mai, Thailand

3.2 Keerati Wanchai, Sakawdaurn Yasom, Wannipa Tunapong, Titikorn Chunchai, Nipon Chattipakorn, Siriporn Chattipakorn, Anchalee Pongchaidecha and **Anusorn Lungaphin.** Prebiotic Xylooligosaccharide Attenuates Kidney Dysfunction by Improving Insulin Resistance in High-Fat Diet Induced-Obese Rats. Presentation at the International Graduate Research Conference 2015: 11 December 2015; Chaing Mai, Thailand

ภาคผนวก

The additive effects of atorvastatin and insulin on renal function and renal organic anion transporter 3 function in diabetic rats

Laongdao Thongnak[1], Anchalee Pongchaidecha[1], Krit Jaikumkao[1], Varanuj Chatsudthipong[2], Nipon Chattipakorn[1,3] and Anusorn Lungkaphin[1*]

[1]Department of Physiology, Faculty of Medicine, Chiang Mai University, Chiang Mai, Thailand

[2]Department of Physiology, Faculty of Science, Mahidol University, Bangkok, Thailand

[3]Cardiac Electrophysiology Research and Training Center, Faculty of Medicine, Chiang Mai University, Chiang Mai, Thailand

*** Corresponding author**

Anusorn Lungkaphin, Department of Physiology, Faculty of Medicine,

Chiang Mai University, Intravaroros Road, Chiang Mai, Thailand 50200

Tel.: 6653-945362-4; fax: 6653-945365

E-mail address: onanusorn@yahoo.com; anusorn.lungka@cmu.ac.th

ABSTRACT

Hyperglycemia-induced oxidative stress is usually found in diabetic condition. 3-hydroxy-3-methylglutaryl coenzyme-A (HMG-CoA) reductase inhibitors, statins, are widely used as cholesterol-lowering medication with several “pleiotropic” effects in diabetic patients. This study aims to evaluate whether the protective effects of atorvastatin and insulin on renal function and renal organic anion transporter 3 (Oat3) function involve the modulation of oxidative stress and pancreatic function in type 1 diabetic rats. Type 1 diabetes was induced by intraperitoneal injection of streptozotocin (50 mg/kg BW). Atorvastatin and insulin as single or combined treatment were given for 4 weeks after diabetic condition had been confirmed. Diabetic rats demonstrated renal function and renal Oat3 function impairment with an increased MDA level and decreased SOD protein expression concomitant with stimulation of renal Nrf2 and HO-1 protein expression. Insulin plus atorvastatin (combined) treatment effectively restored renal function as well as renal Oat3 function which correlated with the decrease in hyperglycemia and oxidative stress. Moreover, pancreatic inflammation and apoptosis in diabetic rats were ameliorated by the combined drugs treatment. Therefore, atorvastatin plus insulin seems to exert the additive effect in improving renal functionby alleviating hyperglycemiaand the modulation of oxidative stress, inflammation and apoptosis.

Keywords: Diabetes Mellitus; Renal function; Renal Oat3; Atorvastatin; Oxidative stress; Inflammation

Introduction

Type 1 diabetes (T1D) is an autoimmune disease characterized by low plasma insulin due to a destruction of the pancreatic β-cells which synthesize insulin[1] leading to the development of hyperglycemia. Diabetic nephropathy (DN) is a devastating complication of type 1 diabetes, which is the leading cause of end-stage renal disease (ESRD) and a major cause of morbidity and mortality in T1D patients[2]. Although the pathogenesis of DN is still not fully understood it has been suggested that long-term hyperglycemia activates reactive oxygen species (ROS) production by increasing advanced glycation end products (AGE). Subsequently, AGE activates the polyol pathway resulting in the activation of Nicotinamide adenine dinucleotide phosphate (NADPH) oxidase causing cell damage and dysfunction[3-5]. These conditions can lead to diabetic nephropathy and diabetic-induced complications in several organs including the pancreas. DN is characterized by various ultrastructural changes of nephrons including basement membrane thickening, glomerular and tubular hypertrophy, glomerulosclerosis and tubulointerstitial fibrosis[6]. This pathology markedly affects the secretory and excretory capacities of transporters in renal proximal tubules.

The organic anion transporter 3 (Oat3) is an important renal transporter which is localized in the basolateral membrane of the renal proximal tubule. It plays an essential role in renal excretion of a variety of drug metabolites, endogenous substances, and environmental toxins. Our previous study has demonstrated that a decrease in function and expression of renal Oat3 in diabetic rats were associated with an increased oxidative stress level from hyperglycemia[7]. Moreover, we found that an impairment of

renal Oat3 transport function and expression in diabetic rats was restored by insulin treatment[7,8].

Atorvastatin, an 3-hydroxy-3-methylglutaryl coenzyme-A (HMG-CoA) reductase inhibitor, is widely used to treat hypercholesterolemia and dyslipidemia in diabetic patients. A recent study demonstrated the pleiotropic effects of statins in attenuating oxidative stress, inflammation, apoptosis and thrombosis[9]. In addition, cardioprotective effects of statins in an angiotensin II (Ang II)-induced cardiac hypertrophy and fibrosis mice model[10] and the renoprotective effects of statins in gentamicin-induced nephropathy in rats through the attenuation of oxidative stress leading to improving renal Oat3 and renal function[11] have been reported by our team. We also demonstrated that renal inflammation, endoplasmic reticulum (ES) stress and apoptosis were ameliorated by atorvastatin in gentamicin-induced nephrotoxicity in rats[12]. In contrast-induced nephropathy, rosuvastatin was found to modulate nitric oxide synthesis, inflammation, oxidative stress and apoptosis in diabetic male rats[13]. Taken together, either insulin or atorvastatin can improve renal function in diabetic rats but their combined effect has not been investigated. In addition, we were very interested in the effect of the combined treatment on pancreatic function and whether it was effective in the modulation of insulin secretion in diabetic condition. Therefore, in this study we have evaluated the renoprotective effects of atorvastatin plus low dose insulin treatment on renal function and the function of the important renal transport protein, renal Oat3, in modulation of the renal oxidative stress pathway, and its effect on the inflammation and apoptosis of the pancreas in streptozotocin (STZ)-induced diabetic rats.

Results

Effects of pharmacological intervention on metabolic parameters in STZ-induced diabetic rats

As shown in Table 1, type 1 diabetic rats showed a significant decrease in body weight and plasma insulin level when compared with those of the control and control plus atorvastatin rats ($p<0.05$). Plasma glucose, cholesterol, triglyceride, urine glucose and urine volume were significantly increased in diabetic rats when compared with control or control plus atorvastatin-treated rats ($p<0.05$). Treatment with insulin as a single entity or combined with atorvastatin correlated with significantly increased body weight compared with diabetic rats ($p<0.05$). Similarly, the rats that received the combined drug treatment (atorvastatin plus insulin) had significantly higher body weight than those receiving only a single treatment of either insulin or atorvastatin-treated rats ($p<0.05$). Rats on insulin or atorvastatin treatment alone and combined drugs treatment showed significantly decreased fasting blood glucose levels when compared with those of diabetic rats ($p<0.05$). However, the fasting blood glucose in the combined drug treatment was lowest and significantly different from that of insulin or atorvastatin-treated rats ($p<0.05$). Co-administration of insulin and atorvastatin had a marked effect on the restoration of plasma insulin which nearly returned to normal levels and was significantly different when compared to that of diabetic, insulin or atorvastatin-treated rats ($p<0.05$). Also, rats having the combined drug treatment showed a significantly lower plasma cholesterol level when compared to diabetic and atorvastatin-treated rats ($p<0.05$). In addition, rats receiving insulin or atorvastatin alone or the combined

therapy showed significantly lowered urine glucose concentration when compared to that of diabetic rats ($p<0.05$). Rats having insulin as a single or combined treatment with atorvastatin showed a significantly decreased 24-hr urine volume in comparison with that of diabetic rats ($p<0.05$). Surprisingly, atorvastatin treatment significantly increased 24-hr urine volume with respect to diabetic, insulin-treated and combined-treated rats ($p<0.05$).

Effects of pharmacological intervention on kidney weight, kidney weight to body weight ratio, and renal function in STZ-induced diabetic rats

Type 1 diabetic rats showed significant increases in kidney weight (KW) and kidney weight to body weight (KW/BW) ratio compared with the control and control plus atorvastatin rats ($p<0.05$) (Table 2). Although, the KW/BW ratio of both insulin and combined drug treatment rats ($p<0.05$) was significantly lower than that of diabetic rats. The greater reduction in KW/BW ratio was observed in the combined drug treatment (insulin plus atorvastatin) group ($p<0.05$).

Significant increases in serum blood urea nitrogen (BUN) and creatinine levels, along with a decrease in urine creatinine level and estimated glomerular filtration rate (eGFR) in diabetic rats, compared with that of the control or control plus atorvastatin rats ($p<0.05$) were observed which indicated an impairment in renal function in rats with the diabetic condition (Table 2). The greatest reduction in BUN was found in the combined drug treatment group. Of note, the decreased serum BUN and creatinine levels, in this group showed a strong correlation with an improved eGFR. The results

suggested that combined drug treatment produced the greatest effect in improving kidney function in the diabetic rats.

Effects of atorvastatin on kidney histological change in STZ-induced diabetic rats

As shown in Figure 1A, moderate glomerular lesions were found in diabetic rats when compared with control and control plus atorvastatin rats. Glomerular capillaries were attached to the Bowman's capsule, their wide and irregular morphology leading to increased capsule space in the diabetic group. In the kidneys from the diabetic rats, tubulointerstitial damage was found with epithelial cell atrophy. Furthermore, a small amount of focal interstitial fibrosis with neutrophil accumulation was observed. These results were supported by the significant increase in renal injury score when compared with control ($p<0.05$) (Figure 1B). Atorvastatin plus insulin (combined) treatment led to a decrease in these morphological changes as indicated by a significant improve in renal injury score when compared with diabetic group ($p<0.05$). Moreover, the combined treatment found to have a significant different in renal injury score when compared to insulin or atorvastatin treatment alone ($p<0.05$).

Effects of pharmacological intervention on renal Oat3 function and expression in STZ-induced diabetic rats

An impairment in renal Oat3 function in diabetic rats was indicated by a significant decrease in [^{3}H]estrone sulfate (ES) uptake when compared with the control or control plus atorvastatin rats ($p<0.05$) (Figure 2A). Insulin as a single or combined treatment with atorvastatin led to significantly elevated [^{3}H]ES uptake in comparison

with diabetic rats ($p<0.05$). Although, atorvastatin treatment led to a tendency to increase [^{3}H]ES uptake it was still significantly lower than that of the control group. As presented in Figure 2B and 2C, the expression of renal Oat3 in the whole cell lysate of cortical tissues was comparable among the experimental groups while renal Oat3 expression in the membrane fraction was significantly decreased in diabetic rats ($p<0.05$). All drug treatment groups indicated a tendency to increase [^{3}H]ES uptake. However, a significant increase in renal Oat3 expression in the membrane fraction was only observed in the combined drug treatment rats ($p<0.05$) but there was an increasing trend noted in insulin-treated rats. These findings indicated that the decreased Oat3 function associated with the down-regulation of Oat3 in the membrane of renal tubular cells in cases of diabetes mellitus may well be improved by insulin or insulin plus atorvastatin treatment.

Effects of pharmacological intervention on oxidative stress status in STZ-induced diabetic rats

As shown in Figure 3, significant increases in malondialdehyde (MDA) level and protein kinase C alpha (PKC-α) expression along with an apparent decrease in superoxide dismutase (SOD) expression were observed in the renal cortical tissues of diabetic rats compared with that of the control rats ($p<0.05$) reflecting an increase in oxidative stress in diabetes. Insulin as a single or combined treatment with atorvastatin led to a significantly decreased renal cortical MDA level when compared with diabetic rats ($p<0.05$) and this value was approaching the control level. The atorvastatin treatment alone seemed to have no effect on cortical MDA. Interestingly, diabetic rats on the combined drug treatment showed a significant increase in the expression of SOD

(p<0.05) with compared to diabetic rats and the ones with insulin or atorvastatin treatment alone. Moreover, rats on the combined drug treatment showed a significant decrease in the expression of PKC-α when compared with the diabetic rats (p<0.05). The results from this study suggested that atorvastatin plus insulin treatment could markedly decrease oxidative stress in the diabetic condition.

Effects of pharmacological intervention on the oxidative stress pathway in STZ-induced diabetic rats

To further study the mechanism by which combined drug treatment led to decreased hyperglycemia-induced oxidative stress, the expression of proteins involved in the oxidative stress pathway, including nuclear factor erythroid 2-related factor 2 (Nrf2), glutamate-cysteine ligase catalytic subunit (GCLC), and heme oxygenase-1 (HO-1) were investigated in the renal cortical tissues. Diabetic rats showed a significant increase in the expression of Nrf2 in both the nuclear and whole cell lysate fractions of renal cortical tissues compared with the control and control plus atorvastatin rats (p<0.05) (Figure 4). These results indicated, not only was there an increase in Nfr2 protein synthesis in the cell, but there was also increased translocation of Nrf2 from the cytoplasm to nucleus occurring in the diabetic rats. Interestingly, the combined drug treatment significantly reversed the expression of Nrf2 in both the whole cell lysate and the nuclear fraction when compared with that of diabetic rats (p<0.05). Rats on atorvastatin alone had significantly attenuated Nrf2 expression in whole cell lysate fractions but there was no significant effect on Nrf2 in the nuclear fraction compared with diabetic rats (p<0.05). Of note, Nrf2 induced a significant increase in antioxidant

enzyme HO-1 in diabetic rats compared to that of control or control plus atorvastatin rats ($p<0.05$) whereas there was no change of GCLC expression among the experimental groups. All types of drug treatment showed a significant lowering of the expression of HO-1 in comparison with that of the diabetic rats ($p<0.05$). The results indicated that combined drug treatment inactivated Nrf2 translocation to nucleus which was related to the reduced HO-1 expression.

Effects of pharmacological intervention on the pancreatic apoptotic pathway in STZ-induced diabetic rats

Atorvastatin has been shown to inhibit the apoptosis of myocardial cells in cases of heart failure following myocardial infarction in rats[14]. As plasma insulin levels were found to decrease in diabetic type 1 rats and the combined drug treatment led to the restoration of these levels to within normal limits, it is likely that pancreas function recovered after the treatment. To verify this hypothesis the expression of apoptotic proteins in pancreatic tissue was investigated. As shown in Figure 5, diabetic rats showed a significant increase in B-cell lymphoma 2 (Bcl-2) associated X (Bax) protein and cleaved caspase-3 expression, and marked reduction of Bcl-2 expression in pancreatic tissue when compared with that of the control or control plus atorvastatin rats ($p<0.05$). The combined drug treatment led to a significant reduction of Bax and cleaved caspase-3 expression and apparently enhanced the expression of Bcl-2 in comparison with diabetic rats ($p<0.05$) whereas insulin or atorvastatin treatment alone had no effects on these parameters. These results suggested that combined drug

treatment protected against pancreatic apoptosis which helps preserve the pancreas tissue and function in diabetic rats.

Effects of pharmacological intervention on pancreatic inflammation pathways in STZ-induced diabetic rats

It has been reported that chronic hyperglycemia can cause β-cell degranulation and reduction[15]. It has been shown that statins have anti-inflammatory effects in asymmetrical dimethylarginine-induced inflammatory endothelial cells[16]. We, therefore, went on to investigate the effect of atorvastatin treatment on the inflammation of pancreatic tissues. As shown in Figure 6, there was significantly increased interferon gamma (IFN-γ) and interleukin-6 (IL-6) protein expression in diabetic rats when compared with that of the control and control plus atorvastatin rats ($p<0.05$). The single treatment with either insulin or atorvastatin tended to lower levels of inflammatory proteins but the significant difference in IFN-γ was only observed in insulin-treated rats ($p<0.05$) whereas the combined drug treatment led to the significant decreases seen in both IFN-γ and IL-6 protein expression when compared with diabetic rats ($p<0.05$).

Discussion

The STZ-induced diabetes type 1 in the rats in this study was characterized by body weight loss, hyperglycemia, decreased plasma insulin level, renal dysfunction and renal histological changes which were shown to have a correlation with an increase in renal oxidative stress. In addition, hyperglycemia-induced oxidative stress was found to activate the oxidative defense mechanisms through the Nrf2 pathway to protect

cytotoxicity. This was consistent with findings from our previous study[7] which reported that the increased ROS generation in diabetes activated the PKC signaling pathway resulting in the downregulation of renal Oat3 function and expression in the renal tissues. Of note, hyperglycemia also increased pancreatic expression of IL-6 and IFN-γ, indicators of inflammation, leading to pancreatic apoptosis as shown by the increase in Bax, cleaved caspase-3 protein expression and the Bax/Bcl-2 ratio. Interestingly, atorvastatin plus insulin (combined) treatment led to amelioration of the inflammation and destruction of pancreatic cells leading to an increase in insulin secretion which subsequently improved conditions of hyperglycemia. Thus, combined drug treatment could exert additive effects in preserving both renal and pancreatic functions via modulation of oxidative stress, inflammation and apoptotic pathways.

Long-term hyperglycemia leads to an increase in reactive oxygen species and reactive nitrogen species (ROS&RNS) leading to increased oxidative stress[17]. The condition of increased oxidative stress in the diabetic rats in this study was confirmed by the elevation of renal MDA, the stimulation of HO-1 expression and the reduction of antioxidant enzyme expression, SOD2. Antioxidant mechanisms are usually activated when oxidative stress occurs. The Nrf2-Kelch-like ECH-associated protein 1 (Keap1) pathway is the major regulator of cytoprotective responses and regulates the expression of antioxidant proteins which protect against oxidative damage triggered by injury and inflammation[18,19]. In the presence of ROS, cysteine residues in Keap1 are oxidized leading to a conformational change of Keap1, which prevents its binding to Nrf2. After that, Nrf2 passes by translocation into the nucleus to promote the translation of oxidative-stress-inducible genes, including HO-1[20]. In this study, an increased oxidative

stress, induced by hyperglycemia in diabetic rats, led to activated Nrf2 expression and translocation, which subsequently promoted the expression of HO-1 proteins. It is now widely accepted that induction of HO-1 expression represents an adaptive response that increases cellular defense to oxidative injury. It has been reported that HO-1 is increased in livers of obese versus lean individuals and of diabetic versus nondiabetic subjects[21]. These results are supported by the previous study that found high-glucose-induced upregulation of Nrf2 and HO-1 gene expression[22]. This is in agreement with our previous reports showing the increased expression of renal Nrf2, NAD(P)H quinone dehydrogenase 1 (NQO1) and HO-1 due to oxidative stress in gentamicin-induced nephrotoxicity in rats[11,23].

An increased expression of PKC-α in diabetic rats was also consistent with the previous report that PKC-α was activated in hyperglycemia[7]. Moreover, the decreased renal Oat3 function and expression in the present study when PKC-α was activated due to oxidative stress were similar to that observed previously in diabetic[7,8] and gentamicin-induced nephrotoxicity in rats[11,23].

In this study, increased pancreatic apoptosis was found to be significantly related to the decreased plasma insulin levels in diabetic rats. Hyperglycemia may negatively affect β-cell mass by inducing apoptosis without a compensatory increase in β-cell proliferation and neogenesis. It has been reported that chronic hyperglycemia can cause β-cell degranulation and reduction[15]. The increased pancreatic expression of IL-6, and IFN-γ, indicating inflammation in diabetic rats in the present study, was found to be correlated with the findings of an *in vitro* study demonstrating that the exposure of β-

cells to high glucose induced interleukin 1 beta (IL-1β) which activated nuclear factor-kappa B (NF-kB) and Fas signaling and consequently triggered apoptosis[24,25]. Moreover, both IL-1β and IFN-γ also activated NF-kB and appeared to increase inducible nitric oxide synthase (iNOS) expression resulting in the stimulation of ER stress conditions and mononuclear cell activation and infiltration leading to β-cell death[26].

Atorvastatin is a lipid-lowering agent in statins or the HMG-CoA reductase inhibitor group which inhibit the HMG-CoA reductase enzyme, the catalyst of the rate-limiting step of the mevalonate pathway[27]. It has been reported as having pleiotropic effects including anti-apoptosis[28,29], anti-inflammation[30], antioxidant[11,31] and anti-thrombotic effects[32]. Although the direct effect of atorvastatin in reducing plasma levels of cholesterol was not observed in this study, the beneficial effects of the restoration of plasma insulin, reduced blood glucose, improved renal function, as well as decreased pancreatic inflammation and apoptosis were demonstrated in the diabetic rats that had undergone the combined treatment (atorvastatin with a low dose of insulin). It initiated a greater effect than that observed in the rats undergoing insulin or atorvastatin treatment alone. These pleiotropic effects of atorvastatin which led to the adjustment of glucose homeostasis and renoprotection observed in this study might be due to the additive effect of atorvastatin and insulin in controlling metabolic parameters and subsequently protect kidney dysfunction in diabetes. This proposed mechanism is supported by the previous study reporting that atorvastatin can increase β-cell function by increasing β-cell proliferation and decreasing ER stress conditions[33]. The increased insulin secretion and the attenuation of apoptosis of pancreatic tissue seen in rats on the combined

treatment in this study reflected an improvement in β-cell function. The dosage of insulin used in this study had no effect on the lowering of plasma glucose to normal levels as indicated in the group on insulin treatment alone. Thus, the effective reduction of the hyperglycemic condition in the group on the combined drug treatment corroborated the pleiotropic effects of atorvastatin in the reduction of oxidative stress leading to the improvement of renal and pancreatic functions seen in this study. We found that only combined treatment had the significant effect on Nrf-2 expression while insulin, atorvastatin and combined treatment had similar effect on HO-1 expression. The results indicated that combined drug treatment inactivated Nrf2 translocation to nucleus which was related to the reduced HO-1 expression. However, the reduced HO-1 expression in insulin or atorvastatin treatment alone might be involved the other regulated mechanisms such as inflammation or insulin. Insulin has been reported to stimulate HO-1 expression in skeletal myoblast[34]. The decreased HO-1 expression might be related to the low level of plasma insulin in insulin or atorvastatin treatment alone. Thus, the combined drug treatment produced highly effective effects in the control of glucose homeostasis and the prevention of organ dysfunction when compared to of the insulin or atorvastatin treatment alone.

In conclusion, the results obtained from this study indicate that combined atorvastatin and low dose insulin treatment exhibit renoprotective effects and lead to the reversal of pancreatic β-cell function in streptozotocin-induced diabetes in rats. These improvements occurred via the modulation of oxidative stress, pancreatic inflammation and apoptotic pathways. Moreover, the reduced insulin injection dosage could prevent the adverse effect of insulin in prolonged treatment especially in Type 1 diabetes. Since

the use of atorvastatin and insulin showed great potential benefits in the preservation of renal and pancreatic function in rats with diabetes type 1, further study is recommended to investigate whether these benefits could also be conferred in humans.

Materials and methods

Animals. Male Wistar rats (200-250 g) were obtained from the National Animal Center, Salaya Campus, Mahidol University, Thailand. The animal facilities and protocols involved in the study were approved by the Laboratory Animal Care and Use Committees at the Faculty of Medicine, Chiang Mai University, Chiang Mai, Thailand (Permit No: 12/2557). All methods were performed in accordance with the relevant guidelines and regulations. All experimental rats were housed under controlled temperatures of 25±1°C and lighting in a 12 h-light/dark cycle with food and water *ad libitum*. After seven days of acclimatization, thirty-six rats were randomly divided into control (12 rats) and diabetic (24 rats) groups. The control group was divided into 2 groups, control (C), and control plus atorvastatin (CS) (six rats per group). Rats in the diabetic group were intraperitoneally (i.p.) injected with 50 mg/kg BW of streptozotocin in 10 mM citrate buffer pH 4.5 while the control rats received the equivalent dose of citrate buffer solution as a vehicle. After 7 days, rats with fasting blood glucose ≥ 250 mg/dl were included in the diabetic group and assigned into four sub-groups (six rats per group): diabetic (DM), diabetic plus insulin (DMI), diabetic plus atorvastatin (DMS), and diabetic plus insulin and atorvastatin (DMIS). Insulin (4 units/day) was injected subcutaneously while 10 mg/kg/day of atorvastatin dissolved in saline was administered orally for 4 weeks. All rats had free access to water and food and body weight was recorded daily. At the end of the experimental period, a 24-hr urine sample was

collected using a metabolic cage. Rats were killed after being anesthetized using isoflurane inhalation. Blood samples were collected. Plasma and serum were separated and then stored at -20°C until use. The kidneys were removed immediately, decapsulated and weighed to facilitate further use for the determination of renal Oat3 transporter function, malondialdehyde (MDA) concentration, hematoxylin and eosin (H&E) staining, and western blot analysis. Pancreatic tissue was collected and kept at -80°C for further western blot analysis.

Biochemical parameters. The plasma glucose, triglyceride, cholesterol and urine glucose levels were determined by the enzymatic colorimetric method using a commercial kit (ErbaLachemas.r.o., Brno, CZ). Plasma insulin concentration was evaluated by the Sandwich ELIZA method using a commercial kit (Rat/Mouse Insulin ELISA kit, Merck Millipore, MA, USA). Renal function was estimated by the determination of serum and urine creatinine, serum blood urea nitrogen (BUN) levels and estimated glomerular filtration rate (eGFR). Serum and urine creatinine and serum blood urea nitrogen (BUN) levels were measured using an automatic biochemical analyzer at the Clinical Laboratory, Maharaj Nakorn Chiang Mai Hospital, Chiang Mai, Thailand. eGFR was calculated using the following equation :-

$$\text{eGFR} = (\text{urine creatinine} \times \text{urine flow rate}) / \text{serum creatinine} \quad (1)$$

Determination of renal Oat3 function. The decapsulated kidneys were placed into freshly-oxygenated ice-cold modified Cross and Taggart saline buffer (contain: 95 mM NaCl, 80 mM mannitol, 5 mM KCl, 0.74 mM $CaCl_2$, and 9.5 mM Na_2HPO_4, pH 7.4). Thin renal cortical slices (≤ 0.5 mm; 5-15 mg, wet weight) were cut using a Stadie-Riggs

microtome and incubated in 1 ml of buffer containing 50 nM [^{3}H] estrone sulfate (ES), a prototypical organic anion that is preferentially transported by Oat3[35,36], to enable an uptake study for 30 mins at room temperature. At the end of the uptake period, the slices were washed in 0.1 M $MgCl_2$, blotted on filter paper, weighed and dissolved in 0.4 ml of 1 M NaOH, and neutralized with 0.6 ml of 1 N HCl. Five renal cortical slices were used for each rat (5-6 rats per group). The radioactivity was measured using a liquid scintillation analyzer (Perkin Elmer, MA, USA). The transport of ES was calculated as tissue to medium (T/M) ratio.

T/M ratio= dpm/g tissue ÷ dpm/ml medium (2)

Determination of renal oxidative stress and pancreatic apoptosis.

Determination of MDA in renal cortical tissue

The renal cortical tissue was cut and suspended in Cell Lytic MT mammalian tissue lysis/extraction reagent (Sigma Aldrich, MO, USA) containing a 1% complete protease inhibitor cocktail (Roche Applied Science, IN, USA). After being homogenized and centrifuged at 1,600 g for 10 min at 4°C, the supernatants were collected. The MDA concentration as an indicator of renal oxidative stress condition was determined by using a commercial thiobarbituric acid reactive substance (TBARS) assay kit from Cayman Chemical (Ann Arbor, MI, USA) in line with the manufacturer's protocol.

Western blot Analysis

The renal cortical or pancreatic tissues were homogenized in Cell Lytic MT mammalian tissue lysis/extraction reagent (Sigma Aldrich, MO, USA) containing a 1% complete protease inhibitor cocktail (Roche Applied Science, IN, USA) and centrifuged

at 5,000 g for 10 minutes. The supernatant was collected and served as the whole cell lysate fraction and the pellet served as the nuclear fraction. The remaining supernatant was centrifuged at 100,000 g for 2 hrs, then the collected pellet served as the membrane fraction. Protein concentration was measured using a colorimetric Bradford protein assay commercially available kit (Bio-Rad, PA, USA). Total cell lysates, nuclear and membrane fractions from the renal cortex were subjected to 10% SDS-polyacrylamide gel electrophoresis (SDS-PAGE). Proteins were transferred onto PVDF membrane (Millipore, MA, USA) and were allowed to react with primary antibodies overnight at 4 °C. Antibodies against Nrf-2, IL-6, IFN-γ and PKC-α were obtained from Santa-cruz Biotechnology (CA, USA). Antibodies against GCLC and HO-1 were obtained from Abcambiochemicals (MA, USA). Antibodies against SOD2, Bcl-2, β-actin and Lamin B were obtained from Cell signaling Technology (MA, USA). Antibodies against Oat3 were obtained from Cosmo Bio Co. Ltd., (Tokyo, Japan) and antibodies against Bax, cleaved caspase-3, Na^+-K^+-ATPase from Merck Millipore (MA, USA). Membranes were developed using an ECL enhanced chemiluminescence agent (BioRad Laboratory Ltd., HemelHemstead, UK) and exposed using the ChemiDoc™ Touch Imaging system (BioRad Laboratory Ltd., HemelHemstead, UK). Relative molecular mass of the labeled protein bands was estimated using a Page Ruler Prestained Protein Ladder (Fermentas, MA, USA), and the density was determined by the software ImageJ (National Institutes of Health, Bethesda, MD, USA). Density of the protein bands was expressed in arbitrary units relative to the respective β-actin.

Histopathological study

To determine the changes in kidney morphology, kidneys were cut along the transverse axis then fixed in 10% neutral buffered formalin and embedded in paraffin. Paraffin-embedded specimens were cut into 2 μm-thick sections, mounted on glass slides and stained with hematoxylin and eosin (H&E) for histological assessment. The samples were observed by an observer blinded to animal treatment groups to determine the presence of glomerular and tubular changes or damage. Five slices of kidney section from each group of experiments were examined and scored under light microscope (Olympus Co., Tokyo, Japan) and evaluated the severity of renal injury score (0-4) by estimating the percentage of tubules in cortex or outer medullar and glomerulus that exhibited increases capsular space of glomerular capsule, peritubular leukocyte infiltration, tubular dilatation, and interstitial fibrosis. The histopathological evaluation was performed as follows: 0-none; 1-<5%; 2-5-25%; 3-25-75% and 4->75%[37,38].

Statistical analysis

All data were expressed as mean ± standard error (SEM). A one-way ANOVA was used to compare the data from the various treatments followed by Fisher's Least significant difference test (LSD). A *p* value of less than 0.05 was considered to be statistically significant.

Acknowledgement

This work was supported by Thailand Research Fund Grant number RSA5780029 (AL); National Research Council of Thailand (Grant #347682/2560) (AL); CMU Mid-Career Research Fellowship program (AL), the Faculty of Medicine Research

Fund, Chiang Mai University (AL, LT and AP) and the NSTDA Research Chair grant from the National Science and Technology Development Agency of Thailand (NC.).

Additional Information

Competing financial interests

The author(s) declare no competing financial interests.

References

1. Diagnosis and Classification of Diabetes Mellitus. *Diabetes Care* **37**, S81-S90 (2014).

2. Reutens, A. T. &Atkins, R. C. Epidemiology of diabetic nephropathy. *Contrib Nephrol* **170**, 1-7 (2011).

3. Duran-Salgado, M. B. & Rubio-Guerra, A. F. Diabetic nephropathy and inflammation. *World J Diabetes* **5**, 393-398 (2014).

4. Ramasamy, R., Yan, S. F. & Schmidt, A. M. Receptor for AGE (RAGE): signaling mechanisms in the pathogenesis of diabetes and its complications. *Ann N Y Acad Sci* **1243**, 88-102 (2011).

5. Tang, S. C. &Lai, K. N. The pathogenic role of the renal proximal tubular cell in diabetic nephropathy. *Nephrol Dial Transplant* **27**, 3049-3056 (2012).

6. Jefferson, J. A., Shankland, S. J.& Pichler, R. H. Proteinuria in diabetic kidney disease: a mechanistic viewpoint. *Kidney Int* **74**, 22-36 (2008).

7. Phatchawan, A., Chutima, S., Varanuj, C. & Anusorn, L. Decreased renal organic anion transporter 3 expression in type 1 diabetic rats. *Am J Med Sci* **347**, 221-227 (2014).

8. Lungkaphin, A., Arjinajarn, P., Pongchaidecha, A., Srimaroeng, C., Chatsudthipong, L., et al. Impaired insulin signaling affects renal organic anion transporter 3 (Oat3) function in streptozotocin-induced diabetic rats. *PLoS One* **9**, e96236 (2014).

9. Satoh, M., Takahashi, Y., Tabuchi, T., Minami, Y., Tamada, M., et al. Cellular and molecular mechanisms of statins: an update on pleiotropic effects. *Clin Sci (Lond)* **129**, 93-105 (2015).

10. Kudo, S., Satoh, K., Nogi, M., Suzuki, K., Sunamura, S., et al. SmgGDS as a Crucial Mediator of the Inhibitory Effects of Statins on Cardiac Hypertrophy and Fibrosis: Novel Mechanism of the Pleiotropic Effects of Statins. *Hypertension* **67**, 878-889 (2016).

11. Jaikumkao, K., Pongchaidecha, A., Chattipakorn, N., Chatsudthipong, V., Promsan, S., et al. Atorvastatin improves renal organic anion transporter 3 and renal function in gentamicin-induced nephrotoxicity in rats. *Exp Physiol* **101**, 743-753 (2016).

12. Jaikumkao, K., Pongchaidecha, A., Thongnak, L. O., Wanchai, K., Arjinajarn, P., et al. Amelioration of Renal Inflammation, Endoplasmic Reticulum Stress and Apoptosis Underlies the Protective Effect of Low Dosage of Atorvastatin in Gentamicin-Induced Nephrotoxicity. *PLoS One* **11**, e0164528 (2016).

13. Deng, J., Wu, G., Yang, C., Li, Y., Jing, Q., et al. Rosuvastatin attenuates contrast-induced nephropathy through modulation of nitric oxide, inflammatory responses, oxidative stress and apoptosis in diabetic male rats. *J Transl Med* **13**, 53 (2015).

14. Song, X. J., Yang, C. Y., Liu, B., Wei, Q., Korkor, M. T., et al. Atorvastatin inhibits myocardial cell apoptosis in a rat model with post-myocardial infarction heart failure by downregulating ER stress response. *Int J Med Sci* **8**, 564-572 (2011).

15. Kaiser, N., Leibowitz, G. & Nesher, R. Glucotoxicity and beta-cell failure in type 2 diabetes mellitus. *J Pediatr Endocrinol Metab* **16**, 5-22 (2003).

16. Jiang, J. L., Wang, S., Li, N. S., Zhang, X. H., Deng, H. W., et al. The inhibitory effect of simvastatin on the ADMA-induced inflammatory reaction is mediated by MAPK pathways in endothelial cells. *Biochem Cell Biol* **85**, 66-77 (2007).

17. Busik, J. V., Mohr, S. & Grant, M. B. Hyperglycemia-induced reactive oxygen species toxicity to endothelial cells is dependent on paracrine mediators. *Diabetes* **57**, 1952-1965 (2008).

18. Baird, L.& Dinkova-Kostova, A. T. The cytoprotective role of the Keap1-Nrf2 pathway. *Arch Toxicol* **85**, 241-272 (2011).

19. Motohashi, H. & Yamamoto, M. Nrf2-Keap1 defines a physiologically important stress response mechanism. *Trends Mol Med* **10**, 549-557 (2004).

20. Ishii, T., Itoh, K., Takahashi, S., Sato, H., Yanagawa, T., et al. Transcription factor Nrf2 coordinately regulates a group of oxidative stress-inducible genes in macrophages. *J Biol Chem* **275**, 16023-16029 (2000).

21. Jais, A., Einwallner, E., Sharif, O., Gossens, K., Lu, T. T., et al. Heme oxygenase-1 drives metaflammation and insulin resistance in mouse and man. *Cell* **158**, 25-40 (2014).

22. Ungvari, Z., Bailey-Downs, L., Gautam, T., Jimenez, R., Losonczy, G., et al. Adaptive induction of NF-E2-related factor-2-driven antioxidant genes in endothelial cells in response to hyperglycemia. *Am J Physiol Heart Circ Physiol* **300**, H1133-1140 (2011).

23. Promsan, S., Jaikumkao, K., Pongchaidecha, A., Chattipakorn, N., Chatsudthipong, V., et al. Pinocembrin attenuates gentamicin-induced nephrotoxicity in rats. *Can J Physiol Pharmacol* **94**, 808-818 (2016).

24. Donath, M. Y.& Halban, P. A. Decreased beta-cell mass in diabetes: significance, mechanisms and therapeutic implications. *Diabetologia* **47**, 581-589 (2004).

25. Donath, M. Y., Storling, J., Maedler, K. & Mandrup-Poulsen, T. Inflammatory mediators and islet beta-cell failure: a link between type 1 and type 2 diabetes. *J Mol Med (Berl)* **81**, 455-470 (2003).

26. Cnop, M., Welsh, N., Jonas, J. C., Jorns, A., Lenzen, S., et al. Mechanisms of pancreatic beta-cell death in type 1 and type 2 diabetes: many differences, few similarities. *Diabetes* **54 Suppl 2**, S97-107 (2005).

27. Chogtu, B., Magazine, R. & Bairy, K. L. Statin use and risk of diabetes mellitus. *World J Diabetes* **6**, 352-357 (2015).

28. Buranrat, B., Senggunprai, L., Prawan, A. & Kukongviriyapan, V. Simvastatin and atorvastatin as inhibitors of proliferation and inducers of apoptosis in human cholangiocarcinoma cells. *Life Sci* **153**, 41-49 (2016).

29. Wang, H., Yin, Y., Wang, P., Xiong, C., Huang, L., et al. Current situation and future usage of anticancer drug databases. *Apoptosis* **21**, 778-794 (2016).

30. He, X., Li, L., Tan, H., Chen, J. & Zhou, Y. Atorvastatin attenuates contrast-induced nephropathy by modulating inflammatory responses through the regulation of JNK/p38/Hsp27 expression. *J Pharmacol Sci* **131**, 18-27 (2016).

31. Tian, S., Zhao, W., Yang, D., Yu, Y., Zou, J., et al. Atorvastatin inhibits miR-143 expression: A protective mechanism against oxidative stress in cardiomyocytes. *Int J Cardiol* **211**, 115-118 (2016).

32. Violi, F., Carnevale, R., Pastori, D. & Pignatelli, P. Antioxidant and antiplatelet effects of atorvastatin by Nox2 inhibition. *Trends Cardiovasc Med* **24**, 142-148 (2014).

33. Chen, Z. Y., Liu, S. N., Li, C. N., Sun, S. J., Liu, Q., et al. Atorvastatin helps preserve pancreatic beta cell function in obese C57BL/6 J mice and the effect is related to increased pancreas proliferation and amelioration of endoplasmic-reticulum stress. *Lipids Health Dis* **13**, 98 (2014).

34. Aggeli, I. K., Theofilatos, D., Beis, I. & Gaitanaki, C. Insulin-induced oxidative stress up-regulates heme oxygenase-1 via diverse signaling cascades in the C2 skeletal myoblast cell line. *Endocrinology* **152**, 1274-1283 (2011).

35. Sweet, D. H., Miller, D. S., Pritchard, J. B., Fujiwara, Y., Beier, D. R., et al. Impaired organic anion transport in kidney and choroid plexus of organic anion transporter 3 (Oat3 (Slc22a8)) knockout mice. *J Biol Chem* **277**, 26934-26943 (2002).

36. Aslamkhan, A. G., Thompson, D. M., Perry, J. L., Bleasby, K., Wolff, N. A., et al. The flounder organic anion transporter fOat has sequence, function, and substrate specificity similarity to both mammalian Oat1 and Oat3. *Am J Physiol Regul Integr Comp Physiol* **291**, R1773-1780 (2006).

37. Ma, L., Fei, J., Chen, Y., Zhao, B., Yang, Z. T., et al. Vitamin C Attenuates Hemorrhagic Shock-induced Dendritic Cell-specific Intercellular Adhesion Molecule 3-grabbing Nonintegrin Expression in Tubular Epithelial Cells and Renal Injury in Rats. *Chin Med J (Engl)* **129**, 1731-1736 (2016).

38. Zhao, B., Fei, J., Chen, Y., Ying, Y. L., Ma, L., et al. Vitamin C treatment attenuates hemorrhagic shock related multi-organ injuries through the induction of heme oxygenase-1. *BMC Complement Altern Med* **14**, 442 (2014).

Author Contributions

Conceived and designed the experiments: AL AP LT NC VC. Performed the experiments: AL AP LT KJ. Analyzed the data: AL LT. Investigation: AL AP KJ LT. Wrote the main manuscript text: AL AP LT. Software: LT KJ. Edited and revised the manuscript: AL AP VC NC. Final approved the version to be published: AL AP LT VC NC.

Table 1 Effects of pharmacological interventions on metabolic parameters

	Control	DM	DMI	DMS	DMIS	CS
Body weight (g)	396.67±17.21	245±14.50*	302.5±17.69*†#	219±6.11*	344.17±14.17*†‡#	400±12.18†‡#
Fasting blood glucose (mg/dl)	154.85±13.93	565.57±37.03*	467.04±40.30*†	422.94±31.92*†	254.92±32.82*†‡#	131.08±5.45†‡#
Plasma insulin (U/ml)	2.47±0.43	0.57±0.24*	0.85±0.19*	0.65±0.20*	2.20±0.71†‡#	3.23±0.48†‡#
Plasma cholesterol (mg/dl)	74.71±3.99	102.92±5.97*	91.88±1.55*	95.01±4.89*	81.13±1.67†#	70.87±4.62†‡#
Plasma triglyceride (mg/dl)	75.27±6.98	166.65±28.62*	163.18±16.23*	154.62±26.57*	122.22±12.35	78.51±8.09†‡#
Urine glucose (mg/dl)	115.84±5.84	8834.1±375.5*	6350.6±831.9*†	6136.9±802.7*†	6056.9±426.5*†	110.41±3.08†‡#
Urine volume (ml/24h.)	18.83±0.83	216.33±14.70*	133.67±15.75*†#	251.67±6.60*†	135.50±8.43*†#	18.67±1.61†‡#

Data presented are means ± SEM. n=6 rats per group. C - control group; DM - diabetic group; DMI - diabetic plus insulin group; DMS - diabetic plus atorvastatin group; DMIS - diabetic and insulin plus atorvastatin group; CS - control plus atorvastatin group. *$p < 0.05$ vs. control and control plus atorvastatin groups, †$p < 0.05$ vs. diabetic group, ‡$p < 0.05$ vs. diabetic plus insulin group, #$p < 0.05$ vs. diabetic plus atorvastatin group

Table 2 Effects of pharmacological interventions on renal functions

	Control	DM	DMI	DMS	DMIS	CS
Kidney weight (g)	1.10±0.02	1.34±0.06*	1.38±0.06*	1.25±0.03*	1.29±0.04*	1.05±0.03$^{\dagger\ddagger\#}$
Kidney weight / Body weight ratio (10^{-3})	2.79±0.01	5.55±0.38*	4.66±0.36*$^{\dagger\#}$	5.81±0.28*	3.79±0.21*$^{\dagger\ddagger\#}$	2.64±0.10$^{\dagger\ddagger\#}$
BUN (mg/dl/g BW)	0.05±0.01	0.22±0.03*	0.10±0.01*$^{\dagger\#}$	0.19±0.01*	0.06±0.01$^{\dagger\#}$	0.05±0.01$^{\dagger\ddagger\#}$
Creatinine (10^{-3}mg/dl/g BW)	1.15±0.04	2.13±0.15*	1.82±0.22*	1.74±0.12*†	1.08±0.06$^{\dagger\ddagger\#}$	0.99±0.07$^{\dagger\ddagger\#}$
Urine creatinine (mg/dl)	56.64±7.42	6.37±0.92*	14.45±3.95*	5.88±0.57*	29.36±9.61*$^{\dagger\#}$	54.57±7.59$^{\dagger\ddagger\#}$
eGFR (% of control)	100±1.29	52.69±4.43*	67.11±2.67*$^{\dagger\#}$	50.58±1.41*	75.77±3.30*$^{\dagger\ddagger\#}$	92.31±2.81$^{\dagger\ddagger\#}$

Data presented are means ± SEM. n=6 rats per group. C - control group; DM - diabetic group; DMI - diabetic plus insulin group; DMS - diabetic plus atorvastatin group; DMIS - diabetic and insulin plus atorvastatin group; CS - control plus atorvastatin group. eGFR, estimated glomerular filtration rate calculated as follow :- eGFR= (urine creatinine x urine flow rate) / serum creatinine. *$p < 0.05$ vs. control and control plus atorvastatin groups, $^{\dagger}p < 0.05$ vs. diabetic group, $^{\ddagger}p < 0.05$ vs. diabetic plus insulin group, $^{\#}p < 0.05$ vs. diabetic plus atorvastatin group

Figure legends

Figure 1. A. Photomicrographs of histological sections of kidney stained with hematoxylin and eosin (H&E) (x40); images of glomeruli and renal tubules from control, diabetic (DM), diabetic plus insulin (DMI), diabetic plus atorvastatin (DMS), diabetic and insulin plus atorvastatin (DMIS) groups, and control plus atorvastatin (CS) are indicated. (▲) shows dilatation of renal tubular; (arrow) represents interstitial fibrosis; (white arrow) represents capsular space of the glomerular capsule; (black arrow) represents neutrophil accumulation; (yellow arrow) represents tubular atrophy. B. Quantitative analysis of diabetic injury kidney was determined by semi-quantitative kidney injury scoring (0-4); Bar graphs presented show mean ± SEM. n=5 rats per group. C - control group; DM - diabetic group; DMI - diabetic plus insulin group; DMIS - diabetic and insulin plus atorvastatin group; DMS - diabetic plus atorvastatin group; CS - control plus atorvastatin. *$p < 0.05$ vs. control group and control plus atorvastatin groups, $^{\dagger}p < 0.05$ vs. diabetic group, $^{\ddagger}p < 0.05$ vs. diabetic plus insulin group, and $^{\#}p < 0.05$ vs. diabetic plus atorvastatin group.

Figure 2. Effects of pharmacological intervention on renal cortical Oat3 function and expression. [^{3}H]ES uptake calculated from tissue/medium ratio (A). Western blot analysis of Oat3 expression in whole cell lysate fraction normalized by β-actin (B) and in membrane lysate fraction (cropped blots) normalized by β-actin (C). Na^{+}-K^{+} ATPase was used as a marker for the membrane fraction. Full-length blots are presented in Supplementary Figure 1. Bar graphs presented show mean ± SEM. n=6 rats per group. C - control group; DM - diabetic group; DMI - diabetic plus insulin group; DMIS -

diabetic and insulin plus atorvastatin group; DMS - diabetic plus atorvastatin group; CS - control plus atorvastatin. *p < 0.05 vs. control group and control plus atorvastatin groups, †p < 0.05 vs. diabetic group, ‡p < 0.05 vs. diabetic plus insulin group, and $^{\#}$p <0.05 vs. diabetic plus atorvastatin group.

Figure 3. Effects of pharmacological intervention on renal cortical MDA level (A), renal cortical expression of SOD (B) and PKC-α (C). Western blot analysis of SOD and PKC-α expression in the whole cell lysate fraction of renal cortical tissues (cropped blots) normalized by β-actin. Full-length blots are presented in Supplementary Figure 2. Bar graphs presented show mean ± SEM. n=6 rats per group. C - control group; DM - diabetic group; DMI - diabetic plus insulin group; DMIS - diabetic plus insulin and atorvastatin group; DMS - diabetic plus atorvastatin group; CS - control plus atorvastatin.*p < 0.05 vs. control group and control plus atorvastatin groups, †p < 0.05 vs. diabetic group, ‡p < 0.05 vs. diabetic plus insulin group, and $^{\#}$p <0.05 vs. diabetic plus atorvastatin group.

Figure 4. Effects of pharmacological intervention on the renal cortical expression of Nrf-2, GCLC and HO-1. Western blot analysis of Nrf2 expression in nuclear (A), Nrf2 in whole cell lysate fractions (B), GCLC (C), and HO-1 (D) of renal cortical tissues (whole cell lysate fraction) (cropped blots) normalized to β-actin. Lamin B1 was used as a marker for the nuclear fraction. Full-length blots are presented in Supplementary Figure 3. Bar graphs presented show mean ± SEM. n=6 rats per group. C - control group; DM - diabetic group; DMI - diabetic plus insulin group; DMIS - diabetic and insulin plus atorvastatin group; DMS - diabetic plus atorvastatin group; CS - control plus

atorvastatin. *p < 0.05 vs. control group and control plus atorvastatin groups, †p < 0.05 vs. diabetic group, ‡p < 0.05 vs. diabetic plus insulin group, and $^{\#}$p <0.05 vs. diabetic plus atorvastatin group.

Figure 5. Effects of pharmacological intervention on the expression of Bax, Bcl-2, and cleaved caspase-3 in pancreatic tissues. Western blot analysis showing the expressions of Bax (A), Bcl-2 (B), and cleaved caspase-3 (C) in pancreatic tissues (cropped blots) normalized to β-actin. Full-length blots are presented in Supplementary Figure 4. Bar graphs presented show mean ± SEM. n=6 rats per group. C - control group; DM - diabetic group; DMI - diabetic plus insulin group; DMIS - diabetic and insulin plus atorvastatin group; DMS - diabetic plus atorvastatin group; CS - control plus atorvastatin.*p < 0.05 vs. control group and control plus atorvastatin groups, †p < 0.05 vs. diabetic group, ‡p < 0.05 vs. diabetic plus insulin group, and $^{\#}$p <0.05 vs. diabetic plus atorvastatin group.

Figure 6. Effects of pharmacological intervention on the expression of IL-6, and IFN-γ in pancreatic tissues. Western blot analysis showing the expression of IL-6 (A), and IFN-γ (B) in pancreatic tissues (cropped blots) normalized to β-actin. Full-length blots are presented in Supplementary Figure 5. Bar graphs presented show mean ± SEM. n=6 rats per group. C - control group; DM - diabetic group; DMI - diabetic plus insulin group; DMIS - diabetic and insulin plus atorvastatin group; DMS - diabetic plus atorvastatin group; CS - control plus atorvastatin. *p < 0.05 vs. control group and control plus atorvastatin groups, †p < 0.05 vs. diabetic group, ‡p < 0.05 vs. diabetic plus insulin group, and $^{\#}$p <0.05 vs. diabetic plus atorvastatin group.

A.

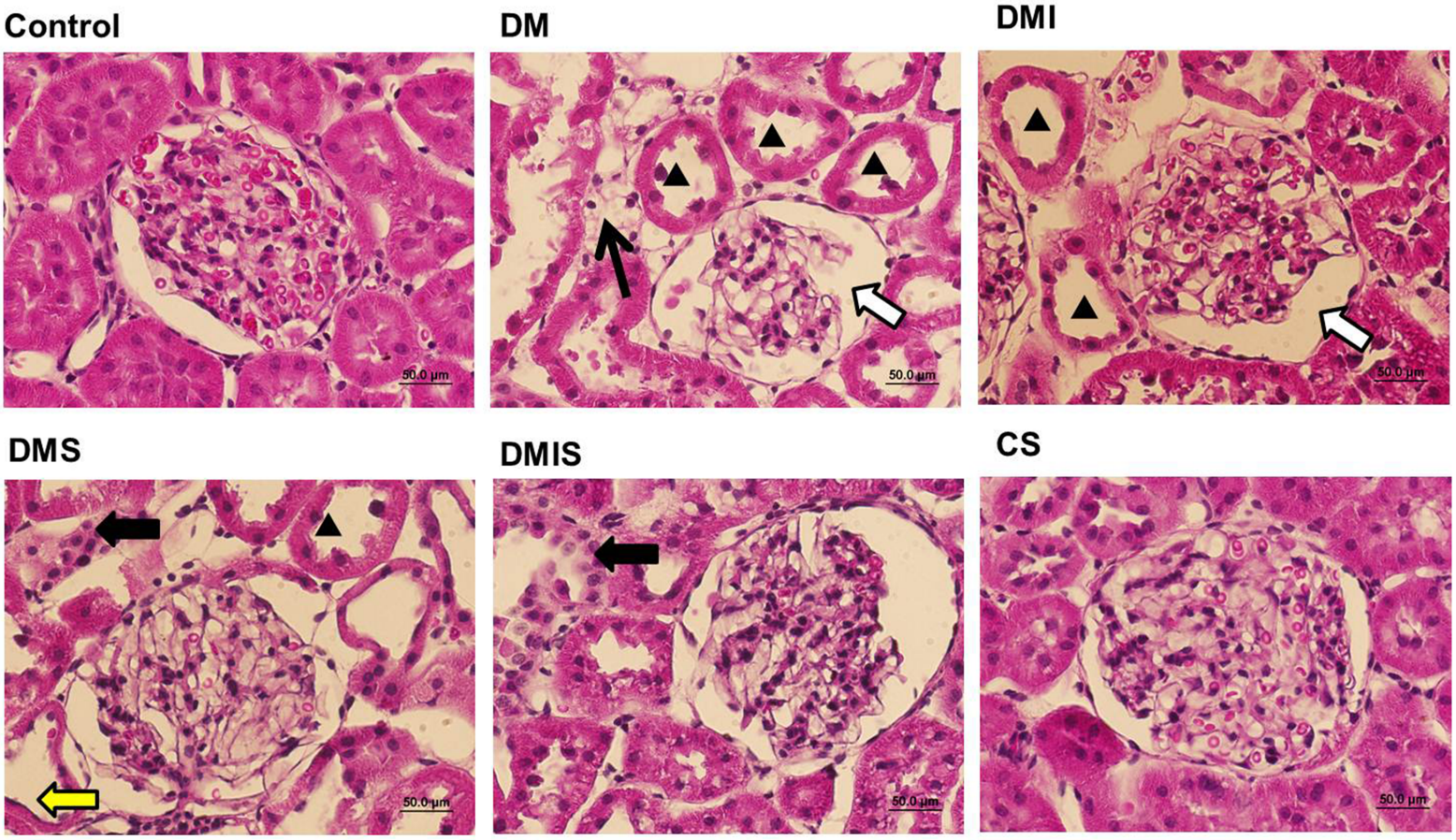
Control
DM
DMI
DMS
DMIS
CS
50.0 μm

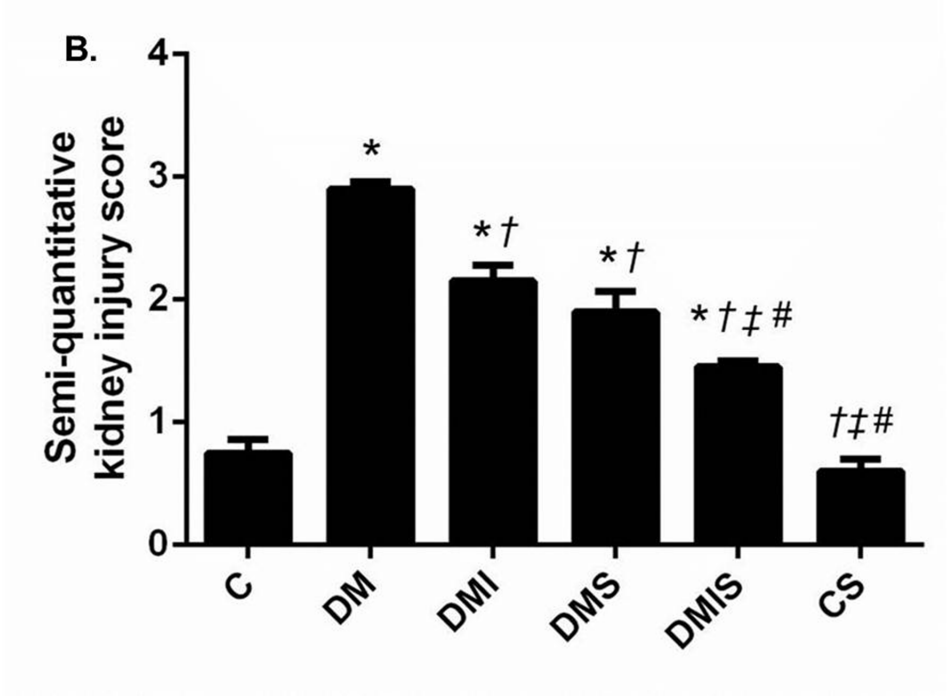
B.
Semi-quantitative kidney injury score
0
1
2
3
4
*
*†
*†
*†‡#
†‡#
C
DM
DMI
DMS
DMIS
CS

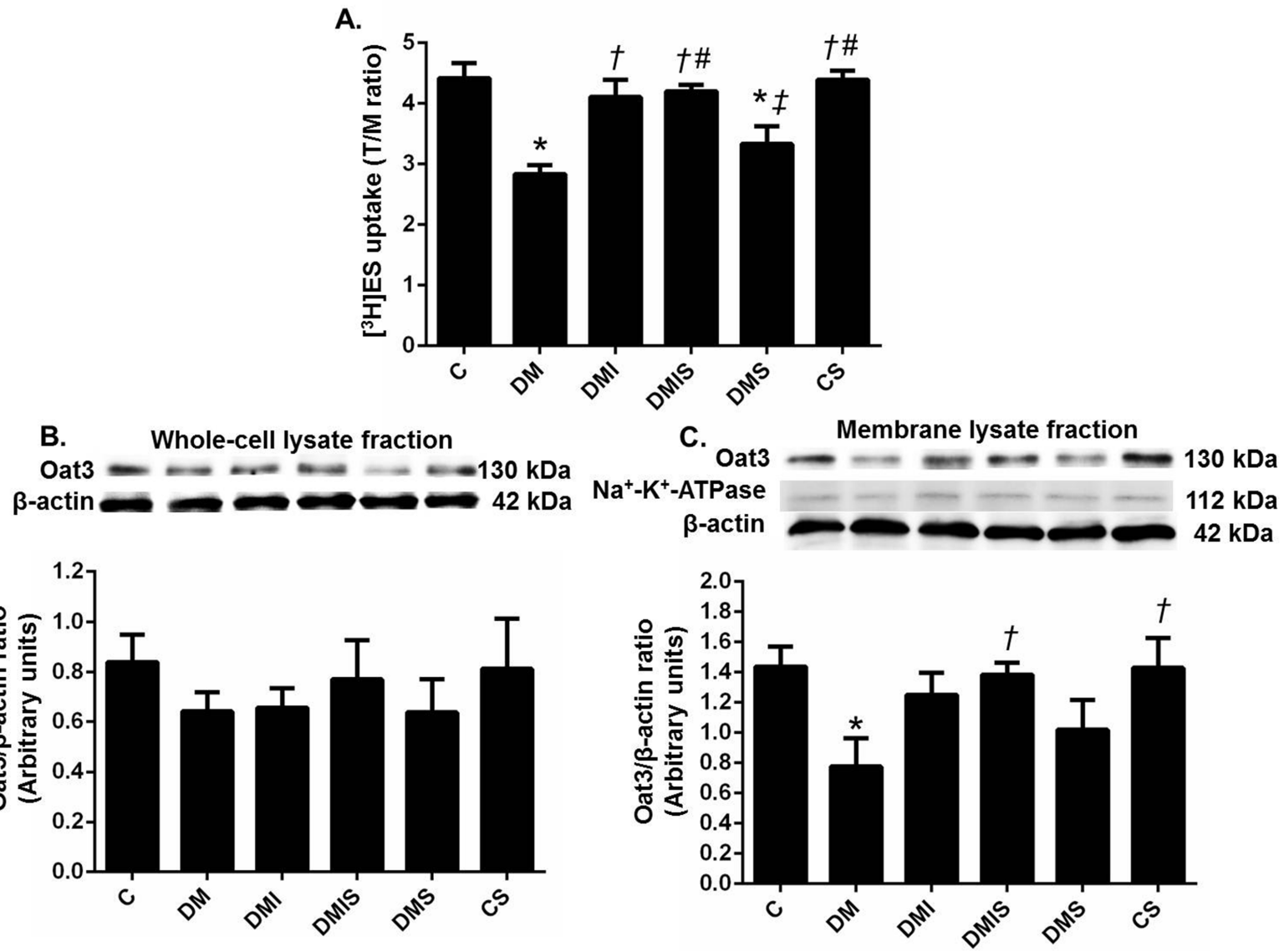
A.
[3H]ES uptake (T/M ratio)
0
1
2
3
4
5
*
†
†#
*‡
†#
C
DM
DMI
DMIS
DMS
CS
B.
Whole-cell lysate fraction
Oat3
β-actin
130 kDa
42 kDa
Oat3/β-actin ratio (Arbitrary units)
0.0
0.2
0.4
0.6
0.8
1.0
1.2
C.
Membrane lysate fraction
Oat3
Na+-K+-ATPase
β-actin
130 kDa
112 kDa
42 kDa
Oat3/β-actin ratio (Arbitrary units)
0.0
0.2
0.4
0.6
0.8
1.0
1.2
1.4
1.6
1.8
2.0
*
†
†

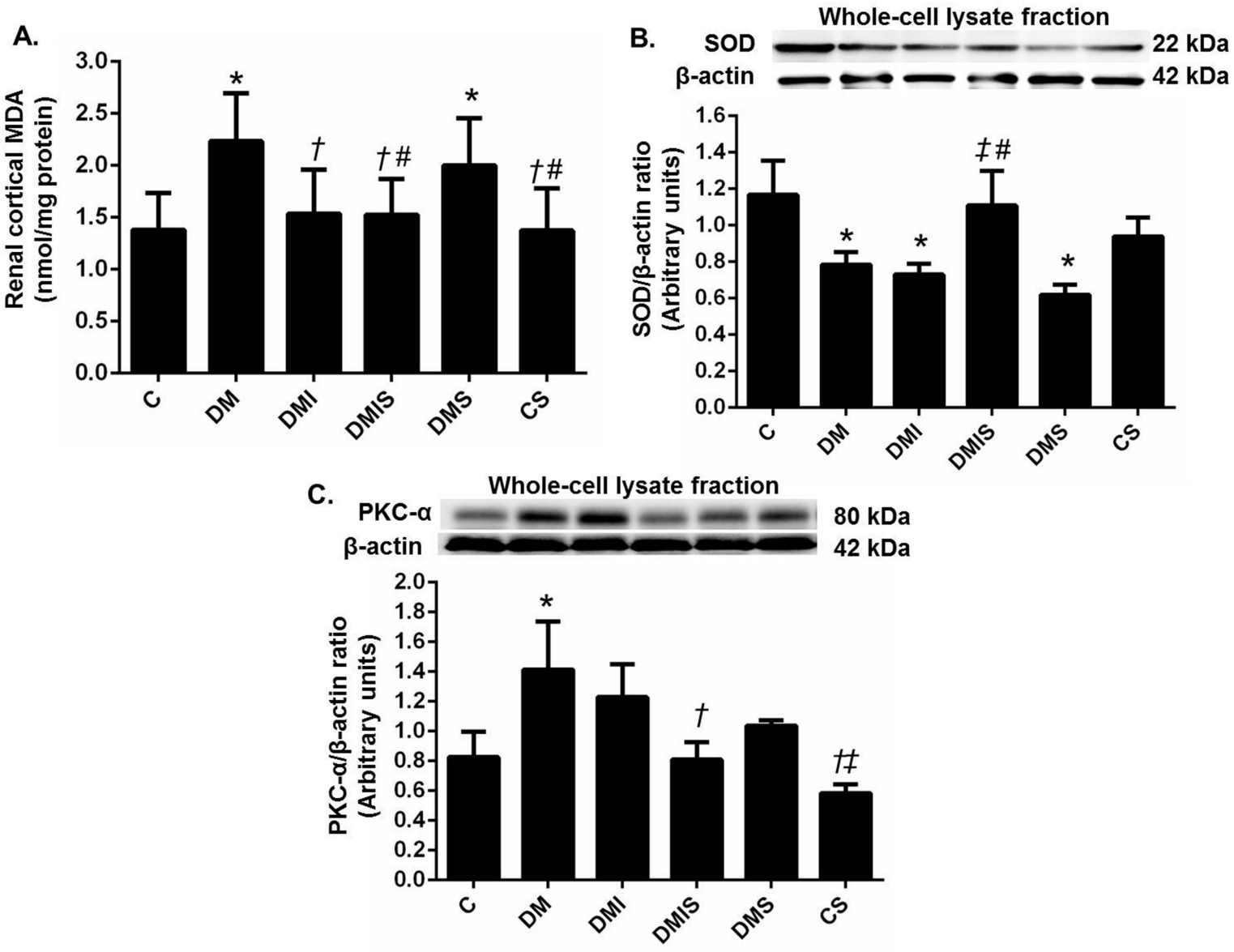
A.
Renal cortical MDA (nmol/mg protein)
3.0
2.5
2.0
1.5
1.0
0.5
0.0
*
*
†
†#
†#
C
DM
DMI
DMIS
DMS
CS
B.
Whole-cell lysate fraction
SOD
β-actin
22 kDa
42 kDa
SOD/β-actin ratio (Arbitrary units)
1.6
1.4
1.2
1.0
0.8
0.6
0.4
0.2
0.0
*
*
*
‡#
C
DM
DMI
DMIS
DMS
CS
C.
Whole-cell lysate fraction
PKC-α
β-actin
80 kDa
42 kDa
PKC-α/β-actin ratio (Arbitrary units)
2.0
1.8
1.6
1.4
1.2
1.0
0.8
0.6
0.4
0.2
0.0
*
†
‡#
C
DM
DMI
DMIS
DMS
CS

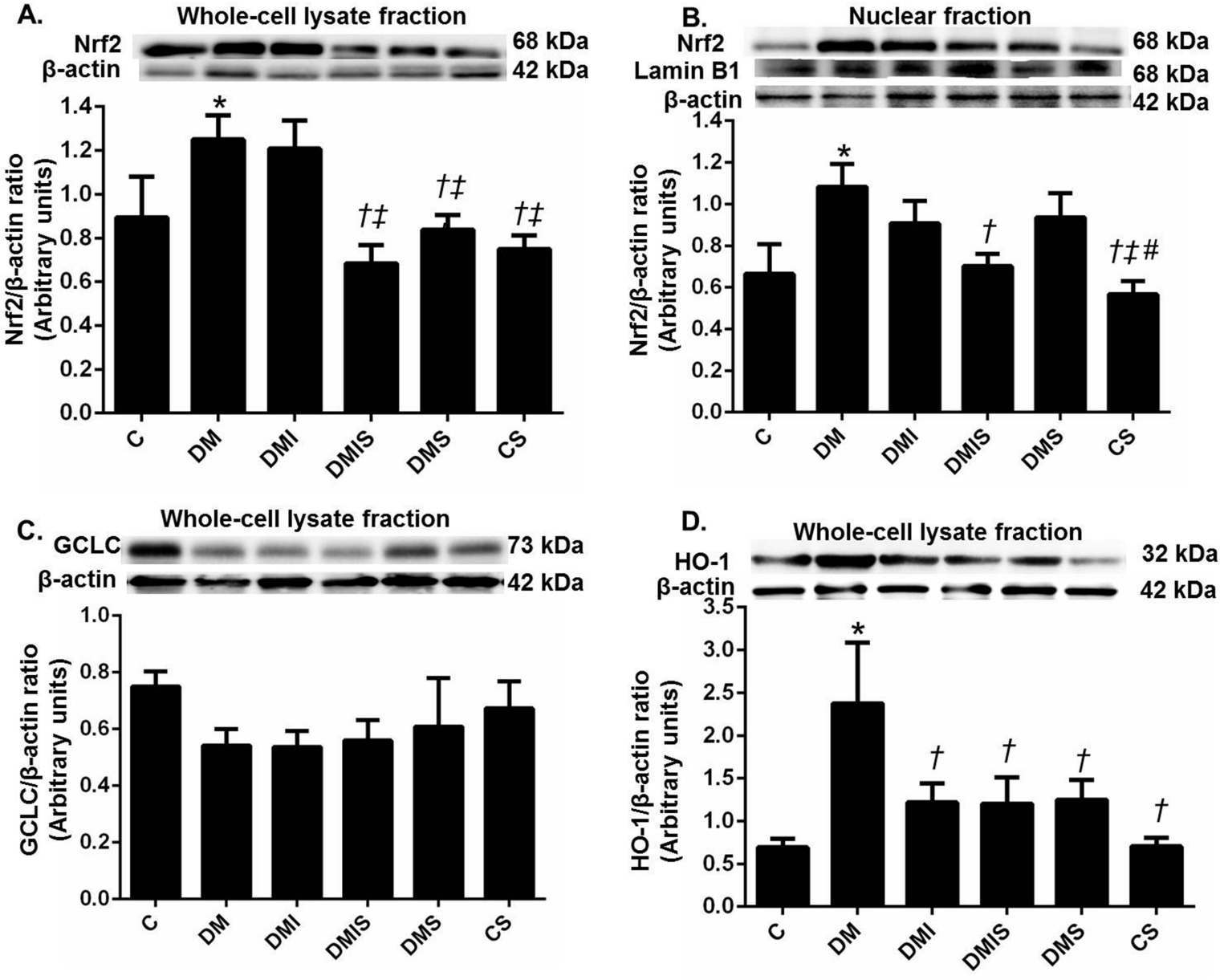
A.
Whole-cell lysate fraction
Nrf2
β-actin
68 kDa
42 kDa
Nrf2/β-actin ratio (Arbitrary units)
1.4
1.2
1.0
0.8
0.6
0.4
0.2
0.0
*
†‡
†‡
†‡
C
DM
DMI
DMIS
DMS
CS
B.
Nuclear fraction
Nrf2
Lamin B1
β-actin
68 kDa
68 kDa
42 kDa
Nrf2/β-actin ratio (Arbitrary units)
1.4
1.2
1.0
0.8
0.6
0.4
0.2
0.0
*
†
†‡#
C
DM
DMI
DMIS
DMS
CS
C.
Whole-cell lysate fraction
GCLC
β-actin
73 kDa
42 kDa
GCLC/β-actin ratio (Arbitrary units)
1.0
0.8
0.6
0.4
0.2
0.0
C
DM
DMI
DMIS
DMS
CS
D.
Whole-cell lysate fraction
HO-1
β-actin
32 kDa
42 kDa
HO-1/β-actin ratio (Arbitrary units)
3.5
3.0
2.5
2.0
1.5
1.0
0.5
0.0
*
†
†
†
†
C
DM
DMI
DMIS
DMS
CS

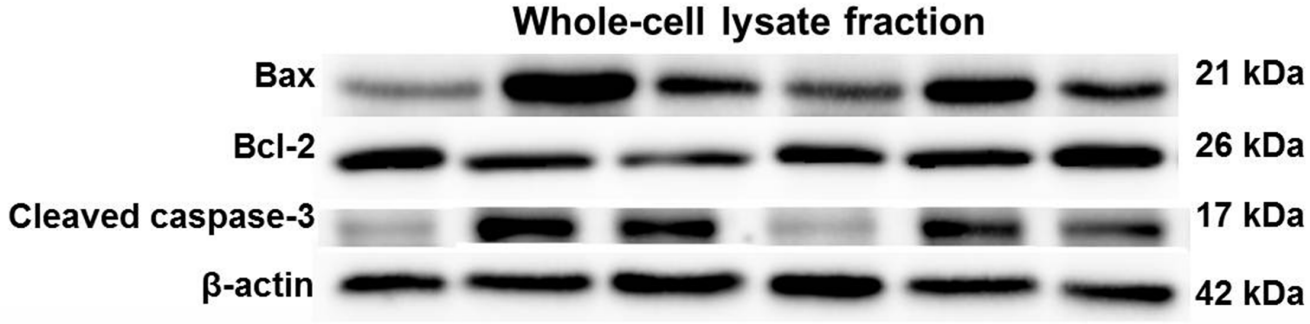
Whole-cell lysate fraction
Bax
Bcl-2
Cleaved caspase-3
β-actin
21 kDa
26 kDa
17 kDa
42 kDa

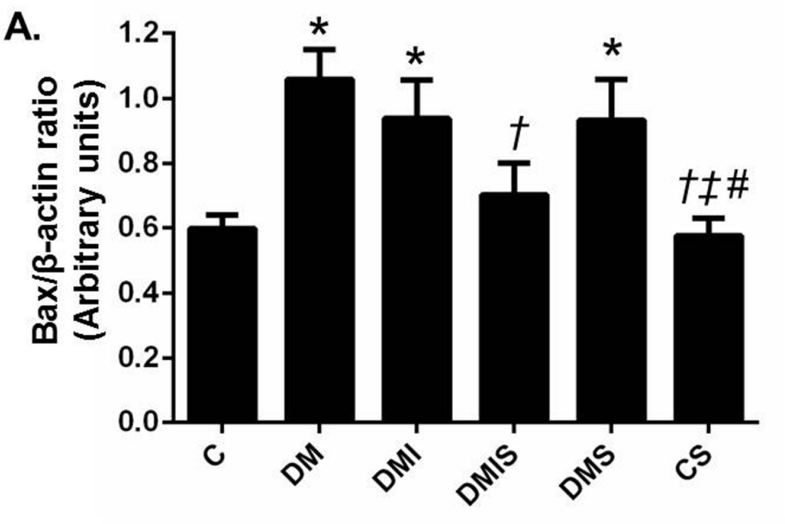
A.
Bax/β-actin ratio
(Arbitrary units)
1.2
1.0
0.8
0.6
0.4
0.2
0.0
*
*
†
*
†‡#
C
DM
DMI
DMIS
DMS
CS

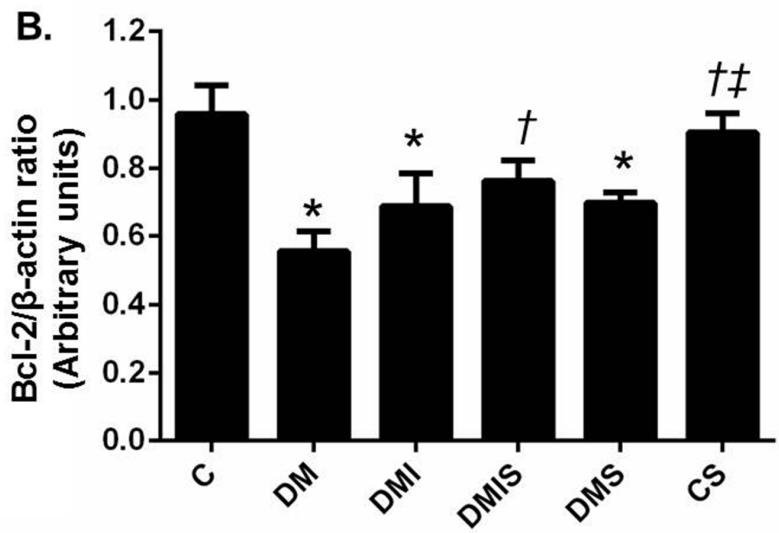
B.
Bcl-2/β-actin ratio
(Arbitrary units)
1.2
1.0
0.8
0.6
0.4
0.2
0.0
*
*
†
*
†‡
C
DM
DMI
DMIS
DMS
CS

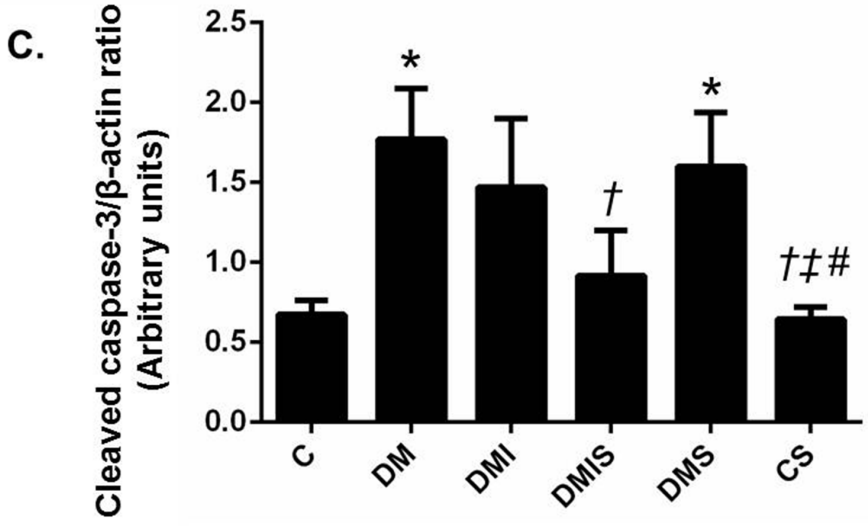
C.
Cleaved caspase-3/β-actin ratio
(Arbitrary units)
2.5
2.0
1.5
1.0
0.5
0.0
*
*
†
†‡#
C
DM
DMI
DMIS
DMS
CS

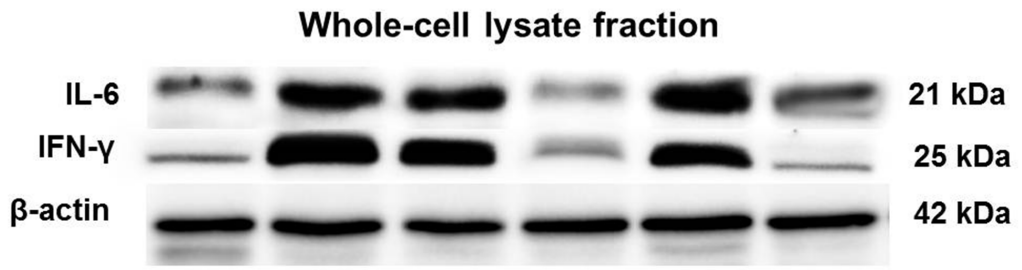
Whole-cell lysate fraction
IL-6
IFN-γ
β-actin
21 kDa
25 kDa
42 kDa

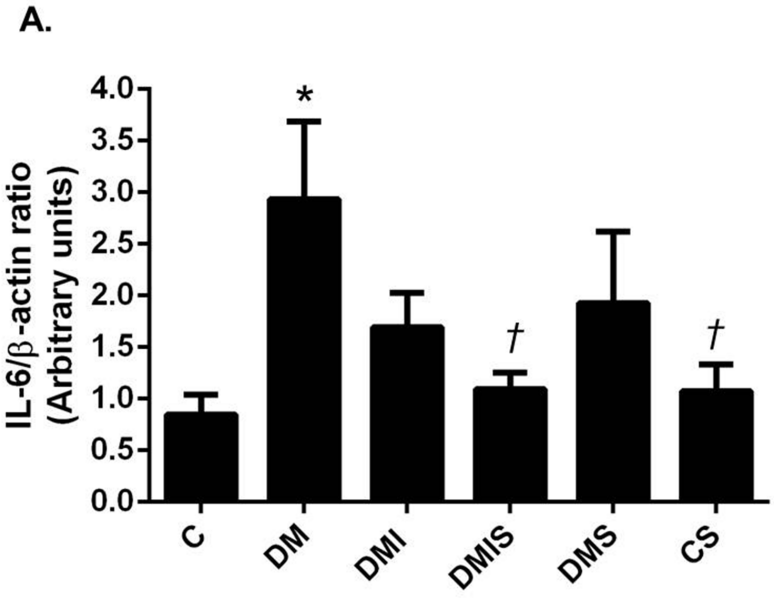
A.
IL-6/β-actin ratio
(Arbitrary units)
4.0
3.5
3.0
2.5
2.0
1.5
1.0
0.5
0.0
*
†
†
C
DM
DMI
DMIS
DMS
CS

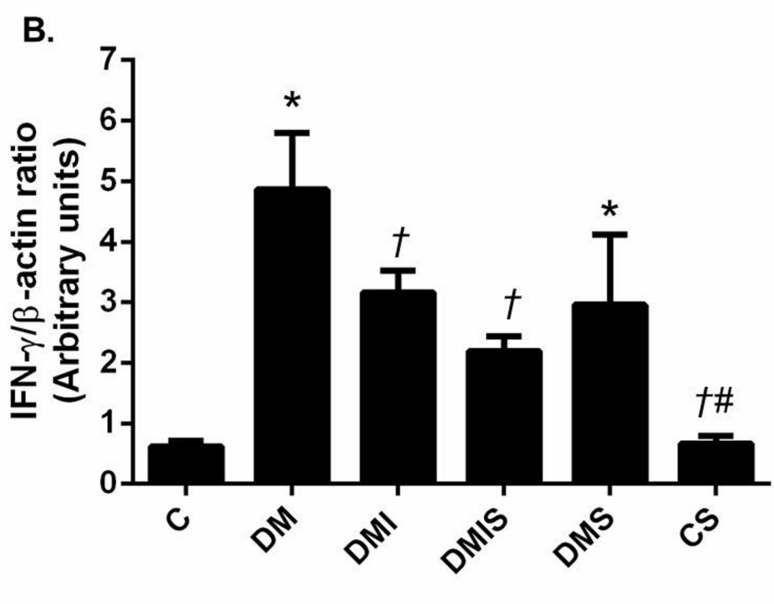
B.
IFN-γ/β-actin ratio
(Arbitrary units)
7
6
5
4
3
2
1
0
*
†
†
*
†#
C
DM
DMI
DMIS
DMS
CS

Role of Gastrointestinal Microbiota on Kidney Injury and the Obese Condition

Keerati Wanchai, MSc, Anchalee Pongchaidecha, PhD, Varanuj Chatsudthipong, PhD, Siriporn C. Chattipakorn, DDS, PhD, Nipon Chattipakorn, MD, PhD and Anusorn Lungkaphin, PhD

ABSTRACT

Obesity is associated with kidney disease, probably due to obesity-mediated inflammation, podocyte injury and oxidative stress in the kidney It is also linked to other diseases, for example, diabetes and hypertension, which are associated with the development and progression of chronic kidney disease. Interestingly, gastrointestinal dysbiosis has been demonstrated in cases of obesity with the development and progression of kidney disease. Thus, modification of gastrointestinal microbiota using probiotics or prebiotics or both to improve the balance of bacterial flora is a potential approach for the management of obesity-associated kidney disease. This review covers information regarding the association between obesity and kidney injury, and it examines evidence for a hypothesized role of gastrointestinal microbiota in this setting. Studies describing the effects of probiotic and prebiotic treatments on kidney disease show mixed results, although several suggest benefits indicated by biomarkers associated with kidney injury, uremia and inflammation. Additional studies are needed to determine whether these interventions are clinically effective in managing kidney injury and kidney disease.

Key Indexing Terms: Obesity; Kidney; Gastrointestinal microbiota; Probiotic; Prebiotic. **[Am J Med Sci 2017;353(1):59–69.]**

INTRODUCTION

Obesity is defined by the World Health Organization as a body mass index (BMI) >30 kg/m^2 and can lead to conditions affecting metabolism such as dyslipidemia, insulin resistance and hypertension. These alterations are components of metabolic syndrome and promote type 2 diabetes and cardiovascular disease. It has also been shown that obesity increases the occurrence of chronic kidney disease (CKD).[1] Previous studies found that serum lipid abnormalities, including reduced high-density lipoprotein cholesterol or high triglyceride levels, significantly increased risk factors for CKD.[2,3] The commonly used measurements for kidney function are estimated glomerular filtration rate (GFR) and urine albumin. A cohort study of more than 300,000 individuals, followed up for between 15 and 35 years, showed that the rate of end-stage renal disease had a strong correlation with the increase in BMI.[4] Increased BMI and waist circumference were also associated with the reduction of GFR and the progression of CKD in a study of non-diabetic participants.[5] These data suggest that obesity may be the initiating factor in the induction of renal injury and contributes to CKD.

An increase in the number and size of adipocytes in obesity can lead to reduced blood flow to adipose tissue, which decreases interstitial oxygen tension in the tissue, eventually causing hypoxia.[6] This event initiates cell death and promotes macrophage infiltration, leading to localized inflammation in the adipose tissue and dysregulation of the production and secretion of adipokines, including leptin and proinflammatory mediators such as tumor necrosis factor α and interleukin 6.[7] These adipokines have been shown to activate overall low-grade systemic inflammation.[8] Previous studies have demonstrated that an increased plasma level of leptin in obesity induces the upregulation of transforming growth factor (TGF-β1) in the kidney and promotes an accumulation of an extracellular matrix. This contributes to glomerular and tubular basement membrane thickening and results in glomerulosclerosis and tubulointerstitial fibrosis.[9] Obesity-associated glomerulosclerosis could be supported by the hypertrophy of podocytes. Podocyte hypertrophy has been shown as an accommodation response to the enlargement of the glomerulus in rats fed *ad libitum*. This change could cause the development of podocyte stress, podocyte loss and glomerulosclerosis.[10] In addition, an elevation of plasma free fatty acids leads to increased fatty acid beta oxidation, triglyceride synthesis and endoplasmic reticulum stress, all of which could cause podocyte death.[11] Proinflammatory cytokines released during obesity also impair insulin signaling pathways, leading to insulin resistance.[12] Furthermore, hyperinsulinemia, a consequence of diabetic nephropathy, induces the production of an insulin-like growth factor 1 that stimulates the activity of connective tissue growth factor, resulting in chronic tubulointerstitial fibrosis.[13] It has been reported that high glucose levels promote kidney fibrosis by the stimulation of NADPH Oxidase 4-induced TGF-β1 production.[14] As insulin has a role in anti-inflammation, systemic insulin resistance in obesity can induce kidney inflammation and can increase oxidative stress, leading to deterioration of kidney function.[15,16]

Metabolic and inflammatory changes occurring in obesity also activate the sympathetic nervous system.[17] Increased sympathetic activity activates renin release from the juxtaglomerular apparatus, which subsequently

enhances angiotensin II (AngII) production, leading to the activation of the renin-angiotensin system (RAS). This occurrence is supported by the finding that RAS overactivation has been shown in cases of obesity.[18] Overproduction of AngII could lead to high blood pressure in obesity by increasing tubular sodium reabsorption and sodium retention. In addition, sodium delivery to macula densa cells could be reduced, promoting a compensatory or feedback mechanism that increases renal blood flow through vasodilation and finally leads to an increase in GFR.[19] High blood flow to the glomeruli and high blood pressure in the glomeruli would cause glomerular hypertrophy and bring changes in the fibrotic pathway, ultimately presenting as glomerulosclerosis.[20] AngII also promotes the progression of kidney injury by increased renal cell hypertrophy, causing microvascular injury and tubulointerstitial damage, increased reactive oxygen species production and induced inflammation and apoptosis.[21,22] Recent studies in daunorubicin-induced nephrotoxicity in rats have shown that RAS activation, indicated by increased AngII type 1 receptor expression, promoted renal inflammation and oxidative and endoplasmic reticulum stress by induction of the extracellular signal–regulated kinases 1 and 2 (ERK1 and 2)-induced endothelin 1-endothelin receptor type A-nuclear factor -kappa-B p65 (ET1-ETAR-NF-kBp65) signaling pathway.[23] In the obese KKAy mouse, a model of type 2 diabetes, the AngII type 1 receptor blocker, olmesartan, has been shown to lead to a reduction in proinflammatory cytokines such as plasminogen activator inhibitor 1, monocyte chemoattractant protein 1 and oxidative stress markers.[24]

Interestingly, a study in animal models reported that a high-fat diet could modulate the composition of intestinal bacteria, leading to microbiota dysbiosis and could also induce inflammation and oxidative stress in obesity.[25] Moreover, the progression of kidney injury and dysfunction in obesity may potentiate the disruption of intestinal microbiota. This microbiota has an influence on host metabolism and the maintenance of gastrointestinal homeostasis that can protect against systemic inflammation. Therefore, modulation of intestinal bacteria may be an effective targeted therapy for inflammation and oxidative stress–induced kidney injury and dysfunction in obesity. This review focuses on the association between the alteration of gastrointestinal microbiota in cases of obesity and kidney injury. In addition, the effects and possible underlying mechanisms of prebiotics and probiotics on kidney injury and dysfunction in obesity-related conditions are discussed. The findings available from clinical research and the relevant evidence from animal studies are comprehensively summarized and discussed.

GASTROINTESTINAL MICROBIOTA AND OBESITY

The human gastrointestinal tract (GI tract) consists of approximately 10^{13}–10^{14} bacteria of up to 2,000 different species.[26] Four bacteria phyla that dominate the adult GI tract include Firmicutes, Bacteroidetes, Actinobacteria and Proteobacteria.[27] The intestinal bacteria promote normal physiological conditions in the human body including energy balance and glucose metabolism. They also produce vitamins and help to ferment some food components that are not digested by the host.[26,28]

To date, it has been reported that changes in microbiota composition of the GI tract are involved in the development of obesity and associated conditions such as insulin resistance.[29,30] A previous study found that obesity and consumption of a high-fat diet modulated the gastrointestinal microbiota by decreasing the abundance of *Bacteroidetes* species and increasing *Firmicutes* species.[29] *Lactobacilli* species were found to decrease in the distal esophagus of rats fed on a high-fat diet.[31] This modulation of bacteria induced metabolic changes in the host, such as increased fatty acid oxidation, triglyceride storage and alteration of short-chain fatty acid proportions, subsequently promoting a high risk of developing the disease.[32,33] In addition to diet, antibiotics also affect the composition of gastrointestinal microbiota and obesity. One study demonstrated that administration of antibiotics in children is associated with increased risk of obesity.[34] In addition, a study in obese prediabetic subjects showed that antibiotics reduced Firmicutes associated with altered short-chain fatty acid metabolism and increased gene expression of the oxidative stress pathway in adipose tissue.[35]

Gastrointestinal bacteria also play an important role in regulating intestinal epithelial homeostasis. They maintain the gastrointestinal barrier by restoring tight-junction protein structure that can suppress intestinal inflammation.[36-38] The impairment of the gastrointestinal barrier by dysbiosis leads to the release of endotoxins such as lipopolysaccharides (LPS), constituents of the outer membrane of gram-negative bacteria cell walls, through the gastrointestinal barrier into the circulatory system.[39] An increased level of LPS in the circulation is called metabolic endotoxemia. It has been reported that plasma LPS is an important factor for the early development of insulin resistance and obesity in an animal study.[40] LPS circulates in the plasma to various organs and activates the immune system in those organs stimulating them to secrete numerous proinflammatory cytokines, leading to an induction of a low-grade systemic inflammatory response.[41] Previous studies have shown that a high-fat diet impaired intestinal permeability and reduced intestinal tight-junction protein expression, leading to an increased LPS level both in the intestinal lumen and plasma, and it also induced inflammation and oxidative stress.[39,42] These data demonstrate that gastrointestinal microbiota disruption in obesity might be a causative factor inducing the inflammation that affects the progression of the disease.

THE RELATIONSHIP OF OBESITY, GASTROINTESTINAL MICROBIOTA AND KIDNEY INJURY

The data cited above suggest that gastrointestinal dysbiosis due to a high-fat diet induces impairment of the barrier of the GI tract leading to metabolic endotoxemia and initiation of systemic inflammation and insulin resistance. These alterations could ultimately promote damage in various organs such as the kidney. It has been reported that LPS could circulate to the kidney, induce inflammation, stimulate oxidative stress pathways and promote kidney injury.[43] The kidney injury and dysfunction found in obesity may lead to the accumulation of toxic metabolites such as urea in the circulation, which then pass into the gastrointestinal lumen. Urea may subsequently be converted to ammonia by urease-processing bacteria, resulting in a high alkaline pH environment in the GI tract, which can promote the growth of proteolytic bacteria and favor dysbiosis.[44] Protein fermentation by proteolytic bacteria leads to the production of waste metabolites, uremic toxins such as indoxyl sulfate and p-cresyl sulfate (PCS).[45] Under normal conditions, these GI tract–derived uremic toxins are removed by renal tubular secretion through organic anion transporters (OAT) especially OAT1 and OAT3, occurring in the proximal tubular cells.[46]

Increased uremic toxin levels are usually observed in the plasma of uremic patients. As these uremic toxins are the metabolites of protein digestion, their levels also depend on the absorption or in the intake of protein in the diet, or on both. Brunori et al[47] reported that a very low-protein diet was effective for postponing dialysis in elderly patients. However, not all the patients with decreased GFR had uremic symptoms. These data suggest that dietary protein intake may be a factor for this critical difference. Although the benefits of dietary protein restriction in patients with CKD have been reported,[48] one study showed that the progression of kidney failure cannot be delayed by a long-term administration of a very low-protein diet.[49]

The correlating effects of obesity and gastrointestinal dysbiosis can affect kidney function by the induction of systemic inflammation. Moreover, kidney injury and dysfunction in obesity may potentiate the severity of this dysbiosis and increase uremic toxin levels, promoting the progression of kidney injury. Therefore, modulation of the intestinal bacteria by selectively increasing or decreasing bacterial composition in the colon, or doing both, including the use of probiotics and prebiotics, may be a targeted therapy for reducing inflammation-induced kidney injury and dysfunction in obesity.

THE EFFECT OF PROBIOTICS IN CLINICAL AND ANIMAL STUDIES OF KIDNEY INJURY AND DYSFUNCTION

The modulation of intestinal bacterial composition by the intake of live microorganisms, known as probiotics, is one of the methods used in attenuating organ injury and dysfunction induced by gastrointestinal dysbiosis. The most common live bacteria used include *Lactobacilli, Streptococci* and *Bifidobacteria*.[50] Previous studies showed that probiotics could prevent renal injury in both clinical and animal studies. The effects of probiotics on kidney disease in clinical studies are presented in Table 1. Two clinical trials evaluating CKD stage 3, with 4 patients treated with *Streptococcus thermophiles*, *Lactobacillus acidophilus* and *Bifidobacteria longum*, demonstrated improved quality of life.[51,52] The decrease in blood urea nitrogen might be because of the effect of the species specificity of probiotics on urea metabolism. Inconsistent findings in the reduction of serum uric acid from these 2 studies that use the same strain of probiotics might be due in part to the differences in food intake of the patients studied. Interestingly, the management of patients with CKD who are undergoing peritoneal dialysis (PD) may also affect the composition of gastrointestinal microbiota, and attenuation of inflammation has been reported to be affected by probiotics in patients undergoing PD. This study showed that the levels of serum endotoxin and proinflammatory cytokines (tumor necrosis factor and interleukin 6) were decreased while the anti-inflammatory cytokine was increased after 6 months of probiotic treatment.[53] These results are associated with preserved kidney function in these patients. However, the evaluation of the microbiotic composition in the patients undergoing PD should be confirmed. In contrast, in another study, treatment with probiotics failed to improve the inflammation in patients undergoing dialysis for end-stage renal disease.[54] This might depend on the severity of the kidney dysfunction and species specificity of the probiotics used.

Table 2 presents the effect of probiotics in animal studies on kidney injury and dysfunction. Treatment with *L plantarum* has been shown to decrease body weight and improve plasma lipid profile in rats with obesity induced by a high-fat diet by decreasing the expression of genes involved in obesity and the inhibition of enzymes involved in the production of cholesterol. These results were accompanied by the attenuation of systemic inflammation and the reduction of kidney injury.[55] The results imply that probiotics potentially have the effect of attenuating obesity-induced systemic inflammation. A study in rats with diabetes induced by streptozotocin and treated with kefir, a beverage of fermented milk containing *L lactis* subspecies, *Leuconostoc* species, *S thermophilus* and *Lactobacillus* species, demonstrated an improvement in their diabetic condition and significantly reduced oxidative stress–induced renal injury; however, serum creatinine and the kidney dysfunction represented by proteinuria was not improved.[56] In addition, increased levels of serum creatinine were improved in type 2 diabetic rats treated with *L plantarum*.[57] The difference in the severity of the diabetic condition and the bacterial species used may

TABLE 1. Effects of probiotics in clinical studies of kidney disease.

Type of study (n)	Kidney injury model	Probiotic species, Dose, Route, Duration	Kidney parameter			Inflammation	Other findings	Interpretation	Reference
			BUN	Serum creatinine	Uric acid				
• A prospective, randomized, double-blind, crossover, placebo-controlled trial (13)	• CKD (stage 3 and 4)	• *S thermophilus* KB27, *L acidophilus* KB31 and *B longum* KB35, 90 billion CFU/day, Oral, 6 months	↓	↔	↓	-	• improved quality of life	• Probiotics may improve kidney function.	51
• A prospective, randomized, double-blind, crossover, placebo-controlled trial (46)	• CKD (stage 3 and 4)	• *S thermophilus, L acidophilus* and *B longum*, 90 billion CFUs/day, Oral, 6 months	↓	↔	↔	-	• improved quality of life	• Probiotics may have an effect to improve kidney function.	52
• A randomised, double-blind, placebo-controlled trial (39)	• Peritoneal dialysis (PD) patients	• *Bifobacterium bifidum* A218, *Bifidobacterium catenulatum* A302, *Bifidobacterium longum* A101, *Lactobacillus plantarum* A87, 10^9 CFUs/day, Oral, 6 months	-	-	-	• ↓Serum TNF-α, IL-5, IL-6, and endotoxin • ↑ IL-10	-	• Probiotics attenuated systemic inflammation in PD patients.	53
• Randomized, double-blind, placebo-controlled crossover study (22)	• ESRD dialysis patients	• *S thermophilus* KB 19, *L acidophilus* KB 27 and *B longum* KB 31, 180 billion CFU/day, Oral, 6 months	-	-	-	• ↔ WBC count • ↔ CRP level	• ↔ total indoxyl glucoronide	• Probiotics have no effect on inflammation in ESRD.	54

BUN, blood urea nitrogen; CFU, colony-forming unit; CKD, chronic kidney disease; CRP, C-reactive protein; ESRD, end-stage renal disease; IL-5, interleukin 5; IL-6, interleukin 6; IL-10, interleukin 10; TNF-α, tumor necrosis factor alpha; WBC, white blood cell.

TABLE 2. Effects of probiotics on kidney injury and dysfunction in animal studies.

Animal	Kidney injury model	Probiotic species, Dose, Route, Duration	Kidney parameter		Kidney injury	Inflammation	Oxidative stress	Other findings	Interpretation	Reference
			BUN	Serum creatinine						
• Wistar rat	• HFD-induced obesity • 2% cholesterol fat /kg diet for 6 weeks	• *Lactobacillus plantarum* TN8, 1x10^9 cells/day, drinking water, 30 days	↓ (serum urea)	↓	• ↓ capsular space shrinkage • ↓ glomerular hypertrophy	• ↓ IL-12, IFN-gamma, and TNF-α (released by PBMC) • ↑ IL-10	-	• ↓ body weight • ↓ total cholesterol • ↓ plasma TG	• Probiotics attenuated systemic inflammation and kidney injury.	55
• Wistar rat	• T1DM • 45 mg/kg BW STZ for 3 days	• *Lactococcus lactis* subspecies, *Leuconostoc* species, *Streptococcus termophilus* and *Lactobacillus* species, 1x10^{10} CFU in 1.8 ml/day of fermented milk (Kefir), oral gavage, 8 weeks	↓	-	-	-	• ↓ kidney TBARS • ↓ kidney superoxide anion • ↓ kidney NO level	• ↑ urinary urea • ↔ proteinuria • ↓ diuresis • ↓ water and chow intake • ↓ blood glucose • ↓ glucose intolerance • ↓ kidney glycogen storage	• Probiotics improved glycemic control, renal injury, and decreased kidney oxidative stress.	56
• Wistar rat	• T2DM • 2.5% cholesterol + STZ 30 mg/kg BW for 8 weeks	• *Lactobacillus. Plantarum* NCU116, 1x10^9 CFU/ml/day, oral gavage, 5 weeks	↓	↓	-	-	-	• ↓ uric acid • improved diabetic condition	• Probiotics improved kidney injury and the diabetic condition.	57
• Spontaneous hypertensive rat (Wistar Kyoto rat)	• CKD • 5/6 Nephrectomy for 12 weeks	• *Lactobacillus acidophilus* NT, 1 ×10^{10} CFU/kg/day, 12 weeks	↓	↔	• ↓ glomerulosclerosis	• ↓ Systemic IL-6, LPS, and CRP	-	• ↓ urinary protein • ↓ Uremic toxins (IS, PCS, and IAA) • ↑ Gut epithelial tight-junction protein (Occuldin and ZO-1) • ↑ Gastrointestinal permeability • ↑ TL2 expression	• Probiotics slowed the progression of CKD and decreased systemic inflammation.	58
• Wistar rat	• Uremia • 500 mg/kg BW/day acetaminophen for 7 days	• *Sporosarcina pasteurii*, 1x10^9 cells/day, food ball, 5 weeks	↓	↓	-	-	• ↓ blood and kidney MDA • ↑ blood and kidney SOD, CAT, GPT, and GOT activity	• ↑ body weight • ↑ Hb level and RBC count	• Probiotics attenuated kidney injury and decreased oxidative stress.	59

(continued on next page)

Table 2. *(continued)*

Animal	Kidney injury model	Probiotic species, Dose, Route, Duration	Kidney parameter		Kidney injury	Inflammation	Oxidative stress	Other findings	Interpretation	Reference
			BUN	Serum creatinine						
• Wistar rat	• Uremia • 500 mg/kg BW/day acetaminophen for 5 days	• *Lactobacillus fermentum* (MTCC 903), *Lactobacillus plantarum* (MTCC 4462) and *Lactobacillus rhamnosus* (MTCC 1408), $1x10^9$ CFU/ml/100g BW/day, oral gavage, 15 days	↓	↓	-	-	• ↓ blood and kidney MDA • ↑ blood and kidney CAT and SOD	• ↓ kidney necrosis	• Probiotics attenuated kidney injury and decreased oxidative stress.	60
• Wistar rat	• Oxidative stress • 10 mg/kg BW chromium(VI), single dose	• *Lactobacillus casei* strain 17, $1x10^9$ CFU/day, 14 days	↓	↓	• Vacuole degeneration	-	• ↓ TBARS and protein carbonyls • ↑ Kidney SOD and GSH	• ↑ body weight	• Probiotics decreased kidney injury and kidney oxidative stress.	61
• Wistar rat (pregnant)	• Nephrotoxicity • 4 mg/kg BW endosulfan by gavage from the 6th to 20th day of gestation	• *Lactobacillusplantarum* BJ0021, 0.1 ml one hour before the administration of endosulfan, oral gavage, 20 days	↓ (serum urea)	↔	-	-	• ↓ kidney MDA • ↔ CAT and SOD activity	• ↑ urinary urea • ↓ kidney apoptotic nucleus	• Probiotics restored kidney injury, reduced kidney oxidative stress, and apoptosis.	62
• Sprague-Dawley rat	• Unhypertensive and nephrotoxicity in rat • salt diet for 4 weeks	• Lactic acid bacteria in fermented Kefir milk, 10% w/v Kefir, drinking water, 4 weeks	-	-	• partial prevention in kidney morphology	-	-	• ↑ creatinine clearance • ↓ kidney apoptosis	• Probiotics improved kidney function and decreased kidney apoptosis.	63

BUN, blood urea nitrogen; BW, body weight; CAT, catalase; CFU, colony-forming unit; CKD, chronic kidney disease; CRP, C-reactive protein; GOT, glutamic oxaloacetic transaminase; GPT, glutamic pyruvate transaminase; GSH, glutathione; HFD, high-fat diet; IAA, indole acetic acid; IFN-gamma, interferon gamma; IL-2, interleukin 2; IL-6, interleukin 6; IL-10, interleukin 10; LPS, lipopolysaccharide; MDA, malondialdehyde; NO, nitric oxide; PBMC, peripheral blood mononuclear cell; SOD, superoxide dismutase; STZ, streptozotocin; T1DM, type 1 diabetes mellitus; T2DM, type 2 diabetes mellitus; TBARS, thiobarbituric acid reactive substances; TG, triglyceride; TL2, toll-like receptor 2; TNF-α, tumor necrosis factor alpha.

TABLE 3. Effects of prebiotics in clinical studies of kidney disease.

Type of study (*n*)	Kidney injury model	Prebiotic, Dose, Route, Duration	Kidney parameter		Other findings	Interpretation	Reference
			BUN	Serum creatinine			
A single center, nonrandomized, open-label phase I/II study (22)	CKD	Oligofructose-enriched inulin, 10 g/day at first week and escalated to 10 g twice a day for 4 weeks	↓	↔	↓Serum PCS	Prebiotics may have an effect to improve kidney function in patients with CKD	70
					↔Serum IS		

BUN, blood urea nitrogen; CKD, chronic kidney disease; IS, indoxyl sulfate; PCS, p-cresol sulfate.

give different results regarding these parameters. However, decreased serum creatinine after probiotic treatment might be caused by decreased production in muscle tissue that might not be related to kidney function. These results imply that probiotics may have an antidiabetic effect that subsequently improves oxidative stress and attenuates injury of the kidney in this condition. Recently, a study has shown that spontaneous hypertensive 5/6 nephrectomized rats (a typical model for CKD) treated with *L acidophilus* showed an improved gastrointestinal tight-junction barrier, decreased systemic inflammation and uremic toxin accumulation. These improvements were accompanied by attenuation in kidney injury.[58] Treatment with different bacterial species decreased lipid peroxidation and enhanced antioxidant enzymes such as superoxide dismutase, and catalase in rats with uremia induced by acetaminophen, and in rats with chromium-induced oxidative stress.[59-61] Moreover, reduced oxidative stress was associated with decreased kidney necrosis.[60] Treatment with *L plantarum* had no effect on antioxidant enzyme activities in rats with nephrotoxicity induced by endosulfan.[62] However, decreased renal lipid oxidation may account for partial improvement of kidney injury and decreased kidney apoptosis. In another study, treatment with lactic acid bacteria in nonhypertensive and nephrotoxic rats was shown to attenuate kidney dysfunction, partially prevent kidney injury and reduce renal apoptosis.[63]

These findings may indicate that probiotic supplements could reverse gastrointestinal dysbiosis and reduce uremic toxin production. In CKD, the concentrations of uremic solutes are increased during the progression of disease. The reduced uremic toxin levels and the upregulation of tight-junction protein expression in the barrier of the GI tract by probiotics leads to decreased translocation of toxins such as LPS to the circulation, and therefore, reduced systemic inflammation may be a possible mechanism that can attenuate kidney injury and dysfunction.

However, not all studies have shown positive results from studies regarding the effect of probiotics. *L casei* 431 treatment had no effect on the immune response to influenza vaccination in healthy adults,[64] and women with gestational diabetes mellitus also did not show positive effects for the probiotic, *L salivarius* UCC118, on glycemic control.[65] A study in overweight and obese women consuming probiotic yogurt during a weight loss program has shown that there was no effect on weight loss after 12 weeks of probiotic consumption, but there may have been a positive effect on lipid profile and insulin sensitivity.[66] Moreover, the administration of probiotics (*L acidophilus La5*, *Bifidobacterium lactis Bb-12*, *S thermophilus* and *L bulgaricus*) combined with prebiotics (oligofructose) for 2 weeks to preoperative patients had no effect on bacterial translocation, gastrointestinal barrier function and systemic inflammation.[67]

In conclusion, probiotics may have a protective effect on kidney injury and dysfunction by partially attenuating inflammation, oxidative stress and apoptosis. However, negative data have also been reported. Therefore, more experimental and clinical data are needed to support these proposed mechanisms. The inconsistency of some results might be because of the difference between bacterial species or the patient population or animal models used in the studies. However, the concept that obesity could alter the intestinal environment through bacterial composition might be considered as a cause of kidney injury. Modulation of intestinal bacterial composition by using probiotics may be a good choice for improving kidney function in cases of obesity.

THE EFFECT OF PREBIOTICS IN CLINICAL AND ANIMAL STUDIES OF KIDNEY INJURY AND DYSFUNCTION

Prebiotics are referred to as nondigestible food ingredients that exert positive effects on the health of the host. They provide nutrients enabling the growth and activity of bacteria in the colon.[68] Prebiotics include inulin, fructo-oligosaccharides, xylo-oligosaccharide (XOS), pyodextrins and soya-oligosaccharide. A recent study found that XOS supplementation increased the population of the *Lactobacillus* genus and promoted intestinal health in chickens.[69] This result suggested that prebiotics could modulate the composition of intestinal

TABLE 4. Effects of prebiotics on kidney injury and dysfunction in animal studies.

Animal	Kidney injury model	Prebiotic, Dose, Route, Duration	Kidney parameter			Kidney injury	Inflammation	Oxidative stress	Other findings	Interpretation	Reference
			Serum urea	Serum creatinine	Urinary protein						
Wistar rat	• T1DM • 40 mg/kg BW STZ for 1 week	• FOS and XOS, 10%, added to diet, 6 weeks	↓	↓	↓	• ↓ renal AGE • ↓ glomerulosclerosis • ↓ tubular lesion	-	-	• ↓ kidney weight • ↑ body weight • ↓ blood glucose	• Prebiotics improved diabetic condition and decreased kidney dysfunction.	71
Sprague-Dawley rat	• CKD • 5/6 Nephrectomy for 1 week	• GOS, 5%, added to diet, 2 weeks	↔ (BUN)	↔	-	• ↓ tubulointerstitial injury	• ↓ kidney macrophage	-	• ↓ ER stress • ↓ apoptosis • ↓ serum IS • ↓ cecal indole	• Prebiotics restored kidney injury, reduced kidney inflammation, uremic toxin, kidney ER stress, and apoptosis. No effect on kidney function.	72
Sprague-Dawley rat	• Chronic interstitial nephropathy • 0.7% adenine for 2 weeks	• High amylose maize resistant starch type, 59%, added to diet, 3 weeks	↔	↓	↓	• ↓ kidney fibrotic pathway (TGF-β1, PAI-1, α-SM actin)	• ↓ NF-kBp65 • ↓ MCP-1	• ↓ ROS generating molecules (iNOS, COX1, COX2, and NOX4) • ↓ nitrotyrosine • ↑ Nrf2 • ↑ anti-oxidant enzyme (HO1, SOD, catalase, and GPX)	• ↓ urine volume • ↑ creatinine clearance • ↑ urine specific gravity • ↑ colonic epithelial tight-junction protein (occludin and claudin-1)	• Prebiotics decreased kidney dysfunction, reduced kidney inflammation, oxidative stress, and improved colonic epithelial barrier.	73

α-SM, alpha smooth muscle; BUN, blood urea nitrogen; BW, body weight; CKD, chronic kidney disease; COX1, cyclooxygenase 1; COX2, cyclooxygenase 2; ER, endoplasmic reticulum; FOS, fructo-oligosaccharidel; GOS, galacto-oligosaccharide; GPX, glutathione peroxidase; HO1, heme oxygenase 1; iNOS, inducible nitric oxide synthase; IS, indoxyl sulfate; MCP-1, monocyte chemoattractant protein 1; NF-κBp65, nuclear factor kappa-light-chain-enhancer of activated B cells; NOX4, NADPH oxidase 4; Nrf2, nuclear factor erythroid 2–related factor 2; PAI-1, plasminogen activator inhibitor 1; ROS, reactive oxygen species; SOD, superoxide dismutase; STZ, streptozotocin; T1DM, type 1 diabetes mellitus; TGF-β1, transforming growth factor beta 1; XOS, xylo-oligosaccharide.

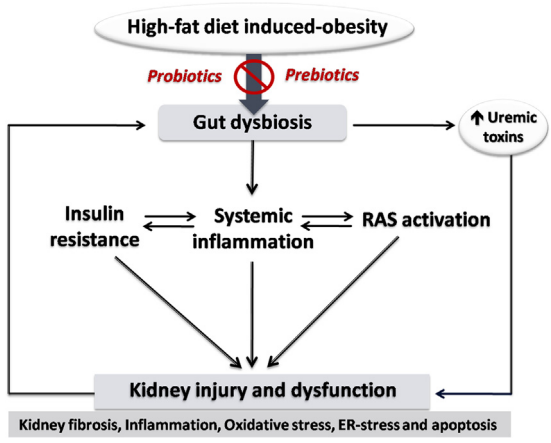

FIGURE. Obesity-induced kidney injury and dysfunction and the potential benefits of using probiotics and prebiotics to improve gastrointestinal microbiota that could attenuate the progression of kidney damage. RAS, renin-angiotensin system; ER-stress, endoplasmic reticulum-stress.

bacteria, which might improve dysbiosis conditions. A clinical study involving the prebiotic supplement, oligofructose-enriched inulin, administered to patients with CKD for 4 weeks demonstrated that blood urea nitrogen and serum PCS were decreased, whereas serum creatinine and serum indoxyl sulfate were not different.[70] The data could indicate that gastrointestinal microbiota, especially PCS-producing bacteria, may be altered by this type of prebiotic that may affect the generation of uremic toxins. In addition, different nutrient intake by patients during the study may be a factor affecting this alteration. Further data on the effects of prebiotics and the underlying mechanism on kidney function need to be evaluated in clinical trials (Table 3).

The effects of prebiotics on animal models of kidney injury and dysfunction are presented in Table 4. In a study of rats with diabetes induced by streptozotocin, 10% XOS and fructo-oligosaccharide supplementation for 6 weeks showed a correlation with decreased blood glucose levels together with the amelioration of diabetic nephropathy.[71] Moreover, a supplement of 5% galacto-oligosaccharide given for 2 weeks to rats with CKD that had undergone 5/6 nephrectomy showed an altered intestinal bacterial composition and a reduced serum indoxyl sulfate. These findings were accompanied by an attenuation of renal injury and decreased endoplasmic reticulum stress and apoptosis.[72] The potential role of prebiotics on kidney injury and dysfunction has also been shown in chronic interstitial nephropathic rats.[73] This study demonstrated not only an improvement in kidney function but also in the reduction of inflammation and oxidative stress after treatment with a dietary supplement of high-amylose maize-resistant starch type 2. Moreover, this prebiotic supplementation showed results correlating with restored colonic tight-junction protein structure. From this evidence, it can be suggested that prebiotics may promote the growth of bacteria that have positive effects for the host, including improvement in the gastrointestinal barrier and in systemic inflammation, eventually reducing kidney injury and preserving kidney function.

In summary, evidence from both clinical and animal studies demonstrated that prebiotics have protective effects against kidney injury and dysfunction by modulating intestinal bacteria composition or attenuating inflammation, oxidative stress and apoptosis or by doing both. However, some kidney parameters such as serum urea and creatinine show discrepancies. These may be because of the types of prebiotic used in the experiments or the difference in nutrient consumption or because of both the reasons. Further investigations evaluating various types of prebiotics in animal and clinical models are needed.

CONCLUSIONS

The increased prevalence of metabolic syndrome is proving to be a progressively important concern worldwide. Some changes in dietary habit and lifestyle are important factors leading to increased levels of obesity, which have an important effect on kidney injury and dysfunction. Alteration of gastrointestinal microbiota instigated by obesity induced by a high-fat diet promotes systemic inflammation and affects kidney function through several mechanisms, such as insulin resistance and RAS activation. The changes in microbiota also had a correlation with increased production of a toxic metabolite called uremic toxin, which has a deleterious effect on the kidney. Moreover, the impairment of kidney function could in turn increase the severity of gastrointestinal dysbiosis, which then further promotes the progression of kidney injury and dysfunction. Thus, the gastrointestinal microbiota is considered to be an important target for future management of obesity-induced kidney injury (Figure). Therefore, the use of probiotics and prebiotics has potential benefits in the treatment of kidney disease and requires further study.

REFERENCES

1. **Iglesias P, Diez JJ.** Adipose tissue in renal disease: clinical significance and prognostic implications. Nephrol Dial Transplant 2010;25(7):2066–77.
2. **Chen J, Muntner P, Hamm LL, et al.** The metabolic syndrome and chronic kidney disease in U.S. adults. Ann Intern Med 2004;140(3):167–74.
3. **Muntner P, Coresh J, Smith JC, et al.** Plasma lipids and risk of developing renal dysfunction: the atherosclerosis risk in communities study. Kidney Int 2000;58(1):293–301.
4. **Hsu CY, McCulloch CE, Iribarren C, et al.** Body mass index and risk for end-stage renal disease. Ann Intern Med 2006;144(1):21–8.
5. **Burton JO, Gray LJ, Webb DR, et al.** Association of anthropometric obesity measures with chronic kidney disease risk in a non-diabetic patient population. Nephrol Dial Transplant 2012;27(5):1860–6.
6. **Cinti S, Mitchell G, Barbatelli G, et al.** Adipocyte death defines macrophage localization and function in adipose tissue of obese mice and humans. J Lipid Res 2005;46(11):2347–55.
7. **Lau DC, Dhillon B, Yan H, et al.** Adipokines: molecular links between obesity and atheroslcerosis. Am J Physiol Heart Circ Physiol 2005;288(5):H2031–41.
8. **Trayhurn P, Wood IS.** Adipokines: inflammation and the pleiotropic role of white adipose tissue. Br J Nutr 2004;92(3):347–55.

9. **Wolf G, Hamann A, Han DC, et al.** Leptin stimulates proliferation and TGF-beta expression in renal glomerular endothelial cells: potential role in glomerulosclerosis [see comments]. Kidney Int 1999;56(3):860–72.
10. **Wiggins JE, Goyal M, Sanden SK, et al.** Podocyte hypertrophy, adaptation and decompensation associated with glomerular enlargement and glomerulosclerosis in the aging rat: prevention by calorie restriction. J Am Soc Nephrol 2005;16(10):2953–66.
11. **Sieber J, Jehle AW.** Free fatty acids and their metabolism affect function and survival of podocytes. Front Endocrinol (Lausanne) 2014;5:186.
12. **Qatanani M, Lazar MA.** Mechanisms of obesity-associated insulin resistance: many choices on the menu. Genes Dev 2007;21(12):1443–55.
13. **Wang S, Denichilo M, Brubaker C, et al.** Connective tissue growth factor in tubulointerstitial injury of diabetic nephropathy. Kidney Int 2001; 60(1):96–105.
14. **Papadimitriou A, Peixoto EB, Silva KC, et al.** Increase in AMPK brought about by cocoa is renoprotective in experimental diabetes mellitus by reducing NOX4/TGFbeta-1 signaling. J Nutr Biochem 2014;25(7): 773–84.
15. **Locatelli F, Pozzoni P, Del Vecchio L.** Renal manifestations in the metabolic syndrome. J Am Soc Nephrol 2006;17(4 suppl 2):S81–5.
16. **Cheng HT, Huang JW, Chiang CK, et al.** Metabolic syndrome and insulin resistance as risk factors for development of chronic kidney disease and rapid decline in renal function in elderly. J Clin Endocrinol Metab 2012;97(4):1268–76.
17. **Lambert GW, Straznicky NE, Lambert EA, et al.** Sympathetic nervous activation in obesity and the metabolic syndrome—causes, consequences and therapeutic implications. Pharmacol Ther 2010;126(2):159–72.
18. **Tuck ML, Sowers J, Dornfeld L, et al.** The effect of weight reduction on blood pressure, plasma renin activity and plasma aldosterone levels in obese patients. N Engl J Med 1981;304(16):930–3.
19. **Hall JE, Henegar JR, Dwyer TM, et al.** Is obesity a major cause of chronic kidney disease? Adv Ren Replace Ther 2004;11(1):41–54.
20. **Henegar JR, Bigler SA, Henegar LK, et al.** Functional and structural changes in the kidney in the early stages of obesity. J Am Soc Nephrol 2001;12(6):1211–7.
21. **Nakagawa T, Kang DH, Ohashi R, et al.** Tubulointerstitial disease: role of ischemia and microvascular disease. Curr Opin Nephrol Hypertens 2003;12(3):233–41.
22. **Manucha W, Valles PG.** Apoptosis modulated by oxidative stress and inflammation during obstructive nephropathy. Inflamm Allergy Drug Targets 2012;11(4):303–12.
23. **Karuppagounder V, Arumugam S, Thandavarayan RA, et al.** Naringenin ameliorates daunorubicin induced nephrotoxicity by mitigating AT1R, ERK1/2-NFkappaB p65 mediated inflammation. Int Immunopharmacol 2015;28(1):154–9.
24. **Kurata A, Nishizawa H, Kihara S, et al.** Blockade of angiotensin II type-1 receptor reduces oxidative stress in adipose tissue and ameliorates adipocytokine dysregulation. Kidney Int 2006;70(10):1717–24.
25. **de La Serre CB, Ellis CL, Lee J, et al.** Propensity to high-fat diet-induced obesity in rats is associated with changes in the gut microbiota and gut inflammation. Am J Physiol Gastrointest Liver Physiol 2010;299 (2):G440–8.
26. **Kau AL, Ahern PP, Griffin NW, et al.** Human nutrition, the gut microbiome and the immune system. Nature 2011;474(7351):327–36.
27. **Qin J, Li R, Raes J, et al.** A human gut microbial gene catalogue established by metagenomic sequencing. Nature 2010;464(7285):59–65.
28. **Nicholson JK, Holmes E, Kinross J, et al.** Host-gut microbiota metabolic interactions. Science 2012;336(6086):1262–7.
29. **Ley RE, Backhed F, Turnbaugh P, et al.** Obesity alters gut microbial ecology. Proc Natl Acad Sci U S A 2005;102(31):11070–5.
30. **Rabot S, Membrez M, Bruneau A, et al.** Germ-free C57BL/6J mice are resistant to high-fat-diet-induced insulin resistance and have altered cholesterol metabolism. FASEB J 2010;24(12):4948–59.
31. **Zhao X, Liu XW, Xie N, et al.** Lactobacillus species shift in distal esophagus of high-fat-diet-fed rats. World J Gastroenterol 2011;17(26): 3151–7.
32. **Turnbaugh PJ, Ley RE, Mahowald MA, et al.** An obesity-associated gut microbiome with increased capacity for energy harvest. Nature 2006; 444(7122):1027–31.
33. **Backhed F, Ding H, Wang T, et al.** The gut microbiota as an environmental factor that regulates fat storage. Proc Natl Acad Sci U S A 2004;101(44):15718–23.
34. **Scott FI, Horton DB, Mamtani R, et al.** Administration of antibiotics to children before age 2 years increases risk for childhood obesity. Gastroenterology 2016;151(1):120–9 e5.
35. **Reijnders D, Goossens GH, Hermes GD, et al.** Effects of gut microbiota manipulation by antibiotics on host metabolism in obese humans: a randomized double-blind placebo-controlled trial. Cell Metab 2016;24(1): 63–74.
36. **Ewaschuk JB, Diaz H, Meddings L, et al.** Secreted bioactive factors from Bifidobacterium infantis enhance epithelial cell barrier function. Am J Physiol Gastrointest Liver Physiol 2008;295(5):G1025–34.
37. **Mattar AF, Teitelbaum DH, Drongowski RA, et al.** Probiotics up-regulate MUC-2 mucin gene expression in a Caco-2 cell-culture model. Pediatr Surg Int 2002;18(7):586–90.
38. **Schlee M, Harder J, Koten B, et al.** Probiotic lactobacilli and VSL#3 induce enterocyte beta-defensin 2. Clin Exp Immunol 2008;151(3): 528–35.
39. **Cani PD, Bibiloni R, Knauf C, et al.** Changes in gut microbiota control metabolic endotoxemia-induced inflammation in high-fat diet-induced obesity and diabetes in mice. Diabetes 2008;57(6):1470–81.
40. **Cani PD, Amar J, Iglesias MA, et al.** Metabolic endotoxemia initiates obesity and insulin resistance. Diabetes 2007;56(7):1761–72.
41. **Kronborg G.** Lipopolysaccharide (LPS), LPS-immune complexes and cytokines as inducers of pulmonary inflammation in patients with cystic fibrosis and chronic *Pseudomonas aeruginosa* lung infection. APMIS Suppl 1995;50:1–30.
42. **Kim KA, Gu W, Lee IA, et al.** High fat diet-induced gut microbiota exacerbates inflammation and obesity in mice via the TLR4 signaling pathway. PLoS One 2012;7(10):e47713.
43. **Lassenius MI, Pietilainen KH, Kaartinen K, et al.** Bacterial endotoxin activity in human serum is associated with dyslipidemia, insulin resistance, obesity and chronic inflammation. Diabetes Care 2011;34(8):1809–15.
44. **Poesen R, Meijers B, Evenepoel P.** The colon: an overlooked site for therapeutics in dialysis patients. Semin Dial 2013;26(3):323–32.
45. **Evenepoel P, Meijers BK, Bammens BR, et al.** Uremic toxins originating from colonic microbial metabolism. Kidney Int Suppl 2009;114: S12–9.
46. **Enomoto A, Takeda M, Tojo A, et al.** Role of organic anion transporters in the tubular transport of indoxyl sulfate and the induction of its nephrotoxicity. J Am Soc Nephrol 2002;13(7):1711–20.
47. **Brunori G, Viola BF, Parrinello G, et al.** Efficacy and safety of a very-low-protein diet when postponing dialysis in the elderly: a prospective randomized multicenter controlled study. Am J Kidney Dis 2007;49(5): 569–80.
48. **Mandayam S, Mitch WE.** Dietary protein restriction benefits patients with chronic kidney disease. Nephrology (Carlton) 2006;11(1):53–7.
49. **Menon V, Kopple JD, Wang X, et al.** Effect of a very low-protein diet on outcomes: long-term follow-up of the Modification of Diet in Renal Disease (MDRD) Study. Am J Kidney Dis 2009;53(2):208–17.
50. **Rastall RA, Gibson GR, Gill HS, et al.** Modulation of the microbial ecology of the human colon by probiotics, prebiotics and synbiotics to enhance human health: an overview of enabling science and potential applications. FEMS Microbiol Ecol 2005;52(2):145–52.
51. **Ranganathan N, Friedman EA, Tam P, et al.** Probiotic dietary supplementation in patients with stage 3 and 4 chronic kidney disease: a 6-month pilot scale trial in Canada. Curr Med Res Opin 2009;25(8): 1919–30.
52. **Ranganathan N, Ranganathan P, Friedman EA, et al.** Pilot study of probiotic dietary supplementation for promoting healthy kidney function in patients with chronic kidney disease. Adv Ther 2010;27(9): 634–47.
53. **Wang IK, Wu YY, Yang YF, et al.** The effect of probiotics on serum levels of cytokine and endotoxin in peritoneal dialysis patients: a randomised, double-blind, placebo-controlled trial. Benef Microbes 2015;1–8.
54. **Natarajan R, Pechenyak B, Vyas U, et al.** Randomized controlled trial of strain-specific probiotic formulation (Renadyl) in dialysis patients. Biomed Res Int 2014;2014:568571.

55. **Ben Salah R, Trabelsi I, Hamden K, et al.** *Lactobacillus plantarum* TN8 exhibits protective effects on lipid, hepatic and renal profiles in obese rat. Anaerobe 2013;23:55–61.
56. **Punaro GR, Maciel FR, Rodrigues AM, et al.** Kefir administration reduced progression of renal injury in STZ-diabetic rats by lowering oxidative stress. Nitric Oxide 2014;37:53–60.
57. **Li C, Ding Q, Nie SP, et al.** Carrot juice fermented with *Lactobacillus plantarum* NCU116 ameliorates type 2 diabetes in rats. J Agric Food Chem 2014;62(49):11884–91.
58. **Yoshifuji A, Wakino S, Irie J, et al.** Gut Lactobacillus protects against the progression of renal damage by modulating the gut environment in rats. Nephrol Dial Transplant 2016;31(3):401–12.
59. **Mandal A, Das K, Roy S, et al.** *In vivo* assessment of bacteriotherapy on acetaminophen-induced uremic rats. J Nephrol 2013;26(1):228–36.
60. **Arpita Patraa AM, Roya Suchismita, Mandala Shreya, et al.** Protective effect of selected urease positive Lactobacillus strains on acetaminophen induced uremia in rats. Biomed Prev Nutr 2014;4(2):271–6.
61. **Balakrishnan R, Kumar CSVS, Reddy KK, et al.** Antioxidant activity of coated probiotic *Lactobacillus casei* on chromium(VI) induced oxidative stress in rats. Proc Natl Acad Sci India Sect B Biol Sci 2014;84(2):305–10.
62. **Bouhafs L, Moudilou EN, Exbrayat JM, et al.** Protective effects of probiotic *Lactobacillus plantarum* BJ0021 on liver and kidney oxidative stress and apoptosis induced by endosulfan in pregnant rats. Ren Fail 2015;1–9.
63. **Kanbak G, Uzuner K, Kusat Ol K, et al.** Effect of kefir and low-dose aspirin on arterial blood pressure measurements and renal apoptosis in unhypertensive rats with 4 weeks salt diet. Clin Exp Hypertens 2014;36(1):1–8.
64. **Jespersen L, Tarnow I, Eskesen D, et al.** Effect of *Lactobacillus paracasei* subsp. *paracasei*, *L casei* 431 on immune response to influenza vaccination and upper respiratory tract infections in healthy adult volunteers: a randomized, double-blind, placebo-controlled, parallel-group study. Am J Clin Nutr 2015;101(6):1188–96.
65. **Lindsay KL, Brennan L, Kennelly MA, et al.** Impact of probiotics in women with gestational diabetes mellitus on metabolic health: a randomized controlled trial. Am J Obstet Gynecol 2015;212(4):496 e1–11.
66. **Madjd A, Taylor MA, Mousavi N, et al.** Comparison of the effect of daily consumption of probiotic compared with low-fat conventional yogurt on weight loss in healthy obese women following an energy-restricted diet: a randomized controlled trial. Am J Clin Nutr 2016;103(2):323–9.
67. **Anderson AD, McNaught CE, Jain PK, et al.** Randomised clinical trial of synbiotic therapy in elective surgical patients. Gut 2004;53(2):241–5.
68. **Gibson GR, Roberfroid MB.** Dietary modulation of the human colonic microbiota: introducing the concept of prebiotics. J Nutr 1995;125(6):1401–12.
69. **Pourabedin M, Guan L, Zhao X.** Xylo-oligosaccharides and virginiamycin differentially modulate gut microbial composition in chickens. Microbiome 2015;3:15.
70. **Meijers BK, De Preter V, Verbeke K, et al.** p-Cresyl sulfate serum concentrations in haemodialysis patients are reduced by the prebiotic oligofructose-enriched inulin. Nephrol Dial Transplant 2010;25(1):219–24.
71. **Gobinath D, Madhu AN, Prashant G, et al.** Beneficial effect of xylo-oligosaccharides and fructo-oligosaccharides in streptozotocin-induced diabetic rats. Br J Nutr 2010;104(1):40–7.
72. **Furuse SU, Ohse T, Jo-Watanabe A, et al.** Galacto-oligosaccharides attenuate renal injury with microbiota modification. Physiol Rep 2014;2(7):e12029.
73. **Vaziri ND, Liu SM, Lau WL, et al.** High amylose resistant starch diet ameliorates oxidative stress, inflammation and progression of chronic kidney disease. PLoS One 2014;9(12):e114881.

From the Department of Physiology (KW, AP, NC, AL), Cardiac Electrophysiology Research and Training Center (KW, AP, SCC, NC, AL), Faculty of Medicine, and Department of Oral Biology and Diagnostic Sciences (SCC), Faculty of Dentistry, Chiang Mai University, Chiang Mai, Thailand; School of Medicine (KW), Mae Fah Luang University, Chiang Rai, Thailand; Department of Physiology (VC), Faculty of Science, Mahidol University, Bangkok, Thailand.

Submitted June 7, 2016; accepted November 15, 2016.

This work was supported by the Thailand Research Fund, Thailand (RSA5780029; A.L.), National Research Council of Thailand, Thailand (347682/2560; A.L.), CMU Mid-Career Research Fellowship program, Thailand (13/2558; A.L.), the Faculty of Medicine Research Fund, Chiang Mai University, Thailand (A.L. and A.P.) and the NSTDA Research Chair grant from the National Science and Technology Development Agency, Thailand (N.C.).

The authors have no conflicts of interest to disclose.

Correspondence: Anusorn Lungkaphin, PhD, Epithelial Transport and Intracellular Signaling Regulation Unit, Department of Physiology, Faculty of Medicine, Chiang Mai University, Chiang Mai 50200, Thailand (E-mail: onanusorn@yahoo.com, anusorn.lungka@cmu.ac.th).

PLOS ONE

RESEARCH ARTICLE

Amelioration of Renal Inflammation, Endoplasmic Reticulum Stress and Apoptosis Underlies the Protective Effect of Low Dosage of Atorvastatin in Gentamicin-Induced Nephrotoxicity

Krit Jaikumkao[1], Anchalee Pongchaidecha[1], La-ongdao Thongnak[1], Keerati Wanchai[1,2], Phatchawan Arjinajarn[3], Varanuj Chatsudthipong[4], Nipon Chattipakorn[1,5], Anusorn Lungkaphin[1]*

1 Department of Physiology, Faculty of Medicine, Chiang Mai University, Chiang Mai, Thailand, **2** School of Medicine, Mae Fah Luang University, Chiang Rai, Thailand, **3** Department of Biology, Faculty of Science, Chiang Mai University, Chiang Mai, Thailand, **4** Department of Physiology, Faculty of Science, Mahidol University, Bangkok, Thailand, **5** Cardiac Electrophysiology Research and Training Center, Faculty of Medicine, Chiang Mai University, Chiang Mai, Thailand

* onanusorn@yahoo.com, anusorn.lungka@cmu.ac.th

OPEN ACCESS

Citation: Jaikumkao K, Pongchaidecha A, Thongnak L-o, Wanchai K, Arjinajarn P, Chatsudthipong V, et al. (2016) Amelioration of Renal Inflammation, Endoplasmic Reticulum Stress and Apoptosis Underlies the Protective Effect of Low Dosage of Atorvastatin in Gentamicin-Induced Nephrotoxicity. PLoS ONE 11 (10): e0164528. doi:10.1371/journal.pone.0164528

Editor: Demetrios G. Vavvas, Massachusetts Eye & Ear Infirmary, Harvard Medical School, UNITED STATES

Received: May 24, 2016

Accepted: September 27, 2016

Published: October 11, 2016

Data Availability Statement: All relevant data are within the paper.

Funding: This work was supported by the Thailand Research Fund academic.trf.or.th RSA5780029 (AL) and TRG5780019 (PA), CMU Mid-Career Research Fellowship program http://www.cmu.ac.th (13/2558; AL), the Faculty of Medicine Research Fund, Chiang Mai University

Abstract

Gentamicin is a commonly used aminoglycoside antibiotic. However, its therapeutic use is limited by its nephrotoxicity. The mechanisms of gentamicin-induced nephrotoxicity are principally from renal inflammation and oxidative stress. Since atorvastatin, 3-hydroxy-3-methylglutaryl coenzyme A reductase inhibitors, exerts lipid-lowering effects, antioxidant, anti-inflammatory as well as anti-apoptotic effects, this study aimed to investigate the protective effects of atorvastatin against gentamicin-induced nephrotoxicity. Male Sprague Dawley rats were used and nephrotoxicity was induced by intraperitoneal injection of gentamicin, 100 mg/kg/day, for 15 days. Atorvastatin, 10 mg/kg/day, was administered by orally gavage 30 min before gentamicin injection on day 1 to 15 (pretreatment) or on day 10 to15 (delayed treatment). For only atorvastatin treatment group, it was given on day 1 to 15. At the end of the experiment, kidney weight, blood urea nitrogen and serum creatinine as well as renal inflammation (NF-κB, TNFαR1, IL-6 and iNOS), renal fibrosis (TGFβ1), ER stress (calpain, GRP78, CHOP, and caspase 12) and apoptotic markers (cleaved caspase-3, Bax, and Bcl-2) as well as TUNEL assay were determined. Gentamicin-induced nephrotoxicity was confirmed by marked elevations in serum urea and creatinine, kidney hypertrophy, renal inflammation, fibrosis, ER stress and apoptosis and attenuation of creatinine clearance. Atorvastatin pre and delayed treatment significantly improved renal function and decreased renal NF-κB, TNFαR1, IL-6, iNOS and TGFβ1 expressions. They also attenuated calpain, GRP78, CHOP, caspase 12, Bax, and increased Bcl-2 expressions in gentamicin-treated rat. These results indicate that atorvastatin treatment could attenuate gentamicin-induced nephrotoxicity in rats, substantiated by the reduction of inflammation,

http://www.med.cmu.ac.th (10/2559; AL) and the NSTDA Research Chair grant from the National Science and Technology Development Agency of Thailand http://www.nstda.or.th (NC). The funders had no role in study design, data collection and analysis, decision to publish, or preparation of the manuscript.

Competing Interests: The authors have declared that no competing interests exist.

ER stress and apoptosis. The effect of atorvastatin in protecting from renal damage induced by gentamicin seems to be more effective when it beginning given along with gentamicin or pretreatment.

Introduction

Nephrotoxicity is an adverse effect of gentamicin treatment, despite its positive therapeutic activity against both gram-positive and gram negative bacteria [1–3]. Gentamicin-induced nephrotoxicity occurs by its selective accumulation in the renal proximal convoluted tubules leading to glomerular atrophy, tubular necrosis, tubular fibrosis, and inflammation. The mechanisms of gentamicin-induced nephrotoxicity are principally from renal inflammatory cascades and elevated renal oxidative stress [4]. Renal inflammation is demonstrated by an infiltration of inflammatory cells such as monocytes and macrophages and the subsequent release of proinflammatory cytokines and activation of NF-κB in response to oxidative stress [1,3]. In addition, apoptosis and necrosis of renal tubular epithelial cells [5–7] and activation of renal matrix metalloproteinase [8] are also found in case of gentamicin-induced nephrotoxicity. The accumulation of gentamicin in the endoplasmic reticulum (ER) may induce endoplasmic reticulum (ER) stress which activates the unfolded protein response (UPR) and cell cycle arrest [9]. Under conditions of UPR overload, the cell undergoes apoptosis, which is mediated by the classical route of calpain and caspase 12 [10]. Moreover, when unfolded proteins accumulate, the ER chaperone immunoglobulin heavy-chain-binding protein (BiP; also known as GRP78) expression is increased and dissociates from the ER receptors, leading to their activation and triggering the ER stress response [11]. The transcription factor CCAAT-enhancer-binding protein homologous protein (CHOP) expression is also increased in response to ER stress and plays an important role in the induction of apoptosis [12,13]. Accordingly, the use of several agents with anti-oxidant, anti-inflammation and anti-apoptosis activities and ER stress inhibition or an agent that posses multiple mechanisms of action may successfully prevent or ameliorate gentamicin-induced nephrotoxicity.

Numbers of clinical and experimental evidence demonstrated that the pharmacological effects of statins include not only lowering the levels of cholesterol but also the exertion of a variety of pleiotropic, such as inhibition of inflammatory response, improvement of endothelial function, antioxidant, antithrombotic and anti-apoptotic effects [14]. In patient with hypercholesterolemia, statins were instrumental in reducing the progression of atherosclerosis by inhibiting of monocyte activation, enhancing metalloprotease synthesis in the vessel walls and the production of pro-inflammatory cytokines interleukin (IL)-6, tumor necrosis factors (TNFα) and IL-1β [15,16]. Statins also suppressed acute and chronic inflammation by inhibiting edema formation, leukocyte-endothelial adhesion, production of inflammatory cytokines and transcription factors [17–19]. It has also been reported that atorvastatin prevents the toxic effects of gentamicin in the kidney via the inhibition of MAPK and NF-κB signaling pathways and iNOS expression [20]. However, details of the pleiotropic effects of statins on nephrotoxicity have not been clearly demonstrated.

This study was designed to investigate the protective effects of atorvastatin against gentamicin-induced toxicity in rat kidneys. We hypothesized that atorvastatin improves renal function by ameliorating an inflammation and ER stress related apoptosis pathways in gentamicin-induced nephrotoxicity.

Materials and Methods

Animal preparation and treatment

The 30 male Sprague-Dawley rats (250–300 g), 10–12 weeks of age, used in this study were obtained from the National Laboratory Animal Center, Mahidol University, Salaya, Thailand. The animal facilities and all protocols were approved by the Laboratory Animal Care and Use Committees at the Faculty of Medicine, Chiang Mai University, Chiang Mai, Thailand (Permit Number: 06/2559). All experimental rats were housed in a room maintained at 25 ± 1°C on a 12 h light/dark cycle and fed on a normal laboratory diet and water ad libitum. Only male rats were used to get rid of the fluctuation of sex hormone during menstrual cycle in female rats which might affect our results. It has been reported that gentamicin could induce the sensitivity of renal toxicity in male rats more than female rats [21,22].

Thirty rats were randomly divided into five groups (six rats per group). (1) the vehicle control (C) group received normal saline by gavage; (2) the gentamicin (G) group. The rat was injected intraperitoneally (i.p.) with 100 mg/kg/day of gentamicin (The Govt. Pharm.Org, Thailand) with the volume of 700–800 μl for 15 days; (3) the atorvastatin group, Ator (Lek Pharmaceuticals d.d, Slovenia) dissolved in 500 μl of 0.9% normal saline solution at dose of 10 mg/kg/day was administered by gavage feeding once a day on day 1 to 15; (4) the atorvastatin pretreatment (Pre) group, Ator was administered by gavage 30 min before gentamicin treatment for 15 days; and (5) atorvastatin delayed treatment (Delayed) group, gentamicin was injected every day for 15 days and Ator was administered on days 10 to 15 by gavage 30 min before the gentamicin treatment. Gentamicin was injected at the same period of time, 8.00 to 9.00 am, in all groups of experiment. Atorvastatin treatments were also given at 8:00 to 9:00 am throughout the experiment. The chosen gentamicin dose was based on that given by intraperitoneal administration in previous studies that showed the drug induced nephrotoxicity in rat models [23–25]. Atorvastatin used in this study was chosen from the dose that given by oral gavage in previous studies that showed nephroprotection as well as oxidative stress improvement [18–20] and from preliminary study. Thus, we selected atorvastatin in the minimal effective therapeutic dose 10 mg/kg/day as used in the clinical to evaluate the beneficial effects of this drug to protect the kidney from gentamicin-induced toxicity. The animals were monitored before and after receiving treatments in the morning and again in the evening. Blood samples were collected from tail vein by cutting the tail tip under isoflurane inhalation. After the last injected dose of gentamicin, each rat was kept individually in metabolic cage for 24 h urine collection. Urine was centrifuged at 1000 rpm for 10 min, to remove cells and debris and stored at -20°C until investigation. At the end of study, the animals were deeply anesthetized by sodium pentobarbital injection intraperitoneally at the dose of 100 mg/kg and blood and kidney tissue samples were collected for subsequent experiments. Following intraperitoneal injection (single dose) of pentobarbital, the isoflurane inhalation was used to maintain anesthesia of the animal throughout surgical protocols. The animals were observed throughout the experiment. The rats that have the severity symptoms such as lack of appetite, inanimate and severe diarrhea were killed before the endpoint of experiment by sodium pentobarbital injection intraperitoneally at the dose of 100 mg/kg and verify that an animal is dead before disposing of the carcass, by making sure there is no respiratory movement for at least 3 minutes. If the animal is deeply unconscious but respirations have not ceased, the inhalation of isoflurane is followed for additional security until respirations have stopped.

Determination of renal function

To assess renal function, serum and urine creatinine were measured using an automatic biochemical analyzer at the Clinical Laboratory, Maharaj Nakhon Chiang Mai Hospital, Chiang

Mai, Thailand. Relative kidney weight was calculated according to the formula: kidney weight/ total bodyweight. The creatinine clearance (C_{cr}) reflected to glomerular filtration rate (GFR) was calculated using the following equation:

$$C_{cr}(\text{ml/min}) = (\text{urine creatinine x urine flow rate}) / \text{serum creatinine}$$

Tissue preparation and Western blot analysis

The renal cortical tissues were used to carry out a Western blot analysis. The renal cortex was gently cut from the outer part of the kidney, sections extending down for approximately 3–4 mm were cut using a microtome. Each cellular compartment, whole cell lysate, membrane and cytosolic fractions were prepared from renal cortical tissues using differential centrifugation technique. Briefly, renal cortical slices were homogenized in Mammalian cell Lytic buffer (Sigma, St. Louis, MO, USA) with a protease cocktail inhibitor (Roche Diagnostics, Indianapolis, IN, USA). Homogenates were centrifuged at 5,000 × g for 15 min at 4°C. Some of the supernatants were collected as whole cell lysate, and the remaining portion was centrifuged at 100,000 × g for 2 h at 4°C to obtain the membrane (pellet) fraction. The 5,000 ×g pellet was resuspended and centrifuged at 10,000 × g 4°C for 10 min. The supernatant fraction from the centrifugation was designated as the nuclear fraction.

Whole cell lysate, membrane and nuclear fractions from the renal cortex were subjected to 10% SDS-polyacrylamide gel electrophoresis (SDS-PAGE), and subsequently transferred to a polyvinylidene fluoride (PVDF) membrane (Millipore, Billerica, MA, USA). The membranes were then blocked with 5% nonfat dry milk in Tris-buffered saline (TBS) containing 0.1% tween-20 (TBST) solution for 1 h at room temperature and subsequently probed with primary antibodies overnight at 4°C. The protein expressions of Bax (Millipore, Billerica, MA, USA), Bcl-2 (Cell Signaling Technology, Danvers, MA, USA), cleaved caspase-3 (Millipore, Billerica, MA, USA), NF-κB (Millipore, Billerica, MA, USA), iNOS (Santa Cruz Biotechnology, Santa Cruz, CA, USA), TNFα receptor1 orTNFαR1, IL-6 (Santa Cruz Biotechnology, Santa Cruz, CA, USA), TGFβ1 (Cell Signaling Technology, Danvers, MA, USA), calpain, GRP78, CHOP (Cell Signaling Technology, Danvers, MA, USA) and caspase 12 (Millipore, Billerica, MA, USA) were determined using western blot. Lamin b1 (Cell Signaling Technology, Danvers, MA, USA) or Na^+-K^+ ATPase (Millipore, Billerica, MA, USA) was used as a marker for the nuclear and membrane fraction, respectively. The β-actin (Millipore, Billerica, MA, USA) was used as a loading control for all samples. The membranes were washed three times with TBST and incubated with horseradish peroxidase (HRP)-conjugated goat anti-rabbit or anti-mouse secondary antibodies (Amersham, Arlington Heights, IL, USA) at room temperature for one hour and developed with ECL enhanced chemiluminescence agent (GE Healthcare, Buckinghamshire, UK). Each membrane was stripped and re-probed with mouse anti-β-actin antibody or another antibody for further detection of protein expression. The western blot film images were scanned and were analyzed using Image J (NIH image) analysis software.

Determination of renal apoptosis by TUNEL assay

Apoptosis in renal tissues was identified by a Terminal deoxynucleotidyl transferase dUTP nick end labeling (TUNEL assay) with tissue paraffin blocks using TdT-FragEL™ DNA fragmentation detection kit (Millipore, Billerica, MA, USA) according to the manufacturer's instruction. Tissue sections were treated with proteinase K for 20 min. After TBS washing, the sections were incubated with DNase I for 20 min. Sections were then reacted with 3% H_2O_2 for 5 min, washed with TBS, incubated with TdT equilibration buffer for 20 min, followed by the

incubation with TdT labeling reaction mixture for 1.5 h at 37°C in a humidified chamber. After TBS washing, the reaction was terminated by stop buffer solution for 5 min and washed and then blocked with blocking buffer for 10 min, followed by immersing the slides in conjugate solution for 30 min in a humidified chamber. After TBS washing, the sections were incubated with DAB solution for 15 min and rinsed with dH_2O, followed by the examination under the light microscope. The samples were performed blindly to the animal treatment groups.

Histopathological study

To determine any morphological changes, a kidney was removed and cut in a half along the transverse axis, fixed in 10% neutral buffered formalin and embedded in paraffin. Paraffin-embedded specimens were cut into 5-μm-thick sections, mounted on microscope slides and stained with Haematoxylin and Eosin for general histological assessment. The samples were examined under a light microscope for tubular and glomerular changes by an observer blinded to the animal treatment groups.

Statistical analysis

The data were analyzed using SPSS17.0 statistical software (Chicago, Ill., USA). All data were expressed as the mean ± SEM. For the comparison between multiple treatments, a one-way ANOVA followed by Fisher's Least significant difference test (LSD) was used. $P < 0.05$ was considered statistically significant.

Results

The effects of atorvastatin on renal function in gentamicin-treated rats

In this study, there was no animal died before the endpoint of experiment. Gentamicin treatment caused a significant decrease in body weight ($P < 0.05$) when compared with that of the control and atorvastatin groups (Fig 1A). Kidney hypertrophy as indicated by the significant increase in kidney weight and kidney/body weight ratio was observed in gentamicin-treated group ($P < 0.05$) (Fig 1B and 1C) when compared with the control or atorvastatin group. In addition, the apparent increase in serum BUN and creatinine levels and a significant decrease in creatinine clearance in gentamicin-treated group compared with the control or atorvastatin groups ($P < 0.05$) (Fig 2A, 2B and 2C) indicated that renal function impairment was induced by gentamicin treatment. Kidney hypertrophy was significantly attenuated in atorvastatin pretreatment as compared to gentamicin-treated rats ($P < 0.05$) (Fig 1B and 1C). Atorvastatin could not only prevent kidney dysfunction but also reverse renal impairment, leading to an improvement of renal function when compared with the gentamicin-treated rats (Fig 2). However, only atorvastatin pretreatment could improve kidney hypertrophy. Atorvastatin treatment alone had no effect on renal function when compared with control.

Effect of atorvastatin on gentamicin-induced renal inflammation

The expression of NF-κB in both whole cell lysate and nuclear fractions from renal cortical tissues was significantly higher in gentamicin-treated rats than those of the control and atorvastatin alone groups ($P < 0.05$) (Fig 3A and 3B). These results indicated the activation of NF-κB induced by gentamicin treatment. Moreover, the significant increases in the expressions of IL-6 and iNOS in whole cell lysate fraction and TNFαR1 in the membrane fraction from renal cortical tissues were observed in the gentamicin-treated group compared to those from the control and atorvastatin alone groups ($P < 0.05$) (Fig 3C, 3D and 3E). This study demonstrated that the expressions of NF-κB, IL-6, iNOS and TNFαR1 were markedly decreased by atorvastatin

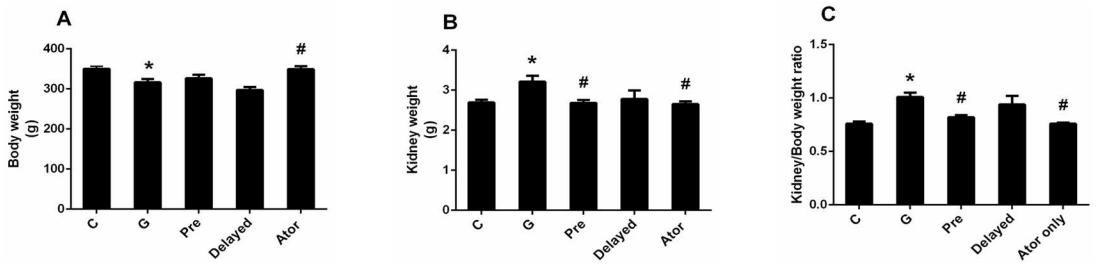

Fig 1. Effects of atorvastatin on the body weight (BW) (A); kidney weight (KW) (B); and KW/BW ratio (C). Bar graph indicates mean ± SEM. (n = 6 rats in each group). *P < 0.05 compared to the control group. #P < 0.05 compared to the gentamicin-treated group. C: control group; G: gentamicin-treated group; Pre: atorvastatin pretreatment group; Delayed: delayed treatment group and Ator: atorvastatin group.

doi:10.1371/journal.pone.0164528.g001

pretreatment ($P < 0.05$). The treatment with atorvastatin on day 10 to 15 of experiment could also reduce the inflammation induced by gentamicin ($P < 0.05$) although IL-6 was still markedly elevated when compared with atorvastatin pretreatment group. In addition, it has been reported that infiltration of macrophage accompanied with myofibroblasts, TGFβ and endothelin might contribute to the development of renal fibrosis in gentamicin-treated rat [26]. The expression of TGFβ1, a key mediator of renal fibrosis, in renal cortical tissues [27], was significantly increased in the gentamicin group when compared to that of the control and atorvastatin groups ($P < 0.05$) (Fig 3F). Atorvastatin pretreatment and delayed treatment shared similar efficacy in attenuating TGFβ1 expression, leading to renal fibrosis reduction compared to that seen in the gentamicin-treated rats ($P < 0.05$). Atorvastatin treatment alone had no effect on NF-κB, iNOS, TNFαR1 and TGFβ1 expressions when compared with control. These findings could indicate that atorvastatin treatment attenuated renal inflammation and fibrosis induced by gentamicin.

The effects of atorvastatin on renal ER stress

To investigate the effect of atorvastatin on the ER stress-mediated cell death signaling pathway in gentamicin-induced nephrotoxicity, the ER stress-related protein expression was determined. Gentamicin treatment caused significant increases in calpain, caspase 12, GRP78 and CHOP protein expressions ($P < 0.05$), indexes of ER stress markers, in renal cortical tissue when compared to both the control and the atorvastatin groups (Fig 4). Atorvastatin pretreatment abolished the increases in calpain, caspase 12, GRP78 and CHOP expressions induced by gentamicin treatment ($P < 0.05$). However, only the significant decreases in calpain and

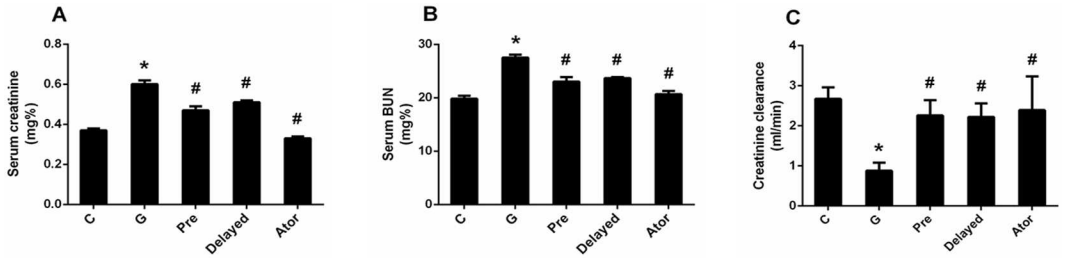

Fig 2. Effects of atorvastatin on serum creatinine (A); serum BUN (B); and creatinine clearance (C). Bar graph indicates mean ± SEM. (n = 6 rats in each group). *P < 0.05 compared to the control group. #P < 0.05 compared to the gentamicin-treated group. C: control group; G: gentamicin-treated group; Pre: atorvastatin pretreatment group; Delayed: delayed treatment group and Ator: atorvastatin group.

doi:10.1371/journal.pone.0164528.g002

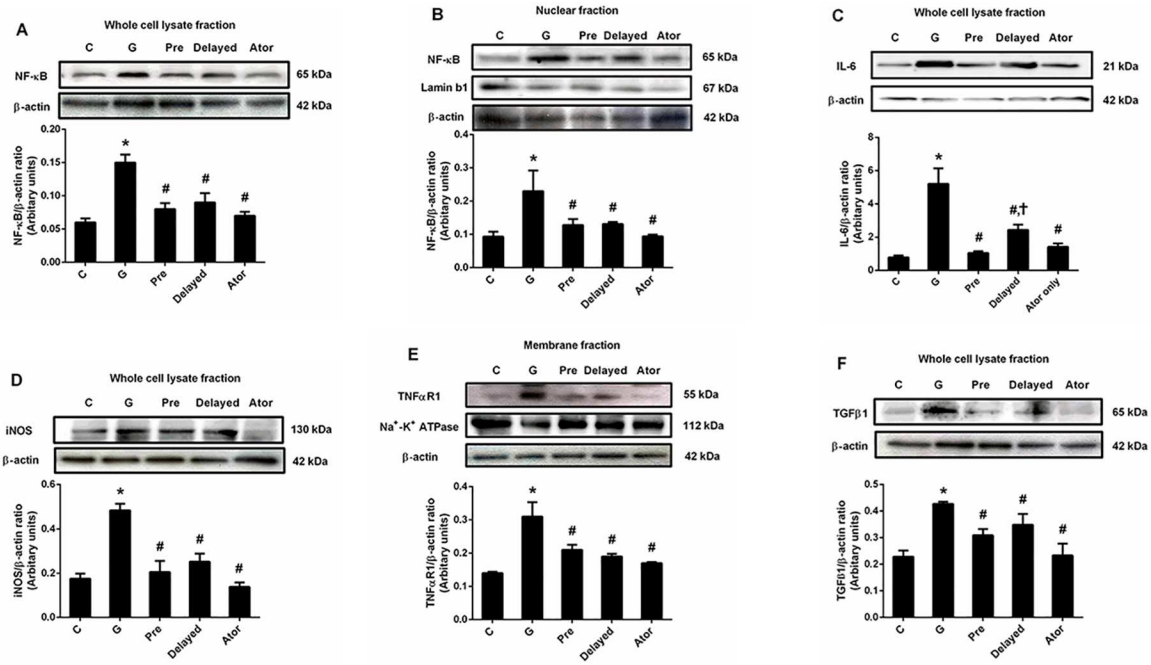

Fig 3. Effects of atorvastatin on the expression of NF-κB, IL-6, iNOS, TNFαR1 and TGFβ1 in the renal cortical tissue. Immunoblot analysis for expressions of NF-κB in the whole cell lysate fraction (A); NF-κB in nuclear fraction (B); IL-6 in whole cell lysate fraction (C); iNOS in whole cell lysate fraction (D); TNFαR1 in membrane fraction (E) and TGFβ1 in whole cell lysate fraction (F) in renal cortical tissues normalized to ß-actin. Lamin b1 or Na^+-K^+ ATPase was used as a marker for the nuclear or membrane fraction, respectively. Bar graph indicates mean ± SEM. (n = 6 rats in each group). *P < 0.05 compared to the control group. #P < 0.05 compared to the gentamicin-treated group. †P < 0.05 compared to the pretreatment group. C: control group; G: gentamicin-treated group; Pre: atorvastatin pretreatment group; Delayed: delayed treatment group and Ator: atorvastatin group.

doi:10.1371/journal.pone.0164528.g003

GRP78 but not caspase 12 and CHOP expressions were observed in atorvastatin delayed treatment ($P < 0.05$) when compared with those of the gentamicin-treated group. Atorvastatin treatment alone had no effect on ER stress when compared with control. These results indicated that atorvastation treatment could inhibit ER stress pathway induced by gentamicin treatment.

The effects of atorvastatin on renal apoptosis

To elucidate the effect of atorvastatin on gentamicin-induced renal cell apoptosis, the apoptosis related pro-apoptotic and anti-apoptotic protein expressions and TUNEL assay were examined. Significant enhanced Bax and cleaved caspase-3 expressions and marked reduced Bcl-2 expression in renal cortical tissue were observed ($P < 0.05$) in the gentamicin group compared to those of the control and atorvastatin groups (Fig 5A, 5B and 5D). The Bax/Bcl-2 ratio was also significantly increased in gentamicin-treated rat ($P < 0.05$) (Fig 5C). The results showed that the numbers of TUNEL-positive cells were observed in gentamicin-treated rats, predominantly located at the renal tubules of the renal cortex when compared with the control group (Fig 6). Atorvastatin pretreatment significantly reduced the expressions of the Bax, cleaved caspase-3 and Bax/Bcl-2 ratio and apparently increased Bcl-2 expression when compared to the gentamicin group ($P< 0.05$). The enhanced expressions of Bax and Bax/Bcl-2 ratio in gentamicin-treated rats were significantly reversed with the delayed treatment with atorvastatin ($P <0.05$). However, delayed treatment with atorvastatin could not down-regulate the expression

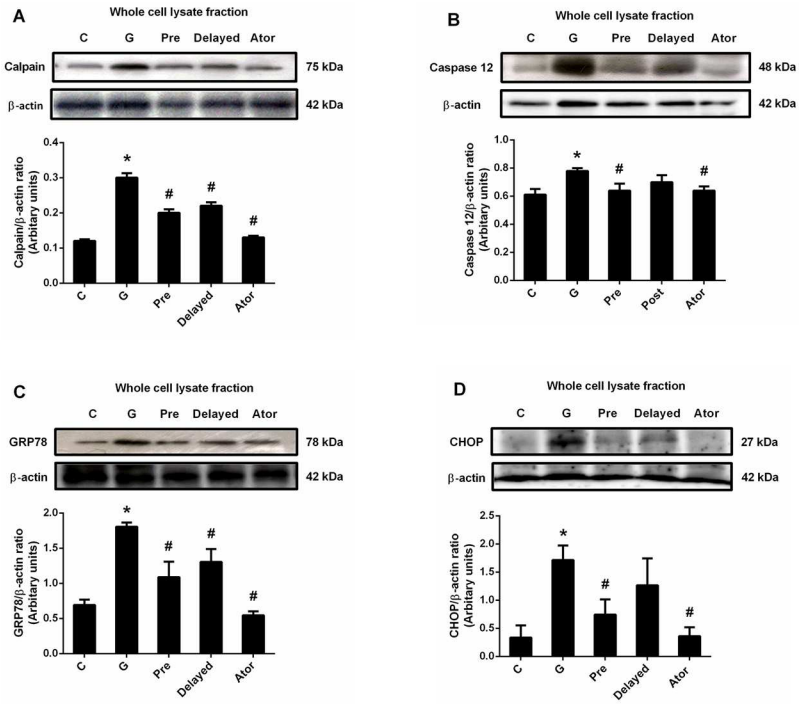

Fig 4. Effects of atorvastatin on the expression of calpain, caspase 12, GRP78 and CHOP. Immunoblot analysis for calpain (A); caspase 12 (B); GRP78 (C) and CHOP (D) expressions in the whole cell lysate fraction of renal cortical tissues normalized to ß-actin. Bar graph indicates mean ± SEM. (n = 6 rats in each group). *P < 0.05 compared to the control group. #P < 0.05 compared to the gentamicin-treated group. C: control group; G: gentamicin-treated group; Pre: atorvastatin pretreatment group; Delayed: delayed treatment group and Ator: atorvastatin group.

doi:10.1371/journal.pone.0164528.g004

of cleaved caspase-3 or enhance Bcl-2 expression. Atorvastatin pre and delayed treatments could reduce TUNEL-positive cells as compared to the gentamicin-treated group. Atorvastatin treatment alone had no effect on Bax, Bcl-2 and cleaved caspase-3 expressions when compared with control. These results suggest that atorvastatin treatment attenuates gentamicin-induced apoptosis in rat renal tubular cells by inhibiting ER stress and apoptosis pathway.

The effects of atorvastatin on renal histology

The results showed that gentamicin-treated rats demonstrated glomerular damage, tubular atrophy, tubular dilatation, cellular desquamation, pyknotic nuclei and interstitial mononuclear cells infiltration. Atorvastatin pre and delayed treatments could preserve kidney morphology in the levels of glomerular, tubular and interstitial cells in this study (Fig 7).

Discussion

Gentamicin, an aminoglycoside antibiotic, is the most clinically used due to its wide spectrum of activities against gram-negative bacterial infections [28]. However, there are limitations to its use due to nephrotoxic side effects. 10–20% of all cases of acute renal failure are due to these nephrotoxicity of this antibiotic. Some clinicians suggest a daily dose of 4 to 7 mg/kg once daily for all patients with normal renal function. In this study, we would like to induce renal dysfunction and use atorvastatin treatment to reverse this impairment. Thus, we selected the supramaximal dosage or 100 mg/kg/day of gentamicin in order to induced nephrotoxicity according to the previous studies [23,24,29]. In addition, the preliminary data, rats receiving gentamicin

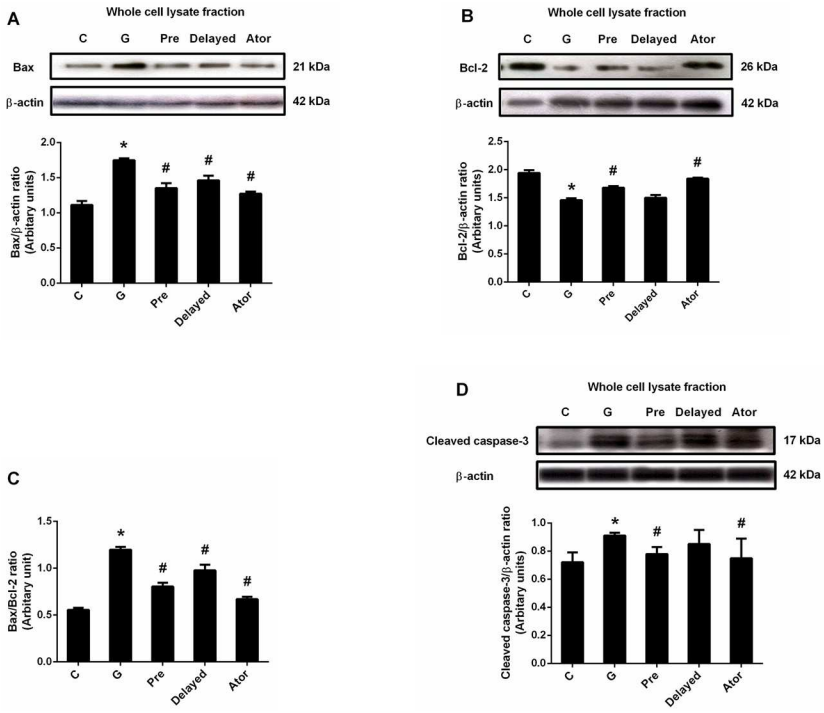

Fig 5. Effects of atorvastatin on the expression of Bax, Bcl-2 and cleaved caspase-3. Immunoblot analysis for Bax (A) Bcl-2 (B) Bax/ Bcl-2 ratio (C) and cleaved caspase-3 (D) expressions in the whole cell lysate fraction of renal cortical tissues normalized to β-actin. Bar graph indicates mean ± SEM. (n = 6 rats in each group). *P < 0.05 compared to the control group. #P < 0.05 compared to the gentamicin-treated group. C: control group; G: gentamicin-treated group; Pre: atorvastatin pretreatment group; Delayed: delayed treatment group and Ator: atorvastatin group.

doi:10.1371/journal.pone.0164528.g005

100 mg/kg/day for 15 days via intraperitoneal injection demonstrated renal dysfunction as shown by the increased serum creatinine and BUN.

Numbers of evidence showing that statins exert beneficial effects independent of its lipid lowering ability, called pleiotropic effects [30]. Clinical studies showed that atorvastatin, a 3-hydroxy-3-methylglutaryl coenzyme A (HMG-CoA) reductase inhibitor, administration improved ventricular ejection fraction, attenuated adverse effect ventricular remodeling and depressed the inflammation process in heart failure patients [31,32]. Furthermore, atorvastatin also decreased the apoptosis of myocardial cells in rat heart failure model [33]. Nevertheless, the role of atorvastatin in gentamicin-induced nephrotoxicity is still poorly known.

Gentamicin cytotoxicity occurs in the cell types in which the drug accumulates. In the kidneys, these cells constitute the tubular epithelial cells in the cortex, mainly in the proximal tubule of experimental animals and humans [34,35]. The expression of a transporter of proteins and cations, the giant endocytic complex formed by megalin and cubilin, which is restricted to the proximal tubule, is consistent with a higher accumulation of gentamicin and responsible for the transport of gentamicin into these cells. We therefore investigated protein expression in the kidney cortex where the proximal tubule is located. The present study showed that nephrotoxicity induced by gentamicin was characterized by a marked increase in serum creatinine and BUN levels along with a significant reduction in rate of creatinine clearance and histological changes. Moreover, kidney injury in gentamicin-treated rats was evidenced by the increased renal expressions of NF-κB as well as IL-6, iNOS and TNFαR1. These effects were accompanied by increases in the ER stress markers (including calpain, caspase 12, GRP78 and

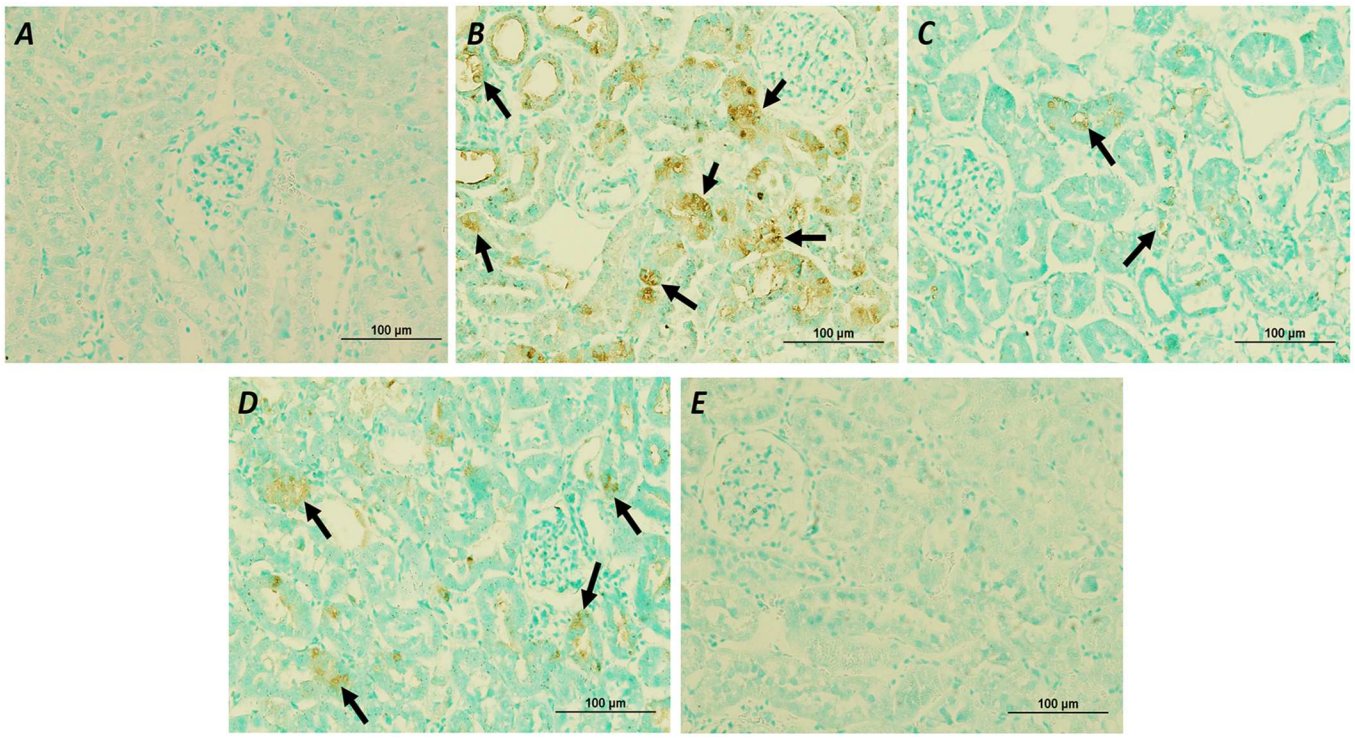

Fig 6. Effects of atorvastatin on apoptotic cells in kidney tissues. Apoptotic cells within kidney tissues were evaluated by TUNEL assays in control (A), gentamicin-treated (B), atorvastatin pretreatment (C), atorvastatin delayed treatment (D) and atorvastatin only (E) rats. TUNEL-positive cells were predominantly located at the renal tubules of the renal cortex (black arrow).

doi:10.1371/journal.pone.0164528.g006

CHOP) and pro-apoptotic Bax and cleaved caspase-3 with a decrease in antiapoptotic Bcl-2 which induced renal apoptosis. Atorvastatin treatment at dose 10 mg/kg significantly improved renal function, and ameliorated renal inflammation, ER stress and apoptosis in gentamicin-treated rat.

Renal injury as a consequence of gentamicin-induced tubular necrosis has been shown to accompany with increased inflammatory events at the site of injury and to enhance the migration of monocytes and macrophages to the site of tissue damage [4]. NF-κB is a key transcription factor in the renal inflammatory process by regulating the gene expression of cytokines, chemokines, adhesion molecules and iNOS which provoke kidney damage [36–38]. We determined the classical pathway of NF-κB which activated by inflammation or ROS induced by gentamicin injection. In the classical pathway, NF-κB proteins are bound and inhibited by IκB proteins. Proinflammatory cytokines including LPS, growth factors, and antigen receptors activate an IKK complex then IκB proteins are phosphorylated. Phosphorylation of IκB leads to its ubiquitination and proteasomal degradation resulting in freeing IκB complexes. Active NF-κB translocates to the nucleus inducing target gene involve proinflammatory cytokine [23,36,39,40]. In this study, gentamicin induced renal injury and activated inflammatory response, free NF-κB dimers translocate to nucleus and activate the target genes such as iNOS and IL-6 expressions. The increased activation and nuclear translocation of the NF-κB were evidenced by the increased NF-κB expression in both whole cell lysate and nuclear fractions in renal cortical tissue. The activation of NF-κB was accompanied with the increased iNOS and TNFαR1 expressions and interstitial mononuclear cells infiltration in gentamicin-treated rats suggesting that NF-κB may play a role in renal inflammation in this study. Previous study in type 2 diabetic rat showed that the endothelial dysfunction was resulted from overexpression of TNFαR [41]. Thus, an increased

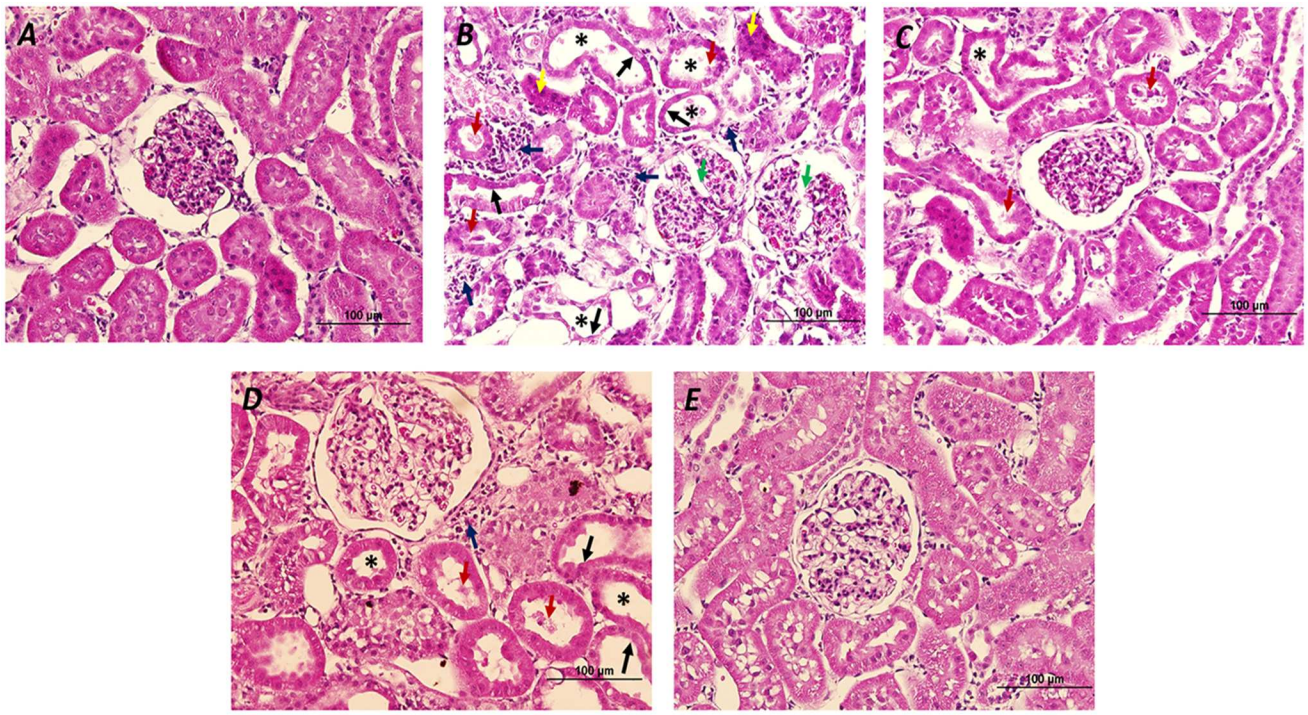

Fig 7. Effects of atorvastatin on histological changes of the kidneys. Hematoxylin- and Eosin-stained kidney tissue sections were performed in control (A); gentamicin-treated (B); atorvastatin pretreatment (C); atorvastatin delayed treatment (D) and atorvastatin only (E) groups. Glomerular degeneration (green arrow), mononuclear cells infiltration (blue arrow), pyknotic nuclei (yellow arrow), renal tubular desquamation (red arrow), renal tubular atrophy (black arrow) and renal tubular dilatation (asterisk) were indicated.

doi:10.1371/journal.pone.0164528.g007

membrane expression of TNFαR1 in the present study might imply an elevation of TNFα activity in the kidneys in gentamicin-treated rat. The results of this study corroborated those found in a previous study which demonstrated that an increased NF-κB activation in gentamicin-treated rats was followed by increasing the synthesis of inflammatory substances. Moreover, TNFα also activates the NF-κB pathway, thus resulting in amplification of the inflammatory response [42]. Atorvastatin pretreatment or delayed treatment decreased the expressions of NF-κB, IL-6, iNOS and TNFαR1 and interstitial mononuclear cells infiltration in gentamicin-treated rat. These findings suggest that atorvastatin improves renal inflammation by attenuating the activation of the NF-κB pathway. This is in agreement with the anti-inflammatory effects of atorvastatin found in heart failure [43], obstructive uropathy [44] and endotoxemia [45]. Additionally, previous studies demonstrated that gentamicin increased macrophage infiltration and elevated TGFβ1 level leading to the progression of tubulointerstitial nephritis [26,46]. An expression of TGFβ1 showed a strong correlation with fibrosis of smooth muscle layer in rats with unilateral ureteral obstruction [44]. In animal models with ureter obstruction, statins have been reported to inhibit inflammatory mediators and macrophage infiltration [47], and to suppress TGFβ1 expression and extracellular matrix production [48,49]. The current results, compatible with the study of Chuang et al [44], showed that atorvastatin pre or delayed treatment markedly down regulated not only IL-6, iNOS and TNFαR1 but also TGFβ1 expression in gentamicin-treated rats. The reduction in inflammatory gene expression is in accordance with the reduced inflammatory infiltrate seen in the histological study in atorvastatin treatment and previous study [15]. These imply that atorvastatin pre or delayed treatment may ameliorate the tissue damage in

gentamicin-induced nephrotoxicity via the inhibition of the TGFβ1 expression and by suppression of pro-inflammation cytokines production.

The significant increases of calpain, caspase 12, GRP78 and CHOP expressions in renal cortical tissue in this study reflected that gentamicin treatment induced ER stress and caused the activation of ER-mediated cell death markers. The activation of ER stress is one of the underlying mechanisms enabling the protection and repair in stress-induced cellular disorder by inducing cell apoptosis [33]. Calpain is responsible for cleaving pro-caspase 12 to active caspase 12. In this study, an up-regulation of cleaved caspase 3 in gentamicin-treated rats showed a correlation with an increased expression of caspase 12. Caspase 12 was translocated from ER to the cytosol and procaspase 9 was directly cleaved, which, in turn, activated caspase 3 leading to cell death [50]. It was noteworthy that the increased expression of calpain, caspase 12, GRP78 and CHOP were significantly suppressed by atorvastatin treatment, particularly pretreatment. Consistently, atorvastatin had been shown to decrease the rate of cell apoptosis and the expression of proteins involved in the ER stress response and apoptosis such as GRP78, caspase 12 and C/EBP homologous protein in myocardial cells in a rat model with post-myocardial infarction heart failure [33]. In this study, gentamicin treatment also caused a reduced expression of Bcl-2 accompanied with the elevated expression of Bax, the Bax/Bcl-2 ratio, cleaved caspase 3 and the increased TUNEL-positive cells, suggesting that gentamicin-induced renal damage was associated with the activation of apoptotic pathway. Atorvastatin pre or delayed treatment provided renoprotection by inhibiting Bax overexpression induced by gentamicin with an enhanced Bcl-2 expression, although the decreased expression of cleaved caspase-3 was presented only in pretreatment. According to the report that NF-κB activation promoted gentamicin-induced apoptosis in rat tubular cells [5], the anti-inflammatory effects of atorvastatin may partly be attributed to its suppression of gentamicin-induced apoptosis. In this study, it might be suggested that atorvastatin protects against renal tubular cell apoptosis induced by gentamicin partly by down-regulating the activation of ER stress and NF-κB pathways. These proposed mechanisms are confirmed by the previous study demonstrating that atorvastatin acts a potent scavenger of free radicals in the kidney leading to the inhibition of MAPK and NF-κB signaling pathways to prevent gentamicin-induced renal toxicity [20].

In conclusion, this study provides evidence that atorvastatin can reduce gentamicin induced NF-κB activation as well as inhibiting inflammatory, ER stress and apoptotic pathways. The effect of atorvastatin in protecting from renal damage induced by gentamicin seems to be more effective when it was given prior to gentamicin exposure.

Author Contributions

Conceptualization: AL AP NC.

Formal analysis: AL AP KJ.

Funding acquisition: AL AP NC VC.

Investigation: AL AP KJ LT KW PA.

Methodology: AL AP KJ NC LT KW PA.

Project administration: AL.

Software: KJ.

Supervision: AL AP NC VC.

Validation: AL AP KJ LT KW PA NC VC.

Visualization: AL AP KJ.

Writing – original draft: AL AP KJ.

Writing – review & editing: AL AP KJ NC VC.

References

1. Ajami M, Eghtesadi S, Pazoki-Toroudi H, Habibey R, Ebrahimi SA (2010) Effect of crocus sativus on gentamicin induced nephrotoxicity. Biol Res 43: 83–90. doi: 10.4067/S0716-97602010000100010 PMID: 21157635
2. Laurent G, Kishore BK, Tulkens PM (1990) Aminoglycoside-induced renal phospholipidosis and nephrotoxicity. Biochem Pharmacol 40: 2383–2392. doi: 10.1016/0006-2952(90)90078-Y PMID: 2268362
3. Martinez-Salgado C, Lopez-Hernandez FJ, Lopez-Novoa JM (2007) Glomerular nephrotoxicity of aminoglycosides. Toxicol Appl Pharmacol 223: 86–98. doi: 10.1016/j.taap.2007.05.004 PMID: 17602717
4. Balakumar P, Rohilla A, Thangathirupathi A (2010) Gentamicin-induced nephrotoxicity: Do we have a promising therapeutic approach to blunt it? Pharmacol Res 62: 179–186. doi: 10.1016/j.phrs.2010.04.004 PMID: 20434560
5. Juan SH, Chen CH, Hsu YH, Hou CC, Chen TH, Lin H, et al. (2007) Tetramethylpyrazine protects rat renal tubular cell apoptosis induced by gentamicin. Nephrol Dial Transplant 22: 732–739. doi: 10.1093/ndt/gfl699 PMID: 17132701
6. Lee IC, Kim SH, Lee SM, Baek HS, Moon C, Kim SH, et al. (2012) Melatonin attenuates gentamicin-induced nephrotoxicity and oxidative stress in rats. Arch Toxicol 86: 1527–1536. doi: 10.1007/s00204-012-0849-8 PMID: 22526374
7. Sue YM, Cheng CF, Chang CC, Chou Y, Chen CH, Juan SH (2009) Antioxidation and anti-inflammation by haem oxygenase-1 contribute to protection by tetramethylpyrazine against gentamicin-induced apoptosis in murine renal tubular cells. Nephrol Dial Transplant 24: 769–777. doi: 10.1093/ndt/gfn545 PMID: 18842672
8. Romero F, Perez M, Chavez M, Parra G, Durante P (2009) Effect of uric acid on gentamicin-induced nephrotoxicity in rats—role of matrix metalloproteinases 2 and 9. Basic Clin Pharmacol Toxicol 105: 416–424. doi: 10.1111/j.1742-7843.2009.00466.x PMID: 19821833
9. Zhang F, Hamanaka RB, Bobrovnikova-Marjon E, Gordan JD, Dai MS, Lu H, et al. (2006) Ribosomal stress couples the unfolded protein response to p53-dependent cell cycle arrest. J Biol Chem 281: 30036–30045. doi: 10.1074/jbc.M604674200 PMID: 16893887
10. Fribley A, Zhang K, Kaufman RJ (2009) Regulation of apoptosis by the unfolded protein response. Methods Mol Biol 559: 191–204. doi: 10.1007/978-1-60327-017-5_14 PMID: 19609758
11. Bertolotti A, Zhang Y, Hendershot LM, Harding HP, Ron D (2000) Dynamic interaction of BiP and ER stress transducers in the unfolded-protein response. Nat Cell Biol 2: 326–332. doi: 10.1038/35014014 PMID: 10854322
12. Kim I, Xu W, Reed JC (2008) Cell death and endoplasmic reticulum stress: disease relevance and therapeutic opportunities. Nat Rev Drug Discov 7: 1013–1030. doi: 10.1038/nrd2755 PMID: 19043451
13. Oyadomari S, Mori M (2004) Roles of CHOP/GADD153 in endoplasmic reticulum stress. Cell Death Differ 11: 381–389. doi: 10.1038/sj.cdd.4401373 PMID: 14685163
14. Reiss AB, Wirkowski E (2009) Statins in neurological disorders: mechanisms and therapeutic value. Scientific World J 9: 1242–1259. doi: 10.1100/tsw.2009.141 PMID: 19882094
15. Ferro D, Parrotto S, Basili S, Alessandri C, Violi F (2000) Simvastatin inhibits the monocyte expression of proinflammatory cytokines in patients with hypercholesterolemia. J Am Coll Cardiol 36: 427–431. doi: 10.1016/S0735-1097(00)00771-3 PMID: 10933353
16. Solheim S, Seljeflot I, Arnesen H, Eritsland J, Eikvar L (2001) Reduced levels of TNF alpha in hypercholesterolemic individuals after treatment with pravastatin for 8 weeks. Atherosclerosis 157: 411–415. PMID: 11472741
17. Garjani A, Andalib S, Ziaee M, Maleki-Dizaji N (2008) Biphasic effects of atorvastatin on inflammation. Pak J Pharm Sci 21: 125–130. PMID: 18390442
18. Niwa S, Totsuka T, Hayashi S (1996) Inhibitory effect of fluvastatin, an HMG-CoA reductase inhibitor, on the expression of adhesion molecules on human monocyte cell line. Int J Immunopharmacol 18: 669–675. doi: 10.1016/S0192-0561(96)00068-9 PMID: 9089010

19. Wahane VD, Kumar VL (2010) Atorvastatin ameliorates inflammatory hyperalgesia in rat model of monoarticular arthritis. Pharmacol Res 61: 329–333. doi: 10.1016/j.phrs.2009.11.006 PMID: 19931618

20. Ozbek E, Cekmen M, Ilbey YO, Simsek A, Polat EC, Somay A (2009) Atorvastatin prevents gentamicin-induced renal damage in rats through the inhibition of p38-MAPK and NF-kappaB pathways. Ren Fail 31: 382–392. PMID: 19839839

21. Eshraghi-Jazi F, Talebi A, Mirsaeedi FS, Ahmadian S, Moslemi F, Nematbakhsh M (2016) Gentamicin Induced Nephrotoxicity: The Role of Sex Hormones in Gonadectomized Male and Female Rats. Scientifica (Cairo) 2016: 5025097. doi: 10.1155/2016/5025097 PMID: 27213082

22. Gautier JC, Gury T, Guffroy M, Masson R, Khan-Malek R, Hoffman D, et al. (2014) Comparison between male and female Sprague-Dawley rats in the response of urinary biomarkers to injury induced by gentamicin. Toxicol Pathol 42: 1105–1116. doi: 10.1177/0192623314524489 PMID: 24717899

23. Promsan S, Jaikumkao K, Pongchaidecha A, Chattipakorn N, Chatsudthipong V, Arjinajarn P, et al. (2016) Pinocembrin attenuates gentamicin-induced nephrotoxicity in rats. Can J Physiol Pharmacol 94: 808–818. doi: 10.1139/cjpp-2015-0468 PMID: 27245556

24. Jaikumkao K, Pongchaidecha A, Chattipakorn N, Chatsudthipong V, Promsan S, Arjinajarn P, et al. (2016) Atorvastatin improves renal organic anion transporter 3 and renal function in gentamicin-induced nephrotoxicity in rats. Exp Physiol 101: 743–753. doi: 10.1113/EP085571 PMID: 27005971

25. Kalayarasan S, Prabhu PN, Sriram N, Manikandan R, Arumugam M, Sudhandiran G (2009) Diallyl sulfide enhances antioxidants and inhibits inflammation through the activation of Nrf2 against gentamicin-induced nephrotoxicity in Wistar rats. Eur J Pharmacol 606: 162–171. doi: 10.1016/j.ejphar.2008.12.055 PMID: 19374873

26. Geleilete TJ, Melo GC, Costa RS, Volpini RA, Soares TJ, Coimbra TM (2002) Role of myofibroblasts, macrophages, transforming growth factor-beta endothelin, angiotensin-II, and fibronectin in the progression of tubulointerstitial nephritis induced by gentamicin. J Nephrol 15: 633–642. PMID: 12495276

27. Lan HY (2011) Diverse roles of TGF-beta/Smads in renal fibrosis and inflammation. Int J Biol Sci 7: 1056–1067. PMID: 21927575

28. Tan KH, Mulheran M, Knox AJ, Smyth AR (2003) Aminoglycoside prescribing and surveillance in cystic fibrosis. Am J Respir Crit Care Med 167: 819–823. doi: 10.1164/rccm.200109-012CC PMID: 12623858

29. Rodrigues FA, Prata MM, Oliveira IC, Alves NT, Freitas RE, Monteiro HS, et al. (2014) Gingerol fraction from Zingiber officinale protects against gentamicin-induced nephrotoxicity. Antimicrob Agents Chemother 58: 1872–1878. doi: 10.1128/AAC.02431-13 PMID: 24395230

30. Liao JK, Laufs U (2005) Pleiotropic effects of statins. Annu Rev Pharmacol Toxicol 45: 89–118. doi: 10.1146/annurev.pharmtox.45.120403.095748 PMID: 15822172

31. Hayashidani S, Tsutsui H, Shiomi T, Suematsu N, Kinugawa S, Ide T, et al. (2002) Fluvastatin, a 3-hydroxy-3-methylglutaryl coenzyme a reductase inhibitor, attenuates left ventricular remodeling and failure after experimental myocardial infarction. Circulation 105: 868–873. doi: 10.1161/hc0702.104164 PMID: 11854129

32. Sola S, Mir MQ, Lerakis S, Tandon N, Khan BV (2006) Atorvastatin improves left ventricular systolic function and serum markers of inflammation in nonischemic heart failure. J Am Coll Cardiol 47: 332–337. doi: 10.1016/j.jacc.2005.06.088 PMID: 16412856

33. Song XJ, Yang CY, Liu B, Wei Q, Korkor MT, Liu JY, et al. (2011) Atorvastatin inhibits myocardial cell apoptosis in a rat model with post-myocardial infarction heart failure by downregulating ER stress response. Int J Med Sci 8: 564–572. doi: 10.7150/ijms.8.564 PMID: 21960749

34. Pattyn VM, Verpooten GA, Giuliano RA, Zheng F, De Broe ME (1988) Effect of hyperfiltration, proteinuria and diabetes mellitus on the uptake kinetics of gentamicin in the kidney cortex of rats. J Pharmacol Exp Ther 244: 694–698. PMID: 3346842

35. Verpooten GA, Giuliano RA, Verbist L, Eestermans G, De Broe ME (1989) Once-daily dosing decreases renal accumulation of gentamicin and netilmicin. Clin Pharmacol Ther 45: 22–27. doi: 10.1038/clpt.1989.4 PMID: 2910634

36. Bae EH, Kim IJ, Joo SY, Kim EY, Choi JS, Kim CS, et al. (2014) Renoprotective effects of the direct renin inhibitor aliskiren on gentamicin-induced nephrotoxicity in rats. J Renin Angiotensin Aldosterone Syst 15: 348–361. doi: 10.1177/1470320312474853 PMID: 23420778

37. Miller RP, Tadagavadi RK, Ramesh G, Reeves WB (2010) Mechanisms of Cisplatin nephrotoxicity. Toxins (Basel) 2: 2490–2518. doi: 10.3390/toxins2112490

38. Tak PP, Firestein GS (2001) NF-kappaB: a key role in inflammatory diseases. J Clin Invest 107: 7–11. doi: 10.1172/JCI11830 PMID: 11134171

39. Lawrence T (2009) The nuclear factor NF-kappaB pathway in inflammation. Cold Spring Harb Perspect Biol 1: a001651. doi: 10.1101/cshperspect.a001651 PMID: 20457564

40. Volpini RA, Costa RS, da Silva CG, Coimbra TM (2004) Inhibition of nuclear factor-kappaB activation attenuates tubulointerstitial nephritis induced by gentamicin. Nephron Physiol 98: p97–106. doi: 10.1159/000081558 PMID: 15627798

41. Gao X, Picchi A, Zhang C (2010) Upregulation of TNF-alpha and Receptors Contribute to Endothelial Dysfunction in Zucker Diabetic Rats. Am J Biomed Sci 2: 1–12. doi: 10.5099/aj100100001 PMID: 20559450

42. Ortiz A, Egido J (1995) Is there a role for specific anti-TNF strategies in glomerular diseases? Nephrol Dial Transplant 10: 309–311. PMID: 7792022

43. Castro PF, Miranda R, Verdejo HE, Greig D, Gabrielli LA, Alcaino H, et al. (2008) Pleiotropic effects of atorvastatin in heart failure: role in oxidative stress, inflammation, endothelial function, and exercise capacity. J Heart Lung Transplant 27: 435–441. doi: 10.1016/j.healun.2008.01.012 PMID: 18374881

44. Chuang YH, Chuang WL, Huang SP, Liu CK, Huang CH (2011) Atorvastatin ameliorates tissue damage of obstructed ureter in rats. Life Sci 89: 795–805. doi: 10.1016/j.lfs.2011.09.010 PMID: 21971118

45. McGown CC, Brookes ZL, Hellewell PG, Ross JJ, Brown NJ (2015) Atorvastatin reduces endotoxin-induced microvascular inflammation via NOSII. Naunyn Schmiedebergs Arch Pharmacol 388: 557–564. doi: 10.1007/s00210-015-1100-y PMID: 25678054

46. Bledsoe G, Crickman S, Mao J, Xia CF, Murakami H, Chao L, et al. (2006) Kallikrein/kinin protects against gentamicin-induced nephrotoxicity by inhibition of inflammation and apoptosis. Nephrol Dial Transplant 21: 624–633. doi: 10.1093/ndt/gfi225 PMID: 16401625

47. Weitz-Schmidt G (2002) Statins as anti-inflammatory agents. Trends Pharmacol Sci 23: 482–486. doi: 10.1016/S0165-6147(02)02077-1 PMID: 12368073

48. Ota T, Takamura T, Ando H, Nohara E, Yamashita H, Kobayashi K (2003) Preventive effect of cerivastatin on diabetic nephropathy through suppression of glomerular macrophage recruitment in a rat model. Diabetologia 46: 843–851. doi: 10.1007/s00125-003-1099-3 PMID: 12774163

49. Vieira JM Jr., Mantovani E, Rodrigues LT, Delle H, Noronha IL, Fujihara CK, et al. (2005) Simvastatin attenuates renal inflammation, tubular transdifferentiation and interstitial fibrosis in rats with unilateral ureteral obstruction. Nephrol Dial Transplant 20: 1582–1591. doi: 10.1093/ndt/gfh859 PMID: 15855201

50. Morishima N, Nakanishi K, Takenouchi H, Shibata T, Yasuhiko Y (2002) An endoplasmic reticulum stress-specific caspase cascade in apoptosis. Cytochrome c-independent activation of caspase-9 by caspase-12. J Biol Chem 277: 34287–34294. doi: 10.1074/jbc.M204973200 PMID: 12097332

Research Paper

Atorvastatin improves renal organic anion transporter 3 and renal function in gentamicin-induced nephrotoxicity in rats

Krit Jaikumkao[1], Anchalee Pongchaidecha[1], Nipon Chattipakorn[2], Varanuj Chatsudthipong[3], Sasivimon Promsan[4], Phatchawan Arjinajarn[5] and Anusorn Lungkaphin[1]

[1]*Department of Physiology, Faculty of Medicine, Chiang Mai University, Chiang Mai, Thailand*
[2]*Cardiac Electrophysiology Research and Training Center, Department of Physiology, Faculty of Medicine, Chiang Mai University, Chiang Mai, Thailand*
[3]*Department of Physiology, Faculty of Science, Mahidol University, Bangkok, Thailand*
[4]*Department of Physiology, Faculty of Medical Sciences, The University of Phayao, Phayao, Thailand*
[5]*Department of Biology, Faculty of Science, Chiang Mai University, Chiang Mai, Thailand*

Experimental Physiology

New Findings

- **What is the central question of this study?**
  This study was designed to determine the renoprotective effects of atorvastatin treatment in an experimental model of gentamicin-induced nephrotoxicity through modulating the Nrf2 pathway by decreasing the oxidative stress.
- **What is the main finding and its importance?**
  Atorvastatin exerts a nephroprotective effect by attenuating oxidative stress, protecting renal function and renal organic anion transporter 3 function from the effects of gentamicin. Atorvastatin might protect the tissues via its antioxidant property and by modulating the antioxidant enzymes through the Nrf2 signalling pathway, which may be the underlying mechanisms of these protective effects.

Recent evidence demonstrates that statins, 3-hydroxy-3-methylglutaryl coenzyme A reductase inhibitors, exert not only lipid-lowering effects but also antioxidant, anti-inflammatory and anti-apoptotic effects. Nephrotoxicity, a serious side-effect of gentamicin, is related to an increase in reactive oxygen species in the kidney. This study was designed to determine the renoprotective effects of atorvastatin treatment in an experimental model of gentamicin-induced nephrotoxicity. Male Sprague–Dawley rats were used. Nephrotocixity was induced by I.P. injection of gentamicin, 100 mg kg^{-1} day^{-1}, for 15 days. Atorvastatin, 10 mg kg^{-1} day^{-1}, was administered by gavage 30 min before gentamicin injection (pretreatment) for 15 days or only on days 10–15 (post-treatment). Renal function and renal organic anion transporter 3 (Oat3) function and expression were examined. Gentamicin-treated rats demonstrated impaired renal function by attenuation of creatinine clearance and increased oxidative stress. Gentamicin treatment also decreased renal Oat3 function and expression as shown by decreased [^{3}H]estrone sulfate uptake into renal cortical slices and decreased expression. The protein expressions of protein kinase C, Nrf2, NAD(P)H:quinone oxidoreductase 1, haeme oxygenase 1 and glutamate–cysteine ligase were markedly increased in gentamicin-treated rats, indicating the increase in oxidative stress. Administration of atorvastatin improved renal function and alleviated oxidative stress, and atorvastatin pretreatment had a greater ability to decrease

 DOI: 10.1113/EP085571

oxidative stress than atorvastatin post-treatment. These effects helped to preserve renal function and Oat3 function and expression. These results indicate that atorvastatin has a renoprotective effect against gentamicin-induced nephrotoxicity by decreasing overoxidation in the kidney, and might be used in conjunction with gentamicin to protect against renal damage.

(Received 20 October 2015; accepted after revision 18 March 2016; first published online 23 March 2016)
Corresponding author A. Lungkaphin: Department of Physiology, Faculty of Medicine, Chiang Mai University, Chiang Mai, 50200, Thailand. Email: onanusorn@yahoo.com, anusorn.lungka@cmu.ac.th

Introduction

Atorvastatin (Ator) is a well-tolerated cholesterol-lowering statin that acts through the inhibition of 3-hydroxy-3-methylglutaryl coenzyme A (HMG-CoA) reductase, the rate-limiting enzyme in cholesterol biosynthesis via the mevalonate pathway (Liao & Laufs, 2005). During the past decade, evidence has emerged that statins also have overall beneficial effects greater than those expected from cholesterol lowering, such as antioxidant, anti-inflammatory and anti-apoptotic effects (Liao & Laufs, 2005). These effects appear to be independent of cellular cholesterol homeostasis and are collectively termed 'pleiotropic effects'. In addition to lowering cholesterol synthesis, inhibition of the HMG-CoA reductase reduces the synthesis of intermediates of the mevalonate pathway (Goldstein & Brown, 1990). It has been demonstrated that atorvastatin reduced lipoprotein oxidation and ameliorated free radical injury in lipoprotein isolated from hyperlipidaemic patients (Aviram *et al.* 1998). Study in diabetic mice demonstrated that the protective antioxidant effect of atorvastatin on vascular function in diabetes mellitus was mediated by inhibition of the activity of Rac-1, a small G-protein (Vecchione *et al.* 2007). However, at present little is known about the effects of statins on kidney function.

Aminoglycoside antibiotics, such as gentamicin, are the most commonly used antibiotics for treatment of Gram-negative bacterial infections (Ali, 2002). Despite their beneficial effects, gentamicin has a considerable nephrotoxic effect, which occurs in ∼20% of patients. The renal toxicity of gentamicin is related to its selective accumulation in the renal cortex, especially in the renal proximal convoluted tubules (Nagai & Takano, 2004), where it causes apoptosis and necrosis of the tubular epithelial cells (Quiros *et al.* 2011). Nephrotoxicity induced by gentamicin is related to an increase in the kidney of in reactive oxygen species (ROS), such as superoxide anions (O_2^-), hydrogen peroxide (H_2O_2) and hydroxyl radicals, released by renal cortical mitochondria (Walker & Shah, 1987; Du & Yang, 1994). Administration of antioxidant enzymes, such as superoxide dismutase (SOD), glutathione peroxidase, glutathione reductase and catalase, has been shown to ameliorate the severity of gentamicin-induced renal damage (Nasri *et al.* 2013).

The cellular response to oxidative stress is regulated by the Nrf2 signalling pathway (Zou *et al.* 2013). Oxidative and electrophilic stresses disrupt the Keap1–Nrf2 complex, which allows Nrf2 translocation into the nucleus, leading to the activation of the antioxidant response element (ARE) and upregulation of antioxidant-related enzyme expressions. Typical genes driven by Nrf2 include haeme oxygenase 1 (*HO1*), NAD(P)H:quinone oxidoreductase 1 (*NQO1*), glutamate–cysteine ligase (*GCL*), the rate-limiting enzyme in glutathione (GSH) synthesis, glutathione peroxidase (*GPx*) and superoxide dismutase (Yang *et al.* 2005; Franklin *et al.* 2009). In triptolide-induced renal injury, the Nrf2–ARE pathway showed a protective role by counteracting oxidative stress (Li *et al.* 2012). Thus, Nrf2–ARE responses are predicted to be activated by an increase in oxidative stress in the injured kidney induced by gentamicin.

Organic anion transporters 1 and 3 (Oat1 and Oat3), the important transporters located in the basolateral membrane of the renal proximal tubule, have roles in actively eliminating endogenous substances or organic anion compounds and their metabolites from the body (Habu *et al.* 2005). The Oat3 protein consists of 536–542 amino acids with 12 transmembrane domains and has potential phosphorylation sites that are regulated by protein kinase C (PKC; Saito, 2010). The regulation of Oat3 function has been studied extensively in the last decade. Recently, the downregulation of expression of Oat1 and Oat3 has been reported in rats with gentamicin-induced nephrotoxicity (Guo *et al.* 2013). Reduced renal Oat1 and Oat3 expression and function would contribute significantly to gentamicin-induced acute renal failure. It is therefore interesting to study the potential effect of atorvastatin on renal function and on Oat3 function and expression in nephrotoxicity induced by gentamicin.

Here, we examined the contribution of Nrf2 to renal protection in gentamicin-induced nephrotoxicity in rats. Furthermore, renal function and renal Oat3 function and expression were also examined. It was hypothesized that atorvastatin could preserve renal function in gentamicin-induced nephrotoxicity through modulation of the Nrf2 pathway.

Methods

Ethical approval, animal preparation and animal treatment

The male Sprague–Dawley rats (250–300 g), 10–12 weeks of age, used in this study were obtained from the National Laboratory Animal Center, Mahidol University, Salaya, Thailand. The animal facilities and protocols were approved by the Laboratory Animal Care and Use Committees at the Faculty of Medicine, Chiang Mai University, Chiang Mai, Thailand (permit no. 36/2557). All experimental rats were housed in a room maintained at 25 ± 1 °C on a 12 h–12 h light–dark cycle and fed with normal pelleted diet and water *ad libitum*. An *in vivo* study was performed to determine renal function, and an *in vitro* study (renal cortical slices) was carried out to determine the renal Oat3 function in an uptake experiment.

Thirty rats were randomly divided into five groups (six rats per group) as follows: (i) the vehicle control (C) group received normal saline by gavage; (ii) the gentamicin (G) group were injected I.P. with gentamicin at a dose of 100 mg kg^{-1} day^{-1} in a volume of 700–800 μl (The Government Pharmaceutical Organization, Thailand) for 15 days; (iii) in the atorvastatin (Ator) group, Ator (Lek Pharmaceuticals d.d., Ljubljana, Slovenia) dissolved in 500 μl of normal saline solution at a dose of 10 mg kg^{-1} day^{-1} was administered by gavage once a day for 15 days; (iv) in the atorvastatin pretreatment group, Ator was administered by gavage 30 min before the gentamicin treatment for 15 days; and (v) in the atorvastatin post-treatment group, gentamicin was injected every day for 15 days and Ator was administered only on days 10–15 by gavage 30 min before the gentamicin treatment on those days. After the last injected dose of gentamicin, a 24 h urine sample was collected. At the end of the study, the animals were killed by I.P. injection of sodium pentobarbital (Ceva Santé Animale, Libourne, France) at a dose of 100 mg kg^{-1}, after which inhalation of isofurane was used to maintain anaesthesia of the animal throughout the experiment. Then blood and kidney tissue samples were collected for subsequent experiments.

Determination of renal function

Serum blood urea nitrogen (BUN) and serum and urine creatinine were measured using an automatic biochemical analyser at the Clinical Laboratory, Maharaj Nakhon Chiang Mai Hospital, Chiang Mai, Thailand. Relative kidney weight was calculated according to the formula: (kidney weight/total body weight) × 100. The creatinine clearance (C_{cr}), which reflects glomerular filtration rate, was calculated using the following equation:

$$C_{cr}(\text{in ml min}^{-1}) = \frac{\text{Urine creatinine} \times \text{Urine flow rate}}{\text{Serum creatinine}}$$

Histopathological study

To determine any morphological changes, a kidney was removed and cut in a half along the transverse axis, fixed in 10% neutral buffered formalin and embedded in paraffin. Paraffin-embedded specimens were cut into 2-μm-thick sections, mounted on microscope slides and stained with Haematoxylin and Eosin for general histological assessment. The samples were examined under a light microscope for tubular and glomerular changes by an observer blinded to the animal treatment groups.

Determination of renal oxidative stress

In order to determine renal oxidative stress, the renal cortical tissue was cut and suspended in CellLyticMT/ extraction reagent (Sigma Aldrich, MO, USA). The tissues were homogenized and centrifuged at 1600 *g* at 4 °C for 10 min. The supernatant was collected to determine malondialdehyde (MDA) and GSH concentrations. Malondialdehyde is one of the end-products of lipid peroxidation in the cells. An increase in free radicals causes overproduction of MDA. The MDA level was determined using the thiobarbituric acid reactive substances (TBARS) assay kit (Cayman Chemical Company, Ann Arbor, MI, USA). The amount of MDA was expressed as nanomoles per milligram of protein. The total protein content of the renal cortical tissues was determined using a DC protein assay kit (Bio-Rad Laboratories, Hercules, CA, USA). The GSH level was determined by colorimetry using the QuantiChrom™ Glutathione Assay Kit (DIGT-250; BioAssay Systems, Hayward, CA, USA). The supernatant was used, and the GSH level was determined by spectrophotometry at an absorbance of 400–450 nm.

In addition, the renal cortical tissue was homogenized in cold lysis buffer (Sigma Aldrich) and centrifuged at 12,000 *g* at 4 °C for 5 min. The supernatant was analysed to calculate the total SOD activity according to the manufacturer's instructions using the EnzyChrom™ Superoxide Dismutase Assay Kit (ESOD-100; BioAssay Systems).

Determination of renal Oat3 function

Renal Oat3 function was determined using a renal cortical slice uptake experiment. After the rat had been killed, the kidneys were removed, decapsulated and placed in PBS. Renal cortical slices (≤0.5 mm thick; 5–15 mg, wet weight) were cut with a Stadie-Riggs microtome and maintained in ice-cold oxygenated modified Cross and Taggart pH 7.4 buffer containing 95 mM NaCl, 80 mM mannitol, 5 mM KCl, 0.74 mM $CaCl_2$ and 9.5 mM Na_2HPO_4. The renal cortical slices were pre-incubated in the buffer for 10 min. Then, slices were incubated in 1 ml of uptake buffer containing 50 nM [^{3}H]estrone

sulfate ([^{3}H]ES; Perkin Elmer, Waltham, MA, USA) for 30 min at room temperature. The uptake was stopped by the addition of ice-cold buffer. Slices were rinsed, blotted, weighed and lysed in 0.5 ml of 1 N NaOH and neutralized with 0.5 ml of 1 N HCl. The radioactivity in the lysate was measured using a liquid scintillation analyser (Perkin Elmer). Transport of [^{3}H]ES into the cell/tissue was calculated as the tissue to medium (T/M) ratio [d.p.m. (g tissue)$^{-1}$ ÷ d.p.m. (ml medium)$^{-1}$].

Tissue preparation and Western blot analysis

The renal cortical tissues were used to carry out Western blot analysis. The renal cortex was gently cut from the outer part of the kidney, in sections extending down for approximately 3–4 mm, using a microtome. Each cellular compartment, whole-cell lysate, membrane and cytosolic fractions were prepared from renal cortical tissues using differential centrifugation techniques. Briefly, renal cortical slices were homogenized in mammalian cell lytic buffer (Sigma Aldrich) with a protease cocktail inhibitor (Roche, Indianapolis, IN, USA). Homogenates were centrifuged at 5000 *g* for 15 min at 4 °C. Some of the supernatants were collected as total cell lysates, and the remaining portion was centrifuged at 100,000 *g* for 2 h at 4 °C to obtain the membrane (pellet) and cytosolic (supernatant) fractions. The 5000 *g* pellet was resuspended and centrifuged at 10,000 *g* at 4 °C for 10 min. The supernatant fraction from the centrifugation was designated as the nuclear fraction.

Total cell lysates, cytosolic, nuclear and membrane fractions from the renal cortex were subjected to 10% SDS-PAGE, and subsequently, transferred to a polyvinylidene fluoride membrane (Millipore, Billerica, MA, USA). The membranes were then blocked with 5% non-fat dry milk in Tris-buffered saline (TBS) containing 0.1% Tween-20 (TBST) for 1 h at room temperature, and subsequently, probed with primary antibodies overnight at 4 °C. The primary antibodies for PKCα (Santa Cruz Biotechnology, Santa Cruz, CA, USA), Nrf2 (Santa Cruz Biotechnology), HO-1 (Abcam, Cambridge, MA, USA), NQO1 (Abcam), GCL (Abcam) and renal Oat3 (Cosmo Bio Co. Ltd., Tokyo, Japan) were used to determine protein expressions. Lamin b1 (Cell Signaling Technology, Danvers, MA, USA) or Na^+, K^+-ATPase (Millipore) was used as a marker for the nuclear or membrane fraction, respectively. β-Actin (Millipore) was used as a loading control for all samples. The membranes were washed three times with TBST and incubated with horseradish peroxidase-conjugated goat anti-rabbit or anti-mouse secondary antibodies (Amersham, Arlington Heights, IL, USA) at room temperature for 1 h and developed with ECL enhanced chemiluminescence agent (GE Healthcare, Little Chalfont, UK). Each membrane was stripped and re-probed with mouse anti-β-actin antibody or another antibody for further detection of protein expression. The densities of the protein signals on Hyperfilms (GE Healthcare) were analysed using ImageJ software (NIH, Bethesda, MD, USA). Protein levels were normalized to β-actin as a loading control.

Statistical analysis

Statistical analyses were conducted using SPSS (version 17; SPSS Inc., Chicago, IL, USA). All data were expressed as the means ± SEM. For comparison between multiple treatments, a one-way ANOVA followed by Fisher's least significant difference test was used. A value of $P < 0.05$ was considered significant.

Results

Effect of atorvastatin on renal function in gentamicin-treated rats

Gentamicin treatment resulted in a significant decrease in body weight (318.33 ± 8.78 g) and an increase in kidney weight (3.12 ± 0.17 g) when compared with the vehicle control group (350 ± 6.19 and 2.68 ± 0.05 g, respectively; $P < 0.05$; Table 1). In addition, gentamicin administration induced kidney hypertrophy, as demonstrated by a significant increase in kidney/body weight ratio in gentamicin-treated rats (0.98 ± 0.05) compared with the control group (0.76 ± 0.21; $P < 0.05$). Atorvastatin pretreatment significantly attenuated kidney weight (2.65 ± 0.08 g) and kidney/body weight ratio (0.84 ± 0.25) when compared with the gentamicin group ($P < 0.05$). However, atorvastatin post-treatment could not reverse these morphological alterations caused by gentamicin. The serum BUN and creatinine showed significant increases by 34 and 55% (26.83 ± 0.60 and 0.58 ± 0.03 mg dl^{-1}), respectively, in the gentamicin-treated group compared with the vehicle control group (20.00 ± 0.52 and 0.37 ± 0.01 mg dl^{-1}, respectively; $P < 0.05$). Moreover, C_{cr}, which reflects glomerular filtration rate, showed a significant decrease by 40% (1.10 ± 0.19 ml min^{-1}) in the gentamicin-treated group when compared with the vehicle control group (1.86 ± 0.28 ml min^{-1}; $P < 0.05$). Interestingly, atorvastatin pre- and post-treatment resulted in an improvement in renal function compared with the gentamicin-treated group ($P < 0.05$; Table 1).

Effect of atorvastatin on renal morphology

Hematoxylin- and Eosin-stained kidney tissue sections from rats in each group are shown in Fig. 1. Kidney tissue from the control (Fig. 1*A*) and atorvastatin (Fig. 1*E*) groups showed normal glomerular and tubular structures, including interstitial cell, tubular and vessel structures. Gentamicin-treated rats demonstrated tubular

Table 1. Effects of atorvastatin on physiological and renal function parameters

Group	Body weight (g)	Kidney weight (g)	Kidney/body weight ratio	Serum creatinine (mg dl^{-1})	Serum blood urea nitrogen (mg dl^{-1})	Creatinine clearance (ml min^{-1})
Control	350.00 ± 6.19	2.68 ± 0.05	0.76 ± 0.21	20.00 ± 0.52	0.37 ± 0.01	1.86 ± 0.28
Gentamicin only	318.33 ± 8.78*	3.12 ± 0.17*	0.98 ± 0.05*	26.83 ± 0.60*	0.58 ± 0.03*	1.10 ± 0.19*
Gentamicin with atorvastatin pretreatment	323.00 ± 8.73	2.65 ± 0.08†	0.84 ± 0.25†	23.50 ± 0.99†	0.48 ± 0.02†	2.02 ± 0.23†
Gentamicin with atorvastatin post-treatment	289.00 ± 12.08	2.71 ± 0.24	0.92 ± 0.09	23.33 ± 0.80†	0.49 ± 0.02†	1.76 ± 0.05†
Atorvastatin only	349.16 ± 6.09†	2.60 ± 0.07†	0.74 ± 0.01†	20.85 ± 0.95†	0.34 ± 0.01†	1.79 ± 0.17†

Values are means ± SEM ($n = 6$ rats in each group). *$P < 0.05$ *versus* control. †$P < 0.05$ *versus* gentamicin.

atrophy, tubular dilatation, cellular desquamation, tubular epithelial cell damage and interstitial inflammation, while normal glomerular structure and blood vessels were noted (Fig. 1*B*). Atorvastatin pre- and post-treatments could preserve kidney morphology in this study (Fig. 1*C* and *D*, respectively).

Effects of atorvastatin on renal Oat3 function and expression

Gentamicin treatment significantly reduced [^{3}H]ES uptake into renal cortical slices ($P < 0.05$; Fig. 2) concomitant with a significant decrease in the expression of renal Oat3 protein in the membrane fraction ($P < 0.05$; Fig. 3*B*) when compared with the vehicle control rats. There was no significant difference in renal Oat3 expression in the whole-cell lysate fraction among experimental groups (Fig. 3*A*). Compared with the gentamicin-treated group, atorvastatin pre- and post-treatments significantly increased both the uptake of [^{3}H]ES into the renal cortical slices by 43 and 27%, respectively (Fig. 2) and the renal Oat3 protein expression by 39 and 23%, respectively (Fig. 3*B*), reflecting the improved renal Oat3 function ($P < 0.05$).

Effects of atorvastatin on renal oxidative damage

The renal cortical level of MDA, an end-product of lipid peroxidation, was significantly increased after gentamicin treatment when compared with that of the vehicle control group (Fig. 4*A*). In the gentamicin-treated group, the GSH level showed a marked increase (Fig. 4*B*),

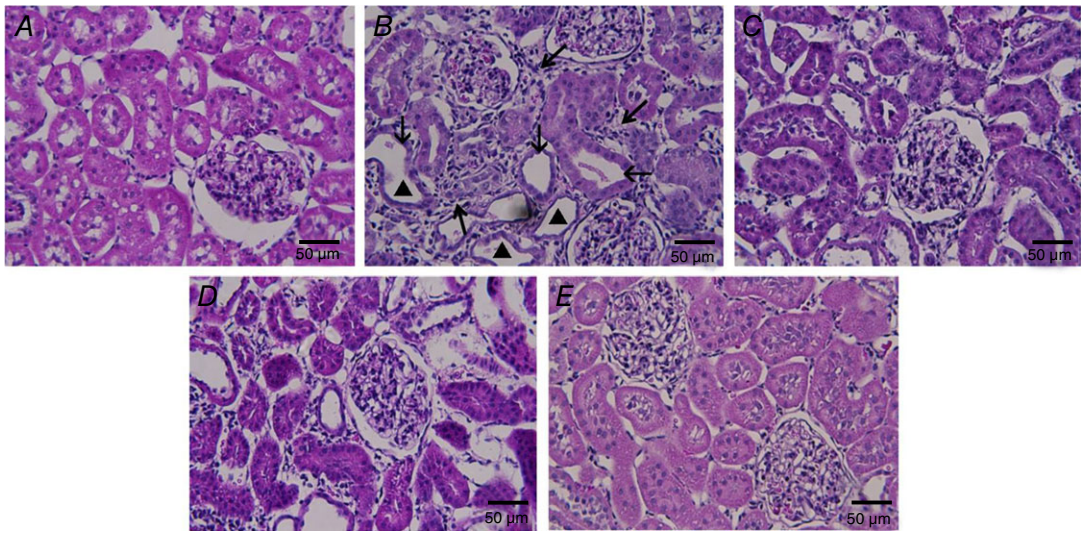

Figure 1. Photograph of histological sections of the kidney
Haematoxylin and eosin stain (scale bar = 50 μm); *A*, *B*, *C*, *D* and *E* are images of glomeruli and renal tubules from control, gentamicin-treated, atorvastatin pretreatment, atorvastatin post-treatment and atorvastatin -treated rats, respectively. The tubular atrophy, dilatation and interstitial inflammation (*B*) in kidney from gentamicin-treated rats are indicated with the arrowheads, arrows and black arrows, respectively.

whereas SOD activity was significantly reduced (Fig. 4*C*) in relation to the vehicle control group. Atorvastatin pre- and post-treatments significantly reduced the MDA level when compared with the gentamicin-treated group ($P < 0.05$; Fig. 4*A*). Moreover, the decreased MDA level in atorvastatin-pretreated rats (35%) was significantly greater than that in atorvastatin post-treated rats (21%; $P < 0.05$; Fig. 4*A*). The SOD activities were significantly increased by 14 and 9% in atorvastatin pre- and post-treatments, respectively (Fig. 4*C*), whereas the

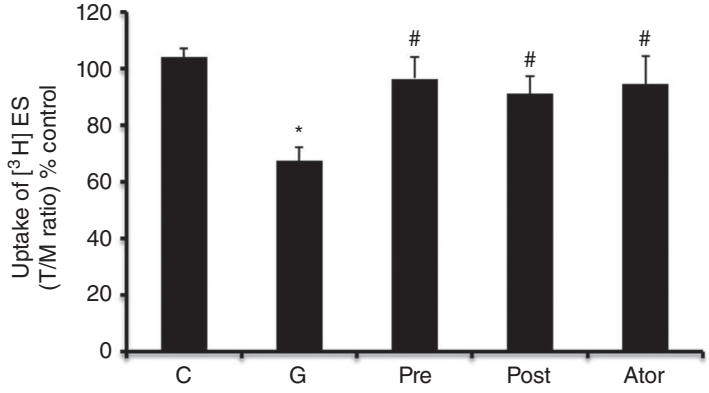

Figure 2. Effect of atorvastatin on [^{3}H]estrone sulfate ([^{3}H]ES) uptake into renal cortical slices
Renal cortical slices were incubated in an uptake buffer containing 50 nM [^{3}H]ES for 30 min at room temperature. The uptake was calculated as tissue/medium (T/M) ratio and then converted to a mean percentage of the control value. Values are shown as means + SEM ($n = 6$ rats in each group and five renal slices per animal were used). For comparison between multiple treatments, a one-way ANOVA followed by Fisher's least significant difference test was used. $^*P < 0.05$ compared with the control group. $^\#P < 0.05$ compared with the gentamicin-treated group. Abbreviations: Ator, atorvastatin group; C, control group; G, gentamicin-treated group; Pre, atorvastatin-pretreated group; and Post, atorvastatin post-treated group.

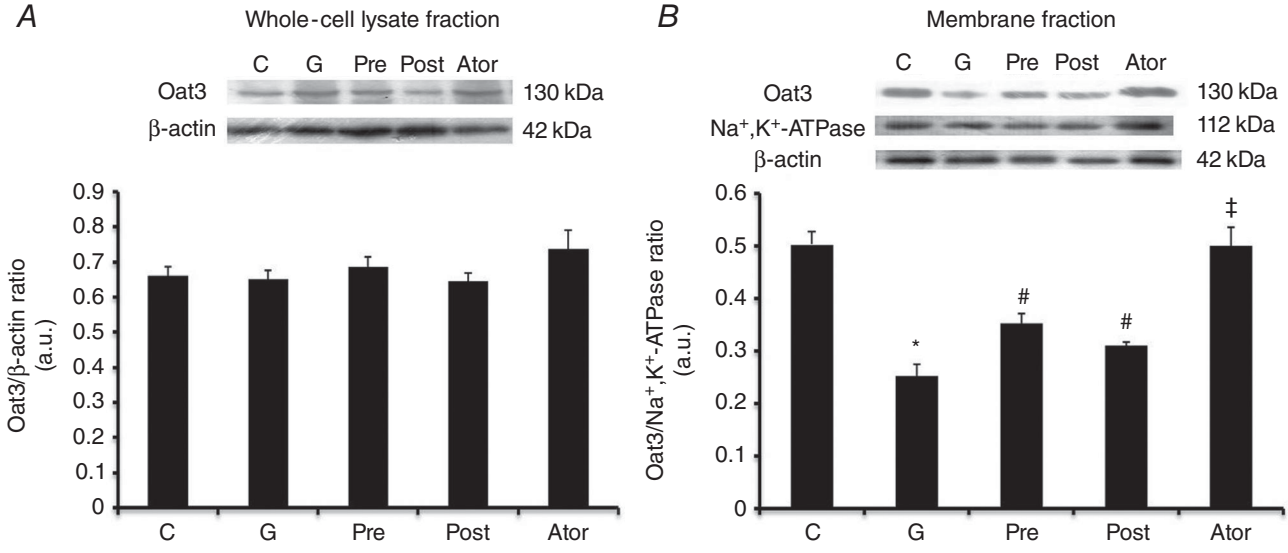

Figure 3. Effect of atorvastatin on the protein expression of renal organic anion transporter 3 (Oat3) in renal cortical tissues
A and *B* show the representative immunoblot analyses for Oat3 in the whole-cell lysate and membrane fraction of renal cortical tissues normalized by Na^+, K^+-ATPase. The bar graphs show the means + SEM ($n = 6$ rats in each group). For comparison between multiple treatments, a one-way ANOVA followed by Fisher's least significant difference test was used. $^*P < 0.05$ compared with the control group. $^\#P < 0.05$ compared with the gentamicin-treated group. Abbreviations are as in Fig. 2.

GSH level was significantly decreased by 27 and 24%, respectively, compared with the gentamicin-treated group ($P < 0.05$; Fig. 4*B*).

As shown in Fig. 5, a significant increase in PKCα protein expression in gentamicin-treated rats in this study was consistent with the previous reports showing that the overproduction of ROS could activate PKCα, which in turn inhibited Oat3 translocation to the membrane and decreased Oat3 function (Arjinajarn *et al.* 2014). Atorvastatin pre- and post-treatment significantly reduced PKCα expression when compared with the gentamicin-treated rats ($P < 0.05$).

Effects of atorvastatin on renal protein expression of Nrf2 and antioxidant enzymes

To gain further insight into the mechanisms underlying the beneficial effects of atorvastatin on gentamicin-induced oxidative stress in the kidney, the expressions of proteins that are involved in the oxidative stress pathway, including Nrf2, NQO1, HO-1 and GCL, in the renal cortex were investigated. Gentamicin treatment induced a significant increase in Nrf2 expression in the nucleus when compared with the vehicle control rats, suggesting an increase in Nrf2 activation ($P < 0.05$; Fig. 6*B*). In fact, a high expression of Nrf2 in gentamicin-treated rats was also observed in the whole-cell lysate fraction, reflecting the increase in Nfr2 protein synthesis inside the cells (Fig. 6*A*). The activation of Nrf2 induced an increase in the protein expressions of antioxidant enzymes, including NQO1, HO-1 and GCL, in gentamicin-treated rats (Fig. 6*C*, *D* and *E*, respectively). Atorvastatin pre- and post-treatment resulted in a significant inactivation of Nrf2 protein as shown by decreased nuclear translocation and protein expression. The protein expressions of NQO1, HO-1and GCL in atorvastatin pre- and post-treatments were significantly reduced when compared with those of the gentamicin-treated rats ($P < 0.05$), which were related to the expression of Nrf-2.

Discussion

The results obtained from this study showed that gentamicin administration produced a typical pattern of nephrotoxicity, which was manifested by markedly elevated serum BUN and creatinine levels, decreased creatinine clearance (or glomerular filtration rate), reduced renal Oat3 function and increased oxidative stress in renal cortical tissues. Atorvastatin pre- and post-treatments significantly improved renal function. In addition, treatment with atorvastatin showed ameliorative effects against gentamicin-induced nephrotoxicity by reducing oxidative stress and improving renal function and Oat3 function and expression.

A previous study has reported that the elevations in serum creatinine and BUN levels in gentamicin-induced

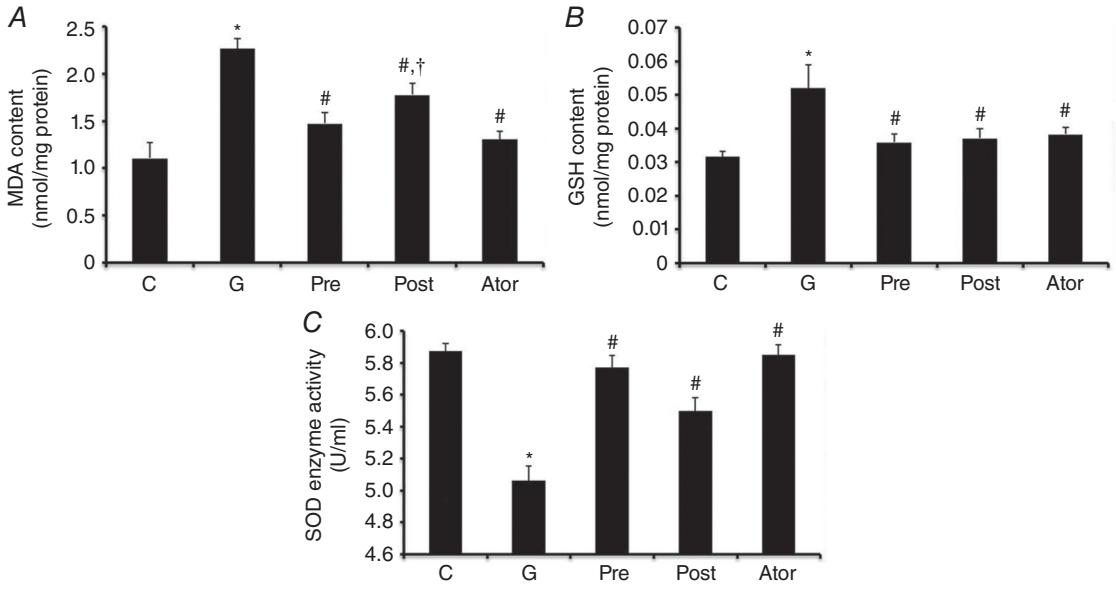

Figure 4. Effect of atorvastatin on renal cortical malondialdehyde (MDA; *A*) and glutathione contents (GSH; *B*) and superoxide dismutase (SOD) activity (*C*)
Values are shown as means + SEM ($n = 6$ rats in each group). For comparison between multiple treatments, a one-way ANOVA followed by Fisher's least significant difference test was used. $^{*}P < 0.05$ compared with the control group. $^{\#}P < 0.05$ compared with the gentamicin-treated group. $^{\dagger}P < 0.05$ compared with the atorvastatin-pretreated group. Abbreviations are as in Fig. 2.

nephrotoxicity are associated with the overproduction of free radicals (Balakumar *et al.* 2010). Increased hydrogen peroxide generation and lipid peroxidation, concomitant with a decreased glutathione level in the renal cortex, were observed in gentamicin-treated rats (Nasri *et al.* 2013). Gentamicin induces oxidative stress in renal tubular cells, principally involving ROS production of mitochondrial ROS, such as superoxide anions and hydroxyl radicals, from the respiratory chain (Ahn *et al.* 2012). The interaction of ROS with cellular components may result in damage to DNA, cellular proteins and lipids by inhibition of the electron transport chain and subsequent ATP production. Moreover, the release of cytochrome *c*, an inducer of caspase-dependent death, from the mitochondrial intermembrane space, induces cell cycle arrest as a result of DNA damage, lipid peroxidation, membrane destabilization, inhibition of the Na^+, K^+-ATPase pump, which leads to cellular swelling, loss of membrane integrity and necrosis (Yazar *et al.* 2003; Quiros *et al.* 2011). Malondialdehyde, an indicator of peroxidative damage, can be identified easily in the biological structures in terms of the lipid peroxidation and is generally used for the evaluation of lipid peroxidation. These observations were confirmed by histopathological changes, such as tubular dilatation or tubular epithelial call damage, and an elevation in the renal cortical MDA level, in gentamicin-treated rats in the present study.

A significant decrease in the activity of renal SOD following gentamicin treatment in this study was in accordance with a previous report demonstrating the suppression of endogenous enzymatic antioxidant machinery in gentamicin-induced nephrotoxicity (Thounaojam *et al.* 2010). In addition, after gentamicin treatment there were increases in the nuclear accumulation of Nrf2, which plays a role in promoting the antioxidant defense system or protecting against oxidative stress, and the protein expressions of GCL, NQO1 and HO-1 in the renal tissues. Oxidative stress disrupts the Keap1–Nrf2 complex, which allows Nrf2 translocation into the nucleus, leading to activation of the ARE and upregulation of the expression of antioxidant-related enzymes. Nrf2 is expressed in many tissues, particularly those associated with detoxification and exposed to the external environment, such as the liver and kidney (Copple *et al.* 2007). These findings might be attributed to oxidative stress-induced disruption of the Keap1–Nrf2 complex, resulting in Nrf2 translocation into the nucleus and subsequent activation of the ARE and upregulation of GCL, NQO1 and HO-1 expressions to counteract these conditions. Similar results were also observed in an earlier study, in which Nrf2 was shown to protect against progression of hair cell damage through regulation of antioxidant enzymes, including NQO1, GCL, SOD and HO-1 (Hoshino *et al.* 2011). Furthermore, a significant increase in the GSH level was consistent with a marked increase in expression of GCL, the enzyme that catalyses the rate-limiting step for GSH synthesis, in the gentamicin-treated group. Therefore, it is likely that Nrf2 plays a crucial role in preventing gentamicin-induced nephrotoxicity via induction of detoxification and antioxidant enzymes. However, activation of the Nrf2 pathway could not overdrive the gentamicin-induced oxidative damage in this study.

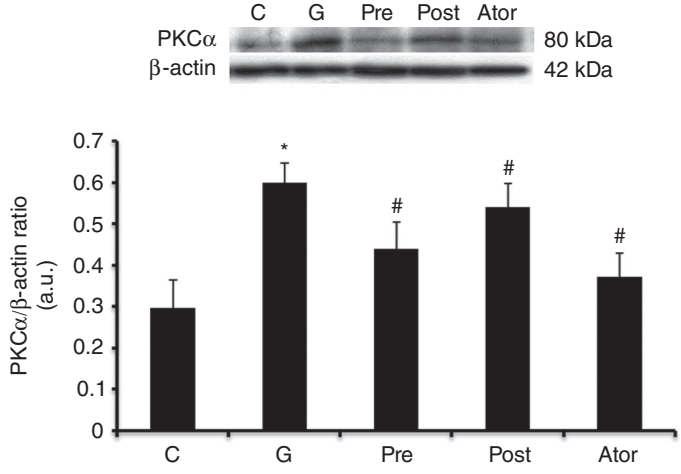

Figure 5. Effect of atorvastatin on the protein expression of protein kinase Cα (PKCα) in renal cortical tissues
Immunoblot analysis for PKCα expression in the whole-cell lysate fraction of renal cortical tissues normalized to β-actin. Bar graph shows the means + SEM ($n = 6$ rats in each group). For comparison between multiple treatments, a one-way ANOVA followed by Fisher's least significant difference test was used. $^*P < 0.05$ compared with the control group. $^\#P < 0.05$ compared with the gentamicin-treated group. Abbreviations are as in Fig. 2.

The present study showed a significant decrease of MDA levels accompanied by a substantial increase of SOD activity in the kidneys of the atorvastatin-treated rats, indicating attenuation of the oxidative stress induced by gentamicin. Interestingly, the decreased MDA level was greater with atorvastatin pretreatment than atorvastatin post-treatment, implying that the preventive effect of atorvastatin on oxidative stress generation was more effective than the post-treatment. Previous studies demonstrated the antioxidant effects of statins against cardiac hypertrophy (Lee *et al.* 2002; Custodis *et al.* 2006) and diabetes-induced endothelial dysfunction (Ting *et al.* 1996), which are independent of their effect on cholesterol synthesis. Statins can block the isoprenylation of small G-proteins, such as Ras and Rho/Rac/Cdc42, by inhibition of the mevalonate pathway. It has been shown that Rac-GTPase contributes to oxidative stress induction in the hippocampus by facilitating activation of NADPH oxidase, a key membrane enzyme that generates O_2^- ions (Raz *et al.* 2010). A study in microglial cells demonstrated that statins suppress translocation of the small GTPase Rac to the plasma membrane, leading to reduced free radical generation (Cordle *et al.* 2005). The antioxidant effect of atorvastatin in the present study was supported by the significantly reduced nuclear translocation of Nrf2, implying the inactivation of Nrf2 secondary to the decreased ROS production. These findings demonstrate that statins can contribute to renal protection against oxidative injury.

The important findings of the present study are the impaired renal Oat3 function and reduced Oat3 membrane expression in gentamicin-treated rats. Similar results were also observed in a recent study by Guo *et al.* (2013). The mechanisms of these changes were also investigated in this study. A previous study demonstrated that the activation of PKCα could stimulate the internalization of renal Oat3, accounting for the decreased membrane expression (Takeda *et al.* 2000). Furthermore, we have previously reported that overproduction of ROS in diabetic rats activates PKCα expression, and subsequently, leads to downregulation of renal Oat3 expression and therefore a reduction in renal Oat3 function (Arjinajarn

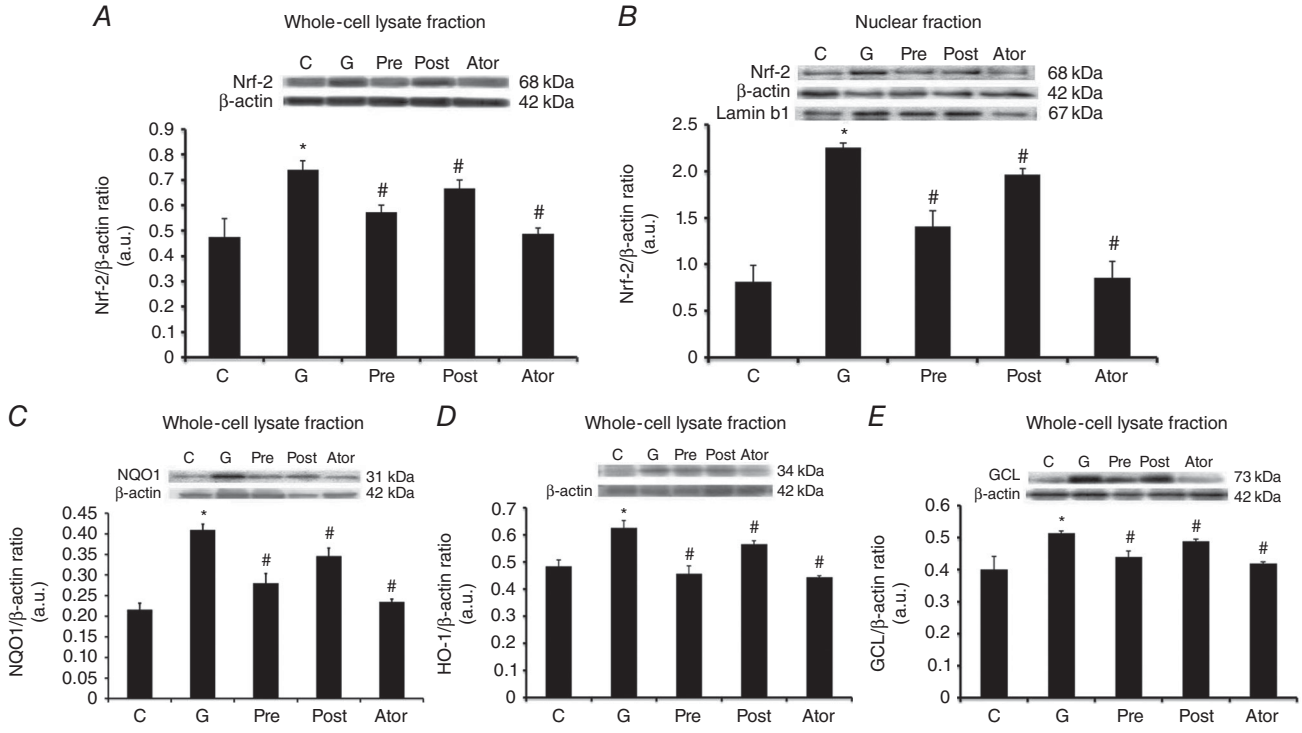

Figure 6. Effect of atorvastatin on the protein expression of Nrf2, haeme oxygenase 1 (HO-1), NAD(P)H:quinone oxidoreductase 1 (NQO1) and glutamate–cysteine ligase (GCL) in the renal cortical tissue

Immunoblot analysis for protein expression of Nrf2 in whole-cell lysate (*A*) and nuclear fractions (*B*) and NQO1 (*C*), HO1 (*D*) and GCL (*E*) expressions of renal cortical tissues (whole-cell lysate fraction) normalized to β-actin. Bar graphs show the means + SEM ($n = 6$ rats in each group). For comparison between multiple treatments, a one-way ANOVA followed by Fisher's least significant difference test was used. $^*P < 0.05$ compared with the control group. $^\#P < 0.05$ compared with the gentamicin-treated group. Abbreviations are as in Fig. 2.

et al. 2014). Consistent with this recent finding, the increased expression of PKCα in gentamicin-treated rats might cause the downregulation of renal Oat3 expression on the tubular membranes through the activation of transporter internalization, resulting in decreased renal Oat3 function. The present study showed that atorvastatin treatment recovered the function and expression of renal Oat3 in gentamicin-treated rats. Results from the previous study demonstrated that the decreased overoxidation of the kidney could reverse the impairment of Oat1 and Oat3 function and expression in gentamicin-induced acute renal failure (Guo *et al.* 2013). It is likely that the antioxidant effect of atorvastatin in reducing oxidative stress could be responsible for the improved renal Oat3 expression and function. Supporting this statement is the decreased expression of PKCα in accordance with the increased renal Oat3 expression in atorvastatin-treated rats.

In conclusion, we have demonstrated that atorvastatin has a protective role against nephrotoxicity induced by gentamicin treatment. The results obtained from this study are the first to provide evidence that atorvastatin exerts a nephroprotective effect from the effects of gentamicin by attenuating oxidative stress and improving renal function and renal Oat3 function. Therefore, we propose that atorvastatin might protect the tissues via its antioxidant property and by modulating the antioxidant enzymes through the Nrf2 signalling pathway, which may be the underlying mechanisms of these protective effects.

References

Ahn JM, You SJ, Lee YM, Oh SW, Ahn SY, Kim S, Chin HJ, Chae DW & Na KY (2012). Hypoxia-inducible factor activation protects the kidney from gentamicin-induced acute injury. *PLoS ONE* **7**, e48952.

Ali BH (2002). The effect of treatment with the medicinal plant *Rhazya stricta* Decne on gentamicin nephrotoxicity in rats. *Phytomedicine* **9**, 385–389.

Arjinajarn P, Srimaroeng C, Chatsudthipong V & Lungkaphin A (2014). Decreased renal organic anion transporter 3 expression in type 1 diabetic rats. *Am J Med Sci* **347**, 221–227.

Aviram M, Rosenblat M, Bisgaier CL & Newton RS (1998). Atorvastatin and gemfibrozil metabolites, but not the parent drugs, are potent antioxidants against lipoprotein oxidation. *Atherosclerosis* **138**, 271–280.

Balakumar P, Rohilla A & Thangathirupathi A (2010). Gentamicin-induced nephrotoxicity: do we have a promising therapeutic approach to blunt it? *Pharmacol Res* **62**, 179–186.

Brown MS & Goldstein JL (1980). Multivalent feedback regulation of HMG CoA reductase, a control mechanism coordinating isoprenoid synthesis and cell growth. *J Lipid Res* **21**, 505–517.

Copple IM, Goldring CE, Kitteringham NR & Park BK (2007). The Nrf2–Keap1 defence pathway: role in protection against drug-induced toxicity. *Toxicology* **246**, 24–33.

Cordle A, Koenigsknecht-Talboo J, Wilkinson B, Limpert A & Landreth G (2005). Mechanisms of statin-mediated inhibition of small G-protein function. *J Biol Chem* **280**, 34202–34209.

Custodis F, Eberl M, Kilter H, Böhm M & Laufs U (2006). Association of RhoGDIα with Rac1 GTPase mediates free radical production during myocardial hypertrophy. *Cardiovasc Res* **71**, 342–351.

Du XH & Yang CL (1994). Mechanism of gentamicin nephrotoxicity in rats and the protective effect of zinc-induced metallothionein synthesis. *Nephrol Dial Transplant* **9** Suppl 4, 135–140.

Franklin CC, Backos DS, Mohar I, White CC, Forman HJ & Kavanagh TJ (2009). Structure, function, and post-translational regulation of the catalytic and modifier subunits of glutamate cysteine ligase. *Mol Aspects Med* **30**, 86–98.

Goldstein JL & Brown MS (1990). Regulation of the mevalonate pathway. *Nature* **343**, 425–430.

Guo X, Meng Q, Liu Q, Wang C, Sun H, Peng J, Ma X, Kaku T & Liu K (2013). JBP485 improves gentamicin-induced acute renal failure by regulating the expression and function of Oat1 and Oat3 in rats. *Toxicol Appl Pharmacol* **271**, 285–295.

Habu Y, Yano I, Okuda M, Fukatsu A & Inui K (2005). Restored expression and activity of organic ion transporters rOAT1, rOAT3 and rOCT2 after hyperuricemia in the rat kidney. *Biochem Pharmacol* **69**, 993–999.

Hoshino T, Tabuchi K, Nishimura B, Tanaka S, Nakayama M, Ishii T, Warabi E, Yanagawa T, Shimizu R, Yamamoto M & Hara A (2011). Protective role of Nrf2 in age-related hearing loss and gentamicin ototoxicity. *Biochem Biophys Res Commun* **415**, 94–98.

Lee TM, Chou TF & Tsai CH (2002). Association of pravastatin and left ventricular mass in hypercholesterolemic patients: role of 8-iso-prostaglandin F2α formation. *J Cardiovasc Pharm* **40**, 868–874.

Li J, Jin J, Li M, Guan C, Wang W, Zhu S, Qiu Y, Huang M & Huang Z (2012). Role of Nrf2 in protection against triptolide-induced toxicity in rat kidney cells. *Toxicol Lett* **213**, 194–202.

Liao JK & Laufs U (2005). Pleiotropic effects of statins. *Annu Rev Pharmacol Toxicol* **45**, 89–118.

Lungkaphin A, Arjinajarn P, Pongchaidecha A, Srimaroeng C, Chatsudthipong L & Chatsudthipong V (2014). Impaired insulin signaling affects renal organic anion transporter 3 (Oat3) function in streptozotocin-induced diabetic rats. *PLoS ONE* **9**, e96236.

Nagai J & Takano M (2004). Molecular aspects of renal handling of aminoglycosides and strategies for preventing the nephrotoxicity. *Drug Metab Pharmacokinet* **19**, 159–170.

Nasri H, Nematbakhsh M & Rafieian-Kopaei M (2013). Ethanolic extract of garlic for attenuation of gentamicin-induced nephrotoxicity in Wistar rats. *Iran J Kidney Dis* **7**, 376–382.

Quiros Y, Vicente-Vicente L, Morales AI, López-Novoa JM & López-Hernández FJ (2011). An integrative overview on the mechanisms underlying the renal tubular cytotoxicity of gentamicin. *Toxicol Sci* **119**, 245–256.

Raz L, Zhang QG, Zhou CF, Han D, Gulati P, Yang LC, Yang F, Wang RM & Brann DW (2010). Role of Rac1 GTPase in NADPH oxidase activation and cognitive impairment following cerebral ischemia in the rat. *PLoS ONE* **5**, e12606.

Saito H (2010). Pathophysiological regulation of renal SLC22A organic ion transporters in acute kidney injury: pharmacological and toxicological implications. *Pharmacol Ther* **125**, 79–91.

Takeda M, Sekine T & Endou H (2000). Regulation by protein kinase C of organic anion transport driven by rat organic anion transporter 3 (rOAT3). *Life Sci* **67**, 1087–1093.

Thounaojam MC, Jadeja RN, Devkar RV & Ramachandran AV (2010). *Sida rhomboidea*.Roxb leaf extract ameliorates gentamicin induced nephrotoxicity and renal dysfunction in rats. *J Ethnopharmacol* **132**, 365–367.

Ting HH, Timimi FK, Boles KS, Creager SJ, Ganz P & Creager MA (1996). Vitamin C improves endothelium-dependent vasodilation in patients with non-insulin-dependent diabetes mellitus. *J Clin Invest* **97**, 22–28.

Vecchione C, Gentile MT, Aretini A, Marino G, Poulet R, Maffei A, Passarelli F, Landolfi A, Vasta A & Lembo G (2007). A novel mechanism of action for statins against diabetes-induced oxidative stress. *Diabetologia* **50**, 874–880.

Walker PD & Shah SV (1987). Gentamicin enhanced production of hydrogen peroxide by renal cortical mitochondria. *Am J Physiol Cell Physiol* **253**, C495–C499.

Yang H, Magilnick N, Lee C, Kalmaz D, Ou X, Chan JY & Lu SC (2005). Nrf1 and Nrf2 regulate rat glutamate-cysteine ligase catalytic subunit transcription indirectly via NF-κB and AP-1. *Mol Cell Biol* **25**, 5933–5946.

Yazar E, Elmas M, Altunok V, Sivrikaya A, Oztekin E & Birdane YO (2003). Effects of aminoglycoside antibiotics on renal antioxidants, malondialdehyde levels, and some serum biochemical parameters. *Can J Vet Res* **67**, 239–240.

Zou Y, Hong B, Fan L, Zhou L, Liu, Y, Wu Q, Zhang X & Dong M (2013). Protective effect of puerarin against beta-amyloid-induced oxidative stress in neuronal cultures from rat hippocampus: involvement of the GSK-3β/Nrf2 signaling pathway. *Free Radic Res* **47**, 55–63.

Additional information

Completing interests

None declared.

Author contributions

A.L., A.P., K.J., N.C., V.C., S.P. and P.A. designed and substantially performed the experiments, analysed the data, prepared the figures and wrote the manuscript. S.P., K.J. and P.A. helped with the biochemical assays and animal experiments. A.L. and N.C. collaborated by providing expert advice. A.L., N.C. and A.P. collaborated by analysing and interpreting the data and developing, co-writing and editing the manuscript. A.L., A.P., V.C. and N.C. oversaw the experiments, supervised the project and wrote and revised the manuscript. All authors approved the final version of the manuscript and agree to be accountable for all aspects of the work in ensuring that questions related to the accuracy or integrity of any part of the work are appropriately investigated and resolved. All persons designated as authors qualify for authorship, and all those who qualify for authorship are listed.

Funding

This work was supported by the Thailand Research Fund RSA5780029 (to A.L.) and TRG5780019 (to P.A.), National Research Council of Thailand (164368;2558A10402068; to A.L.), CMU Mid-Career Research Fellowship program (13/2558; to A.L.), the Faculty of Medicine Research Fund, Chiang Mai University (10/2559; to A.L.) and the NSTDA Research Chair grant from the National Science and Technology Development Agency of Thailand (to N.C.).

Acknowledgements

We thank Associate Professor Suree Lakawanvijit, Department of Pathology, Faculty of Medicine, Chiang Mai University for the valuable suggestions in renal histology.

NRC Research Press

ARTICLE

Pinocembrin reduces cardiac arrhythmia and infarct size in rats subjected to acute myocardial ischemia/reperfusion

Anusorn Lungkaphin, Anchalee Pongchaidecha, Siripong Palee, Phatchawan Arjinajarn, Wilart Pompimon, and Nipon Chattipakorn

Abstract: Oxidative stress plays an important role in the pathogenesis of ischemia/reperfusion (I/R) injury induced by cardiac dysfunction. Pinocembrin (5,7-dihydroxyflavanone) is a flavonoid found in propolis and in rhizomes of fingerroot (*Boesenbergia pandurata*) that is reported to have pharmacological properties including antimicrobial, antioxidant, and anti-inflammatory activities. The cardioprotective effects of pinocembrin in an I/R model were investigated in this study. Male Wistar rats (n = 20) were randomly divided into 2 groups to receive either pinocembrin (30 mg/kg body weight) or the vehicle intravenously. Thirty minutes later, the left anterior descending coronary artery of each rat was ligated for 30 min, and then reperfusion was allowed for 120 min. Cardiac function improved in the pinocembrin-treated group: the time to first ventricular fibrillation (VF) was significantly longer in the treated group (550 ± 54 s) than in the vehicle-only control group (330 ± 27 s) ($p < 0.05$). VF incidence and arrhythmia score were lower and infarcts were 49% smaller in the pinocembrin-treated group than in the control group ($p < 0.05$). In the pinocembrin-treated group, malondialdehyde levels and Bax/Bcl-2 ratios decreased, and the ratio of phosphorylated connexin 43 (phospho-Cx43) to total Cx43 increased in infarcted tissues compared with the non-infarcted area ($p < 0.05$). Pinocembrin exhibited cardioprotective effects during I/R, evidenced by improved cardiac function, fewer arrhythmias, and smaller infarcts in treated hearts than in controls. These benefits may be due to pinocembrin's antiapoptotic and anti-oxidative stress effects and its ability to increase the phosphorylation of Cx43 in ischemic myocardium.

Key words: acute myocardial ischemia/reperfusion, cardiac function, pinocembrin.

Résumé : Le stress oxydatif joue un important rôle dans la pathogenèse des lésions d'ischémie/reperfusion (I/R) suscitées par un dysfonctionnement cardiaque. La pinocembrine (5,7-dihydroxyflavanone) est un flavonoïde trouvé dans la propolis et les rhizomes du krachaï (*Boesenbergia pandurata*) ayant, selon des études, des propriétés pharmacologiques entre autres antimicrobiennes, antioxydantes et anti-inflammatoires. Cette étude analyse les effets cardioprotecteurs de la pinocembrine dans un modèle d'ischémie/reperfusion. On répartit aléatoirement des rats mâles Wistar (n = 20) en 2 groupes, l'un recevant par voie intraveineuse la pinocembrine (30 mg/kg) et l'autre, un véhicule. Trente minutes plus tard, on ligature durant 30 minutes l'artère interventriculaire antérieure gauche de chaque rat, puis on effectue une reperfusion durant 120 minutes. Chez le groupe traité à la pinocembrine, la fonction cardiaque s'améliore : le temps de déclenchement de la première fibrillation ventriculaire (VF) est significativement plus long (550 ± 54 s) comparativement au groupe de contrôle recevant seulement le véhicule (330 ± 27 s) ($p < 0,05$). L'incidence de VF et le score de l'arythmie présentent des valeurs plus faibles et l'étendue de l'infarctus est 49 % moins grande comparativement au groupe de contrôle ($p < 0,05$). Chez le groupe traité à la pinocembrine, la concentration de MDA et le ratio Bax/Bcl-2 diminuent; on observe en outre une augmentation du ratio phosphorylation-connexine 43 (phospho-Cx43)/Cx43 totale dans les tissus infarcis comparativement aux tissus épargnés ($p < 0,05$). La pinocembrine procure un effet cardioprotecteur à la suite d'une lésion I/R comme le révèlent une meilleure fonction cardiaque, une diminution des arythmies et de l'étendue de la lésion comparativement au groupe de contrôle. Ces bienfaits seraient probablement dus aux propriétés anti-apoptotiques et antioxydantes de la pinocembrine et à sa capacité d'accroître la phosphorylation de la Cx43 dans le myocarde ischémique. [Traduit par la Rédaction]

Mots-clés : ischémie/reperfusion aigüe du myocarde, fonction cardiaque, pinocembrine.

Introduction

Acute myocardial infarction is the most common cause of sudden cardiac death, with the vast majority of these deaths being caused by polymorphic ventricular tachycardia and ventricular fibrillation (Wang et al. 2005; Lerner et al. 2000). Interventions for this condition include coronary reperfusion and thrombolytic treatment. However, early reperfusion after coronary occlusion is the most effective means of therapy. However, there is a great deal of evidence to suggest that reperfusion may contribute to additional cardiac injury and cause structural, functional, and biochemical abnormalities (Wang et al. 2005; Lerner et al. 2000; Temsah et al. 2003). One of the proposed major mechanisms for

Received 18 March 2015. Accepted 4 June 2015.

A. Lungkaphin, A. Pongchaidecha, and N. Chattipakorn.* Cardiac Electrophysiology Research and Training Center, Faculty of Medicine, Chiang Mai University, Chiang Mai, Thailand; Department of Physiology, Faculty of Medicine, Chiang Mai University, Chiang Mai, Thailand; Center of Excellence in Cardiac Electrophysiology Research, Chiang Mai University, Chiang Mai, Thailand.
S. Palee. Cardiac Electrophysiology Research and Training Center, Faculty of Medicine, Chiang Mai University, Chiang Mai, Thailand; Center of Excellence in Cardiac Electrophysiology Research, Chiang Mai University, Chiang Mai, Thailand; School of Medicine, Mae Fah Luang University, Chiang Rai, Thailand.
P. Arjinajarn. Department of Biology, Faculty of Science, Chiang Mai University, Chiang Mai, Thailand.
W. Pompimon. Department of Chemistry and Center of Excellence for Innovation in Chemistry, Faculty of Science, Lampang Rajabhat University, Lampang, Thailand.

Corresponding author: Nipon Chattipakorn (e-mail: nchattip@gmail.com).

*Present address: Cardiac Electrophysiology Research and Training Center, Faculty of Medicine, Chiang Mai University, Chiang Mai, 50200, Thailand.

ischemia/reperfusion (I/R)-induced subcellular remodeling and subsequent contractile dysfunction and cardiac arrhythmias is oxidative stress (Dhalla et al. 2000). Direct and indirect evidence demonstrates that during the reperfusion period, one finds not only elevated oxygen free radicals due to the failure of metabolic reactions during ischemia but also a marked increase in oxygen-derived free radicals (Temsah et al. 2003; Dhalla et al. 2000). Potent oxidant radicals, such as superoxide anion, hydroxyl radical, and peroxynitrite, are produced within the first few minutes of reperfusion and play a crucial role in the development of reperfusion injury (Bolli et al. 1989). The occurrence of oxidative stress critically impairs the antioxidant defense system in ischemic myocardial tissues, which is followed by increased formation of reactive oxygen species (ROS), which subsequently cause significant myocardial cell damage and heart dysfunction during myocardial I/R injury (Valko et al. 2007; Kasparová et al. 2005). It has been reported that ROS may injure cells by causing peroxidation of membrane lipids, denaturation of proteins including enzymes and ion channels, and breakage of DNA strands. Subsequently, peroxidation of membrane lipids triggers loss of membrane integrity, necrosis, and cell death (Park and Lucchesi 1999). The available reports also show that inflammation is one of the major pathophysiological mechanisms leading to myocardial I/R injury (Ottani et al. 2010; Jolly et al. 1986). During the myocardial I/R process, complement activation and ROS release stimulate the infiltration of inflammatory cells into the myocardial tissues (Birdsall et al. 1997; Kloner et al. 1991). Thereafter, massive amounts of inflammatory cytokines, such as TNF-α and IL-6, are released from the inflammatory cells, resulting in myocardial injury (Birdsall et al. 1997; Dhalla et al. 2000; Zhang et al. 2006).

Connexin 43 (Cx43) is a predominant connexin in cardiac myocyte gap junctions (Gros and Jongsma 1996; Severs et al. 2001). Gap junctions mediate electrical coupling between cardiac myocytes, allowing the spreading of electrical waves responsible for synchronized contraction in the heart. The function of gap junctions can be regulated at different levels by a variety of mechanisms such as modulation of connexon densities on cell membranes and Cx phosphorylation, which leads to modification of channel conductance as well as Cx trafficking and degradation (Goodenough and Paul 2009). In myocardial ischemia, the dephosphorylation of Cx43 induces the loss of cellular communication via gap junctions, resulting in cardiac arrhythmias (Palee et al. 2013; Beardslee et al. 2000; Lampe et al. 2000). Moreover, reperfusion is reported to activate myocardial tissue apoptosis, resulting in increased expression of the apoptotic marker protein Bax (Eefting et al. 2004).

Pinocembrin (5,7-dihydroxyflavonone, $C_{15}H_{12}O_4$, Fig. 1) is a flavonoid that is abundant in honeybee propolis (Bankova et al. 1982) and in rhizomes of the culinary herb *Boesenbergia pandurata* (family Zingiberaceae), known as fingerroot, lesser galangal, Chinese keys, and Chinese ginger (Punvittayagul et al. 2011). Pinocembrin has been proven to have several biological effects, including antimicrobial, antioxidant, and anti-inflammatory activities (Santos et al. 1998). Recently, its protective effects against ischemic injury have been reported. For example, pinocembrin was found to improve cognition by protecting cerebral mitochondrial structure and function during chronic cerebral hypoperfusion in rats (Guang and Du 2006). It was also found to alleviate cerebral ischemic injury following experimental focal cerebral I/R (Gao et al. 2010; Liu et al. 2008) and decrease brain injury after global cerebral I/R (Shi et al. 2011; Meng et al. 2011) in rats.

Although pinocembrin's protective effects against ischemic injury in the brain have been well studied, its 'potential beneficial effects on the heart have not been investigated. Moreover, the mechanisms underlying pinocembrin's antioxidant and antiapoptotic activities and its effect on the modification of myocardial electrical activity in rat hearts subjected to I/R need to be elucidated. We tested the hypothesis that administration of pinocembrin reduces the occurrence of arrhythmia and alleviates cardiac injury in a rat model of myocardial I/R. The expression of protein markers associated with altered electrical coupling and mitochondria-dependent apoptosis (Cx43 and Bax/Bcl-2, respectively) was also investigated.

Fig. 1. The chemical structure of pinocembrin (5,7-dihydroxyflavonone, $C_{15}H_{12}O_4$) (Punvittayagul et al. 2011).

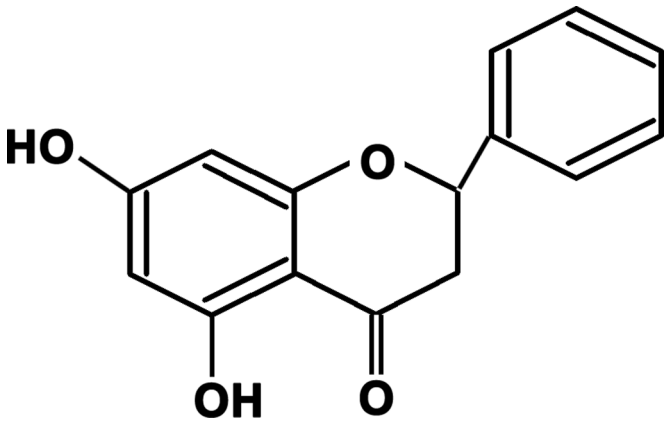

Materials and methods

Animal preparation and in vivo study procedure

A total of 20 male Wistar rats 10–12 weeks of age, weighing between 350 g and 400 g, were used in this study, which was approved by the Institutional Animal Care and Use Committees of the Faculty of Medicine of Chiang Mai University. All animals were fed normal rat chow and water ad libitum before the study. Each was anesthetized by an intramuscular injection of Zoletil (50 mg/kg; Virbac Laboratories, Carros, France) and xylazine (0.15 mL/kg; Laboratorios Calier, Barcelona, Spain) and ventilated with room air via a tracheostomy tube from a positive-pressure rodent ventilator (Model 683, Harvard Apparatus, Holliston, Mass., USA). Nominal respiratory volume was 200–250 μL and the ventilation rate was 70–110 breaths/min to maintain pCO_2, pO_2, and pH at normal physiological values (Palee et al. 2013). The left femoral vein was cannulated with a polyethylene tube (PE-60, Intramedic, Clay Adams, N.J., USA) for drug and vehicle administration. The electrocardiogram (lead II) was recorded continuously throughout the experiment (PowerLab 4/25 T, ADInstruments, Colorado Springs, Colo., USA).

Pinocembrin was isolated from the rhizomes of *B. pandurata* by the Department of Chemistry and Center of Excellence for Innovation in Chemistry of the Faculty of Science of Lampang Rajabhat University, Lampang, Thailand. Pinocembrin doses for the experimental group were prepared by adding sufficient drug of 95% purity to the vehicle, consisting of 150 μL of β-cyclodextrin (Sigma–Aldrich, St. Louis, Mo., USA) and 850 μL of sterile normal saline, to produce an individualized dose of 30 mg/kg body weight. Control rats received 1 mL of β-cyclodextrin/saline vehicle without pinocembrin. The chosen pinocembrin dose was based on that given by intravenous administration in previous studies that showed the drug gave neurovascular protection as well as cognitive improvement (Liu et al. 2008).

Under deep anesthesia, the rats were opened by left thoracotomy at the 4th intercostal space using aseptic techniques. An incision was made in the pericardium and the heart was exposed. Then, the rats were randomly assigned to receive either pinocembrin or the vehicle alone (sham operated) by intravenous infusion over 3 min. Ischemia was induced 30 min after the infusion of pinocembrin or the vehicle alone. For the I/R procedure, the left anterior descending coronary artery (LAD) was ligated approximately 2 mm from its origin using a 5-0 silk suture with a traumatic needle. The ends of this ligature were passed through a

small vinyl tube, which was used to occlude the coronary artery by pulling the thread. Ischemia was confirmed by ST elevation on the electrocardiogram and progressive darkening of the myocardial tissues distal to the occlusion point. The occlusion was held for 30 min, and then a 120-min reperfusion was carried out (Palee et al. 2013).

Arrhythmia determination

In each experiment, the occurrence of cardiac arrhythmia was determined in accordance with the Lambeth Conventions II, and scores were tabulated for the entire 150-min I/R period using criteria previously described (Curtis et al. 2013). The score was based on the following scale: 0, <50 ventricular premature beats (VPB); 1, ≥50 to 499 VPB; 2, ≥500 VPB or 1 episode of <1 min of ventricular tachycardia (VT) or ventricular fibrillation (VF); 3, ≥2 episodes of VT or VF totaling <1 min combined; 4, ≥1 to 2 min of total VT or VF; and 5, >2 min of total VT or VF.

Cardiac function determination

In each rat, left ventricular (LV) function was determined using a pressure–volume recording system (Transonic Scisense, London, Ont., Canada). The pressure–volume catheter was inserted via the common carotid artery and placed in the left ventricle. LV function parameters such as cardiac output (CO), end-systolic volume, end-diastolic volume, end-systolic pressure, end-diastolic pressure, and maximum and minimum rise in LV pressure over time (dP/dt max and dP/dt min, respectively) were recorded throughout the experiment (Palee et al. 2013).

Infarct size determination

At the end of each experiment, the animal was sacrificed by bolus anesthesia and the heart was removed. Cold normal saline was used to flush blood from the chambers and vessels of the hearts of 10 rats (5 from the pinocembrin group and 5 from the control group), after which the LAD was reoccluded at the same site that had been ligated during the ischemic period. Then, catheters were inserted into the right and left coronary ostia to facilitate the infusion of 1 mL of Evans blue (0.5%). The area into which Evans blue did not infuse was considered that into which blood did not flow during the in vivo ischemic period. The hearts were then frozen overnight and 1-mm-thick slices were cut horizontally, starting at the apex and stopping 1 mm above the occlusion site. Each slice was then immersed in 1% buffered 2,3,5-triphenyltetrazolium chloride (pH 7.4) at 37 °C for 5 min. The red areas were considered viable tissue, while those not stained with Evans blue were considered the area at risk (AAR). Areas stained neither blue nor red were defined as the infarct. The areas were measured using ImageTool software version 3.0. Infarct size was determined according to the formula of Riess et al. (2009) and was recorded as a percentage of the AAR (Palee et al. 2013).

Western blot analysis

Whole ventricles were separated from the hearts of the remaining 10 rats (5 from the pinocembrin group and 5 from the control group), quickly frozen in liquid nitrogen, and stored at −80 °C until analysis. Myocardial protein extract was prepared by homogenizing nitrogen-frozen myocardial tissues in CelLytic MT mammalian tissue lysis/extraction reagent (Sigma Aldrich, St. Louis, Mo., USA) with a protease inhibitor cocktail (Roche Applied Science, Indianapolis, Ind., USA). Tissues were homogenized at 4 °C, incubated on ice for 30 min, and then centrifuged at 5000*g* for 15 min at 4 °C. The total protein, amounting to 50–80 mg, was separated by electrophoresis on 10% or 15% sodium dodecyl sulfate–polyacrylamide gels. The proteins were then transferred to a polyvinylidene difluoride membrane (Millipore, Billerica, Mass., USA) in glycine–methanol transfer buffer (20 mmol/L Tris base, 0.15 mol/L glycine, and 20% methanol) using a wet transfer system (Trans-Blot SD, Bio-Rad Laboratories, Hercules, Calif., USA). The membranes were blocked with 5% nonfat dry milk in TBS-T buffer (20 mmol/L Tris–HCl, pH 7.6, 137 mmol/L NaCl, and 0.05% Tween-20) for 1 h at room temperature. The membranes were subsequently exposed to antibodies against Bax (Santa Cruz Biotechnology, Santa Cruz, Calif., USA), Bcl-2, total Cx43, Cx43 phosphorylated at Ser368 (phospho-Cx43) (Cell Signaling Technology, Danvers, Mass., USA), or actin (Millipore, Billerica, Mass., USA) for 12 h at room temperature. We determined the expression of Cx43 to study the conduction of electrical activity though the muscle fibers. The expression levels of Bax and Bcl-2 reflect apoptotic conditions involving the mitochondrial pathway in the myocardium. The membranes with bound antibody were then incubated with horseradish peroxidase-conjugated secondary antibody (Amersham, Arlington Heights, Ill., USA) for 1 h. Finally, enhanced chemiluminescence detection reagents were used to visualize the products of the peroxidase reaction. The X-ray films were scanned and the densities of protein signals were analyzed using the histogram function of Adobe Photoshop CS5 (Adobe, San Jose, Calif., USA). The protein levels were normalized using β-actin as the loading control.

Determination of oxidative stress in cardiac tissue

The level of myocardial oxidative stress was determined by measuring the level of malondialdehyde (MDA) in cardiac tissue using a thiobarbituric acid-reactive substance assay kit (Cayman Chemical Company, Ann Arbor, Mich., USA); the MDA level was expressed as nanomoles per milligram of protein. The total protein content of the cardiac tissues was determined using a DC protein assay kit (Bio-Rad Laboratories, Hercules, Calif., USA).

Statistical analysis

Data are presented as the mean ± SEM. Statistical analyses were conducted using SPSS (version 17; Chicago, Ill., USA). Alterations of the phospho-Cx43/total Cx43 ratio, arrhythmia score, time to VT or VF onset, and infarct size were analyzed using a 1-way ANOVA followed by a Fisher least significant difference test. The hemodynamic parameters at baseline and during the ischemic and reperfusion periods, the Bax/Bcl-2 ratio, and the MDA level were analyzed using a 2-way ANOVA with multiple comparisons. A p value <0.05 was considered statistically significant.

Results

Effect on hemodynamic parameters

At baseline, no differences in LV function or hemodynamic parameters were found between the pinocembrin-treated and control groups (Table 1). In both control and pinocembrin-treated groups, dP/dt max (baseline: 7984 ± 567 and 7861 ± 373 mm Hg/s, respectively) and end-systolic volume (baseline: 241 ± 10 and 250 ± 20 μL, respectively) worsened significantly during the ischemic period (6341 ± 234 and 6266 ± 328 mm Hg/s; 456 ± 17 and 435 ± 23 μL, respectively) ($p < 0.05$ vs. baseline).

In the pinocembrin group, CO during the ischemia and reperfusion periods was not significantly different from that at baseline. However, in the control group, CO decreased significantly during ischemia and reperfusion, to 85% and 87% of baseline CO, respectively ($p < 0.05$). These findings support our conclusion that pinocembrin improves LV function during cardiac I/R injury.

Arrhythmia and infarct size during I/R

The arrhythmia score showed a significant decrease in the pinocembrin-treated group (3.2 ± 0.20) compared with the vehicle-treated group (4.2 ± 0.25) ($p < 0.05$) (Fig. 2A). Also, the interval from the onset of LAD ligation until the onset of the first VT or VF episode was significantly longer in the pinocembrin-treated group (550 ± 54 s) than in the vehicle-treated group (330 ± 27 s) ($p < 0.05$) (Fig. 2B). Infarct size in the pinocembrin-treated group (24% ± 5.00% of AAR) was 49% smaller than that in the vehicle-treated

Table 1. Hemodynamic and cardiac function parameters in hearts subjected to ischemia/reperfusion.

	Control group			Pinocembrin group		
Parameter	Baseline	Ischemia	Reperfusion	Baseline	Ischemia	Reperfusion
Heart rate (beats/min)	324±2	311±9	290±7	329±21	296±17	299±13
End-systolic blood pressure (mm Hg)	151±15	134±22	130±6	128±9	129±17	102±23
End-diastolic blood pressure (mm Hg)	13±3	16±1	16±2	10±1	12±2	12±1
d*P*/d*t* max (mm Hg/s)	7984±567	6341±234*	6213±193*	7861±373	6266±328*	6782±429
d*P*/d*t* min (mm Hg/s)	−5041±497	−4653±121	−5529±533	−4547±158	−4298±286	−4467±202
End-systolic volume (μL)	241±10	456±17*	366±41*,†	250±20	435±23*	349±47*,†
End-diastolic volume (μL)	640±14	730±33*	650±31	630±10	716±31*	655±23
Stroke volume (μL)	399±22	274±22*	284±29*	380±23	280±10*	306±29*
Cardiac output (%)	100	85±2*	87±5*	100	92±4	93±1

Note: d*P*/d*t* max, maximum slope of left ventricle pressure waveform; d*P*/d*t* min, minimum slope of left ventricle pressure waveform. Results are the mean ± SE (n = 10 for all groups).

*$p < 0.05$ versus baseline.

†$p < 0.05$ versus ischemia in the same group.

Fig. 2. The effects of pinocembrin on arrhythmia scores (A) and time to onset of the first spontaneous ventricular tachycardia or fibrillation event (VT/VF) (B) during 30 min of ischemia and 120 min of reperfusion of rat hearts. Either 1 mL of pinocembrin (30 mg/kg body weight) or 1 mL of β-cyclodextrin/saline vehicle alone (control) was administered 30 min before coronary occlusion. Results are means ± SE; n = 5 for both groups. *, $p < 0.05$ versus the control group.

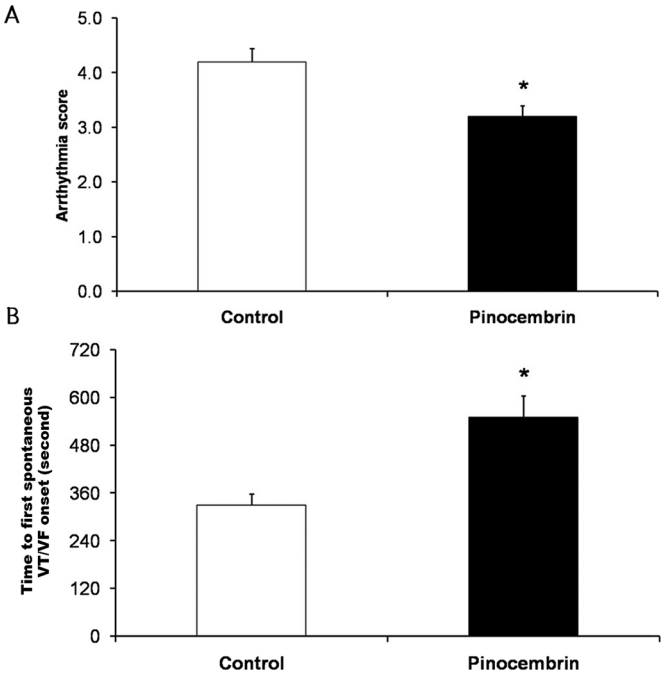

Fig. 3. The effect of pinocembrin on infarct size, expressed as a percentage of the area at risk, following 30 min of ischemia and 120 min of reperfusion of rat hearts. Either 1 mL of pinocembrin (30 mg/kg body weight) or 1 mL of β-cyclodextrin/saline vehicle alone (control) was administered 30 min before coronary occlusion. Results are means ± SE; n = 5 for both groups. *, $p < 0.05$ versus the control group.

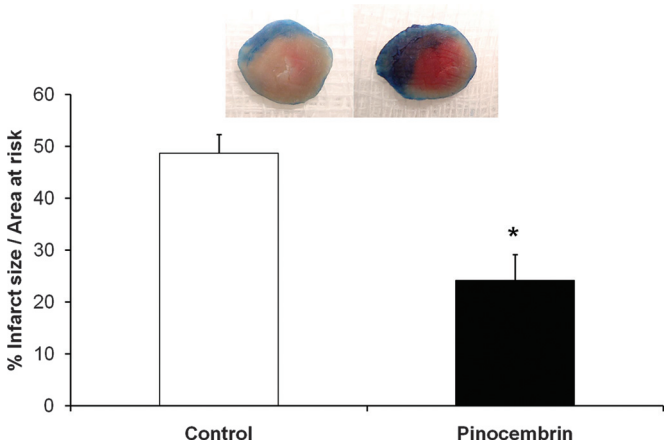

group (48% ± 3.60%), representing a significant reduction of infarct size ($p < 0.05$) (Fig. 3).

Effects on Cx43 phosphorylation and Bax and Bcl-2 levels

Pinocembrin administration significantly increased the phospho-Cx43/total Cx43 ratio, expressed as the ratio in ischemic myocardium relative to the ratio in non-ischemic myocardium, compared with that in the vehicle-treated group ($p < 0.05$) (Fig. 4A).

The Bax/Bcl-2 ratio in the ischemic myocardium of pinocembrin-treated rats (0.12 ± 0.06) was significantly lower than the ratio in the ischemic myocardium of control rats (1.43 ± 0.20) ($p < 0.05$) (Fig. 4B). In the pinocembrin group, the Bax/Bcl-2 ratio was not significantly different between ischemic and non-ischemic myocardium (0.12 ± 0.06 and 0.23 ± 0.09, respectively). However, in the control group, the Bax/Bcl-2 ratio differed significantly between ischemic and non-ischemic myocardium (1.43 ± 0.20 and 0.57 ± 0.15, respectively) ($p < 0.05$).

Effect of pinocembrin on oxidative stress

In the vehicle-treated group, MDA levels were higher in the ischemic myocardium (0.19 ± 0.01 nmol/mg protein) than in the non-ischemic muscle (0.13 ± 0.03 nmol/mg protein) ($p < 0.05$). However, in rats treated with pinocembrin, MDA levels were not increased in the ischemic myocardium compared with the non-ischemic tissue (0.12 ± 0.02 versus 0.15 ± 0.01 nmol/mg protein, respectively) (Fig. 5). When ischemic myocardium was compared between control and pinocembrin-treated rats, there was a significant difference in MDA level ($p < 0.05$).

Discussion

Previous studies have demonstrated that pinocembrin protects the brain against I/R injury and that this protective effect might be attributed to inhibition of apoptosis (Wu et al. 2013; Zhao et al. 2014). In these studies, pinocembrin decreased neurological deficit scores, infarct volume, and neuron apoptosis in the rats subjected to I/R. Our work here appears to be the first to show that pinocembrin may provide some protection against myocardial I/R injury in an in vivo rat model. Administration of pinocembrin before myocardial ischemia (*i*) improved LV function, which was impaired by I/R, (*ii*) decreased cardiac arrhythmia by increasing

Fig. 4. The effects of pinocembrin (Pino), compared with vehicle only (Con), on the expression of phosphorylated Cx43 (p-Cx43), total Cx43 (T-Cx43), and their ratio (A) and Bax, Bcl-2, and their ratio (B) in rat heart tissues. The p-Cx43/T-Cx43 ratio is expressed as the ratio in ischemic myocardium relative to the ratio in non-ischemic myocardium. The upper panels show representative immunoblots of ventricular tissues (IC, ischemic-control; IP, ischemic-pinocembrin; NC, non-ischemic-control; NP, non-ischemic-pinocembrin). The lower panels show quantitative data for Cx43, Bax, and Bcl-2 normalized to their total protein level. Rat hearts were subjected to 30 min of ischemia and 120 min of reperfusion. Either 1 mL of pinocembrin (30 mg/kg body weight) or 1 mL of β-cyclodextrin/saline vehicle alone (control) was administered 30 min before coronary occlusion. Results are means ± SE; $n = 5$ for all groups. *, $p < 0.05$ versus the control group (A) or non-ischemic myocardium of the control group (B); †, $p < 0.05$ versus ischemic myocardium of the control group (B).

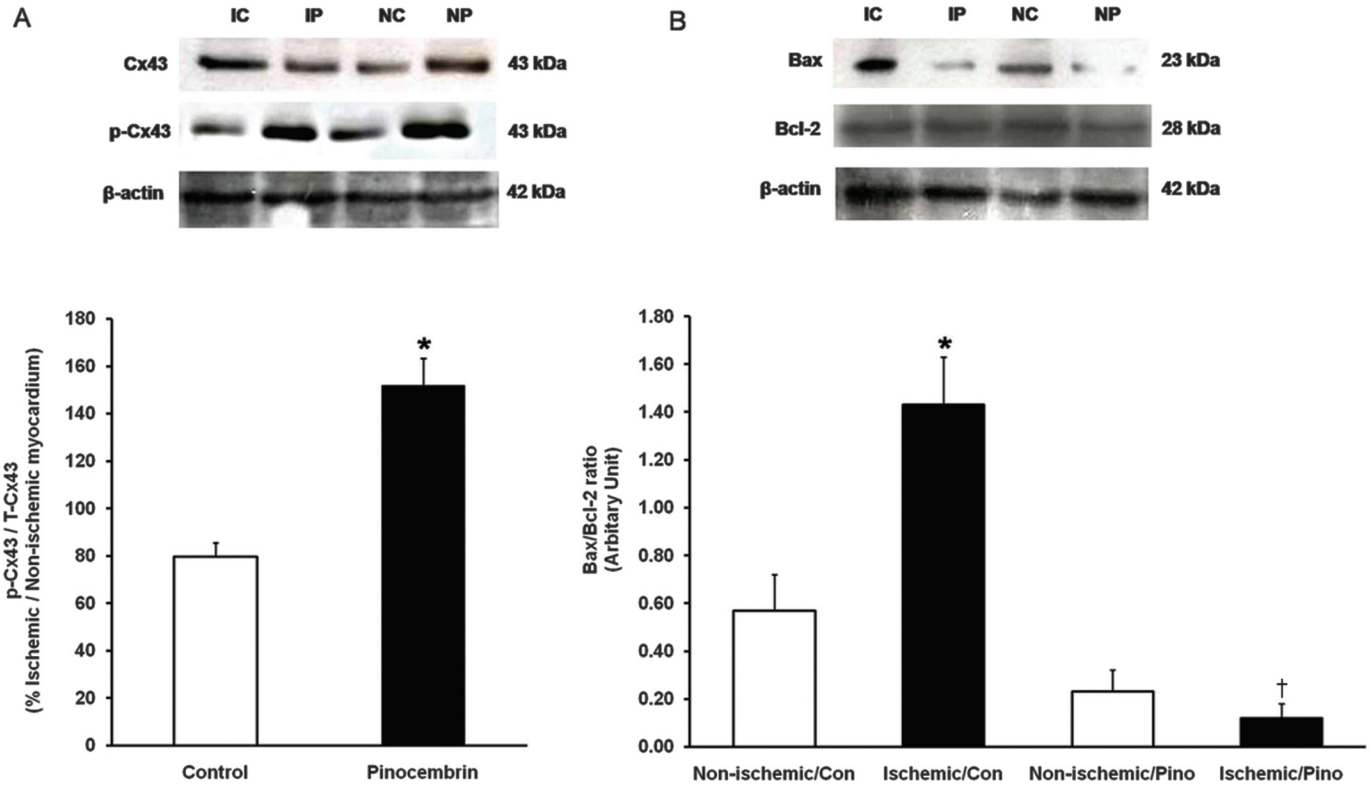

Fig. 5. Malondialdehyde (MDA) levels in non-ischemic and ischemic myocardium of rats treated with vehicle (Con) or pinocembrin (Pino). Rat hearts were subjected to 30 min of ischemia and 120 min of reperfusion. Either 1 mL of pinocembrin (30 mg/kg body weight) or 1 mL of β-cyclodextrin/saline vehicle alone (control) was administered 30 min before coronary occlusion. Results are means ± SE; $n = 5$ for all groups. *, $p < 0.05$ versus non-ischemic myocardium of the control group; †, $p < 0.05$ versus ischemic myocardium of the control group.

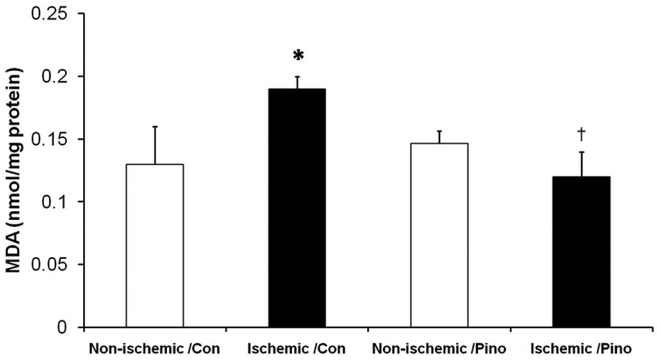

the ratio of phospho-Cx43 to total Cx43, (*iii*) reduced myocardial infarct size by decreasing the Bax/Bcl-2 ratio, and (*iv*) ameliorated cardiac oxidative stress.

Our results clearly demonstrate that during the I/R period, pinocembrin-treated rats had a lower incidence of VF and longer intervals before the onset of VT or VF than control rats. This antiarrhythmic effect might be due to the increased Cx43 phosphorylation that was observed in the ischemic myocardium. Experimental and clinical work by others has demonstrated that reperfusion of previously ischemic myocardium contributes to additional tissue injury and structural, functional, and biochemical abnormalities (Zhao et al. 2000; Temsah et al. 2003). During I/R, dephosphorylation of Cx43 occurs, leading to the loss of intercellular electrical communication via gap junctions in the ischemic heart and thus to conduction abnormalities and re-entrant arrhythmias (Peters et al. 1997; Saffitz et al. 1999). In myocardial ischemia, the dephosphorylation of Cx43 induces the loss of cellular communication via gap junctions, resulting in cardiac arrhythmias, as reported by Palee et al. (2013), who found that decreases in Cx43 phosphorylation during I/R could lead to increases in both VF frequency and arrhythmia scores. In our study, the marked increase in the phospho-Cx43/total Cx43 ratio in the pinocembrin-treated rats compared with the controls was associated with decreased arrhythmia scores. This antiarrhythmic effect of pinocembrin is consistent with prior reports that the phosphorylation of Cx43 at Ser368 could prevent phosphorylation at other Cx43 residues, leading to the preservation of cell-to-cell communication via gap junctions and thus reducing fatal arrhythmias (Beardslee et al. 2000; Lampe et al. 2000).

The present study also shows that pinocembrin can reduce the size of infarcts resulting from myocardial I/R injury. Reperfusion injury is reported to activate apoptosis, which causes further damage to the cardiac tissues after ischemia (Eefting et al. 2004). In apoptosis, the Bax and Bcl-2 proteins play important roles in the

regulation of mitochondrial outer membrane permeabilization (Murphy et al. 2000). Bax promotes pore formation, whereas Bcl-2 blocks it. Bax can also alter mitochondrial function to trigger the activation of terminal caspases, which results in the release into the cytoplasm of apoptosis-promoting factors (Adams and Cory 1998). Therefore, Bax and Bcl-2 have been used as marker proteins for apoptosis. Our findings demonstrate that pinocembrin inhibited increased expression of the proapoptotic protein Bax following myocardial I/R injury without affecting expression of the antiapoptotic protein Bcl-2. This led to a large shift in the Bax/Bcl-2 ratio in favor of Bcl-2, which may have protected the integrity of the mitochondria. This suggests that pinocembrin exerts an anti-apoptotic effect and may contribute to infarct size reduction via either an intrinsic or a mitochondrion-dependent apoptotic signaling pathway. In addition, an increase in Cx43 phosphorylation at Ser368 has been shown to enhance myocardial resistance to ischemic injury (Srisakuldee et al. 2009). These beneficial effects of pinocembrin during I/R might be responsible for the reduction in infarct size that was observed in this study.

During I/R, oxygen-derived free radicals are markedly elevated when metabolic reactions are impaired, resulting in deterioration of the electron-transport chain (Tompkins et al. 2006), activation of the apoptotic pathway (Loor et al. 2011), and eventual myocardial cell death. In addition, the elevation of ROS could cause cardiac mitochondrial membrane depolarization, a condition that has been shown to be responsible for cardiac arrhythmia (Aon et al. 2009). It has also been shown that the mitochondrial permeability transition is induced by ROS and in turn triggers mitochondrial ROS generation. This phenomenon has been termed mitochondrial ROS-induced ROS release (Zorov et al. 2000). A reduced MDA level was found in the ischemic myocardium of pinocembrin-treated rat hearts in our study, suggesting that pinocembrin has an anti-oxidative stress effect. This antioxidative effect could be responsible for the reduced myocardial vulnerability to arrhythmia and the decreased infarct size observed in the study. These various effects of pinocembrin could explain the improved cardiac function observed in pinocembrin-treated hearts stressed by I/R during the study. Although the protective effects of pinocembrin during cardiac I/R have been established, future studies are needed to investigate the cardioprotective effects of pinocembrin administration at different time points during cardiac I/R (i.e., during ischemia or reperfusion), since this information will enable direct application in a clinical setting.

Conclusion

In a rat model of myocardial I/R, acute pinocembrin administration 30 min prior to occlusion reduced the incidence of lethal arrhythmias, improved LV function, and decreased infarct size. These potential cardioprotective effects of pinocembrin may be the result of its antiapoptotic and antioxidative effects and its ability to increase the phosphorylation of Cx43 in ischemic myocardium.

Conflict of interest statement

The authors have no conflicts of interest to disclose.

Acknowledgements

We thank Sasivimol Promsan for her excellent technical assistance. This work was supported by grants from the Thailand Research Fund (RSA5780029 to AL and TRG5780007 to SP), the National Research Council of Thailand (2558A10402068 to AL), the Faculty of Medicine Research Fund, Chiang Mai University (AL), the Chiang Mai University Excellence Center Award (NC), and a Research Chair grant from the National Science and Technology Development Agency (NC).

References

Adams, J.M., and Cory, S. 1998. The Bcl-2 protein family: arbiters of cell survival. Science, **281**: 1322–1326. doi:10.1126/science.281.5381.1322. PMID:9735050.

Aon, M.A., Cortassa, S., Akar, F.G., Brown, D.A., Zhou, L., and O'Rourke, B. 2009. From mitochondrial dynamics to arrhythmias. Int. J. Biochem. Cell Biol. **41**: 1940–1948. doi:10.1016/j.biocel.2009.02.016. PMID:19703656.

Bankova, V.S., Popov, S.S., and Marekov, N.L. 1982. High-performance liquid chromatographic analysis of flavonoids from propolis. J. Chromatogr. A, **242**: 135–143. doi:10.1016/S0021-9673(00)87255-6.

Beardslee, M.A., Lerner, D.L., Tadros, P.N., Laing, J.G., Beyer, E.C., Yamada, K.A., et al. 2000. Dephosphorylation and intracellular redistribution of ventricular connexin43 during electrical uncoupling induced by ischemia. Circ. Res. **87**: 656–662. doi:10.1161/01.RES.87.8.656. PMID:11029400.

Birdsall, H.H., Green, D.M., Trial, J., Youker, K.A., Burns, A.R., MacKay, C.R., et al. 1997. Complement C5a, TGF-b1, and MCP-1, in sequence, induce migration of monocytes into ischemic canine myocardium within the first one to five hours after reperfusion. Circulation, **95**(3): 684–692. 21. doi:10.1161/01.CIR.95.3.684.

Bolli, R., Jeroudi, M.O., Patel, B.S., DuBose, C.M., Lai, E.K., Roberts, R., and McCay, P.B. 1989. Direct evidence that oxygen-derived free radicals contribute to postischemic myocardial dysfunction in the intact dog. Proc. Natl. Acad. Sci. U.S.A. **86**: 4695–4699. doi:10.1073/pnas.86.12.4695. PMID:2543984.

Curtis, M.J., Hancox, J.C., Farkas, A., Wainwright, C.L., Stables, C.L., Saint, D.A., et al. 2013. The Lambeth Conventions (II): Guidelines for the study of animal and human ventricular and supraventricular arrhythmias. Pharmacol. Ther. **139**: 213–248. doi:10.1016/j.pharmthera.2013.04.008. PMID:23588158.

Dhalla, N.S., Elmoselhi, A.B., Hata, T., and Makino, N. 2000. Status of myocardial antioxidants in ischemia-reperfusion injury. Cardiovasc. Res. **47**: 446–456. doi:10.1016/S0008-6363(00)00078-X. PMID:10963718.

Eefting, F., Rensing, B., Wigman, J., Pannekoek, W.J., Liu, W.M., Cramer, M.J., et al. 2004. Role of apoptosis in reperfusion injury. Cardiovasc. Res. **61**(3): 414–426. doi:10.1016/j.cardiores.2003.12.023. PMID:14962473.

Gao, M., Zhu, S.Y., Tan, C.B., Xu, B., Zhang, W.C., and Du, G.H. 2010. Pinocembrin protects the neurovascular unit by reducing inflammation and extracellular proteolysis in MCAO rats. J. Asian Nat. Prod. Res. **12**: 407–418. doi:10.1080/10286020.2010.485129. PMID:20496198.

Goodenough, D.A., and Paul, D.L. 2009. Gap junctions. Cold Spring Harb. Perspect. Biol. **1**(1): a002576. PMID:20066080.

Gros, D.B., and Jongsma, H.J. 1996. Connexins in mammalian heart function. Bioessays, **18**: 719–730. doi:10.1002/bies.950180907. PMID:8831288.

Guang, H.M., and Du, G.H. 2006. Protections of pinocembrin on brain mitochondria contribute to cognitive improvement in chronic cerebral hypoperfused rats. Eur. J. Pharmacol. **542**: 77–83. doi:10.1016/j.ejphar.2006.04.054. PMID:16806158.

Jolly, S.R., Kane, W.J., Hook, B.G., Abrams, G.D., Kunkel, S.L., and Lucchesi, B.R. 1986. Reduction of myocardial infarct size by neutrophil depletion: effect of duration of occlusion. Am. Heart. J. **112**(4): 682–690. 20. doi:10.1016/0002-8703(86)90461-8. PMID:3766367.

Kasparová, S., Brezová, V., Valko, M., Horecký, J., Mlynárik, V., Liptaj, T., et al. 2005. Study of the oxidative stress in a rat model of chronic brain hypoperfusion. Neurochem. Int. **46**: 601–611. doi:10.1016/j.neuint.2005.02.006. PMID:15863238.

Kloner, R.A., Giacomelli, F., Alker, K.J., Hale, S.L., Matthews, R., and Bellows, S. 1991. Influx of neutrophils into the walls of large epicardial coronary arteries in response to ischemia/reperfusion. Circulation, **84**(4): 1758–1772. 22. doi:10.1161/01.CIR.84.4.1758.

Lampe, P.D., TenBroek, E.M., Burt, J.M., Kurata, W.E., Johnson, R.G., and Lau, A.F. 2000. Phosphorylation of connexin43 on serine368 by protein kinase C regulates gap junctional communication. J. Cell Biol. **149**: 1503–1512. doi:10.1083/jcb.149.7.1503. PMID:10871288.

Lerner, D.L., Yamada, K.A., Schuessler, R.B., and Saffitz, J.E. 2000. Accelerated onset and increased incidence of ventricular arrhythmias induced by ischemia in Cx43-deficient mice. Circulation, **101**: 547–552. doi:10.1161/01.CIR.101.5.547. PMID:10662753.

Liu, R., Gao, M., Yang, Z.H., and Du, and G.H. 2008. Pinocembrin protects rat brain against oxidation and apoptosis induced by ischemia–reperfusion both in vivo and in vitro. Brain Res. **1216**: 104–115. doi:10.1016/j.brainres.2008.03.049. PMID:18495093.

Loor, G., Kondapalli, J., Iwase, H., Chandel, N.S., Waypa, G.B., Guzy, R.D., et al. 2011. Mitochondrial oxidant stress triggers cell death in simulated ischemia–reperfusion. Biochim. Biophys. Acta, **1813**: 1382–1394.

Meng, F., Liu, R., Gao, M., Wang, Y., Yu, X., Xuan, Z., et al. 2011. Pinocembrin attenuates blood–brain barrier injury induced by global cerebral ischemia–reperfusion in rats. Brain Res. **1391**: 93–101. doi:10.1016/j.brainres.2011.03.010. PMID:21435338.

Murphy, K.M., Ranganathan, V., Farnsworth, M.L., Kavallaris, M., and Lock, R.B. 2000. Bcl-2 inhibits Bax translocation from cytosol to mitochondria during drug-induced apoptosis of human tumor cells. Cell Death Differ. **7**: 102–111. doi:10.1038/sj.cdd.4400597. PMID:10713725.

Ottani, A., Giuliani, D., Galantucci, M., Spaccapelo, L., Novellino, E., Grieco, P., et al. 2010. Melanocortins counteract inflammatory and apoptotic responses to prolonged myocardial ischemia/reperfusion through a vagus nerve-mediated

mechanism. Eur. J. Pharmacol. **637**(1–3): 124–130. doi:10.1016/j.ejphar.2010.03.052. PMID:20385118.

Palee, S., Weerateerangkul, P., Chinda, K., Chattipakorn, S., and Chattipakorn, N. 2013. Mechanisms responsible for beneficial and adverse effects of rosiglitazone in a rat model of acute cardiac ischaemia-reperfusion. Exp. Physiol. **98**: 1028–1037. doi:10.1113/expphysiol.2012.070433. PMID:23291914.

Park, J.L., and Lucchesi, B.R. 1999. Mechanisms of myocardial reperfusion injury. Ann. Thorac. Surg. **68**: 1905–1912. doi:10.1016/S0003-4975(99)01073-5. PMID:10585102.

Peters, N.S., Coromilas, J., Severs, N.J., and Wit, A.L. 1997. Disturbed connexin43 gap junction distribution correlates with the location of reentrant circuits in the epicardial border zone of healing canine infarcts that cause ventricular tachycardia. Circulation, **95**: 988–996. doi:10.1161/01.CIR.95.4.988. PMID:9054762.

Punvittayagul, C., Wongpoomchai, R., Taya, S., and Pompimon, W. 2011. Effect of pinocembrin isolated from *Boesenbergia pandurata* on xenobiotic-metabolizing enzymes in rat liver. Drug Metab. Lett. **5**: 1–5. doi:10.2174/187231211794455226. PMID:20942797.

Riess, M.L., Rhodes, S.S., Stowe, D.F., Aldakkak, M., and Camara, A.K. 2009. Comparison of cumulative planimetry versus manual dissection to assess experimental infarct size in isolated hearts. J. Pharmacol. Toxicol. Methods, **60**: 275–280.

Saffitz, J.E., Schuessler, R.B., and Yamada, K.A. 1999. Mechanisms of remodeling of gap junction distributions and the development of anatomic substrates of arrhythmias. Cardiovasc. Res. **42**: 309–317. doi:10.1016/S0008-6363(99)00023-1. PMID:10533569.

Santos, A.C., Uyemura, S.A., Lopes, J.L., Bazon, J.N., Mingatto, F.E., and Curti, C. 1998. Effect of naturally occurring flavonoids on lipid peroxidation and membrane permeability transition in mitochondria. Free Radic. Biol. Med. **24**: 1455–1461. doi:10.1016/S0891-5849(98)00003-3. PMID:9641263.

Severs, N.J., Rothery, S., Dupont, E., Coppen, S.R., Yeh, H.I., Ko, Y.S., et al. 2001. Immunocytochemical analysis of connexin expression in the healthy and diseased cardiovascular system. Microsc. Res. Tech. **52**: 301–322. doi:10.1002/1097-0029(20010201)52:3<301::AID-JEMT1015>3.0.CO;2-Q. PMID:11180622.

Shi, L.L., Chen, B.N., Gao, M., Zhang, H.A., Li, Y.J., Wang, L., and Du, G.H. 2011. The characteristics of therapeutic effect of pinocembrin in transient global brain ischemia/reperfusion rats. Life Sci. **88**: 521–528. doi:10.1016/j.lfs.2011.01.011. PMID:21262238.

Srisakuldee, W., Jeyaraman, M.M., Nickel, B.E., Tanguy, S., Jiang, Z.S., and Kardami, E. 2009. Phosphorylation of connexin-43 at serine 262 promotes a cardiac injury-resistant state. Cardiovasc. Res. **83**: 672–681. doi:10.1093/cvr/cvp142. PMID:19423616.

Temsah, R.M., Netticadan, T., and Dhalla, N.S. 2003. Mechanisms of cellular alterations due to ischemia-reperfusion injury in the heart. *In* Myocardial Ischemia and Preconditioning. *Edited by* N.S. Dhalla, N. Takeda, M. Singh, and A. Lukas. Kluwer Academic Publishers, Boston, Mass., USA. pp. 149–164.

Tompkins, A.J., Burwell, L.S., Digerness, S.B., Zaragoza, C., Holman, W.L., and Brookes, P.S. 2006. Mitochondrial dysfunction in cardiac ischemia–reperfusion injury: ROS from complex I, without inhibition. Biochim. Biophys. Acta, **762**: 223–231.

Valko, M., Leibfritz, D., Moncol, J., Cronin, M.T., Mazur, M., and Telser, J. 2007. Free radicals and antioxidants in normal physiological functions and human disease. Int. J. Biochem. Cell Biol. **39**: 44–84. doi:10.1016/j.biocel.2006.07.001. PMID:16978905.

Wang, M., Tsai, B.M., Turrentine, M.W., Mahomed, Y., Brown, J.W., and Meldrum, D.R. 2005. P38 mitogen activated protein kinase mediates both death signaling and functional depression in the heart. Ann. Thorac. Surg. **80**: 2235–2241. doi:10.1016/j.athoracsur.2005.05.070. PMID:16305880.

Wu, C.X., Liu, R., Gao, M., Zhao, G., Wu, S., Wu, C.F., et al. 2013. Pinocembrin protects brain against ischemia/reperfusion injury by attenuating endoplasmic reticulum stress induced apoptosis. Neurosci. Lett. **546**: 57–62.

Zhang, C., Xu, X., Potter, B.J., Wang, W., Kuo, L., Michael, L., et al. 2006. TNF-α contributes to endothelial dysfunction in ischemia/reperfusion injury. Arterioscler. Thromb. Vasc. Biol. **26**(3): 475–480. PMID:16385082.

Zhao, G., Zhang, W., Li, L., Wu, S., and Du, G. 2014. Reperfusion induces myocardial apoptotic cell death. Cardiovasc. Res. **45**(3): 651–660.

Zhao, Z.Q., Nakamura, M., Wang, N.P., Wilcox, J.N., Shearer, S., Ronson, R.S., et al. 2000. Reperfusion induces myocardial apoptotic cell death. Cardiovasc. Res. **45**(3): 651–660.

Zorov, D.B., Filburn, C.R., Klotz, L.-O., Zweier, J.L., and Sollott, S.J. 2000. Reactive oxygen species (ROS)-induced ROS release: a new phenomenon accompanying induction of the mitochondrial permeability transition in cardiac myocytes. J. Exp. Med. **192**: 1001–1014. doi:10.1084/jem.192.7.1001. PMID:11015441.

Biomedicine & Pharmacotherapy 92 (2017) 412–420

Available online at
ScienceDirect
www.sciencedirect.com

Elsevier Masson France
EM|consulte
www.em-consulte.com/en

Original article

Anthocyanin-rich Riceberry bran extract attenuates gentamicin-induced hepatotoxicity by reducing oxidative stress, inflammation and apoptosis in rats

Phatchawan Arjinajarn[a], Nuttawud Chueakula[b], Anchalee Pongchaidecha[b], Krit Jaikumkao[b], Varanuj Chatsudthipong[c], Sugunya Mahatheeranont[d], Orranuch Norkaew[d], Nipon Chattipakorn[b,e], Anusorn Lungkaphin[b,*]

[a] Department of Biology, Faculty of Science, Chiang Mai University, Chiang Mai, Thailand
[b] Department of Physiology, Faculty of Medicine, Chiang Mai University, Chiang Mai, Thailand
[c] Department of Physiology, Faculty of Science, Mahidol University, Bangkok, Thailand
[d] Department of Chemistry, Faculty of Science, Chiang Mai University, Chiang Mai, Thailand
[e] Cardiac Electrophysiology Research and Training Center, Faculty of Medicine, Chiang Mai University, Chiang Mai, Thailand

ARTICLE INFO

Article history:
Received 26 January 2017
Received in revised form 15 May 2017
Accepted 22 May 2017

Keywords:
Apoptosis
Gentamicin
Inflammation
Liver
Oxidative stress
Riceberry bran extract

ABSTRACT

Liver plays an important role in the detoxification and metabolic elimination of various drugs and harmful substances. The damaging effects on the liver tissue treated with gentamicin are multi-factorial and their mechanisms remain unclear. This study aimed to investigate the possible protective effects of anthocyanin-rich Riceberry bran extract on gentamicin-induced hepatotoxicity in rats. Riceberry bran extract was given by oral administration 30 min before gentamicin injection for 15 consecutive days. Serum levels of liver marker enzymes, AST and ALT, were significantly elevated and the total serum protein level was markedly reduced in gentamicin-treated rats. Gentamicin injection led to the significant increase in hepatic MDA level and decrease SOD expression. Liver inflammation and apoptosis were observed in gentamicin-treated rats as indicated by the increases in NF-κB, TNF-αR1, COX2, and iNOS, caspase-3, Bax, and decrease in Bcl-XL expressions. Riceberry bran extract significantly prevented gentamicin-induced the elevations of serum AST, ALT and the reduction of serum total protein. These were related to the inhibition of oxidative stress, inflammation and apoptosis in Riceberry bran extract treatment. These findings suggest that anthocyanin-rich Riceberry bran extract can prevent liver dysfunction and damage induced by gentamicin, possibly through its antioxidant, anti-inflammatory and anti-apoptotic effects.

1. Introduction

Liver plays an important role in the detoxification and metabolic elimination of various drugs and harmful substances [1]. Its exposure to hazardous compounds and toxins could lead to injury and reduced function [2]. Gentamicin, an aminoglycoside antibiotic, is a common used drug for the treatment of severe gram-negative bacterial infections [3]. There are several reports concerning the nephrotoxicity and cytotoxicity of gentamicin [4]. The hepatotoxicity of gentamicin as reflected by significant increases in liver enzyme activities and histological lesions were also reported [5–8]. The pathogenesis of gentamicin-induced liver toxicity is multi-factorial and its mechanism is not fully understood. Among these, oxidative stress is suggested to be a major cause of hepatotoxicity [9,10].

Nuclear factor erythroid-2-related factor-2 (Nrf2) is a cellular sensor of oxidative stress and functions in defensing against harmful effect that occurs due to an elevated reactive oxygen species and toxic damage [11,12]. In response to reactive oxygen species (ROS), cytosolic Nrf2 is dissociated from Keap1 and translocated into the nucleus leading to the activation of detoxifying enzymes and antioxidant proteins such as glutathione S-transferase (GST), heme-oxygenase 1 (HO-1), NAD(P)H, quinone reductase (NQO1) and glutathione (GSH) [13–15]. Moreover, oxidative stress leads to the activation of transcription factor like

* Corresponding author at: Department of Physiology, Faculty of Medicine, Chian Mai University, Intravaroros Road, Chiang Mai, 50200, Thailand.
E-mail addresses: onanusorn@yahoo.com, anusorn.lungka@cmu.ac.th (A. Lungkaphin).

http://dx.doi.org/10.1016/j.biopha.2017.05.100
0753-3322/

nuclear factor-κB (NF-κB) which plays a crucial role in the regulation of genes involved in inflammatory process such as the inducible nitric oxide synthase (iNOS), cycloxygenase-2 (COX2), interleukin-1b (IL-1b) and tumor necrosis factor-α (TNF-α) [16–19]. Excessive intracellular ROS production could lead to cell apoptosis through the modulation of Bcl2 family proteins and caspases [20].

Various kinds of plant extract with strong antioxidant activity have been reported to ameliorate organ toxicities [21,22]. Rice is a main staple food for 3–4 billions of people around the world. Riceberry rice (*Oryza sativa* L.), a Thai black purple rice, is a new breeding line developed by crossing Khao Hom Nin rice with the fragrant Thai Jasmine rice or Khao Dawk Mali [23]. It has recently been developed to provide optimum nutritional benefit to consumers since it contains high iron content and little glucose which is good for anemic and diabetes mellitus patients. It has been found that Riceberry whole-grain rice has a "medium" Glycemic index. Riceberry oil supplementation affected hyperglycemia and change in lipid profile [23] and Riceberry bran can also improve hyperglycemia and hyperlipidemia conditions as well as decrease oxidative stress and inflammation in steptozotocin-induced diabetic rats fed a high fat [24]. Moreover, the bran part of Riceberry shows high levels of antioxidant contents and other significant bioactive compounds, such as anthocyanins (cyanidin 3-glucoside and peonidin-3-glucoside), β-carotene, γ-oryzanol and vitamin E complex (tocopherols and tocotrienols) [25]. These data led us to investigate the hepatoprotective effects of Riceberry bran extract against gentamicin-induced hepatotoxicity. We tested the hypothesis that Riceberry bran extract exerts hepatoprotection against gentamicin-induced hepatotoxicity via its antioxidant, anti-inflammatory and anti-apoptotic effects.

2. Material and methods

2.1. Chemicals and reagents

Gentamicin was purchased from the Pharmaceutical Organization, INC (Bangkok, Thailand). Riceberry bran extract was obtained from Department of Chemistry, Faculty of Science, Chiang Mai University (Chiang Mai, Thailand). Malondialdehyde (MDA) assay kit was obtained from Cayman Chemical Company (Ann Arbor, MI, USA). Mammalian tissue lysis/extraction reagent was purchased from Sigma-Aldrich Corp. (St. Louis, Missouri, USA). Complete protease inhibitor cocktail was purchased from Roche Applied Science (Indianapolis, Indiana, USA). Polyclonal rabbit antibody against Nrf2 was purchased from Santa Cruz Biotechnology (Santa Cruz, CA, USA). Antibodies against nuclear factor erythroid-2-related factor-2 (Nrf2), heme oxygenase-1 (HO-1) and NAD(P)H: quinone reductase-1 (NQO-1) were obtained from Abcam (Cambridge, UK). Antibodies against SOD2, COX-2, TNFα-R1, Lamin B1, NF-κB subunit p65 and β-actin were purchased from Cell Signaling Technology, Inc. (Beverly, MA, USA). A poly-vinylidene fluoride (PVDF) membrane and polyclonal antibodies against caspase 3 and iNOS were obtained from Millipore (Billerica, MA, USA). Monoclonal antibodies against Bax and Bcl-xL were purchased from Upstate (Lake Placid, NY, USA). Secondary antibodies, HRP conjugated anti-rabbit, anti-goat were purchased from Santa Cruz Biotechnology (Santa Cruz, CA, USA). The ECL enhanced chemilunescence agent and Hyperfilm were purchased from GE Healthcare (Buckinghamshire, UK). Other chemicals and reagents were all purchased from commercial sources and were of analytical grade.

2.2. Extract preparation and quantification of its major compounds

Riceberry bran (1 kg) was extracted by 3 L of methanol for 24 h at room temperature. After removing the solvent by evaporation, the bran extract was found to contain two major anthocyanins, cyanidin 3-glucoside and peonidin-3-glucoside at the amount of 13.24 and 5.33 mg/g of crude extract, respectively. Further screening for other bioactive components, apigenin as the main flavonoid determined by LC–MS (Agilent HP1100 and MSD Model G 1946A, Agilent Technologies, Santa Clara, CA, USA) was found but it appeared in only small amount compared with the other two anthocyanins.

2.3. Animals

Male Sprague Dawley rats (180–200 g) from the National Experimental Animal Center, Salaya, Mahidol University, were housed in the animal room at controlled temperature about 25 ± 2 °C with 12 h light–12 h dark cycle and fed with a normal pellet diet and water ad libitum. This study was performed in strict accordance with the recommendations in the Guide for the Care and Use of Laboratory Animals of the National Institutes of Health. The protocol was approved by the Committee on the Ethics of Animal Experiments of the Faculty of Medicine, Chiang Mai University, Chiang Mai, Thailand (Permit No: 10/2557). All surgeries were performed under sodium pentobarbital anesthesia to minimize suffering.

2.4. Experimental design

The rats were randomly assigned into 6 groups (5–7 rats per group) as follows:- (1) the control group, the rats received intraperitoneal (i.p.) saline injection; (2) the gentamicin (GM) group, the rats were i.p. injected with gentamicin 100 mg/kg body weight; (3–5) gentamicin plus Riceberry bran extract (GM + RBE) groups; the rats were pretreated by oral gavage with various doses of RBE (250, 500 and 1000 mg/kg body weight, respectively) 30 min before gentamicin treatment; and (6) Riceberry bran extract (RBE 1000) group, the rats received only RBE at a dose of 1000 mg/kg. All treatments were given to rats for 15 days. Twenty-four hours after the last dose of gentamicin treatment, the rats were sacrificed and then blood and liver samples were collected for subsequent analysis.

2.5. Determination of serum biomarkers for liver function and total serum protein level

The serum alanine transaminase (ALT) and aspartate transaminase (AST) and total serum protein were measured by following enzymatic colorimetric methods using Reflotron Plus Analyzer and Roche Kits (Roche Diagnostics, Indianapolis, Indiana, USA). The data were expressed as mg/dL.

2.6. Determination of lipid peroxidation

Lipid peroxidation was measured in the liver by the method of Ohkawa [26] and was expressed in term of malondialdehyde (MDA) as biomarker for oxidative stress. The tissue was homogenized on ice in Mammalian cell Lytic buffer with protease inhibitor cocktail. The homogenates were centrifuged at 1600 × *g* for 10 min at 4 °C and the supernatants were collected. MDA level was determined by colorimetry using a commercial TBARS assay kit and expressed as nmol/mg protein. Total protein content of the tissues was determined using a DC protein assay kit (Bio-Rad Laboratories, Hercules, CA, USA).

2.7. Tissue preparation and western blot analysis

Whole cell lysate, nuclear, cytosolic and membrane fractions were separated from frozen liver tissue. In brief, the liver was

homogenized in Mammalian Cell Lytic buffer with protease cocktail inhibitor. The total liver homogenate was centrifuged at 5000 × *g* for 15 min at 4 °C to obtain the whole cell lysate (supernatant) fraction. The supernatant was centrifuged again at 100,000 × *g*, for 2 h at 4 °C to obtain the membrane (pellet) and cytosolic (supernatant) fractions. The 5000 × g pellet was resuspended and centrifuged at 10,000 × *g* at 4 °C for 10 min to obtain supernatant containing the nuclear fraction. All the fractions were immediately frozen and kept at −80 °C until use.

For western blot analysis, denatured (95 °C, 5 min) proteins (50 μg) were separated by SDS-PAGE (10% gels), transferred to a PVDF membrane and blocked in Tris-buffered saline containing 0.1% Tween-20(TBST) plus 5% of skim milk at room temperature for 1 h. Membranes were incubated overnight at 4 °C in the appropriate primary antibodies against SOD2, Nrf2, NQO-1, HO-1, NF-κB, iNOS, TNF-αR1, COX-2, Bax, Bcl-XL and cleaved caspase 3and then washed 3 times with TBST followed by incubation for 1 h at room temperature with specific horseradish peroxidase (HRP)-conjugated secondary antibody. Next, the protein bands were detected using ECL plus reagent, then, bands were scanned and quantified by densitometric analysis with ImageJ software(NIH, Bethesda, MD, USA), and signal density was normalized to β-actin density and expressed in arbitrary units (AU).

2.8. Statistical analysis

The results were expressed as means ± standard error of mean (SEM) and analyzed using SPSS software version17statistical program (SPSS Inc., Chicago, Illinois, USA). For comparison between experimental groups, a one way analysis of variance (ANOVA) followed by Tukey's test was used. A value of $P < 0.05$ was considered statistically significant.

3. Results

3.1. Effect of Riceberry bran extract on liver function

As shown in Table 1, the serum levels of liver marker enzymes, AST and ALT, were significantly elevated and the total serum protein level was markedly reduced in gentamicin-treated rats compared with the control ($p < 0.05$). These results indicated that gentamicin injection for 15 days induced liver dysfunction in this study. Gentamicin plus Riceberry bran extract at the dose 500 mg/kg body weight (GM + RBE 500) showed to have the highest efficacy to improve liver function as shown by the significant decreases in serum levels of AST and ALT and increase in serum total protein level when compared with gentamicin-treated group ($p < 0.05$). GM + RBE 250 and GM + RBE 1000 could also restored serum AST and total protein levels which were significantly different when compared with the gentamicin-treated rats ($p < 0.05$). The ALT level in GM + RBE 250 and GM + RBE 1000 was lower when compared with gentamicin group although the significant difference was not observed. Moreover, the levels of AST and ALT in GM + RBE 500 group was significantly different from GM + RBE 250 and GM + RBE 1000 groups ($p < 0.05$). The level of total protein was not significantly different among the three groups of RBE treatments. RBE 1000 had no effect on serum AST and total protein levels when compared with control. However, RBE 1000 showed to increase serum ALT level when compared with control ($p < 0.05$). Therefore, high dose of RBE may be used with cautions. These results demonstrated that the RBE treatment especially RBE at the dose of 500 mg/kg body weight could ameliorate liver dysfunction in gentamicin-treated rats.

Table 1
Effect of RBE on liver function marker enzymes and total protein level.

Parameters	AST (U/L)	ALT (U/L)	Total serum protein (mg/dL)
Control	73.44 ± 2.49^{b}	35.50 ± 4.38^{b}	5.40 ± 0.10^{b}
GM	94.98 ± 5.22^{c}	41.20 ± 3.65^{c}	4.77 ± 0.20^{a}
GM + RBE 250	66.20 ± 3.92^{a}	39.20 ± 3.52^{c}	5.40 ± 0.05^{b}
GM + RBE 500	74.00 ± 6.30^{b}	32.60 ± 1.77^{a}	5.53 ± 0.23^{b}
GM + RBE 1000	67.60 ± 2.38^{a}	40.20 ± 3.67^{c}	5.47 ± 0.03^{b}
RBE 1000	76.60 ± 4.63^{b}	39.00 ± 1.36^{c}	5.56 ± 0.03^{b}

AST: aspartate aminotransferase, ALT: alanine aminotransferase, GM: gentamicin, GM + RBE 250: gentamicin plus RBE at dose of 250 mg/kg body weight, GM + RBE 500: gentamicin plus RBE at dose of 500 mg/kg body weight, GM + RBE 1000: gentamicin plus RBE at dose of 1000 mg/kg body weight, RBE 1000: Riceberry bran extract at dose of 1000 mg/kg body weight. Values are mean ± S.E.M. of 5–7 animals in each group. Values with different superscript letters (a–c) in the same column differ significantly ($p < 0.05$) by the Tukey's test.

3.2. Effect of Riceberry bran extract on liver lipid peroxidation

Gentamicin treatment led to a significant increase in hepatic MDA level, an indicator of lipid peroxidation, compared with the control and RBE 1000 groups ($p < 0.05$) (Fig. 1). The hepatic MDA levels in gentamicin plus RBE treatment in three different doses (250, 500 and 1000 mg/kg body weight) were significantly attenuated when compared with the gentamicin-treated rats ($p < 0.05$). Moreover, in GM + RBE 500 and GM + RBE 1000 groups, the levels of MDA were significantly lower than that of GM + RBE 250 groups ($p < 0.05$). The levels of hepatic MDA were not significantly different when compared between GM + RBE 500 and GM + RBE 1000 groups. RBE treatment (RBE 1000) had no effect on hepatic MDA level when compared with control. These results suggested that lipid peroxidation induced by gentamicin injection could be ameliorated by RBE treatment. Since RBE treatments at the doses of 500 and 1000 mg/kg showed similar degree of hepatoprotective effects, RBE at the dose of 500 mg/kg was selected for the subsequent experiments. In the RBE group, the dose of 1000 mg/kg was used to study the effect of high dose of RBE alone on hepatotoxicity in control rats.

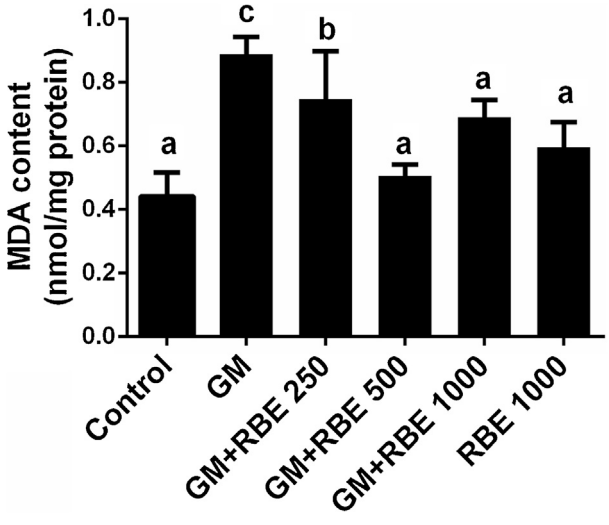

Fig. 1. Effect of RBE on malondialdehyde (MDA). GM: gentamicin, GM + RBE 250: gentamicin plus RBE at dose of 250 mg/kg body weight, GM + RBE 500: gentamicin plus RBE at dose of 500 mg/kg body weight, GM + RBBE 1000: gentamicin plus RBE at dose of 1000 mg/kg body weight, RBE 1000: RBE at dose of 1000 mg/kg body weight. Values are mean ± SEM of 5–7 animals in each group. Values with different superscript letters (a–c) differ significantly ($p < 0.05$) by the Tukey's test.

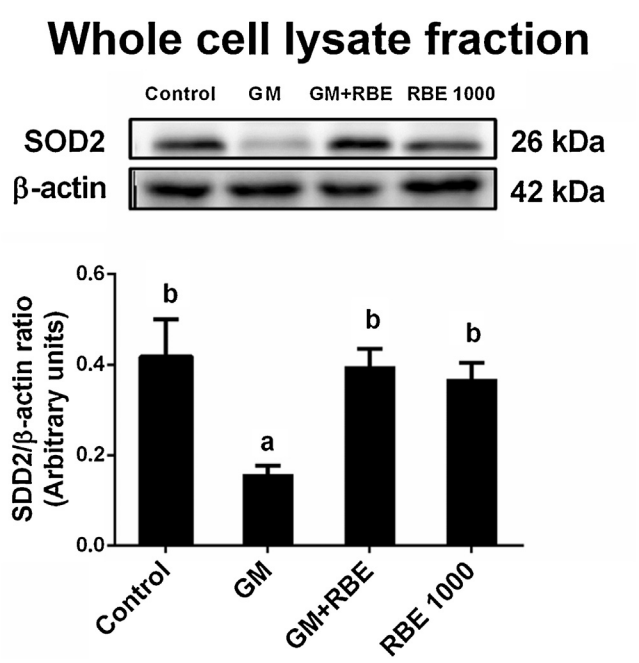

Fig. 2. Effect of RBE on the antioxidant activity. A; Representative immunoblot analysis for SOD2 in the whole cell lysate fraction of liver tissues. B; Representative bar diagram showing relative densities of SOD2 proteins. Lanes 1–4 represent Control, GM: gentamicin, GM + RBE: gentamicin plus RBE at the dose of 500 mg/kg body weight and RBE 1000: RBE alone at the dose of 1000 mg/kg body weight, correspondingly. Bar graphs indicate mean ± SEM of 5–7 animals in each group. Values with different superscript letters (a–c) differ significantly ($p < 0.05$) by the Tukey's test.

3.3. Effect of Riceberry bran extract on antioxidant activity

Fig. 2 showed a marked decrease in SOD2 protein expression in liver tissues of gentamicin-treated rats compared with the control and RBE 1000 rats ($p < 0.05$). There was a significant elevation of SOD2 protein expression in gentamicin plus RBE treatment rats compared to that of the gentamicin-treated rats ($p < 0.05$). This result suggested that treatment with RBE could increase antioxidant activity.

3.4. Effect of Riceberry bran extract on the expressions of Nrf2, HO-1 and NQO-1 protein

Nrf2 and its downstream signaling molecules including HO-1 and NQO-1 have been shown to be important for protecting liver from oxidative damage and are highly upregulated by oxidative stress [27]. Therefore, we next evaluated the effect of RBE on the Nrf2/HO-1/NQO-1signaling pathway. As depicted in Fig. 3, the Nrf2 protein expression in hepatic cytosolic fraction was significantly decreased ($p < 0.05$) while it was apparently elevated in nuclear fraction ($p < 0.05$) in the gentamicin-treated rats compared with the control. These indicated the increased translocation of Nrf2 from cytosol to nucleus in the gentamicin-treated rats. This stimulation had been attenuated in RBE treatment as shown by the reduced Nrf2 expression in nuclear fraction concomitant with the increased expression of Nrf2 in the cytosolic fraction in RBE treatment as compared to gentamicin-treated group ($p < 0.05$). Although RBE 1000 showed to significantly reduced cytosolic Nrf2 expression as compared to control ($p < 0.05$), the translocation of Nrf2 to the nucleus was not significantly different from that of control group. In addition, there were significant increases in HO-1 and NQO-1 expressions in the gentamicin-treated rats compared to the control or RBE 1000 group ($p < 0.05$). The expressions of HO-1 and NQO-1 in gentamicin plus RBE treatment group were significantly decreased ($p < 0.05$) when compared with gentamicin-treated group. No statistically significant differences were observed between control and RBE 1000 group. The results demonstrated that RBE treatment attenuated gentamicin-induced liver oxidative stress through the modulating of Nrf2/HO-1/NQO-1 signaling pathway.

3.5. Effect of Riceberry bran extract on liver inflammation

It has been reported that oxidative stress can activate NF-κB which in turn induces the expressions of inflammatory molecules including iNOS, TNF-α and COX-2 that cause liver damage [28,29]. To determine whether RBE could protect liver inflammation induced by gentamicin, the expressions of NF-κB and proinflammatory cytokines were determined. The significant increases in NF-kB along with iNOS, TNF-αR1 and COX2 expressions in the liver tissues were observed in gentamicin-treated rats compared with the control and RBE1000 rats ($p < 0.05$) (Fig. 4). These findings suggested that gentamicin induced an inflammation via NF-κB pathway. The NF-kB expression was significantly reduced in gentamicin plus RBE treatment compared to that of gentamicin-treated rats ($p < 0.05$). The expressions of iNOS, TNF-αR1 and COX-2 were also significantly lowered in gentamicin plus RBE treatment than that of gentamicin-treated rats. The results suggested that RBE inhibited the activation of NF-kB which in turn downregulated the iNOS, TNF-αR1 and COX-2 protein expressions.

3.6. Effect of riceberry bran extract on liver apoptosis

We hypothesized that RBE might have anti-apoptotic effect that contributed to hepatoprotection induced by gentamicin. Therefore, pro-apoptotic proteins, Bax and anti-apoptotic proteins, Bcl-XL as well as caspase family protein, caspase-3, which play critical roles in the regulation of cell apoptosis [30–32] were evaluated. As shown in Fig. 5, the expression of Bax protein was significantly upregulated, whereas the expression of Bcl-XL protein was apparently downregulated in gentamicin-treated rats in comparison to the control and RBE 1000groups ($p < 0.05$). Moreover, the Bax/Bcl-XL ratio was significantly higher in the gentamicin-treated group than that of in the control and RBE1000 groups ($p < 0.05$). Interestingly, treatment with RBE could reverse Bax and Bcl-XL expressions, Bax/Bcl-XL ratio as well as caspase-3 expression back to the control. These results suggested that RBE had anti-apoptotic effect by modulating the Bcl-2 family proteins, inhibiting the activation of the caspase cascade, and thereby protected liver tissue from gentamicin-induced hepatotoxicity.

4. Discussion

This study showed that administration of gentamicin at the dose of 100 mg/kg body weight for 15 consecutive days induced hepatotoxicity as evidenced by the significant elevation of serum AST and ALT levels and a decrease in serum total protein level. Gentamicin-induced hepatotoxicity was associated with an increased oxidative stress, inflammation and apoptosis. Gentamicin plus RBE treatment showed an improvement of liver function. This study is the first to show that RBE treatment might provide protection against liver injury by ameliorating oxidative stress, inflammation and apoptosis.

A significant increase in the lipid peroxidation product, MDA, in gentamicin-treated rats in this study was consistent with previous report indicating that gentamicin enhanced the production of

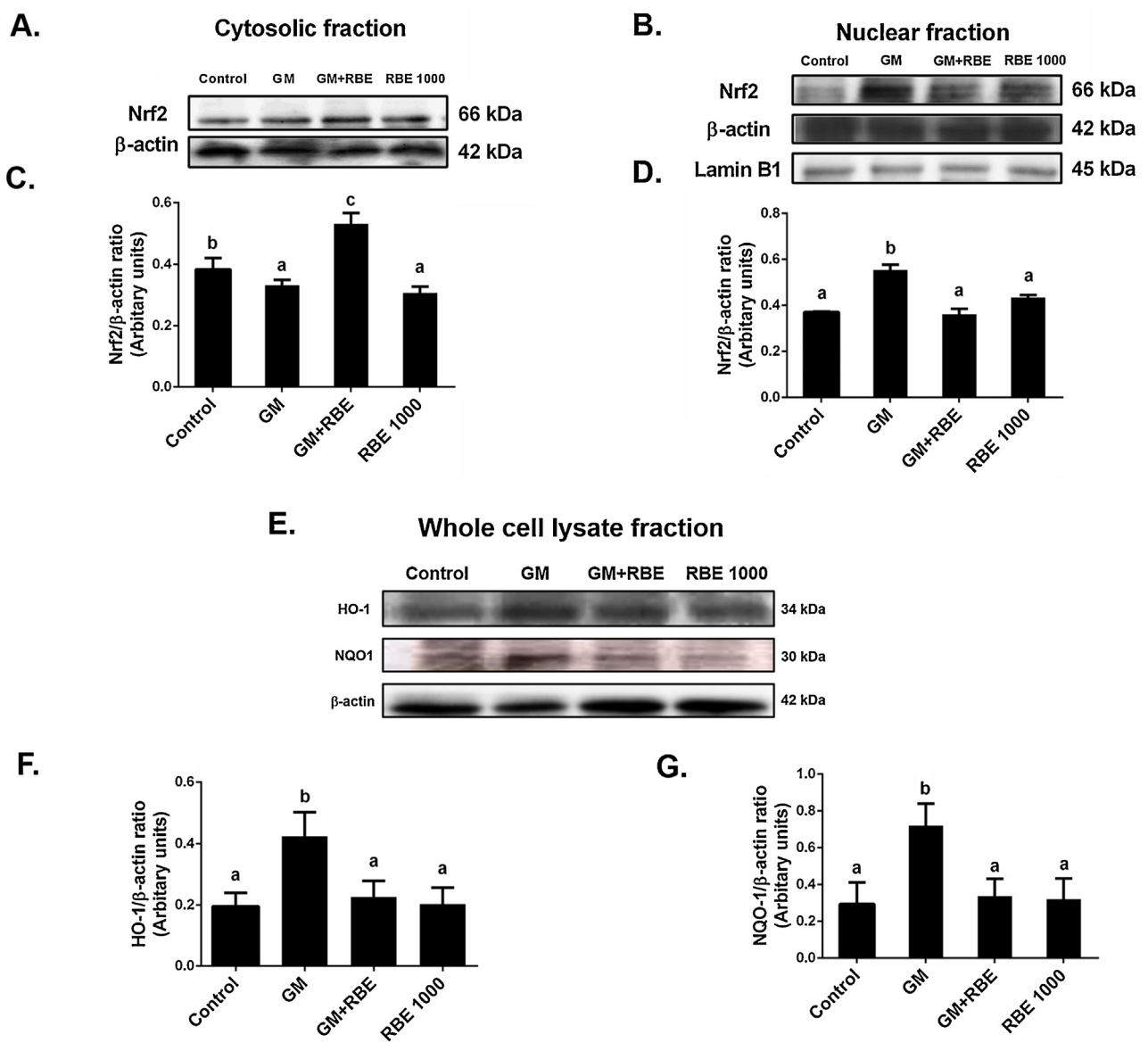

Fig. 3. Effect of RBE on the expressions of Nrf2, HO-1 and NQO-1 protein. A and B; Representative immunoblots analysis for Nrf2 in the cytosolic and nuclear fractions of liver tissues, respectively. C and D; Representative bar diagram showing relative densities of Nrf2 protein in the cytosolic and nuclear fraction of liver tissues, respectively. E; Representative immunoblots analysis for HO-1 and NQO-1 in the whole cell lysate fractions of liver tissues. F and G; Representative bar diagram showing relative densities of HO-1 and NQO-1 proteins, respectively. Lanes 1–4 represent Control, GM: gentamicin, GM + RBE: gentamicin plus RBE at the dose of 500 mg/kg body weight and RBE 1000: RBE alone at the dose of 1000 mg/kg body weight, correspondingly. Lamin B1 is a nuclear protein marker, and β-actin is a loading control. Bar graphs indicate mean ± SEM of 5–7 animals in each group. Values with different superscript letters (a–c) differ significantly ($p < 0.05$) by the Tukey's test.

reactive oxygen species including superoxide anion, hydrogen peroxide and hydroxyl radicals which could further stimulate peroxidation of membrane lipids, protein and nucleic acids [20]. There was also a decreased antioxidant SOD2 in the liver tissue of gentamicin rats. An increased ROS generation and impaired antioxidant defenses contributed to oxidative stress which resulted in liver toxicity, dysfunction and damage. A decreased MDA level along with the increase of SOD2expression in the liver of gentamicin plus RBE treatment rats indicated an amelioration of oxidative stress by RBE. The antioxidant effects of RBE might be due to its anthocyanin components, mainly cyanidin-3-glucoside and peonidin-3-glucoside which were highly expressed in black purple rice bran part. These anthocyanins have shown to possess remarkable antioxidant as well as anti-inflammatory properties [25,33]. This notion was supported by the study in mice by which liver injury was induced by carbon tetrachloride (CCl4). It was reported that anthocyanin-rich RBE administration significantly decreased a lipid peroxidation marker thiobarbituric acid reactive substances (TBARS) level [24]. Pre-incubated the liver L-02 cells with cyanidin-3-glucoside and peonidin-3-glucoside, the predominant anthocyanins, significantly ameliorated CCl4-induced cell injury [34]. Moreover, RBE also contains the flavonoid apigenin and the simple phenols 4-vinylguaiacol. These bioactive compounds have a wide range of pharmacological activities including anti-oxidative, anti-inflammatory and anti-cancer [35,36].

Cellular responses to oxidative stress are regulated by the redox-sensitive transcription factor, NF-E2-related factor 2 (Nrf2) [14]. In the present study, the significant elevation of Nrf2 protein expression in hepatic nuclear fraction was accompanied by the increases in HO-1 and NQO-1 expressions in whole cell lysate

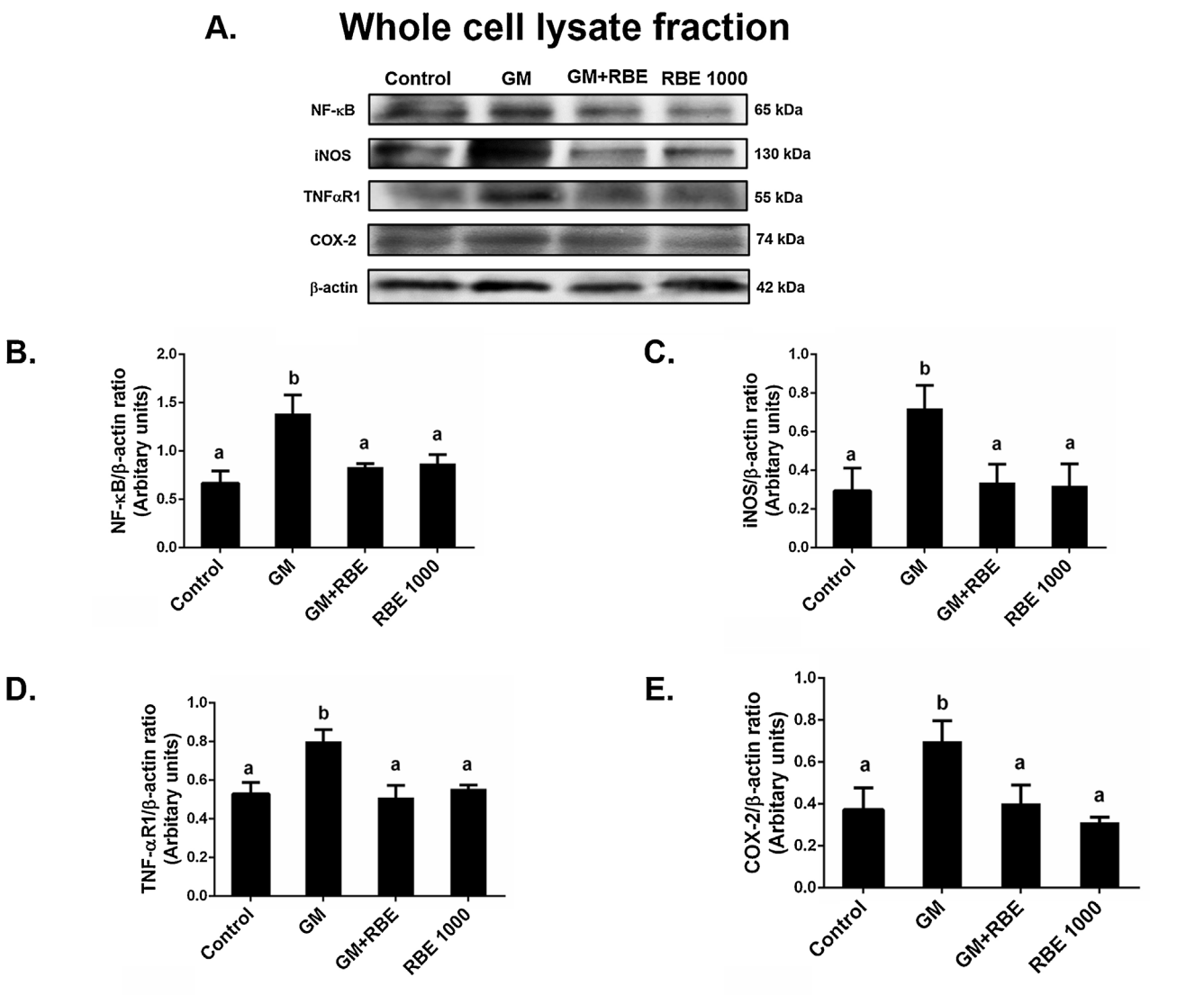

Fig. 4. Effect of RBE on the expressions of inflammatory markers NF-κB, iNOS, TNF-αR1 and COX-2 protein. A; Representative immunoblots analysis for NF-κB, iNOS, TNF-αR1 and COX-2 in the whole cell lysate fractions of liver tissues. B–E; Representative bar diagram showing relative densities of NF-κB, iNOS, TNF-αR1 and COX-2 proteins in the whole cell lysate fractions of liver tissues, respectively. Lanes 1–4 represent Control, GM: gentamicin, GM + RBE: gentamicin plus RBE at the dose of 500 mg/kg body weight and RBE 1000: RBE alone at the dose of 1000 mg/kg body weight, correspondingly. β-actin is a loading control. Bar graphs indicate mean ± SEM of 5–7 animals in each group. Values with different superscript letters (a–c) differ significantly ($p < 0.05$) by the Tukey's test.

fraction in the gentamicin-treated rats. These findings suggested that the increased oxidative stress condition induced by gentamicin might stimulate Nrf2 translocation to the nucleus and subsequent activation the anti-oxidant response element (ARE) leading to upregulation of NQO1 and HO-1 expressions. It was noteworthy that RBE treatment could significantly suppress nuclear translocation of Nrf2 which subsequently decrease NQO1 and HO-1 expressions in gentamicin plus RBE rats. These finding implied that RBE exerted an antioxidant action via modulating Nrf2 signaling pathway. Similar results were reported in our previous studies demonstrating that the increased Nrf2, NQO1 and HO-1 expressions in response to gentamicin-induced oxidative stress could be alleviated through the pleiotropic antioxidant effect of atorvastatin [37] and pinocembrin [38].

Oxidative stress can activate NF-κB, which plays a crucial role in inflammation, cellular proliferation and apoptosis [39,40]. In this study, an increased hepatic NF-κB expression in gentamicin-treated rats indicated the activation of NF-κB by gentamicin treatment. These were accompanied by the increased expressions of COX-2, iNOS and TNF-αR1. Previous study in Zucker diabetic rats has reported the upregulation of TNF-α and receptors associated with endothelial dysfunction [41]. An increased expression of TNF-αR1 in this study might imply an elevation of TNF-α activity in gentamicin-treated rat liver. These data are in concurrence with the previous report [42]. Therefore, NF-κB activation might play a role in hepatic inflammation in this study. Moreover, TNF-α also activates the NF-κB pathway, thus resulting in amplifying the inflammatory response [43]. RBE treatment showed to decrease the expressions of NF-κB, iNOS and TNFα-R1 in gentamicin-treated rats. These findings suggested that RBE improved liver inflammation by attenuating the activation of NF-κB pathway. This was supported by the previous study in mouse macrophage cell linings which demonstrated that two major anthocyanins, cyanidin-3-glucoside and peonidin-3-glucoside could reduce inflammation and enhance anti-inflammation by suppressing nitric oxide synthase [33]. Moreover, feruloyl esters, a part of

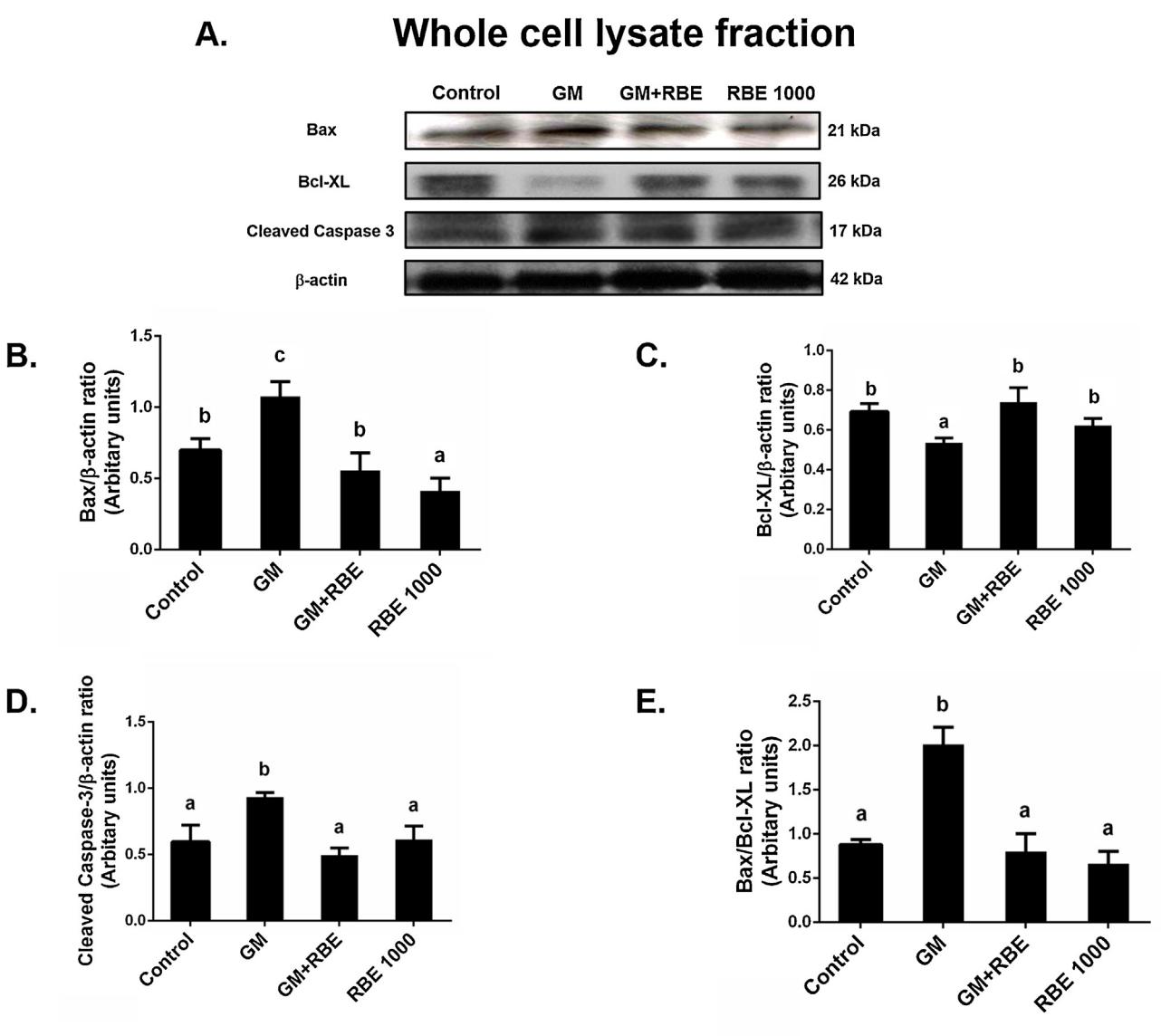

Fig. 5. Effect of RBE on the expressions of apoptotic markers Bax, Bcl-XL and cleaved caspase 3 protein. A; Representative immunoblots analysis for Bax, Bcl-XL and cleaved caspase 3 in the whole cell lysate fractions of liver tissues. B–D; Representative bar diagram showing relative densities of Bax, Bcl-XL and cleaved caspase 3 proteins in the whole cell lysate fractions of liver tissues, respectively. E; Bax/Bcl-xL ratio in liver were measured by immunoblots. Lanes 1–4 represent Control, GM: gentamicin, GM + RBE: gentamicin plus RBE at the dose of 500 mg/kg body weight and RBE 1000: Riceberry bran extract alone at the dose of 1000 mg/kg body weight, correspondingly. β-actin is a loading control. Bar graphs indicate mean ± SEM of 5–7 animals in each group. Values with different superscript letters (a–c) differ significantly ($p < 0.05$) by the Tukey's test.

γ-oryzanol found in rice bran has been reported to reduce nitric oxide in macrophage cell by inhibiting NF-kB activation [44]. Therefore, RBE might have an anti-inflammatory effect to protect liver damage via the modulating of NF-κB pathway.

Apoptosis plays a key role in inflammatory process as well as many liver disease and drug induced hepatotoxicity [45,46]. ROS generation can induce apoptosis through the activation of the intrinsic, mitochondria-dependent pathway. In the present study, gentamicin-induced liver apoptosis was shown by a reduced expression of Bcl-XL accompanied by the elevated expressions of Bax, cleaved caspase 3 and Bax/Bcl-XL ratio. These findings were consistent with the recent study demonstrating that caspase-dependent apoptotic signaling pathway was associated with gentamicin-induced apoptotic liver damage [20]. Under normal condition, the maintenance of mitochondrial membrane potential depends on pro-apoptotic (Bax) and anti-apoptotic (Bcl2) members of Bcl2 family. Interestingly, RBE treatment showed to restore Bcl-XL expression, inhibit Bax and cleaved caspase 3 over-expressions in gentamicin-treated rats. According to the report that NF-κB activation promoted gentamicin-induced apoptosis in rat tubular cells [47], the anti-inflammatory effect of RBE might partly attribute to its suppression of gentamicin-induced apoptosis. The results from this study suggest that RBE could prevent gentamicin-induced apoptotic liver damage partly by attenuating oxidative stress and suppressing the activation of NF-κB pathway.

5. Conclusion

The present results clearly show that RBE can prevent gentamicin-induced liver injury through suppressing oxidative stress and NF-κB activation which lead to attenuate inflammation and apoptotic pathway. This study provides the evidence of RBE as the adjuvant of gentamicin to prevent hepatotoxicity.

Conflicts of interest

The authors declare that they have no conflict of interests

Acknowledgements

This work was supported by the Young Researcher Support Grant, Chiang Mai University (PA), the Thailand Research Fund (TRG-5780019) (PA), (RSA5780029) (AL), National Research Council of Thailand (Grant #347682/2560) (AL), the Faculty of Medicine Research Fund, Chiang Mai University (AL and AP), the Higher Education Commission, Ministry of Education, Thailand, through the Higher Education Research Promotion and National Research University Project of Thailand and the Center of Excellence for Innovation in Chemistry (PERCH-CIC) (SM) and the NSTDA Research Chair grant from the National Science and Technology Development Agency of Thailand (NC).

References

[1] C. Mayuren, V.V. Reddy, S.V. Priya, V.A. Devi, Protective effect of Livactine against CCl(4) and paracetamol induced hepatotoxicity in adult Wistar rats, N. Am. J. Med. Sci. 2 (10) (2010) 491–495.
[2] N. Sultana, S.C. Shimmi, M.T.H. Parash, J. Akhtar, Effects of ashwagandha (Withania somnifera) root extract on some serum liver marker enzymes (AST, ALT) in gentamicin intoxicated rats, J. Bangladesh Soc. Physiol. 7 (1) (2012) 1–7.
[3] C. Martinez-Salgado, F.J. Lopez-Hernandez, J.M. Lopez-Novoa, Glomerular nephrotoxicity of aminoglycosides, Toxicol. Appl. Pharmacol. 223 (1) (2007) 86–98.
[4] W.M. Lee, Drug-induced hepatotoxicity, N. Engl. J. Med. 349 (5) (2003) 474–485.
[5] J. Aubrecht, M.E. Goad, E.M. Simpson, R.H. Schiestl, Expression of hygR in transgenic mice causes resistance to toxic effects of hygromycin B in vivo, J. Pharmacol. Exp. Ther. 281 (2) (1997) 992–997.
[6] A.A. Khan, A.M. Alzohairy, Hepatoprotective effects of camel milk against CCl4-induced hepatotoxicity in Rats, Asian J. Biochem. 6 (2011) 171–180.
[7] E.R. Al-kenanny, L.K. Al-Hayaly, A.G. Al-Badrany, Protective effect of Arabic gum on liver injury experimentally induced gentamycin in mice, Kufa J. Vet. Med. Sci. 3 (1) (2012) 174–189.
[8] A.O. Ademiluyi, G. Oboh, T.R. Owoloye, O.J. Agbebi, Modulatory effects of dietary inclusion of garlic (Allium sativum) on gentamycin-induced hepatotoxicity and oxidative stress in rats, Asian Pac. J. Trop. Biomed. 3 (6) (2013) 470–475.
[9] B.H. Ali, Gentamicin nephrotoxicity in humans and animals: some recent research, Gen. Pharmacol. 26 (7) (1995) 1477–1487.
[10] W. Lesniak, V.L. Pecoraro, J. Schacht, Ternary complexes of gentamicin with iron and lipid catalyze formation of reactive oxygen species, Chem. Res. Toxicol. 18 (2) (2005) 357–364.
[11] Y. Mitsuishi, H. Motohashi, M. Yamamoto, The Keap1-Nrf2 system in cancers: stress response and anabolic metabolism, Front. Oncol. 2 (2012) 200.
[12] A. Lau, S.A. Whitman, M.C. Jaramillo, D.D. Zhang, Arsenic-mediated activation of the Nrf2-Keap1 antioxidant pathway, J. Biochem. Mol. Toxicol. 27 (2) (2013) 99–105.
[13] M. Kobayashi, M. Yamamoto, Molecular mechanisms activating the Nrf2-Keap1 pathway of antioxidant gene regulation, Antioxid. Redox Signal. 7 (3–4) (2005) 385–394.
[14] Q. Zhang, J. Pi, C.G. Woods, M.E. Andersen, A systems biology perspective on Nrf2-mediated antioxidant response, Toxicol. Appl. Pharmacol. 244 (1) (2010) 84–97.
[15] B. Li, X. Li, B. Zhu, X. Zhang, Y. Wang, Y. Xu, H. Wang, Y. Hou, Q. Zheng, G. Sun, Sodium arsenite induced reactive oxygen species generation, nuclear factor (erythroid-2 related) factor 2 activation, heme oxygenase-1 expression, and glutathione elevation in Chang human hepatocytes, Environ. Toxicol. 28 (7) (2013) 401–410.
[16] J.A. Klein, S.L. Ackerman, Oxidative stress, cell cycle, and neurodegeneration, J. Clin. Invest. 111 (6) (2003) 785–793.
[17] R.E. Mrak, W.S. Griffin, Glia and their cytokines in progression of neurodegeneration, Neurobiol. Aging 26 (3) (2005) 349–354.
[18] B. Shukitt-Hale, F.C. Lau, A.N. Carey, R.L. Galli, E.L. Spangler, D.K. Ingram, J.A. Joseph, Blueberry polyphenols attenuate kainic acid-induced decrements in cognition and alter inflammatory gene expression in rat hippocampus, Nutr. Neurosci. 11 (4) (2008) 172–182.
[19] A.K. Talley, S. Dewhurst, S. Perry, S.C. Dollard, S. Gummuluru, S.M. Fine, D. New, L.G. Epstein, H.E. Gendelman, H. Gelbard, Tumor necrosis factor alpha-induced apoptosis in human neural cells: protection by the antioxidant N-acetylcysteine and the genes bcl-2 and crmA, Mol. Cell Biol. 15 (1995) 2359–2366.
[20] S.R. Galaly, O.M. Ahmed, A.M. Mahmoud, Thymoquinone and curcumin prevent gentamicin-induced liver injury by attenuating oxidative stress, inflammation and apoptosis, J. Physiol. Pharmacol. 65 (6) (2014) 823–832.
[21] J. Safa, H. Argani, B. Bastani, N. Nezami, B. Rahimi Ardebili, A. Ghorbanihaghjo, H. Kalagheichi, A. Amirfirouzi, M. Mesgari, J. Soleimany Rad, Protective effect of grape seed extract on gentamicin-induced acute kidney injury, Iran J. Kidney Dis. 4 (4) (2010) 285–291.
[22] I.T. Abdel-Raheem, G.A. El-Sherbiny, A. Taye, Green tea ameliorates renal oxidative damage induced by gentamicin in rats, Pak. J. Pharm. Sci. 23 (1) (2010) 21–28.
[23] R. Kongkachuichai, P. Prangthip, R. Surasiang, J. Posuwan, R. Charoensiri, A. Kettawan, Effect of Riceberry oil (Deep purple oil; Oryza sativaindica) supplementation on hyperglycemia and change in lipid profile in streptozotocin (STZ)-induced diabetic rats fed a high fat diet, Int. Food Res. J. 20 (2) (2013) 873–882.
[24] P. Prangthip, R. Surasiang, R. Charoensiri, V. Leardkamolkarn, S. Komindr, U. Yamborisut, A. Vanavichit, R. Kongkachuichai, Amelioration of hyperglycemia, hyperlipidemia, oxidative stress and inflammation in steptozotocin-induced diabetic rats fed a high fat diet by Riceberry supplement, J. Funct. Food 5 (1) (2013) 195–203.
[25] V. Leardkamolkarn, W. Thongthep, P. Suttiarporn, R. Kongkachuichai, S. Wongpornchai, A. Wanavijitr, Chemopreventive properties of the bran extracted from a newly-developed Thai rice: the Riceberry, Food Chem. 125 (3) (2011) 978–985.
[26] H. Ohkawa, N. Ohishi, K. Yagi, Assay for lipid peroxides in animal tissues by thiobarbituric acid reaction, Anal. Biochem. 95 (2) (1979) 351–358.
[27] A.M. Bataille, J.E. Manautou, Nrf2: a potential target for new therapeutics in liver disease, Clin. Pharmacol. Ther. 92 (3) (2012) 340–348.
[28] T. Luedde, R.F. Schwabe, NF-kappaB in the liver–linking injury, fibrosis and hepatocellular carcinoma, Nat. Rev. Gastroenterol. Hepatol. 8 (2) (2011) 108–118.
[29] S. Nafees, S. Rashid, N. Ali, S.K. Hasan, S. Sultana, Rutin ameliorates cyclophosphamide induced oxidative stress and inflammation in Wistar rats: role of NFkappaB/MAPK pathway, Chem. Biol. Interact. 231 (2015) 98–107.
[30] S.A. Cook, P.H. Sugden, A. Clerk, Regulation of bcl-2 family proteins during development and in response to oxidative stress in cardiac myocytes: association with changes in mitochondrial membrane potential, Circ. Res. 85 (10) (1999) 940–949.
[31] E.A. Slee, M.T. Harte, R.M. Kluck, B.B. Wolf, C.A. Casiano, D.D. Newmeyer, H.G. Wang, J.C. Reed, D.W. Nicholson, E.S. Alnemri, D.R. Green, S.J. Martin, Ordering the cytochrome c-initiated caspase cascade: hierarchical activation of caspases-2, -3, -6, -7, -8, and -10 in a caspase-9-dependent manner, J. Cell Biol. 144 (2) (1999) 281–292.
[32] J.M. Adams, S. Cory, The Bcl-2 protein family: arbiters of cell survival, Science 281 (5381) (1998) 1322–1326.
[33] C. Hu, J. Zawistowski, W. Ling, D.D. Kitts, Black rice (Oryza sativa L. indica) pigmented fraction suppresses both reactive oxygen species and nitric oxide in chemical and biological model systems, J. Agric. Food Chem. 51 (18) (2003) 5271–5277.
[34] F. Hou, R. Zhang, M. Zhang, D. Su, Z. Wei, Y. Deng, Y. Zhang, J. Chi, X. Tang, Hepatoprotective and antioxidant activity of anthocyanins in black rice bran on carbon tetrachloride-induced liver injury in mice, Funct. Foods 5 (4) (2013) 1705–1713.
[35] J.B. Jeong, H.J. Jeong, 2-Methoxy-4-vinylphenol can induce cell cycle arrest by blocking the hyper-phosphorylation of retinoblastoma protein in benzo[a] pyrene-treated NIH3T3 cells, Biochem. Biophys. Res. Commun. 400 (4) (2010) 752–757.
[36] D. Patel, S. Shukla, S. Gupta, Apigenin and cancer chemoprevention: progress, potential and promise (review), Int. J. Oncol. 30 (1) (2007) 233–245.
[37] K. Jaikumkao, A. Pongchaidecha, N. Chattipakorn, V. Chatsudthipong, S. Promsan, P. Arjinajarn, A. Lungkaphin, Atorvastatin improves renal organic anion transporter 3 and renal function in gentamicin-induced nephrotoxicity in rats, Exp. Physiol. 101 (6) (2016) 743–753.
[38] S. Promsan, K. Jaikumkao, A. Pongchaidecha, N. Chattipakorn, V. Chatsudthipong, P. Arjinajarn, W. Pompimon, A. Lungkaphin, Pinocembrin attenuates gentamicin-induced nephrotoxicity in rats, Can. J. Physiol. Pharmacol. 29 (2016) 1–11.
[39] M. Karin, M. Delhase, The I kappa B kinase (IKK) and NF-kappa B: key elements of proinflammatory signalling, Semin. Immunol. 12 (1) (2000) 85–98.
[40] A.R. Brasier, The NF-kappaB regulatory network, Cardiovasc. Toxicol. 6 (2) (2006) 111–130.
[41] X. Gao, A. Picchi, C. Zhang, Upregulation of TNF-alpha and receptors contribute to endothelial dysfunction in zucker diabetic rats, Am. J. Biomed. Sci. 2 (1) (2010) 1–12.
[42] P. Subramanian, R. Anandan, J.J. Jayapalan, O.H. Hashim, Hesperidin protects gentamicin-induced nephrotoxicity via Nrf2/HO-1 signaling and inhibits inflammation mediated by NF-κB in rats, J. Funct. Foods 13 (2015) 89–99.
[43] Y. Yamamoto, R.B. Gaynor, Therapeutic potential of inhibition of the NF-kappaB pathway in the treatment of inflammation and cancer, J. Clin. Invest. 107 (2) (2001) 135–142.
[44] R. Nagasaka, C. Chotimarkorn, I.M. Shafiqul, M. Hori, H. Ozaki, H. Ushio, Anti-inflammatory effects of hydroxycinnamic acid derivatives, Biochem. Biophys. Res. Commun. 358 (2) (2007) 615–619.

[45] E. Song, J. Fu, X. Xia, C. Su, Y. Song, Bazhen decoction protects against acetaminophen induced acute liver injury by inhibiting oxidative stress inflammation and apoptosis in mice, PLoS One 9 (9) (2014) e107405.
[46] K. Wang, Molecular mechanisms of hepatic apoptosis, Cell. Death. Dis. 5 (2014) e996.
[47] A.A. El Gamal, M.S. AlSaid, M. Raish, M. Al-Sohaibani, S.M. Al-Massarani, A. Ahmad, M. Hefnawy, M. Al-Yahya, O.A. Basoudan, S. Rafatullah, Beetroot (Beta vulgaris L.) extract ameliorates gentamicin-induced nephrotoxicity associated oxidative stress, inflammation, and apoptosis in rodent model, Mediat. Inflamm. 2014 (2014) 983952.

Phytomedicine 23 (2016) 1753–1763

Contents lists available at ScienceDirect

Phytomedicine

journal homepage: www.elsevier.com/locate/phymed

Riceberry bran extract prevents renal dysfunction and impaired renal organic anion transporter 3 (Oat3) function by modulating the PKC/Nrf2 pathway in gentamicin-induced nephrotoxicity in rats

Phatchawan Arjinajarn[a], Anchalee Pongchaidecha[b], Nuttawud Chueakula[b], Krit Jaikumkao[b], Varanuj Chatsudthipong[c], Sugunya Mahatheeranont[d], Orranuch Norkaew[d], Nipon Chattipakorn[b,e], Anusorn Lungkaphin[b,*]

[a] Department of Biology, Faculty of Science, Chiang Mai University, Chiang Mai, Thailand
[b] Department of Physiology, Faculty of Medicine, Chiang Mai University, Chiang Mai, Thailand
[c] Department of Physiology, Faculty of Science, Mahidol University, Bangkok, Thailand
[d] Department of Chemistry, Faculty of Science, Chiang Mai University, Chiang Mai, Thailand
[e] Cardiac Electrophysiology Research and Training Center, Faculty of Medicine, Chiang Mai University, Chiang Mai, Thailand

ARTICLE INFO

Article history:
Received 9 December 2015
Revised 18 August 2016
Accepted 12 October 2016

Keywords:
Gentamicin
Nephrotoxicity
Riceberry bran extract
Oxidative stress
Organic anion transporter 3

ABSTRACT

Purpose: This study investigated the protective effects of Riceberry bran extract (RBBE) on renal function, and the function and expression of renal organic anion transporter 3 (Oat3) in gentamicin-induced nephrotoxicity in rats and explored the mechanisms for its protective effects.
Material and methods: Male Sprague Dawley rats ($n = 42$) were divided into six groups to receive normal saline, gentamicin (100 mg/kg), co-treatment of gentamicin and RBBE (at dose of 250, 500 and 1000 mg/kg), and RBBE (at dose of 1000 mg/kg) only, for consecutive fifteen days. Renal function, oxidative and antioxidative markers, the function and expression of Oat3 and histological changes in the kidney were evaluated.
Results: Elevation of BUN, serum creatinine levels and reduction in urine creatinine and creatinine clearance indicated decreased renal function in the gentamicin-treated rats. The decrease of [^{3}H]ES uptake in the renal cortical slices of these rats, reflecting the attenuation of Oat3 transport function that was accompanied by decreased expression of Oat3. Moreover, increased MDA level and reduced superoxide dismutase (SOD) and glutathione (GSH) activities were found in gentamicin-treated rats compared to the control group. These changes were associated with the upregulated PKCα, Nrf-2, Keap 1, NQO-1 and HO-1 expressions in kidneys. RBBE treatment improved the renal function and Oat3 transport function and expression in gentamicin-treated rats. The oxidative status was also restored by RBBE treatment.
Conclusion: RBBE protects kidney injury by its antioxidant effect, subsequently leading to modulation of the PKC/Nrf2 antioxidant defense pathway.

Introduction

Gentamicin is widely used and is an effective aminoglycoside antibiotic used in the treatment of life-threatening gram-negative bacterial infections (Ali, 2003). However, its clinical usefulness is limited due to the development of nephrotoxicity. Renal toxicity from gentamicin administration is related to a selective accumulation of the drug in the renal proximal tubular cells which leads to cell injury, and results in renal dysfunction (Quiros et al., 2011). In vivo and in vitro studies have shown that gentamicin administration can enhance the generation of reactive oxygen species (ROS) such as hydroxyl radical, hydrogen peroxide and superoxide anions mostly in the mitochondria, which subsequently damage some

Abbreviations: **ARE**, antioxidant response element; **ARF**, acute renal failure; **BUN**, blood urea nitrogen; **CAT**, catalase; **ES**, estrone sulfate; **GCL**, glutamate-cysteine ligase; **GC–MS**, gas chromatography-mass spectrometry; **GFR**, glomerular filtration rate; **GM**, gentamicin; **GSH**, glutathione; **GSH-Px**, glutathione peroxidase; **HO-1**, heme oxygenase-1; **HRP**, horseradish peroxidase; **Keap1**, kelch-like ECH associated protein 1; **MAP kinase**, mitogen-activated protein kinase; **MDA**, malondialdehyde; **NQO-1 NAD(P)H**, quinine oxidoreductase-1; **Nrf2**, nuclear factor erythroid-2-related factor-2; **Oat**, organic anion transporter; **PKC**, protein kinase C; **RBBE**, Riceberry bran extract; **ROS**, reactive oxygen species; **SOD**, superoxide dismutase; **TBARS**, thiobarbituric acid reactive substances.

* Corresponding author. Fax. 6653 945365.
E-mail addresses: onanusorn@yahoo.com, anusorn.lungka@cmu.ac.th (A. Lungkaphin).

http://dx.doi.org/10.1016/j.phymed.2016.10.014
0944-7113/

macromolecules and induce cellular injury and necrosis (Du and Yang, 1994). However, the mechanisms in which increased oxidative stress induced renal dysfunction are still unclear.

Nuclear factor erythroid-2-related factor-2 (Nrf2) is a redox-sensitive transcription factor, which plays a crucial role in cellular defense against oxidative stress (Ishii et al., 2000). It activates the antioxidant response element (ARE) to enhance the expression of phase II detoxification enzymes and antioxidant proteins including catalase (CAT), glutathione (GSH), glutathione peroxidase (GSH-Px), superoxide dismutase (SOD), heme oxygenase-1 (HO-1) and NAD(P)H:quinine oxidoreductase-1 (NQO-1) (Kim and Vaziri, 2010). Nrf2 has been reported to protect rat kidneys against oxidative stress induced by gentamicin through the activation of antioxidant and phase II enzymes such as HO-1 (Subramanian et al., 2015).

Renal excretion of organic anions largely occurs at the proximal tubule through the organic anion transporter (Oat) which is one of the major routes for body drug clearance/detoxification. To date, several renal Oat isoforms have been cloned and identified. Among these, only Oat1 and Oat3 have been shown to play a major role in the cellular uptake of organic anions across the basolateral membrane of the renal proximal tubules. Moreover, among the Oat isoforms, Oat3 exhibits the highest mRNA expression level in the human kidneys (Motohashi et al., 2002). Previous studies clearly showed that acute renal failure (ARF) induced by gentamicin treatment decreased the renal excretion of organic anion compounds, and the renal expressions and functions of Oat1 and Oat3 were decreased in gentamicin-treated rats (Guo et al., 2013). The generation of free radicals and oxidative stress condition in proximal tubular epithelial cells has been shown to account for the mechanisms of several xenobiotic toxicities (Cuzzocrea et al., 2002; Du and Yang, 1994). Of interest, hydroxyl radical scavengers and iron chelators have been shown to reduce the severity of gentamicin-induced function and histological tubular damage (Ali, 2003;Guo et al., 2013).

Several natural compounds are demonstrated to exert antioxidants and provide protection against free radical-induced tissue damage. Rice is the staple food for people in the Asia-Pacific region. Riceberry rice (Oryza sativa L.), a Thai black purple rice, has been recently developed by crossing Chao Hom Nin Rice and Khao-Dawk Mali 105 (Kongkachuichai et al., 2013). The bran of Riceberry has been shown to possess high antioxidative activity. It contains a large number of antioxidant compounds, such as anthocyanins (cyanidin 3-glucoside and peonidin-3-glucoside), β-carotene, γ-oryzanol and vitamin E complex (tocopherols and tocotrienols) (Leardkamolkarn et al., 2011). Recent studies reported the antioxidant, anticancer and antidiabetic effects of Riceberry bran extract (RBBE) (Prangthip et al., 2013; Leardkamolkarn et al., 2011). Despite these benefits, the effect of RBBE on renal function in gentamicin-induced nephrotoxicity has not been investigated. We investigated the protective effects of RBBE against gentamicin-induced renal dysfunction and the reduction of Oat3 function and expression in the rat kidney. We hypothesized that the renoprotective effect of RBBE against gentamicin-induced nephrotoxicity mediates through its antioxidative action by modulating the PKC/Nrf2 pathway.

Materials and methods

Chemicals and reagents

Gentamicin was obtained from the Pharmaceutical Organization, INC (Bangkok, Thailand). Malondialdehyde (MDA) assay kit was obtained from Cayman Chemical Company (Ann Arbor, MI, USA). Superoxide dismutase (SOD) and Glutathione (GSH) assay kits were purchased from BioAssay Systems (Hayward, CA, USA). [^{3}H]ES was purchased from Perkin Elmer (Norwalk, CT, USA). Polyclonal antibody against Oat3 was purchased from Cosmo Bio Co. Ltd. (Tokyo, Japan). Antibodies against nuclear factor erythroid-2-related factor-2 (Nrf2) and protein kinase Cα (PKCα) (C-20) were purchased from Santa Cruz Biotechnology (Santa Cruz, CA, USA). Antibodies against heme oxygenase-1 (HO-1) and NAD(P)H:quinine oxidoreductase-1 (NQO-1) were obtained from Abcam (Cambridge, UK). Monoclonal antibody against Lamin B1 and anti-β-actin antibody were purchased from Cell Signaling Technology, Inc. (Beverly, MA, USA). Monoclonal mouse anti-Na^+-K^+-ATPase and kelch-like ECH-associated protein 1(Keap 1) were obtained from Millipore (Billerica, MA, USA). Horseradish peroxidase (HRP) conjugated goat anti-rabbit and anti-mouse secondary antibodies were purchased from Amersham (Arlington Heights, IL, USA). All solvents used for extraction of chemical components from the Riceberry bran; methanol, dichloromethane, and hexane, were analytical grade obtained from Fluka (Buchs, Switzerland). Methanol and water, HPLC grade solvents, were purchased from Merck (Darmstadt, Germany). De-ionized water was obtained from a Mili-Q UV-Plus water purification system (Milipore Corp, USA). Formic acid was purchased from Fluka (Buchs, Switzerland). Standard grade vitamin E was obtained from Wako Pure Chemical Industries, Ltd. (Osaka, Japan). Standard anthocyanins; cyanidin-3-O-glucoside and peonidin-3-O-glucoside, were purchased from Apin Chemicals Ltd. (Oxfordshire, UK). All other chemicals were purchased from a commercial source at the analytical pure grade.

Preparation of Riceberry bran extract

Thai black non-glutinous rice, cv. Riceberry, grown in 2013, was obtained as harvested paddy from an experimental field in Kasetsart University, NakornPathom Province located in Central Thailand. The paddy was dried by modified hot air at a temperature of 40 °C until their moisture content was reduced to approximately 14% by weight. On the day of the experiment, the rice sample was dehusked and milled in a local milling system (Natrawee Technology, Chachoengsao, Thailand) for 30 s to obtain approximately 10% (w/w) fresh rice bran. One kilogram of the Riceberry bran was extracted with methanol (3 l) at room temperature for 24 h. After solvent evaporation, a dark red viscous crude extract of 55.8 g was obtained for further analysis by gas chromatography-mass spectrometry (GC-MS).

GC–MS analysis

A gas chromatograph-mass spectrometer (Agilent 6890 and HP 5973 mass-selective detector, Agilent Technologies, Palo Alto, CA) equipped with a fused silica capillary column having phase HP-5MS with dimension 30 m × 0.25 mm i.d. and 0.25 mm film thickness (Agilent Technologies) was utilized for analysis of chemical components obtained from crude methanol extract of the Riceberry bran. The sample was injected with a split ratio of 20:1. The injection port temperature was 250 °C. The column temperature program started at 60 °C upon injection. The temperature was increased at a rate of 3 °C/min to 285 °C. Purified helium gas at a flow rate of 1 ml/min was used as the GC carrier gas. The mass spectrometer was operated in the electron impact (EI) mode with an electron energy of 70 eV; ion source temperature, 230 °C; quadrupole temperature, 150 °C; mass range m/z 50–550; scan rate, 0.68 s/scan; EM voltage, 1456 V. The GC-MS transfer line was set to 280 °C. Identification of organic components in both extracts was performed by matching their mass spectra with reference spectra in the Wiley 7n Mass Spectral Library and the NIST 08 Mass Spectral Library, both purchased from Agilent Technologies. In addition, Kováts indices and retention times of known standards, for some available compounds, were used to aid structural confirmation. Quantitative analysis of each component in percent was

performed by peak area normalization measurements. Analysis by GC-MS of this methanol extract revealed 34 identified components. Among the group of simple phenolic compounds, 2-methoxy-4-vinylphenol was present as the major constituent.

LC-MS/MS analysis of flavonoids

Five grams of the black rice bran were extracted by 50 ml of formic acid in methanol (0.01:99.9). After being sonicated for 60 min, the methanol solution was concentrated under reduced pressure at temperature below 40 °C until its volume was reduced to 2.0 ml. The extract was then subjected to separation by a 3'100 mm Zorbax Eclipse column (Agilent Technologies, USA) with a particle size of 3.5 mm. The mobile phase consisted of formic acid: deionized water (0.5:99.5) (solvent A) and methanol (solvent B), with gradient elution started at 90:10 (A:B) and remained for 10 min. Its composition was changed to 75:25 over 60 min. The flow rate was 0.4 ml/min. The total HPLC effluent was delivered into a Z-SprayTM ES source of a Micromass Q-TOF 2TM hybrid quadrupole time of flight mass spectrometer (Micromass, Manchester, UK), which was operated in a positive ionization mode at a temperature of 80 °C. Nitrogen was used as a nebulizing gas with a flow rate of 12 l/min and as a desolvation gas at a temperature of 150 °C. The capillary and cone voltages were set at 3.00 kV and 30 V, respectively. Ultra-high purity grade argon was used as the collision gas at a 10 psi inlet pressure for collision-induced dissociation (CID). Collision energy was 35 eV. A scan time of 0.5 s with m/z range of 100–350 was used to obtain the product ions mass spectra. The software used for data acquisition and processing was MassLynx NT, version 4.0 (Micromass, Manchester, UK). The confirmation of chemical structure of the black rice anthocyanins was accomplished by elucidating the fragmentation patterns of their full scan daughter ion mass spectra obtained by LC-MS/MS against those of the standard compounds. The MS/MS spectra were also compared with those reported previously (da Costa et al., 2000; Oliveira et al., 2001; Montoro et al., 2006). The bran extract was found to contain two major anthocyanins, cyanidin 3-glucoside and peonidin-3-glucoside at the amount of 13.24 and 5.33 mg/g of crude extract, respectively. Further screening for other bioactive flavonoids by LC-MS found apigenin as the main flavonoid but it appeared in only small amount compared with the other two anthocyanins. The identified components in crude methanol extract of Ricebery black rice bran are shown in Table 1.

Animal and treatment

Forty-two male Sprague Dawley rats (180–200 g) from the National Experimental Animal Center, Salaya, Mahidol University were housed in a temperature-controlled room with 12 h dark/light cycles and provided food and tap water ad libitum. This study was carried out in strict accordance with the recommendations in the Guide for the Care and Use of Laboratory Animals of the National Institutes of Health. The protocol was approved by the Committee on the Ethics of Animal Experiments of the Faculty of Medicine, Chiang Mai University (Permit Number: 1/2558). All surgery was performed under sodium pentobarbital anesthesia, and all efforts were made to minimize suffering.

The rats were randomly assigned into six groups, each with seven rats. In the control (CON) group, the rats were intraperitoneally (i.p.) injected with normal saline. Rats in the gentamicin (GM) group were i.p. administered with gentamicin (100 mg/kg/day). Rats in the gentamicin plus Riceberry bran extract received gentamicin (100 mg/kg) together with RBBE at doses of 250, 500 or 1000 mg/kg/day (GM + RBBE 250, GM + RBBE 500, GM + RBBE 1000, respectively). RBBE was administered via oral gavage 30 min before gentamicin injection. Rats in the Riceberry bran extract (RBBE) only group received RBBE at a concentration of 1000 mg/kg/day. All treatments were administered for 15 consecutive days.

Blood and renal tissue sampling

After the last dose of gentamicin treatment, a 24 h urine was collected by placing the animal in an individual metabolic cage. Then, the animal was sacrificed under anesthesia with an i.p. injection of pentobarbital sodium (100 mg/kg). Blood samples were collected by cardiac puncture and serum was separated by centrifugation. The abdomen was then opened and the kidneys were flushed through the abdominal aorta with ice-cold HEPES-sucrose buffer (containing 250 mM sucrose, 10 mM HEPES, pH 7.42–7.44), and immediately removed, decapsulated and weighed. One of the kidneys was divided into two longitudinal sections. The renal cortical tissues were isolated and kept for western blot analysis and evaluation of MDA and GSH. The other kidney was cut into two longitudinal sections; one half was fixed in 10% neutralized formalin for further morphological analysis and in the other half, the renal cortical tissues were isolated and kept for SOD determination. Then, the serum and tissue samples were placed in liquid nitrogen and stored at -80 °C until use.

Biochemical analysis

Renal function assessment

To determine kidney function, serum levels of BUN and creatinine were measured using ReflotronPlus Analyzer. Urinary creatinine was determined by a commercial kit (Roche Diagnostics, Indianapolis, IN, USA). Creatinine clearance (C_{cr}) was calculated using the standard formula UxV/P where U = urine creatinine in mg/dl, V = volume of urine in ml/min and P = serum creatinine in mg/dl.

Determination of malondialdehyde

To determine the level of renal oxidative stress, the renal cortical malondialdehyde (MDA) level was assayed by colorimetry as previously described (Ohkawa et al., 1979) using a commercial TBARS assay kit (Cayman Chemical Company, Ann Arbor, MI, USA), and expressed as nmol/mg protein.

Determination of superoxide dismutase activity

The activity of renal cortical superoxide dismutase (SOD) was assayed by colorimetric method using a commercial EnzyChrom Superoxide Dismutase assay kit (BioAssay Systems, Hayward, CA, USA). The activity was expressed as U/ml.

Determination of glutathione (GSH) level

The total GSH in renal cortical tissue was assayed by the colorimetry using a commercial Quantichrom Glutathione assay kit (BioAssay Systems, Hayward, CA, USA). The activity was expressed as mmole/mg protein.

Determination of renal Oat3 function

The uptake of radiolabeled estrone sulfate ([^{3}H]ES), a specific Oat3 substrate (Sweet et al., 2002) into renal cortical slices, which reflects the renal Oat3 function, was examined. After removal, the kidney was decapsulated and placed into freshly oxygenated ice-cold modified Cross and Taggart saline buffer (containing 95 mM NaCl, 80 mM mannitol, 5 mM KCl, 0.74 mM $CaCl_2$ and

Table 1
The identified components in crude methanol extract of Ricebery black rice bran.

	Structural assignment[a]	LRI[b]	Peak area (%)[c]
GC-MS			
	Ketone		
	1,2-Cyclopentanedione[1,2]	938	1.53
	Phenolic compounds		
	1,2-Benzenediol[1,2]	1219	0.58
	2-Methoxy-4-vinylphenol[1,2](4-vinylguaiacol)	1324	0.69
	Methyl 4-hydroxy-3-methoxybenzoate (Methyl vanilate)[1,2]	1527	0.51
	4-Hydroxymethoxybenzoic acid[1,2]	1582	0.46
	3,5-Dihydroxybenzhydrazide[1,2]	1699	0.44
	Pyran		
	2H-Pyran-2,6(3H)-dione[1,2]	1008	0.12
	2,3-Dihydro-3,5-dihydroxy-6-methyl-4H-pyran-4-one[1,2]	1155	0.26
	Furan		
	5-(Hydroxymethyl)-2-furancarboxaldehyde[1,2]	1242	1.05
	Fatty acid		
	Tetradecanoic acid (myristic acid)[1,2]	1871	0.17
	n-Hexadecanoic acid (Pamitic acid)[1,2]	1976	9.72
	(Z,Z)-9,12-Octadecadienoic acid(Linoleic acid)[1,2,3]	2149	18.83
	(E)-9-Octadecenoic acid (Oleic acid)[1,2]	2155	14.55
	Octadecanoic acid (stearic acid)[1,2]	2172	0.70
	Eicosanoic acid[1]		0.16
	Ester of fatty acid		
	Methyl tetradecanoate[1,2]	1832	0.27
	Methyl hexadecanoate (Methyl pamitate)[1,2]	1932	7.35
	Methyl 8,11-octadecadienoate[1,2]	2098	8.66
	Methyl (E)-9-octadecenoate (Methyl elidate)[1,2]	2104	10.65
	Methyl 9-octadecenoate[1,2]	2109	0.26
	Methyl octadecanoate[1,2]	2131	0.07
	Methyl 11-eicosenoate[1]		0.13
	Methyl eicosanoate[1]		0.04
	2-Hydroxy-1-(hydroxypropyl) ethyl hexadecanoate[1]		0.90
	Methyl docosanoate[1]		0.90
	2-Hydroxy-1-(hydroxymethyl)ethyl (Z,Z)-9,12-octadecadienoate[1]		0.91
	3-Hydroxypropyl oleate[1]		1.98
	Methyl tetracosanoate[1]		0.14
	Triterpeoid		
	Squalene[1]		0.23
	(3beta.,24S)-9,19-Cyclolanost-25-en-3ol[1]		0.64
	Steroid		
	Ergost-4,6,22-trien-3-ol[1]		0.40
	Campesterol[1,3]		0.38
	Stigmasterol[1,3]		0.58
	beta.Sitosterol[1,3]		1.24

[a] Identification: 1, mass spectrum (tentative); 2, Retention indices; and 3, standard compound.
[b] Retention indices using a non polar dimethyl polysiloxane column.
[c] Relative areas presented in percentage of the total peak areas.

9.5 mM Na_2HPO_4; pH 7.4). Thin renal cortical slices (< 0.5 mm; 5–15 mg/slice; wet weight) were cut with a Stadie-Riggs microtome, pre-incubated at room temperature in modified Cross and Taggart buffer for 10 min, and then incubated in 1 ml of buffer containing 50 nM [^{3}H]ES for 30 min at room temperature. After incubation, slices were rinsed in 0.1 M $MgCl_2$, blotted with filter paper, weighed and dissolved in 1 M NaOH. Slice samples were then neutralized with 1 M HCl, and assayed for [^{3}H]ES by liquid scintillation counter (Perkin Elmer, MA, USA). The [^{3}H]ES uptake was calculated as tissue to medium ratios (dpm/mg of tissue ÷ dpm/ml of medium).

Western blotting analysis

Protein extraction and western blotting for the determination of Oat3, PKCα, Nrf2, Keap 1, NQO-1 and HO-1 were carried out on frozen renal cortical tissues. Protein extraction was done by homogenizing the rat renal cortex in Mammalian Cell Lytic buffer (Sigma-Aldrich, St. Louis, MO, USA) with protease cocktail inhibitor (Roche, Indianapolis, IN, USA). The homogenates were centrifuged at 5000 g for 15 min at 4 °C, the supernatant was designated as whole cell lysate, and then the supernatant was further centrifuged at 100,000 x g for 2 h at 4 °C to obtain a membrane (pellet) and cytosolic (supernatant) fractions. The 5000 x g pellet was re-suspended and centrifuged at 10,000 x g at 4 °C for 10 min. The supernatant fraction from the spin was designated as the nuclear fraction. All the fractions collected were stored at -80 °C until use.

The renal cortical fractions from whole cell lysates, cytosol, nuclear and membrane fractions were separated on 10% SDS-polyacrylamide gel electrophoresis (PAGE) and subsequently transferred to a polyvinylidenedifluoride (PVDF) membrane (Millipore, MA, USA). The membranes were blocked with 5% non-fat dry milk in TBST solution for 1 h at room temperature and then incubated overnight at 4 °C with primary antibody against Oat3, PKCα, Nrf2, Keap 1, NQO-1 and HO-1. Following incubation with the primary antibody, the membranes were washed, and incubated with horseradish peroxidase (HRP)-conjugated goat anti-rabbit or anti-mouse secondary antibody (Amersham, IL, USA) for 1 h at room temperature. Protein antibody complexes were detected using ECL enhanced chemiluminescence agent (GE Healthcare, Buckinghamshire, UK), visualized by exposure to Hyperfilm (GE Healthcare, Buckinghamshire, UK). The expression levels of target proteins were analyzed as the band density on Hyperfilm using the histogram function of Adobe Photoshop CS5 (Adobe Corp., CA, USA)

Table 2
Effects of Riceberry bran extract on physiological and renal function parameters in gentamicin-induced nephrotoxicity rats.

Parameters	CON	GM	GM + RBBE 250	GM + RBBE 500	GM + RBBE 1000	RBBE
BW (g)	369 ± 5	291 ± 7*	363 ± 9#	351 ± 6#	345 ± 5#	344 ± 6#
KW (g)	1.35 ± 0.03	1.96 ± 0.04*	1.67 ± 0.03*,#,d	1.54 ± 0.05#	1.56 ± 0.06#	1.38 ± 0.06#,a
KW/BW (mg/g)	3.67 ± 0.07	6.78 ± 0.31*	4.91 ± 0.11*,#	4.41 ± 0.14#	4.52 ± 0.17#	4.02 ± 0.11#
Urine output (ml/h)	0.74 ± 0.05	1.40 ± 0.10*	1.00 ± 0.04*,#	0.88 ± 0.02#	0.93 ± 0.06#	0.88 ± 0.06#
BUN (mg/dl)	20.29 ± 1.02	40.57 ± 2.28*	28.00 ± 0.62*,#,b,c,d	21.71 ± 0.84#,a	23.86 ± 0.55#,a	20.00 ± 0.58#,a
S_{cr} (mg/dl)	0.38 ± 0.02	0.66 ± 0.01*	0.51 ± 0.03*,#	0.43 ± 0.04#	0.42 ± 0.03#	0.42 ± 0.03#
U_{cr} (mg/dl)	58.06 ± 4.93	27.19 ± 2.62*	44.42 ± 1.26*,#	52.61 ± 2.79#	50.38 ± 2.56#	56.38 ± 2.70#
C_{cr} (ml/min)	1.84 ± 0.14	1.13 ± 0.06*	1.52 ± 0.09#	1.68 ± 0.23#	1.70 ± 0.18#	2.02 ± 0.19#

BW: body weight; KW: kidney weight; KW/BW: kidney weight to body weight; BUN: blood urea nitrogen; S_{cr}: serum creatinine; U_{cr}: urine creatinine; C_{cr}: creatinine clearance; CON: control, GM: gentamicin, GM + RBBE 250: gentamicin plus Riceberry bran extract at dose of 250 mg/kg, GM + RBBE 500: gentamicin plus Riceberry bran extract at dose of 500 mg/kg, GM + RBBE 1000: gentamicin plus Riceberry bran extract at dose of 1000 mg/kg, and RBBE: Riceberry bran extract at dose of 1000 mg/kg.
Values are mean ± S.E.M. ($n = 7$) *$p < 0.05$ as compared with control group; #$p < 0.05$ as compared with gentamicin group; [a]$p < 0.05$ compared to GM + RBBE 250; [b]$p < 0.05$ compared to GM + RBBE 500; [c]$p < 0.05$ compared to GM + RBBE 1000; [d]$p < 0.05$ compared to RBBE.

and normalized to the β-actin level in its corresponding sample. Lamin B1 and Na^+/K^+-ATPase were used as markers for nuclear and membrane fractions, respectively.

Histological examination

To determine the morphology change, the kidneys were removed, cut in a half along the transverse axis, fixed in 10% neutral buffered formalin and embedded in a paraffin wax. Paraffin-embedded specimens were cut into 2 μm-thick sections, mounted on microscope slides and stained with Hematoxylin and Eosin (H&E) (Bancroft et al., 1996). The samples were examined under light microscope (Olympus Co., Tokyo, Japan) for morphological changes by an observer blinded to the animal treatment group.

Statistical analysis

All values are expressed as mean ± S.E.M and analyzed using SPSS version 17.0 statistical programs (SPSS Inc., Chicago, IL, USA). One-way analysis of variance (ANOVA), followed by Post Hoc Tukey test, was performed. A p-value < 0.05 was considered to be statistically significant.

Results

Effects of RBBE on physiological and renal function parameters

All rats started with similar mean body weight. As shown in Table 2, gentamicin-treated rats had a significant decrease in body weight (291 ± 7 g) and renal hypertrophy as indicated by a significant increase in the kidney weight and kidney weight per body weight ratio (1.96 ± 0.04 g and 6.78 ± 0.31 mg/g, respectively) when compared to the control (369 ± 5 g, 1.35 ± 0.03 g and 3.67 ± 0.07 mg/g, respectively) or RBBE (344 ± 6 g, 1.38 ± 0.06 g and 4.02 ± 0.11 mg/g, respectively) rats ($p < 0.05$). As compared with the control rats, the gentamicin-treated rats showed an impaired renal function as indicated by the significant increase in urine output (1.40 ± 0.10 and 0.74 ± 0.05 ml/h), serum BUN (40.57 ± 2.28 and 20.29 ± 1.02 mg/dl) and serum creatinine (0.66 ± 0.01 and 0.38 ± 0.02 mg/dl) accompanying with the apparent decreases in urine creatinine (27.19 ± 2.62 and 58.06 ± 4.93 mg/dl) and C_{cr} (1.13 ± 0.06 and 1.84 ± 0.14 ml/min) ($p < 0.05$). In the gentamicin plus RBBE (at dose of 250, 500 or 1000 mg/kg)-treated rats, the body weight was significantly higher (363 ± 9, 351 ± 6 and 345 ± 5 g, respectively) while the kidney weight (1.67 ± 0.03; 1.54 ± 0.05; 1.56 ± 0.06 g, respectively) and kidney weight per body weight ratio (4.91 ± 0.11; 4.41 ± 0.14; 4.52 ± 0.17 mg/g, respectively) were lower than those in gentamicin-treated rats ($p < 0.05$). Interestingly, all doses of RBBE treatment significantly decreased urine output (1.00 ± 0.04; 0.88 ± 0.02; 0.93 ± 0.06 ml/h), serum BUN (28.00 ± 0.62; 21.71 ± 0.84; 23.86 ± 0.55 mg/dl) and creatinine (0.51 ± 0.03; 0.43 ± 0.04; 0.42 ± 0.03 mg/dl) levels, and increased urine creatinine (44.42 ± 1.26; 52.61 ± 2.79; 50.38 ± 2.56 mg/dl) and C_{cr} (1.52 ± 0.09; 1.68 ± 0.23; 1.70 ± 0.18 ml/min) compared to those of gentamicin-treated rats ($p < 0.05$). There were no differences in urine output, creatinine levels, and C_{cr} among the gentamicin plus RBBE (at dose of 250, 500 or 1000 mg/kg) treatment groups. Also, administration of RBBE only had no effect on these parameters compared with the control rats. These results suggest that RBBE treatment can ameliorate the impaired renal function in gentamicin-induced nephrotoxicity in rats.

Effects of RBBE on the renal morphology

Sections of renal tissue from control rats showed normal histological structure of the renal corpuscles and renal tubules (Fig. 1a and d). In gentamicin-treated rats, renal sections exhibited changes in the structure of renal corpuscle including swelling appearances, narrowed Bowman's space and periglomerular inflammation (Fig. 1b). Renal tubules were undergoing vacuolization, dilation, necrosis, epithelial desquamation and infiltration with inflammatory cells in gentamicin-treated rats (Fig. 1e). These renal histological changes were significantly attenuated by administration of RBBE prior to gentamicin injection (Fig. 1c and f).

Effects of RBBE on oxidative status in gentamicin-induced nephrotoxicity

Oxidative stress induced by gentamicin treatment was indicated by a significant increase in renal cortical MDA ($p < 0.05$) accompanied with the decreases in renal cortical SOD and GSH levels ($p < 0.05$) in gentamicin-treated rats compared with the control or RBBE rats (Fig. 2). Compared with gentamicin-treated rats, the renal cortical MDA was decreased in all doses of RBBE treatments ($p < 0.05$). Moreover, the renal cortical GSH and SOD levels were also significantly increased with RBBE treatments at doses of 250, 500 and 1000 mg/kg ($p < 0.05$; Fig. 2). In addition, the gentamicin-treated rats received RBBE at dose of 250 mg had significant higher renal cortical MDA and apparent lower renal cortical SOD and GSH levels than those pretreated with RBBE at doses of 500 or 1000 mg/kg ($p < 0.05$). These findings indicate that the increase of renal oxidative stress condition induced by gentamicin administration can be reversed by RBBE treatment.

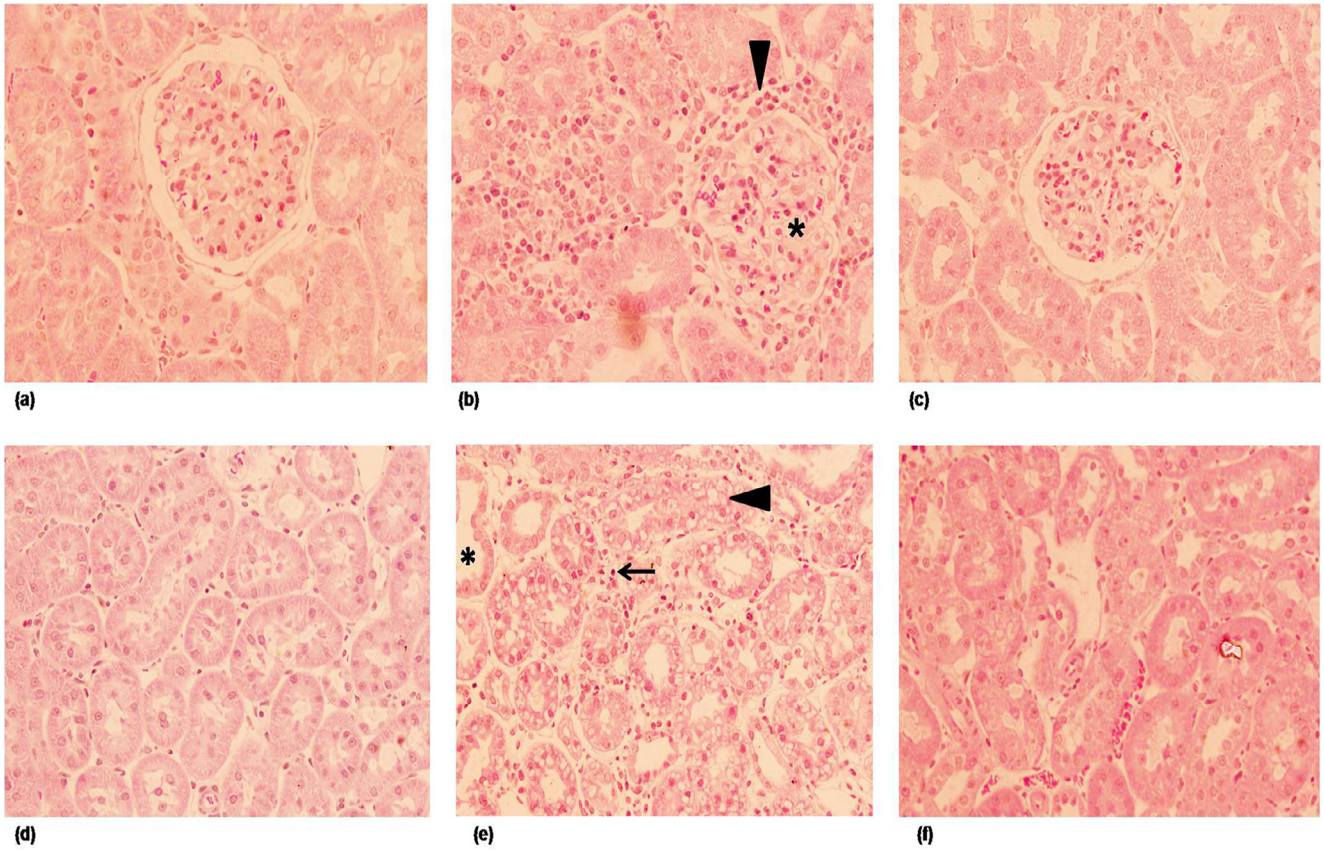

Fig. 1. Photograph of histological sections of kidney using hematoxylin and eosin (H&E) stain (magnification, x40); Panels (a), (b) and (c) are images of glomeruli from control, gentamicin and gentamicin plus Riceberry bran extract at dose of 500 mg/kg, respectively. Panels (d), (e) and (f) are images of tubules from control, gentamicin and gentamicin plus Riceberry bran extract at dose of 500 mg/kg, respectively. Enlargement of glomerulus with reduction of Bowman's space (asterisk) and periglomerular inflammation (arrowhead) were seen in Panel (b). Tubular dilation (asterisk), vacuolization, necrosis and desquamation (arrowhead), and inflammatory cell infiltration (arrow) were seen in Panel (e) in gentamicin-treated rats.

Effects of RBBE on renal Oat3 function and expression in gentamicin-induced nephrotoxicity rats

As demonstrated in Fig. 3, the administration of gentamicin had a significant decrease in [^{3}H]ES uptake in renal cortical slices when compared with that of the control or RBBE rats ($p < 0.05$). The significant increases in [^{3}H]ES uptake were observed in GEN plus RBBE (at dose of 500, or 1000 mg/kg) as compared with that in gentamicin-treated rats ($p < 0.05$). This finding suggested that RBBE treatment could prevent the impairment in Oat3 transport function induced by gentamicin. Additionally, RBBE at doses of 500 and 1000 mg/kg exhibited a comparable result, thus, RBBE treatment at the dose of 500 mg/kg was selected for the subsequent experiments.

There were no significant differences of renal Oat3 expression in the whole lysate fraction among the experimental groups (Fig. 4). However, a membrane expression of Oat3 in the renal cortical tissue was significantly decreased in gentamicin-treated rats in relation to the control or RBBE rats ($p < 0.05$) (Fig. 4). These results indicated that the decreased renal Oat3 function in the gentamicin-treated rats could be due to the down-regulation of membrane Oat3 expression. Interestingly, RBBE treatment showed a significant increase in membrane expression of Oat3 compared with that in the gentamicin-treated rats ($p < 0.05$) which was correlated with the increase in renal Oat3 function in this study.

Effects of RBBE on renal PKCα expression

An overproduction of ROS has been shown to activate PKC in diabetic nephropathy (Arjinajrn et al., 2014). These were in the same line of the results in this study. As illustrated in Fig. 5, the membrane expression of PKCα was significantly increased in renal cortical tissues in gentamicin-treated rats as compared to that of the control or RBBE rats ($p < 0.05$). RBBE treatment exhibited a significant decrease in membrane expression of PKCα to the same level as in the normal control condition. This result confirmed that the decrease in ROS production in gentamicin plus RBBE led to the inactivation of PKCα in the renal cortical tissues in this study.

Effects of RBBE on renal Nrf-2, Keap 1, NQO-1 and HO-1 expressions

The Nrf2 pathway is the cellular responses activated against oxidative stress (Zhang et al., 2014). We examined the potential mechanisms of RBBE in the regulation of the anti-oxidative defense involving the Nrf2 signaling pathway. As presented in Fig. 6, the expression level of Nrf2 in nuclear fraction was significantly elevated whereas it showed significant decline in cytosol fraction in gentamicin-treated rats when compared with the control or RBBE rats ($p < 0.05$). These findings indicated the activation of Nrf2 translocation from the cytosol into the nucleus induced by gentamicin treatment. Concomitantly, the expression of

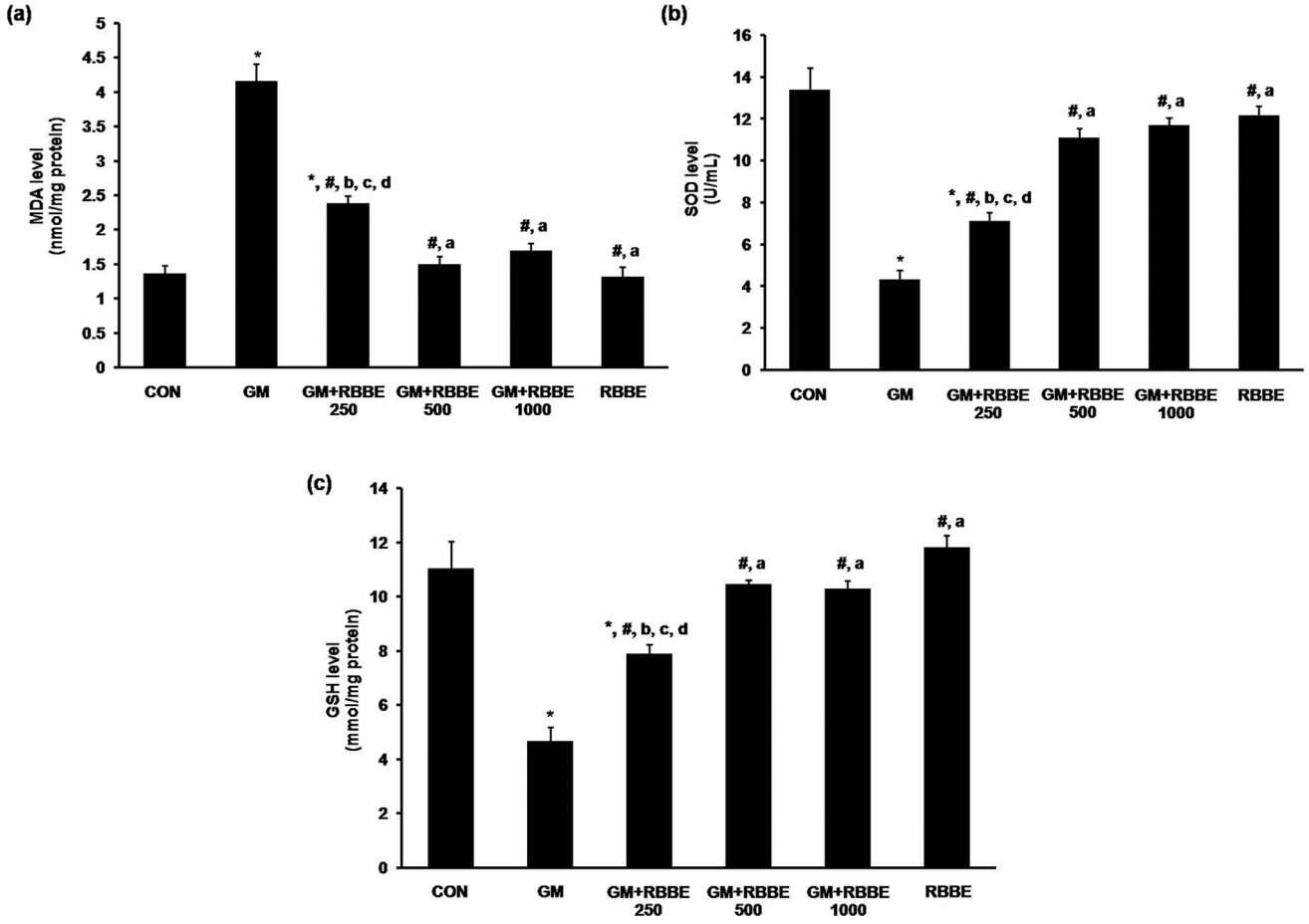

Fig. 2. Effects of RBBE on malondialdehyde (MDA) (a) and superoxide dismutase (SOD) (b) and glutathione (GSH) (c) in renal cortical tissues. CON: control, GM: gentamicin, GM+RBBE 250: gentamicin plus RBBE at dose of 250 mg/kg, GM + RBBE 500: gentamicin plus RBBE at dose of 500 mg/kg, GM + RBBE 1000: gentamicin plus RBBE at dose of 1000 mg/kg, RBBE: Riceberry bran extract at dose of 1000 mg/kg. Values are mean ± S.E.M. ($n = 7$). $^{*}p < 0.05$ as compared with control group; $^{\#}p < 0.05$ as compared with gentamicin group; $^{a}p < 0.05$ as compared with GM + RBBE 250; $^{b}p < 0.05$ as compared with GM + RBBE 500; $^{c}p < 0.05$ as compared with GM + RBBE 1000; $^{d}p < 0.05$ as compared with RBBE.

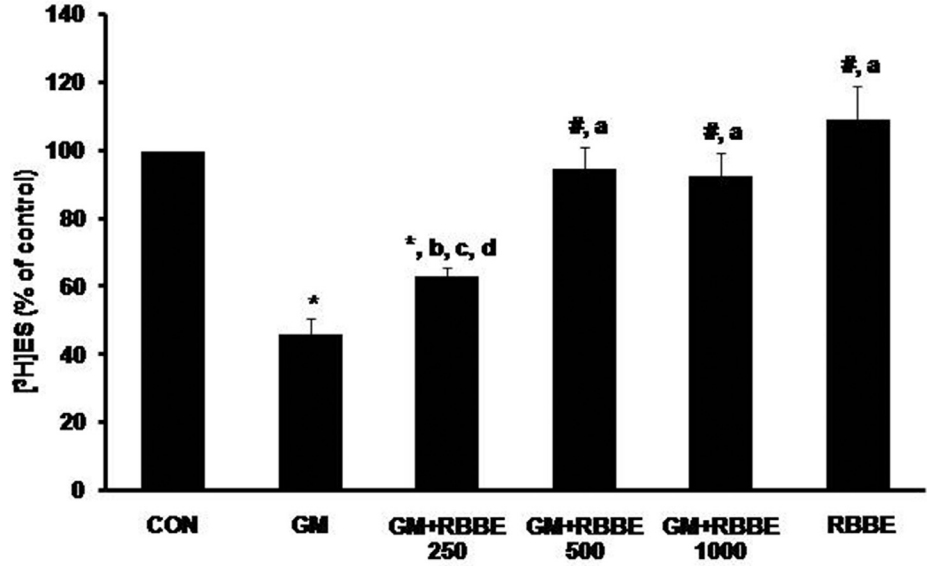

Fig. 3. Effects of RBBE on [^{3}H]ES uptake in renal cortical slices. Renal cortical slices from all six experimental groups were pre-incubated in buffer containing 50 nM [^{3}H]ES for 30 min at 25 °C. Uptake was quantified and expressed as the percentage of control. CON: control, GM: gentamicin, GM + RBBE 250: gentamicin plus RBBE at dose of 250 mg/kg, GM + RBBE 500: gentamicin plus RBBE at dose of 500 mg/kg, GM + RBBE 1000: gentamicin plus RBBE at dose of 1000 mg/kg, RBBE: Riceberry bran extract at dose of 1000 mg/kg. Values are presented as mean ± S.E.M. ($n = 7$). $^{*}p < 0.05$ as compared with control group; $^{\#}p < 0.05$ as compared with gentamicin group; $^{a}p < 0.05$ as compared with GM + RBBE 250; $^{b}p < 0.05$ as compared with GM + RBBE 500; $^{c}p < 0.05$ as compared with GM + RBBE 1000; $^{d}p < 0.05$ as compared with RBBE.

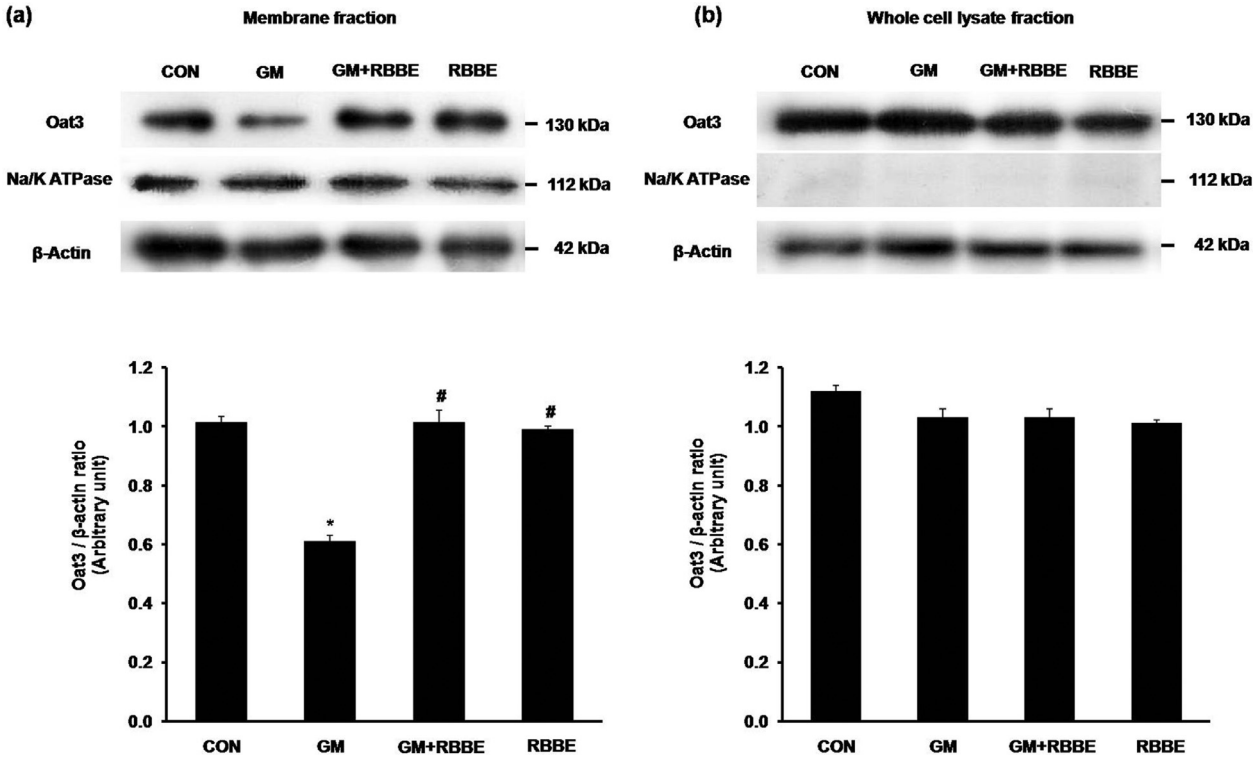

Fig. 4. Effects of RBBE on Oat3 expression in the renal cortex. Western blotting analysis of Oat3 protein (upper panel) and densitometric analysis (lower panel) in the membrane (a) and whole cell lysate (b) fractions. Lanes 1, 2, 3 and 4 represent CON: control, GM: gentamicin, GM + RBBE: gentamicin plus Riceberry bran extract at dose of 500 mg/kg and RBBE: Riceberry bran extract at dose of 1000 mg/kg, correspondingly. Na^+/K^+-ATPase is a marker of membrane fraction, and β-actin is a loading control. Bar graphs indicate mean ± S.E.M. ($n = 7$). $^*p < 0.05$ as compared with control group; $^\#p < 0.05$ as compared with gentamicin group.

Keap1 protein in the whole cell lysate fraction was significantly increased in gentamicin-treated group in comparison to the control or RBBE groups ($p < 0.05$). Also, the expressions of HO-1 and NQO-1 in the whole cell lysate fraction were significantly increased in gentamicin-treated rats as compared with those in the control or RBBE rats ($p < 0.05$). RBBE treatment significantly reversed both the nuclear and cytosol expressions of Nrf2 when compared with those in the gentamicin-treated rats ($p < 0.05$). Moreover, there were the decreases in the expressions of Keap1, HO-1 and NQO-1 in the whole cell lysate fractions in the gentamicin plus RBBE rats compared with those in the gentamicin-treated rats ($p < 0.05$). The results suggest that RBBE treatment exhibits an effective antioxidative effect to attenuate the gentamicin-induced oxidative stress in the kidney that leads to the decrease activation of Nrf2 translocation to the nucleus resulting in the increased Keap 1 and decreased HO-1 and NQO-1 expressions.

Discussion

Nephrotoxicity is the most frequent and serious complication of gentamicin despite its clinical use for treatment of life-threatening gram negative infections (Edson and Terrell, 1999). The selective accumulation of gentamicin in the renal cortex especially in the renal proximal convoluted tubules leads to tubular necrosis without morphological changes in glomerular structures (Martinez-Salgado et al., 2007). In the present study, gentamicin-induced nephrotoxicity was presented with a marked renal hypertrophy as indicated by the greater KW and KW/BW ratio in gentamicin-treated rats, which probably resulted from the edema due to drug-induced tubular necrosis (Erdem et al., 2000). Tubular damage has been shown to impair the normal function of the kidney, generally characterized by increased serum BUN and creatinine as well as decreased urine creatinine and creatinine clearance (C_{cr}) which reflects the poor glomerular filtration rate (GFR) (Dilpesh and Rahul, 2015). Similar results noted in the present study indicated that tubular dysfunction occurred in the gentamicin-induced nephrotoxicity. These findings are firmly confirmed by renal tubular morphologic changes including tubular necrosis, degeneration, desquamation, dilatation, vacuolization and inflammatory cell infiltration. Thus, structural changes in the renal glomerular and tubular support the changes of renal function including elevations of serum BUN and creatinine as well as decreased urine creatinine and creatinine clearance in this study.

Currently, the exact mechanism by which gentamicin-induced nephrotoxicity is still unclear. However, several studies have reported the involvement of oxidative stress in gentamicin-induced renal dysfunction (Cuzzocrea et al., 2002). Gentamicin enhances the production of hydrogen peroxide, superoxide anion and hydroxyl radicals in renal cortical mitochondria, leading to more oxidative stress in renal cortical cells and eventual cell damage (Cuzzocrea et al., 2002; Du and Yang, 1994). Moreover, these free radicals contribute to the peroxidation of lipid, protein and DNA. Also, accumulation of free radicals triggered defense mechanisms against these toxic radical species by using antioxidant enzymes such as superoxide dismutase (SOD), catalase, glutathione peroxidase (GPx) and glutathione (GSH) (Erdem et al., 2000). In this study, gentamicin-induced oxidative stress was indicated by the increased MDA level, a marker of lipid peroxidation, and the decreased SOD and GSH levels. This decrease in renal antioxidant enzymatic protection could aggravate the oxidative damage induce by gentamicin treatment.

It has been reported that Riceberry bran contains high levels of antioxidants such as anthocyanins, flavonoids and phenolic compounds (Prangthip et al., 2013;Leardkamolkarn et al., 2011). RBBE used in this study contains two major anthocyanins, cyanidin 3-glucoside (C-3-G) and peonidin-3-glucoside (P-3-G), thus

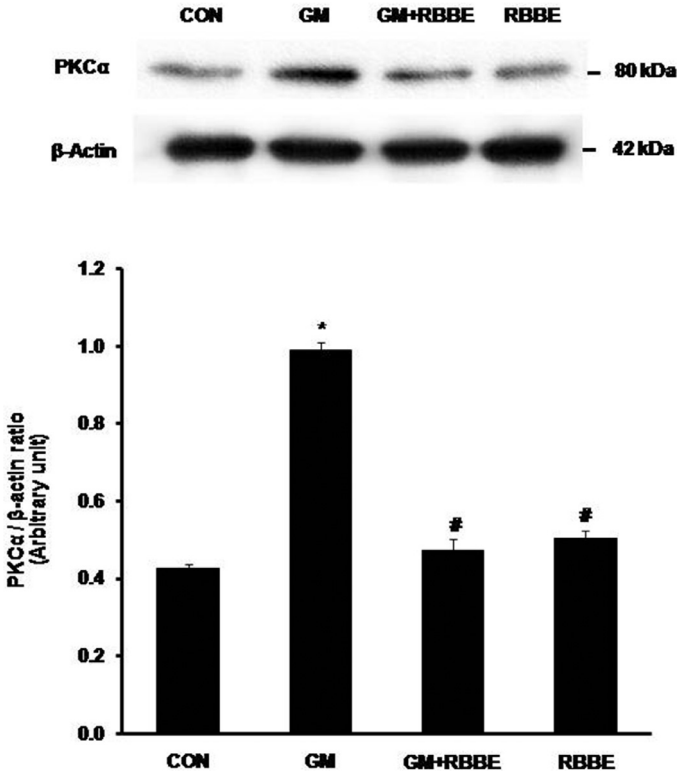

Fig. 5. Effects of RBBE on PKCα expression in the renal cortex. Western blotting analysis of PKCα protein (upper panel) and densitometric analysis (lower panel) in the membrane fraction. Lanes 1, 2, 3 and 4 represent CON: control, GM: gentamicin, GM + RBBE: gentamicin plus Riceberry bran extract at dose of 500 mg/kg and RBBE: Riceberry bran extract at dose of 1000 mg/kg, correspondingly. β-actin is a loading control. Bar graphs indicate mean ± S.E.M. ($n = 7$). $^{*}p < 0.05$ as compared with control group; $^{\#}p < 0.05$ as compared with gentamicin group.

possessing potent antioxidant activity. In addition, the main flavonoid and simple phenolic compounds in RBBE are apigenin and 4-vinylguaiacol, respectively. Anthocyanins have been reported to possess the free radical scavenging abilities in both in vivo and in vitro studies (Wang and Stoner, 2008). At present, little is known about the biological effects of RBBE. The present study showed that RBBE treatment improved the body weight and alleviated the renal hypertrophy in gentamicin-treated rats. Administration of RBBE extract on gentamicin induced nephrotoxic rats significantly prevented the renal injury both functional and histological. Moreover, the decreased kidney MDA and the increased SOD and GSH levels suggested the decreased oxidative stress condition in gentamicin plus RBBE treated rats. These findings indicated that RBBE protected the gentamicin-induced renal damage via its antioxidant property.

Protein kinase C (PKC) is a family of serine-threonine kinases, acting as an excellent target for direct redox-sensitive modifications (Gopalakrishna and Jaken, 2000). Previous studies showed that ROS overproduction under the diabetic condition and gentamicin-induced cytotoxicity were shown to activate PKC signaling (Bertolaso et al., 2003; Arjinajarn et al., 2014). The present result demonstrated that the elevated expression of PKCα in gentamicin-treated rats was restored in gentamicin plus RBBE-treated rats. These findings confirmed the antioxidant effect of RBBE. It has been shown that the activation of PKC mediates the stimulation of Nrf2 in response to oxidative stress (Huang et al., 2000). Nrf2 is a redox-sensitive transcription factor that regulates the expression of several antioxidant and cytoprotective genes. Inactive Nrf2 is retained in the cytoplasm by its association with an actin-binding protein, Keap1. During oxidative stress, Nrf2 is phosphorylated in response to the protein kinase C, phosphatidylinositol 3-kinase, and MAP kinase pathways, and then translocated to the nucleus, being bound to AREs, leading to transactivation of phase II detoxifying enzymes and antioxidant enzymes, such as HO-1, NQO1, CAT, SOD, and GSH-Px (Huang et al., 2000;Ishii et al., 2000; Mann et al., 2007). Previous study demonstrated that Nrf2 induced transcriptional activation of HO-1 and NQO1 (Huang et al., 2000). Overexpression of Nrf2 has been shown to protect the kidney cells against triptolide-induced oxidative stress in vitro study (Li et al., 2012). Moreover, Nrf2 also protected gentamicin-induced ototoxicity by up-regulating antioxidant enzymes including NQO1, HO-1, SOD, and GCL and detoxifying proteins (Hoshino et al., 2011). Consistent with the present results, oxidative stress induced by gentamicin caused the nuclear translocation of Nrf2 as shown by the elevated expression of Nrf2 in the nucleus accompanied with the decreased expression of Nrf2 in the cytoplasm. Also, significant increase in Keap1 expression was observed in gentamicin-treated rats. This finding indicated that the increasing in oxidative stress induced the dissociation of Nrf2 from Keap1 and then translocation of Nrf2 into the nucleus to activate antioxidant gene expression which firmly supported by elevated expressions of HO-1 and NQO1 in gentamicin-treated rats. However, the increased activation of the Nrf2 pathway could not counteract the overproduction of ROS stimulated by gentamicin exposure as shown in this study. Interestingly, the decreased expressions of nuclear Nrf2 and whole cell lysate of Keap 1 and subsequent reduction in HO-1 and NQO1 expressions were found in the gentamicin plus RBBE-treated rats. These findings suggested that the decreased ROS production by RBBE treatment led to the inactivation of Nrf2 to associate with Keap 1, followed by down-regulation of antioxidant enzymes and detoxifying proteins such as HO-1 and NQO1. Thus, it might be proposed that RBBE exerted an antioxidant action, leading to the modulation of Nrf2 signaling pathway.

Organic anion transporters (Oats) play an important role in the excretion of variety of endogenous and toxic exogenous substances including toxins, drugs and their metabolites (Sekine et al., 2000). Oat is also the site for drug–drug interactions and drug-induced nephrotoxicity (You, 2002). The present results demonstrated that nephrotoxicity induced by gentamicin was associated with the impaired function and decreased membrane expression of renal Oat3. Previous study reported down-regulation of renal Oat3 expression stimulated by the activation of PKCα (Takeda et al., 2000). Moreover, the increased PKCα expression induced by the overproduction of ROS in diabetic condition subsequently caused the down-regulation of renal Oat3 expression (Arjinajarn et al., 2014). Consistent with the previous study, our results demonstrated the decreased membrane Oat3 expression and were correlated with the activation of PKCα expression in gentamicin-treated rats. An interesting finding found in this study is the restoration of the function and expression of renal Oat3 in gentamicin-treated plus RBBE treatment. The decreased expression of PKCα and improved renal Oat3 function in gentamicin plus RBBE treatment could be due to the reduced oxidative stress by RBBE treatment. This was supported by the previous study demonstrating that the antioxidant, JBP485, improved acute renal failure by increasing the expression and function of Oat1 and Oat3 along with decreasing overoxidation of the kidney in gentamicin-induced ARF rats (Guo et al., 2013).

Conclusion

The findings of the present study indicated that the impaired renal function and renal Oat3 function and expression in gentamicin-induced nephrotoxicity are closely associated with the increase in oxidative stress condition in the renal cortical tissues. RBBE effectively protected against renal dysfunction and

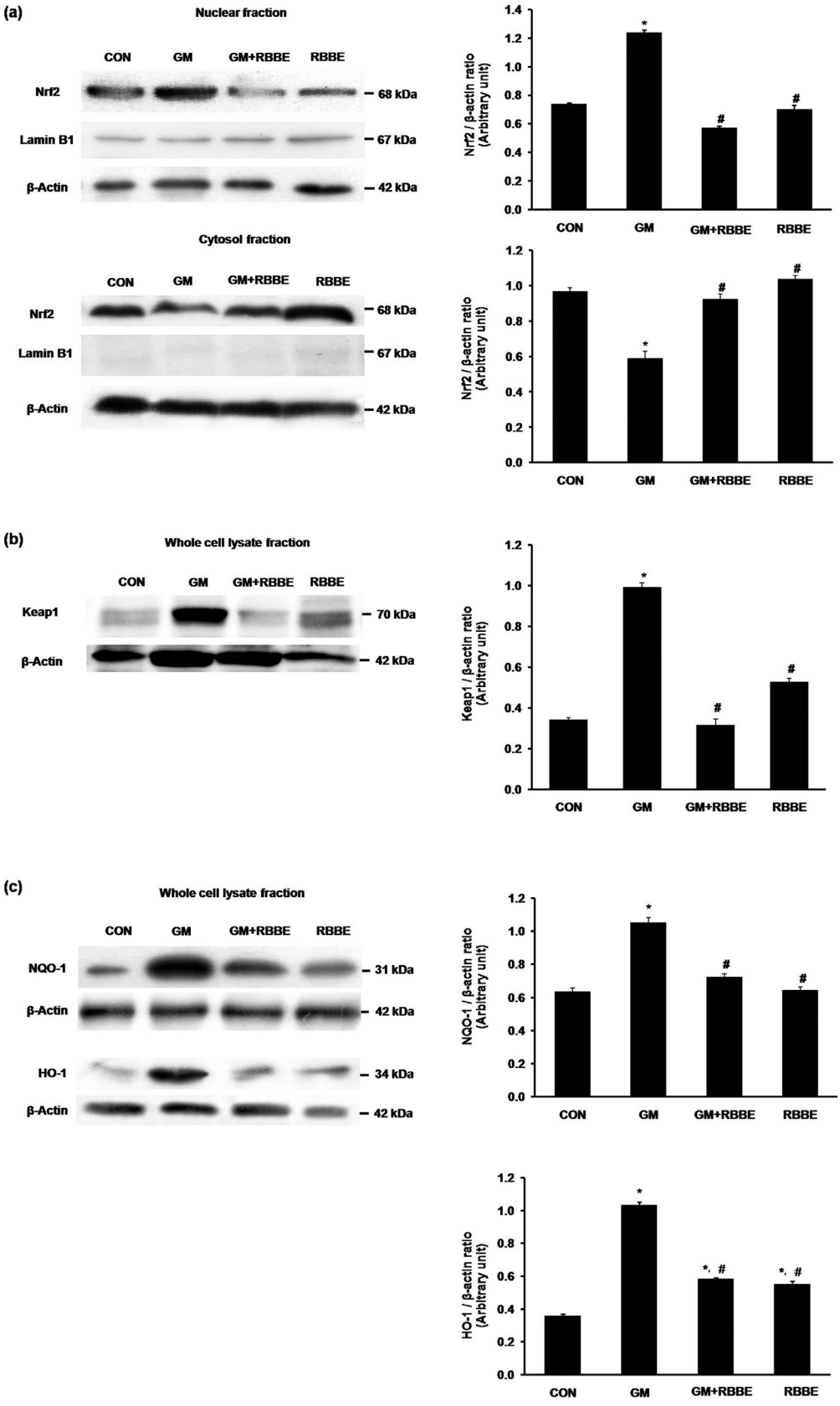

Fig. 6. Effects of RBBE on Nrf2, Keap 1, NQO1 and HO-1 expressions in the renal cortex. (a) Western blotting analysis of Nrf2 protein (left panel) and densitometric analysis (right panel) in the nuclear and cytosol fractions. (b) Western blotting analysis of Keap1 protein (left panel) and densitometric analysis (right panel) in the whole cell lysate fractions. (c) Western blotting analysis of NQO1 and HO1 protein (left panel) and densitometric analysis (right panel) in the whole cell lysate fractions. Lanes 1, 2, 3 and 4 represent CON: control, GM: gentamicin, GM + RBBE: gentamicin plus Riceberry bran extract at dose of 500 mg/kg and RBBE: Riceberry bran extract at dose of 1000 mg/kg, correspondingly. Lamin B1 is a marker of nuclear fraction, and β-actin is a loading control. Bar graphs indicate means ± S.E.M. ($n = 7$). $^{*}p < 0.05$ as compared with control group; $^{\#}p < 0.05$ as compared with gentamicin group.

up-regulated function and expression of renal Oat3 in gentamicin-induced renal toxicity. The renoprotective mechanism of RBBE is due to an antioxidative action, subsequently leading to modulation of the PKC/Nrf2 antioxidant defense pathway.

Conflict of interest

The authors declare that they have no competing interests.

Acknowledgments

This work was supported by the Young Researcher Support Grant, Chiang Mai University (PA), the Thailand Research Fund (TRG-5780019) (PA), the Thailand Research Fund RSA5780029 (AL), National Research Council of Thailand (Grant #164368;2558A10402068) (AL), CMU Mid-Career Research Fellowship program (AL), the Faculty of Medicine Research Fund, Chiang Mai University (AL and AP) and the NSTDA Research Chair grant from the National Science and Technology Development Agency of Thailand (NC.).

References

Ali, B.H., 2003. Agents ameliorating or augmenting experimental gentamicin nephrotoxicity: some recent research. Food Chem.Toxicol. 41, 1447–1452.
Arjinajarn, P., Srimaroeng, C., Chatsudthipong, V., Lungkaphin, A., 2014. Decreased renal organic anion transporter 3 expression in type 1 diabetic rats. In: Am. J. Med. Sci., 347, pp. 221–227.
Bancroft, JD, Steven, A, David, RT, 1996. Theory and Practice of Histological Techniques, fourth ed., p. 303 New York.
Bertolaso, L., Bindini, D., Previati, M., Falgione, D., Lanzoni, I., Parmeggiani, A., Vitali, C., Corbacella, E., Capitani, S., Martini, A., 2003. Gentamicin-induced cytotoxicity involves protein kinase C activation, glutathione extrusion and malondialdehyde production in an immortalized cell line from the organ of corti. Audiol. Neurootol. 8, 38–48.
Cuzzocrea, S., Mazzon, E., Dugo, L., Serraino, I., Di Paola, R., Britti, D., De Sarro, A., Pierpaoli, S., Caputi, A., Masini, E., Salvemini, D., 2002. A role for superoxide in gentamicin-mediated nephropathy in rats. Eur. J. Pharmacol. 450, 67–76.
da Costa, C.T., Horton, D., Margolis, S.A., 2000. Analysis of anthocyanins in foods by liquid chromatography, liquid chromatography-mass spectrometry and capillary electrophoresis. J Chromatogr. A. 881, 403–410.
Dilpesh, J., Rahul, S., 2015. Silibinin: a bioactive flavanonein milk thistle ameliorate gentamicin induced nephrotoxicity in rats. Pharmacologia 6, 38–44.
Du, X.H., Yang, C.L., 1994. Mechanism of gentamicin nephrotoxicity in rats and the protective effect of zinc-induced metallothionein synthesis. Nephrol. Dial. Transplant. 9, 135–140.
Edson, R.S., Terrell, C.L., 1999. The aminoglycosides. Mayo Clin. Proc. 74, 519–528.
Erdem, A., Gundogan, N.U., Usubutun, A., Kilinc, K., Erdem, S.R., Kara, A., Bozkurt, A., 2000. The protective effect of taurine against gentamicin-induced acute tubular necrosis in rats. Nephrol. Dial. Transplant. 15, 1175–1182.
Gopalakrishna, R., Jaken, S., 2000. Protein kinase C signaling and oxidative stress. Free Radic. Biol. Med. 28, 1349–1361.
Guo, X., Meng, Q., Liu, Q., Wang, C., Sun, H., Peng, J., Ma, X., Kaku, T., Liu, K., 2013. JBP485 improves gentamicin-induced acute renal failure by regulating the expression and function of Oat1 and Oat3 in rats. Toxicol. Appl. Pharmacol. 271, 285–295.
Hoshino, T., Tabuchi, K., Nishimura, B., Tanaka, S., Nakayama, M., Ishii, T., Warabi, E., Yanagawa, T., Shimizu, R., Yamamoto, M., Hara, A., 2011. Protective role of Nrf2 in age-related hearing loss and gentamicin ototoxicity. Biochem. Biophys. Res. Commun. 415, 94–98.
Huang, H.C., Nguyen, T., Pickett, C.B., 2000. Regulation of the antioxidant response element by protein kinase C-mediated phosphorylation of NF-E2-related factor 2. Proc. Natl. Acad. Sci. USA. 97, 12475–12480.
Ishii, T., Itoh, K., Takahashi, S., Sato, H., Yanagawa, T., Katoh, Y., Bannai, S., Yamamoto, M., 2000. Transcription factor Nrf2 coordinately regulates a group of oxidative stress-inducible genes in macrophages. J. Biol. Chem. 275, 16023–16029.
Kim, H.J., Vaziri, N.D., 2010. Contribution of impaired Nrf2-Keap1 pathway to oxidative stress and inflammation in chronic renal failure. Am. J. Physiol. Renal Physiol 298, F662–F671.
Kongkachuichai, R., Prangthip, P., Surasiang, R., Posuwan, J., Charoensiri, R., Kettawan, A., Vanavichit, A., 2013. Effect of Riceberry oil (deep purple oil; Oryza sativaindica) supplementation on hyperglycemia and change in lipid profile in streptozotocin (STZ)-induced diabetic rats fed a high fat diet. Int. Food Res. J. 20, 873–882.
Leardkamolkarn, V., Thongthep, W., Suttiarporn, P., Kongkachuichai, R., Wongpornchai, S., Wanavijitr, A., 2011. Chemopreventive properties of the bran extracted from a newly-developed Thai rice: The Riceberry. Food Chem 125, 978–985.
Li, Y., Paonessa, J.D., Zhang, Y., 2012. Mechanism of chemical activation of Nrf2. PLoS One 7, e35122.
Mann, G.E., Niehueser-Saran, J., Watson, A., Gao, L., Ishii, T., de Winter, P., Siow, R.C., 2007. Nrf2/ARE regulated antioxidant gene expression in endothelial and smooth muscle cells in oxidative stress: implications for atherosclerosis and preeclampsia. Sheng Li Xue Bao 59, 117–127.
Martinez-Salgado, C., Lopez-Hernandez, F.J., Lopez-Novoa, J.M., 2007. Glomerular nephrotoxicity of aminoglycosides. Toxicol. Appl. Pharmacol. 223, 86–98.
Montoro, P., Tuberoso, C.I.G., Perrone, A., Piacente, S., Cabras, P., Pizza, C., 2006. Characterisation by liquid chromatography- electrospray tandem mass spectrometry of anthocyanidins in extracts of Myrtus communis L. berries used for the preparation of myrtle liquer. J. Chromatogr. A. 1112, 232–240.
Motohashi, H., Sakurai, Y., Saito, H., Masuda, S., Urakami, Y., Goto, M., Fukatsu, A., Ogawa, O., Inui, K., 2002. Gene expression levels and immunolocalization of organic ion transporters in the human kidney. J. Am. Soc. Nephrol. 13, 866–874.
Ohkawa, H., Ohishi, N., Yagi, K., 1979. Assay for lipid peroxides in animal tissues by thiobarbituric acid reaction. Anal. Biochem. 95, 351–358.
Oliveira, M.C., Esperanca, P., Almoster Ferreira, M.A., 2001. Characterisation of anthocyanidins by electrospray ionization and collision-induced dissociation tandem mass spectrometry. Rapid Commun. Mass Spectrom. 15, 1525–1532.
Prangthip, P., Surasiang, R., Charoensiri, R., Leardkamolkarn, V., Komindr, S., Yamborisut, U., Vanavichitd, A., Kongkachuichaia, R., 2013. Amelioration of hyperglycemia, hyperlipidemia, oxidative stress and inflammation in steptozotocin-induced diabetic rats fed a high fat diet by Riceberry supplement. J. Funct. Food. 5, 195–203.
Quiros, Y., Vicente-Vicente, L., Morales, A.I., Lopez-Novoa, J.M., Lopez-Hernandez, F.J., 2011. An integrative overview on the mechanisms underlying the renal tubular cytotoxicity of gentamicin. Toxicol. Sci. 119, 245–256.
Sekine, T., Cha, S.H., Endou, H., 2000. The multispecific organic anion transporter (OAT) family. Pflugers Arch 440, 337–350.
Subramanian, P., Anandan, R., Jayapalan, P.P., Hashim, O.H., 2015. Hesperidin protects gentamicin-inducednephrotoxicity via Nrf2/HO-1 signaling and inhibits inflammation mediated by NF-Kb in rats. J. Funct. Foods. 13, 89–99.
Sweet, D.H., Miller, D.S., Pritchard, J.B., Fujiwara, Y., Beier, D.R., Nigam, S.K., 2002. Impaired organic anion transport in kidney and choroid plexus of organic anion transporter 3 (Oat3 (Slc22a8)) knockout mice. J. Biol. Chem. 277, 26934–26943.
Takeda, M., Sekine, T., Endou, H., 2000. Regulation by protein kinase C of organic anion transport driven by rat organic anion transporter 3 (rOAT3). Life Sci 67, 1087–1093.
Wang, L.S., Stoner, G.D., 2008. Anthocyanins and their role in cancer prevention. Cancer Lett 269, 281–290.
You, G., 2002. Structure, function, and regulation of renal organic anion transporters. Med. Res. Rev. 22, 602–616.
Zhang, L., Zhu, Z., Liu, J., Hu, Z., 2014. Protective effect of N-acetylcysteine (NAC) on renal ischemia/reperfusion injury through Nrf2 signaling pathway. J. Recept. Signal Transduct. Res. 34, 396–400.

NRC Research Press

ARTICLE

Pinocembrin attenuates gentamicin-induced nephrotoxicity in rats

Sasivimon Promsan, Krit Jaikumkao, Anchalee Pongchaidecha, Nipon Chattipakorn, Varanuj Chatsudthipong, Phatchawan Arjinajarn, Wilart Pompimon, and Anusorn Lungkaphin

Abstract: Oxidative stress mediated apoptosis of renal tubular cells is a major pathology of gentamicin-induced nephrotoxicity, which is one of the prevailing causes of acute renal failure. Pinocembrin is a major flavonoid found in rhizomes of fingerroot (*Boesenbergia pandurata*). It has pharmacological and biological activities including antimicrobial, anti-inflammatory, and antioxidant effects. Preclinical studies have suggested that pinocembrin protects rat brain and heart against oxidation and apoptosis induced by ischemia–reperfusion. The aim of the current study was to investigate the mechanisms of renoprotection elicited by pinocembrin in gentamicin-induced nephrotoxicity. Nephrotoxicity was induced in rats by intraperitoneal injection (i.p.) of gentamicin, and pinocembrin was administered via i.p. 30 min before gentamicin treatment for 10 days. Gentamicin-induced nephrotoxicity was indicated by the reduced renal function and renal Oat3 function and expression. Gentamicin treatment also stimulated Nrf2, HO-1, and NQO1, as well as the pro-apoptotic proteins Bax and caspase-3, concomitant with the attenuation of Bcl-XL expression in the renal cortical tissues. Pinocembrin pretreatment improved renal function and renal Oat3 function and reduced oxidative stress and apoptotic conditions. These findings indicate that pinocembrin has a protective effect against gentamicin-induced nephrotoxicity, which may be due in part to its antioxidant and anti-apoptotic effects, subsequently leading to improved renal function.

Key words: pinocembrin, nephrotoxicity, renal function, organic anion transporter, gentamicin, oxidative stress, apoptosis.

Résumé : L'apoptose dépendant du stress oxydatif dans les cellules tubulaires rénales est un effet néphrotoxique majeur de la gentamicine et une cause prépondérante d'insuffisance rénale aiguë. La pinocembrine est un important composé flavonoïde que l'on trouve dans les rhizomes de gingembre chinois (*Boesenbergia pandurata*). Son activité pharmacologique et biologique entraîne des effets antimicrobiens, anti-inflammatoires et antioxydants. Les résultats des études précliniques laissent présumer que la pinocembrine permet de protéger les cellules du cerveau et du cœur contre l'apoptose dans un modèle d'ischémie–reperfusion chez le rat. Les présents travaux visaient à étudier les mécanismes de néphroprotection mobilisés par la pinocembrine contre la toxicité rénale associée à la gentamicine. Nous avons induit la néphrotoxicité chez le rat en injectant de la gentamicine par voie intrapéritonéale (i.p.) 30 min après l'administration i.p. de pinocembrine pendant 10 jours. La néphrotoxicité induite par la gentamicine se manifestait par la diminution de la fonction rénale de même que de la fonction et de l'expression de l'Oat3. L'administration de gentamicine a aussi activé Nrf2, HO-1 et NQO1 ainsi que la protéine pro-apoptotique Bax et la caspase 3, tout en atténuant l'expression de Bcl-XL dans le cortex rénal. Le prétraitement par la pinocembrine a permis d'améliorer la fonction rénale et la fonction de l'Oat3 dans le rein et d'atténuer le stress oxydatif et de faire rétrocéder d'apoptose. Ces résultats montrent les effets protecteurs que la pinocembrine exerce contre la néphrotoxicité causée par la gentamicine. Ceux-ci pourraient être en partie liés aux effets antioxydants et anti-apoptotiques du traitement qui permettent subséquemment d'améliorer la fonction rénale. [Traduit par la Rédaction]

Mots-clés : pinocembrine, néphrotoxicité, fonction rénale, transporteur anionique organique, gentamicine, stress oxydatif, apoptose.

Introduction

Gentamicin, an aminoglycoside antibiotic, has been widely used as a bactericidal agent against severe Gram-negative infections (Edson and Terrell 1999; Noone et al. 1974). However, prolonged treatment of gentamicin produces serious side effects such as nephrotoxicity and ototoxicity (Lopez-Novoa et al. 2011; Rizzi and Hirose 2007). Gentamicin-induced renal toxicity is related to its preferential accumulation in the renal proximal convoluted tubules (Abdel-Raheem et al. 2009), leading to damage of the tubular epithelial cells, which further progresses to acute renal failure (Nagai and Takano 2004). Although the mechanisms of gentamicin-induced nephrotoxicity are not fully defined, the generation of reactive oxygen species (ROS), mostly in the renal cortical mitochondria (Walker and Shah 1987; Yang et al. 1995), induced vasoconstriction, mesangial cell contraction, cellular damage, and necrosis via lipid peroxidation, and these changes could be pre-

Received 6 October 2015. Accepted 1 March 2016.

S. Promsan. Division of Physiology, School of Medical Sciences, University of Phayao, Phayao, Thailand.
K. Jaikumkao, A. Pongchaidecha, and A. Lungkaphin. Department of Physiology, Faculty of Medicine, Chiang Mai University, Chiang Mai, Thailand.
N. Chattipakorn. Cardiac Electrophysiology Research and Training Center, Chiang Mai University, Chiang Mai, Thailand.
V. Chatsudthipong. Department of Physiology, Faculty of Science, Mahidol University, Bangkok, Thailand.
P. Arjinajarn. Department of Biology, Faculty of Science, Chiang Mai University, Chiang Mai, Thailand.
W. Pompimon. Department of Chemistry and Center of Excellence for Innovation in Chemistry, Faculty of Science, Lampang Rajabhat University, Lampang, Thailand.
Corresponding author: Anusorn Lungkaphin (email: anusorn.lungka@cmu.ac.th).

vented or ameliorated by antioxidants (Abdel-Raheem et al. 2009; Ajami et al. 2010; Mazzon et al. 2001; Nasri et al. 2013).

Nuclear factor E2-related factor-2 (Nrf2), a redox-sensitive transcription factor, is a sensor of oxidative and electrophilic stress (Xing et al. 2012). In vitro and in vivo studies have shown that Nrf2 is essential for the antioxidant response element (ARE) mediated induction of several genes, including phase II detoxifying enzymes such as glutathione-S-transferase and quinone reductase (Kalayarasan et al. 2009). Nrf2 also activates the antioxidant enzymes and many other proteins that detoxify xenobiotics and neutralize ROS and (or) reactive nitrogen species (RNS). In gentamicin-induced ototoxicity, Nrf2 protected hair cell damage by activating Nrf2-mediated antioxidant enzymes, including NAD(P)H dehydrogenase quinone 1 (NQO1), glutamate–cysteine ligase catalytic subunit (GCLC), superoxide dismutase (SOD), and heme oxygenase 1 (HO1) (Hoshino et al. 2011).

Organic anion transporter (Oat) plays a major role in the elimination of organic anion substances. It is a family of solute carrier (SLC) transporters that is classified into many types, e.g., Oat1, Oat2, Oat3, Oat4, Oat5, Oat8, Oat9, and Oat10 (Koepsell 2013; Sekine et al. 2000). Oat3 shows the highest expression at the basolateral membrane of the proximal tubule cell. An impaired renal excretion of various compounds along with down-regulation of Oat3 has been reported in gentamicin-induced acute renal failure (Guo et al. 2013). However, the mechanisms of these alterations have not been clearly elucidated.

Pinocembrin (5,7-dihydroxyflavonone, $C_{15}H_{12}O_4$), a flavonoid found abundantly in honeybee propolis (Bankova et al. 1982) and the rhizomes of *Boesenbergia pandurata* (Punvittayagul et al. 2011), has several biological actions, including anti-microbial (Del Rayo Camacho et al. 1991; Pepeljnjak et al. 1985), antioxidant (Santos et al. 1998), anti-inflammatory (Sala et al. 2003; Soromou et al. 2012), and vasorelaxation (Shi et al. 2011) effects. Recently, preclinical studies have suggested that pinocembrin attenuates cerebral ischemic injury in middle cerebral artery occlusion in rats (Gao et al. 2008). Pinocembrin also reduced compensatory increases in SOD activity, decreased in both malondialdehyde (MDA) content and myeloperoxidase (MPO) activity in global cerebral ischemia–reperfusion (I/R) rat models (Shi et al. 2011). It exhibited cardioprotective effects during I/R by its antioxidant and anti-apoptotic effects (Lungkaphin et al. 2015). These data led us to investigate the renoprotective effect of pinocembrin against gentamicin-induced nephrotoxicity. We tested the hypothesis that the renoprotective mechanisms of pinocembrin against gentamicin-induced nephrotoxicity are due to its antioxidant and anti-apoptotic effects.

Materials and methods

Chemicals and reagents

Gentamicin was acquired from the Government Pharmaceutical Organization (Bangkok, Thailand). The pinocembrin compound (95% purity) was isolated from the rhizomes of *Boesenbergia pandurate*, which was carried out at the Department of Chemistry and Center of Excellence for Innovation in Chemistry, Faculty of Science, Lampang Rajabhat University (Lampang, Thailand). Tween 80 was supplied by Calbiochem, Merck Millipore (Billerica, Massachusetts, USA). Mammalian tissue lysis/extraction reagent was provided by Sigma-Aldrich Corp. (St. Louis, Missouri, USA). Complete protease inhibitor cocktail was acquired from Roche Applied Science (Indianapolis, Indiana, USA). TBARS assay kit was purchased from Cayman Chemical (Ann Arbor, Michigan, USA). SOD activity assay kit was provided by BioAssay Systems (Hayward, California, USA). BUN and creatinine assay kits were purchased from DiaSys Diagnostic Systems GmbH (Holzheim, Germany). The radiolabeled estrone sulfate ([^{3}H]ES) was purchased from PerkinElmer (Sugar Land, Texas, USA). Primary Oat3 antibody was from Cosmo Bio Co. Ltd. (Tokyo, Japan). The Na^+-K^+-ATPase, caspase-3, and Bcl-XL antibodies were acquired from Millipore (Billerica, Massachusetts, USA). The primary anti-HO1 and primary anti-NQO1 antibodies were from Abcam (Cambridge, Massachusetts, USA). The primary PKCα, NADPH oxidase (NOX4), and primary anti-Nrf2 antibodies were from Santa Cruz Biotechnology (Dallas, Texas, USA). The primary anti-Bax and β-actin antibodies were from Cell Signaling Technology (Beverly, Massachusetts, USA). The horseradish peroxidase (HRP) conjugated goat anti-rabbit or anti-mouse secondary antibody was purchased from Amersham (Illinois, USA). A polyvinylidene fluoride (PVDF) membrane was provided by Millipore (Billerica, Massachusetts, USA). The ECL enhanced chemiluminescence agent and Hyperfilm were acquired from GE Healthcare (Buckinghamshire, UK).

The method of pinocembrin preparation

The air-dried powder (1 kg) of *Boesenbergia pandurata* rhizomes was percolated with *n*-hexane at room temperature for 9 days. Subsequently, the residue was percolated with ethyl acetate for 15 days. Then, the filtrate was evaporated to dryness under low pressure to obtain an ethyl acetate crude extract (79.99 g). To obtain pinocembrin, the ethyl acetate extract was first subjected to coarse separation by silica column chromatography. Gradient elution was conducted initially with *n*-hexane, gradually enriched with ethyl acetate, followed by increasing amounts of methanol in ethyl acetate and finally with methanol. The obtained solid was recrystalized from ethanol to obtain pinocembrin (69.32 mg). Finally, structural confirmation was performed using UV spectroscopy, Fourier transform infrared (FTIR) spectroscopy, ^{1}H and ^{13}C nuclear magnetic resonance (^{1}H NMR and ^{13}C NMR, respectively) spectroscopy, and mass spectrometry (MS). The purity of pinocembrin was more than 95% (Charoensin et al. 2010).

A previous study (Charoensin et al. 2010) investigated the toxicity dose of pinocembrin in a rat model. Pinocembrin at the doses of 1–100 mg/kg and 500 mg/kg were administrated by gavage feeding. There was neither toxicity nor death in the rats studied in that model. Recently, there was a report in a double-blind, placebo-controlled, randomized study carried out in 58 healthy subjects (Cao et al. 2015). Single ascending doses of pinocembrin (20–150 mg), as well as a study of multidoses of 60 mg pinocembrin, were investigated. The results showed that pinocembrin was well tolerated and no serious adverse events occurred. No subjects were discontinued because of a treatment-emergent adverse event. These findings indicated that there was no lethal or toxic dose of pinocembrin.

Animals

Male Sprague–Dawley rats (240–250 g) from the National Laboratory Animal Centre, Mahidol University, Salaya, Nakornpathom, were housed in the animal room at controlled temperatures in a 12 h light – 12 h dark cycle and fed with a normal pellet diet and water ad libitum. This study was carried out in strict accordance with the recommendations in the *Guide for the Care and Use of Laboratory Animals* (1996, published by National Academy Press, 2101 Constitution Ave. NW, Washington, DC 20055, USA). The protocol was approved by the Committee on the Ethics of Animal Experiments of the Faculty of Medicine, Chiang Mai University (Permit No. 13/2557). All surgery was performed under sodium pentobarbital anesthesia, and all efforts were made to minimize suffering.

Experimental design

The rats were randomly divided into 5 groups (6 rats per group) and were treated for 10 days as follows: (*i*) the control group, the rats were injected intraperitoneally (i.p.) with Tween 80; (*ii*) the gentamicin group, the rats were treated (i.p.) with gentamicin at a dose of 100 mg/kg daily, (*iii*) the pinocembrin + gentamicin group, the rats were injected (i.p.) with pinocembrin (dissolved in Tween 80 at a dose of 50 mg/kg daily, obtained from air-dried fingerroot weighing 140 g) 30 min prior to the injection of gentamicin; (*iv*) the

Table 1. Effects of pretreatment with pinocembrin (50 or 75 mg/kg) on physiological and renal function parameters in rats treated with gentamicin (100 mg/kg).

	Treatment				
Parameter	Control	Gentamicin	Gentamicin + 50 mg/kg pinocembrin	Gentamicin + 75 mg/kg pinocembrin	Pinocembrin alone (50 mg/kg)
Body mass (g)	337±7.95	294±8.13*	308±2.50#	323±3.30#	324±7.50
Kidney mass (g)	1.33±0.02	2.00±0.16*	1.50±0.03#	1.47±0.06#	1.32±0.02
KM/BM ratio	0.004±0.0001	0.006±0.0003*	0.005±0.0001#	0.004±0.0002#	0.004±0.0001
Renal function					
Serum BUN (mg%)	21.50±0.76	31.16±1.83*	26.33±1.80#	23.33±0.88#	21.40±0.68
Serum Cr (mg%)	0.47±0.02	0.73±0.04*	0.58±0.03#	0.55±0.07#	0.37±0.04
C_{cr} (mL/min)	2.07±0.11	1.17±0.07*	1.35±0.08#	1.51±0.36#	2.40±0.16

Note: Values are mean ± SE (n = 6 rats per group). KM/BM ratio, kidney mass/body mass ratio; BUN, blood urea nitrogen; Cr, creatinine; C_{cr}, creatinine clearance. Asterisk (*) indicates significantly ($P < 0.05$) different compared with control; hashtag (#) indicates significantly ($P < 0.05$) different compared with gentamicin-treated rats.

pinocembrin-50 group, the rats were injected i.p. with pinocembrin (50 mg/kg daily) for 10 days; and (*v*) the pinocembrin-75 group, the rats were injected i.p. with pinocembrin (75 mg/kg daily) for 10 days. The dose of pinocembrin used in this study was chosen from our preliminary experiment and from a previous study (Soromou et al. 2012).

After the treatment on 10th day, the animals were placed into individual metabolic cages for 24 h urine collection and then sacrificed under anesthesia for blood collection from the right atrium. The kidneys were immediately removed, decapsulated, and weighed. One of the kidneys was divided into two longitudinal sections. Renal cortical tissues were isolated and kept for Western blot analysis and evaluation of MDA. The other kidney was perfused with cold PBS and then cut into 2 longitudinal sections: one was fixed in 10% neutralized formalin for further morphological analysis, and in the other, the renal cortical tissues were isolated and kept for SOD determination. Then, the tissue samples were placed in liquid nitrogen and stored at –80 °C until use.

Determination of renal function

The serum and urine creatinine and serum BUN levels were measured by following enzymatic colorimetric methods using commercial kits. The data were expressed as mg/dL. The estimation of glomerular filtration rate (GFR) or creatinine clearance (C_{cr}; mL/min) was carried out using the following equation:

$$C_{cr} = \frac{\text{urine creatine} \times \text{urine flow rate}}{\text{serum creatine}}$$

Determination of renal Oat3 function

The uptake of radiolabeled estrone sulfate ([^{3}H]ES), a specific Oat3 substrate, into the renal cortical slice, which reflects the renal Oat3 function, was examined. After the animals were sacrificed, the kidneys were removed, decapsulated, and placed in freshly oxygenated ice-cold modified Cross and Taggart saline buffer (containing the following: 95 mmol/L NaCl, 80 mmol/L mannitol, 5 mmol/L KCl, 0.74 mmol/L $CaCl_2$, and 9.5 mmol/L Na_2HPO_4, pH 7.4). Thin renal cortical slices (≤0.5 mm; 5–15 mg/slice, wet mass) were cut with a Stadie–Riggs microtome and were preincubated in modified Cross and Taggart buffer for 10 min then incubated in 1 mL of buffer containing 50 nmol/L [^{3}H]ES for 30 min at room temperature. At the end of the uptake period, the slices were washed in 0.1 mol/L $MgCl_2$, blotted on filter paper, weighed, and dissolved in 0.5 mL of 1 mol/L NaOH, and then the preparation was neutralized with 0.5 mL of 1 mol/L HCl. The radioactivity was measured using a liquid scintillation analyzer (PerkinElmer, Massachusetts, USA). The [^{3}H]ES uptake was calculated as a ratio of tissue to medium (T:M) (dpm/g tissue/dpm/mL medium).

Tissue preparation for Western blot analysis

Renal cortical tissue, 0.1 g, was chopped and homogenized on ice in mammalian cell lytic buffer with a protease inhibitor cocktail. Each cellular component, whole-cell lysate, membrane, and cytosolic fractions, were prepared from renal cortical slices using differential centrifugation as previously described (Lungkaphin et al. 2014). Briefly, the homogenate was centrifuged at 5000*g* for 10 min at 4 °C, the supernatant was designated as whole-cell lysate, and then the supernatant was further centrifuged at 100 000*g* for 2 h at 4 °C to obtain membrane (pellet) and cytosolic (supernatant) fractions. The 5000*g* pellet was re-suspended and centrifuged at 10 000*g* 4 °C for 10 min. The supernatant fraction from the spin was designated as the nuclear fraction. All the fractions collected were stored at –80 °C until use.

Determination of renal Oat3 expression

The total cell lysates and the membrane fractions from the renal cortex were subjected to SDS–PAGE and subsequently transferred to a PVDF membrane, as described above. Primary Oat3 antibody at a concentration of 1:500 was added. To confirm the enrichment of the membrane fraction, the Na^+-K^+-ATPase expression was determined as a membrane fraction marker. The density of the protein signal on Hyperfilm was analyzed using the histogram function of Adobe Photoshop CS5 (Adobe Systems Inc., San Jose, California) scanning. The protein level was normalized by β-actin as a loading control.

Determination of renal lipid peroxidation

To determine conditions of renal oxidative stress, measurement of the MDA level, a marker of lipid peroxidation, in the renal cortical tissues was carried out. Briefly, the renal cortical tissues were cut and suspended in CelLyticMT mammalian tissue lysis/extraction reagent containing a 1% complete protease inhibitor cocktail made according to the manufacturer's protocol. The tissues were then homogenized and centrifuged at 1600*g* for 10 min at 4 °C. The supernatants were collected for the determination of MDA concentration using a commercial TBARS assay kit, as previously described (Ohkawa et al. 1979). Each sample was expressed as total MDA level to total protein concentration (nmol/mg protein).

Determination of renal cortical SOD activity

The renal cortex tissue was homogenized at 5 mL/g in cold lysis buffer (50 mmol/L potassium phosphate, 0.1 mmol/L EDTA, 0.5% Triton X-100) and centrifuged at 12 000*g* for 5 min at 4 °C. The supernatants were used for total SOD activity determination according to the manufacturer's protocol.

Determination of renal oxidative stress and apoptosis

The renal oxidative stress pathway and apoptosis protein markers were determined by Western blot analysis. The renal cortical

Fig. 1. Effects of pinocembrin pretreatment on [^{3}H]ES uptake in renal cortical slices. Renal cortical slices were incubated in buffer containing 50 nmol/L [^{3}H]ES for 30 min at room temperature. The uptake was calculated as tissue-to-medium (T/M) ratio and then converted to a mean percentage of the control. Values are expressed as the mean ± SEM from 6 rats per group (5 slices per rat). *, $P < 0.05$ compared with the control group; #, $P < 0.05$ compared with the gentamicin-treated group.

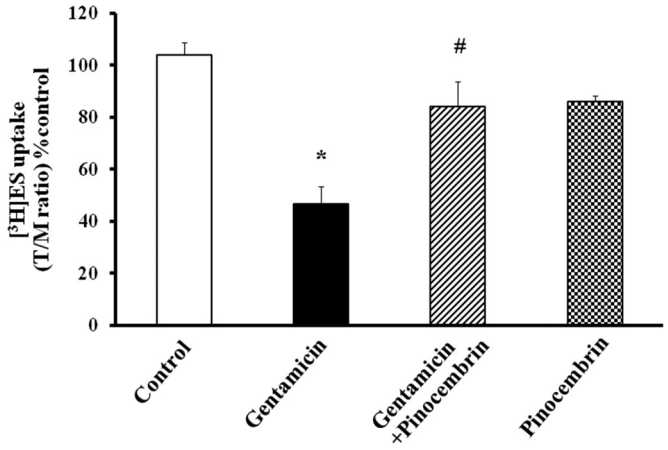

Fig. 2. Effects of pinocembrin pretreatment on Oat3 expression in the renal cortical tissue. Western blot analysis of Oat3 expression in (A) membrane and (B) whole-cell lysate fractions of renal cortical tissues. The signal intensity of Oat3 expression in membrane and whole-cell lysate fractions was normalized to β-actin. Bar graphs indicate mean ± SEM ($n = 6$ rats per group). *, $P < 0.05$ compared with the control group; #, $P < 0.05$ compared with the gentamicin-treated group.

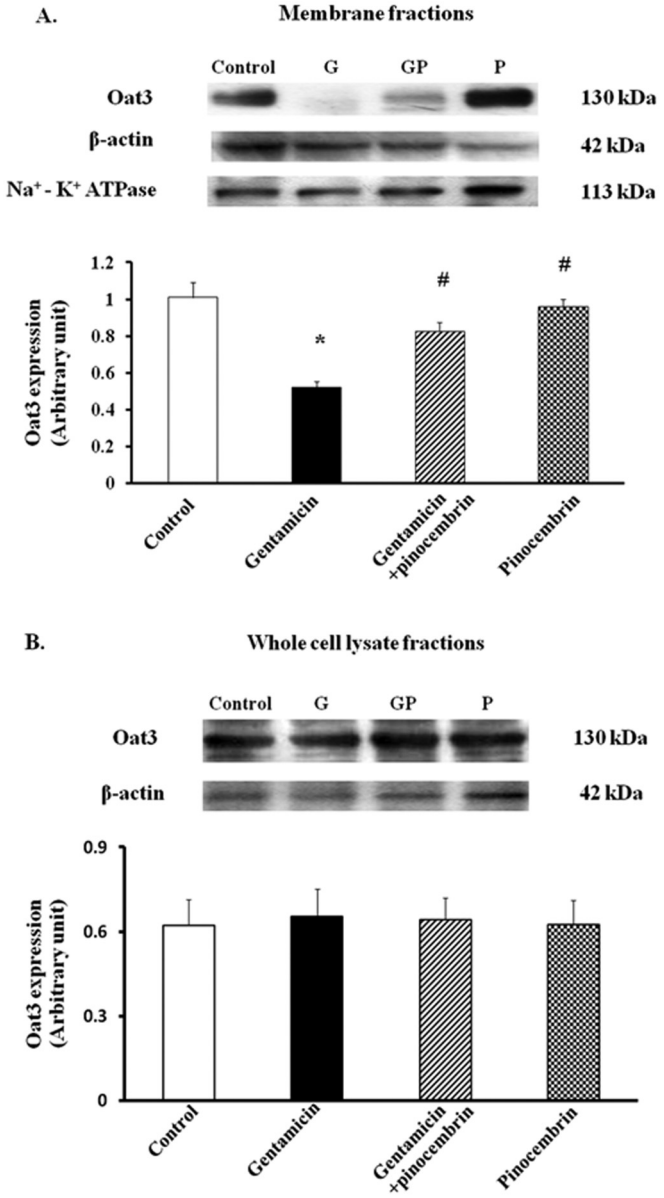

fraction was used to determine the protein expressions of PKCα, Nrf2, HO-1, NQO1, NOX4, Bax, Bcl-XL, and caspase-3. The whole-cell fraction was used to determine the PKCα, HO-1, NQO1, NOX4, caspase-3, and the Bcl-2 protein family (pro-apoptotic Bax and anti-apoptotic Bcl-XL proteins) expressions by Western blot analysis as described above. Briefly, total-cell lysates and cytosolic, membrane, and nuclear fractions from the renal cortex were subjected to 10% SDS–PAGE and subsequently transferred to a PVDF membrane. The primary PKCα antibody at a concentration of 1:2 000, HO-1 antibody at a concentration of 1:2 000, primary anti-NQO1 antibody at a concentration of 1:500, primary anti-NOX4 antibody at a concentration 1:500, primary anti-Bax at a concentration of 1:3 000, Bcl-XL at a concentration of 1:500, and caspase-3 at a concentration 1:250 were used to probe overnight at 4 °C. Determination of the Nrf2 expression was performed using nuclear and cytosolic fractions. Primary anti-Nrf2 antibody at a concentration of 1:250 was added. The membranes were washed three times with TBST (Tris-buffered saline and Tween 20) and incubated with HRP-conjugated goat anti-rabbit or anti-mouse secondary antibody at room temperature for 1 h and developed with an enhanced chemiluminescence (ECL) agent. Each membrane was stripped and re-probed with mouse anti-β-actin antibody that served as a loading control or other antibodies for further detection of the interest protein expression. The densities of the protein signals on the Hyperfilm were analyzed using the histogram function of Adobe Photoshop CS5 (Adobe Systems Inc., San Jose, California) scanning.

Histopathological study

The paraffin-embedded specimen was cut into 2 μm thick sections, which were mounted on microscope slides and stained with hematoxylin and eosin (H&E) for histological assessment. The samples were examined under a light microscope for evaluation of tubular and glomerular changes. Histopathological alteration or tubular damage was assessed by the degree of tubular dilatation, necrosis, apoptosis, and cast formation in the renal tubular cells.

Statistical analysis

The data are expressed as mean ± standard error of mean (SEM) and analyzed using the SPSS version 17 statistical program (SPSS Inc., Chicago, Illinois, USA). One-way analysis of variance (ANOVA), followed by the Newman–Keuls test, was performed. A P value < 0.05 was considered statistically significant.

Results

Effect of pinocembrin pretreatment on physiological and renal function parameters in the gentamicin-induced nephrotoxicity

There was no difference in the mean initial body mass between the experimental groups. After 10 day of treatment, the gentamicin-treated rats had significantly lower body mass and markedly higher kidney mass, as well as higher kidney mass to body mass ratio, than the control rats ($P < 0.05$) (Table 1). Compared with the

Fig. 3. (A) Effects of pinocembrin pretreatment on the renal cortical MDA concentration. Thiobarbituric acid reactive substances (TBARS) were measured in renal cortical tissues. (B) Effects of pinocembrin pretreatment on superoxide dismutase (SOD) enzyme activity in renal cortical tissue. The SOD enzyme activity was expressed as a mean percentage of control. Values are the mean ± SEM (n = 6 rats per group). *, $P < 0.05$ compared with the control; #, $P < 0.05$ compared with the gentamicin-treated group.

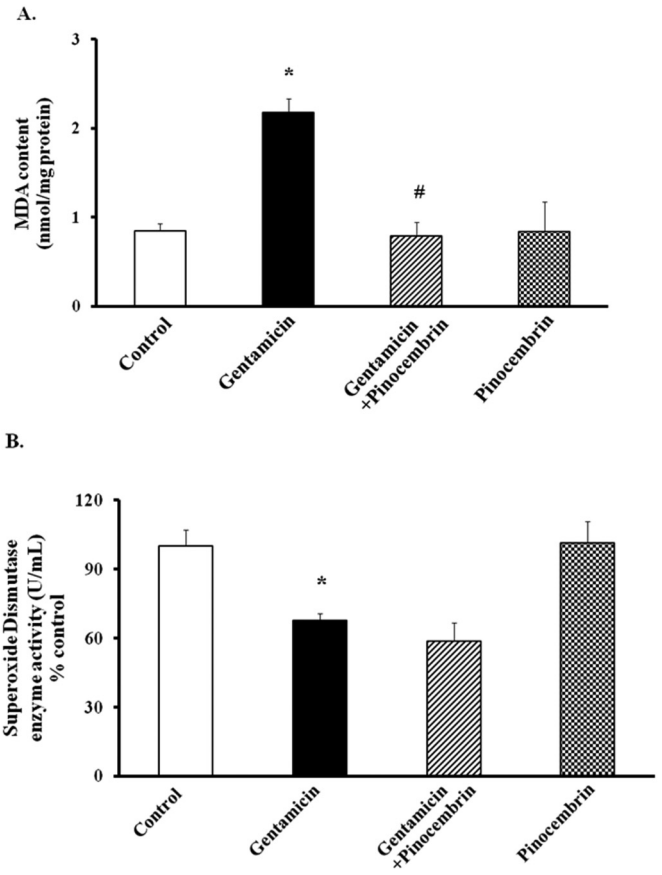

Fig. 4. Effects of pinocembrin pretreatment on the expressions of (A) PKCα and (B) NOX4 in renal cortical tissues. Immunoblot analysis for PKCα and NOX4 expressions in the whole-cell lysate fractions of renal cortical tissue and immunostaining signal intensity of PKCα and NOX4 expressions were normalized to β-actin. Bar graphs indicate mean ± SEM (n = 6 rats in each group). *, $P < 0.05$ compared with the control; #, $P < 0.05$ compared with the gentamicin-treated group.

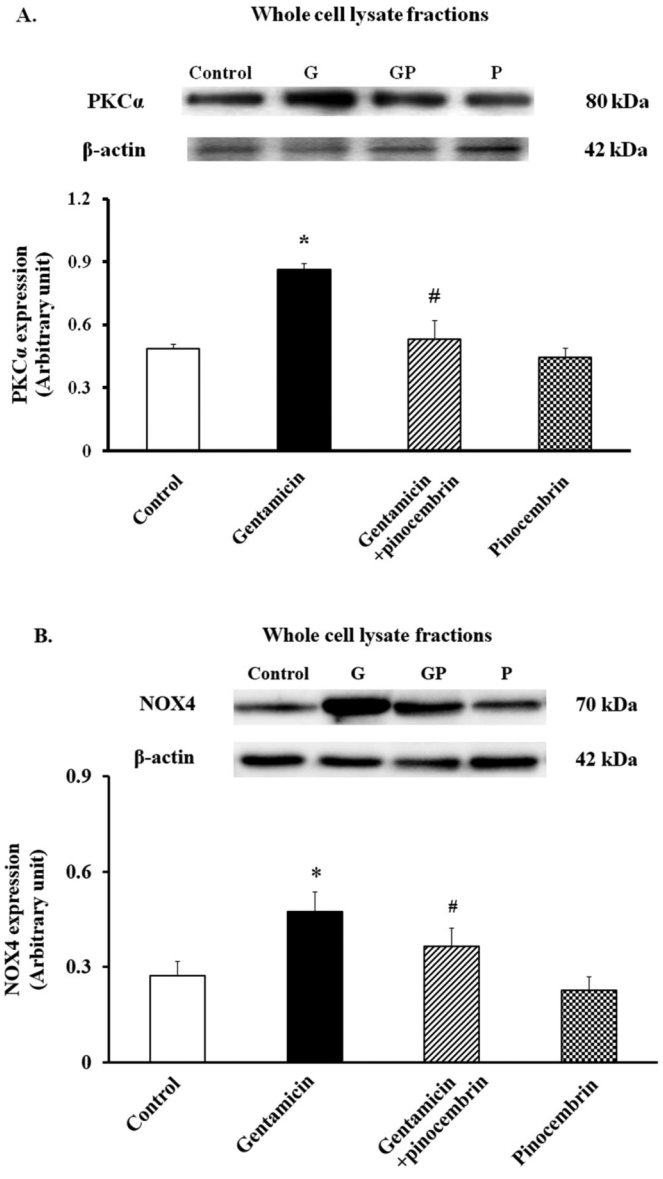

control group, the serum BUN and creatinine levels were significantly higher ($P < 0.05$) and the C_{cr} was markedly lower in the gentamicin group ($P < 0.05$), indicating impaired renal function. Pinocembrin pretreatment (50 or 75 mg/kg) apparently increased the body mass and decreased the kidney mass and kidney mass to body mass ratio ($P < 0.05$). The serum BUN and creatinine levels were also significantly decreased ($P < 0.05$), although the C_{cr} had a tendency to increase in the gentamicin + pinocembrin (50 or 75 mg/kg) group compared with the pinocembrin group. Because the pinocembrin at the doses of 50 and 75 mg/kg showed similar results, we chose to use pinocembrin at the low dose (50 mg/kg) for the subsequent experiments.

Effect of pinocembrin pretreatment on renal Oat3 function and expression in the gentamicin-induced nephrotoxicity

A significant decrease in the [^{3}H]ES uptake into the renal cortical slides was observed in the gentamicin-treated rats compared with the control rats ($P < 0.05$) (Fig. 1). Interestingly, pinocembrin pretreatment led to significantly improved renal Oat3 function as shown by an increase in the [^{3}H]ES uptake compared with the gentamicin group ($P < 0.05$). To determine whether the decreased function of renal Oat3 in the gentamicin-treated rats was partly due to the down-regulated expression of Oat3 at the basolateral membrane, Oat3 expressions in the membrane and whole-cell lysate fractions of the renal cortex were determined by Western blot analysis. The expression level of renal Oat3 from the whole-cell lysate fraction was unchanged in all of the experimental groups (Fig. 2B). However, the membrane expression of Oat3 in the gentamicin-treated rats was significantly decreased compared with the control group ($P < 0.05$) (Fig. 2A). Pinocembrin pretreatment significantly attenuated a decreased membrane expression of Oat3 compared with the gentamicin-treated rats ($P < 0.05$). These results suggest that the decreased renal Oat3 function in the gentamicin-treated rats may result from the down-regulation of Oat3 at the membrane of renal tubular cells. The reduced renal Oat3 function and expression can be improved by pinocembrin pretreatment in this study.

Fig. 5. Effects of pinocembrin pretreatment on the expression of Nrf2 in the renal cortical tissue. Immunoblot analysis for Nrf2 expression in (A) cytosolic fractions and (B) nuclear fractions and for (C) HO-1 and (D) NQO1 expressions in the whole-cell lysate fractions of renal cortical tissues. Immunostaining signal intensity protein expressions were normalized to β-actin. Bar graphs indicate mean ± SEM (n = 6 rats in each group). *, $P < 0.05$ compared with the control; #, $P < 0.05$ compared with the gentamicin-treated group.

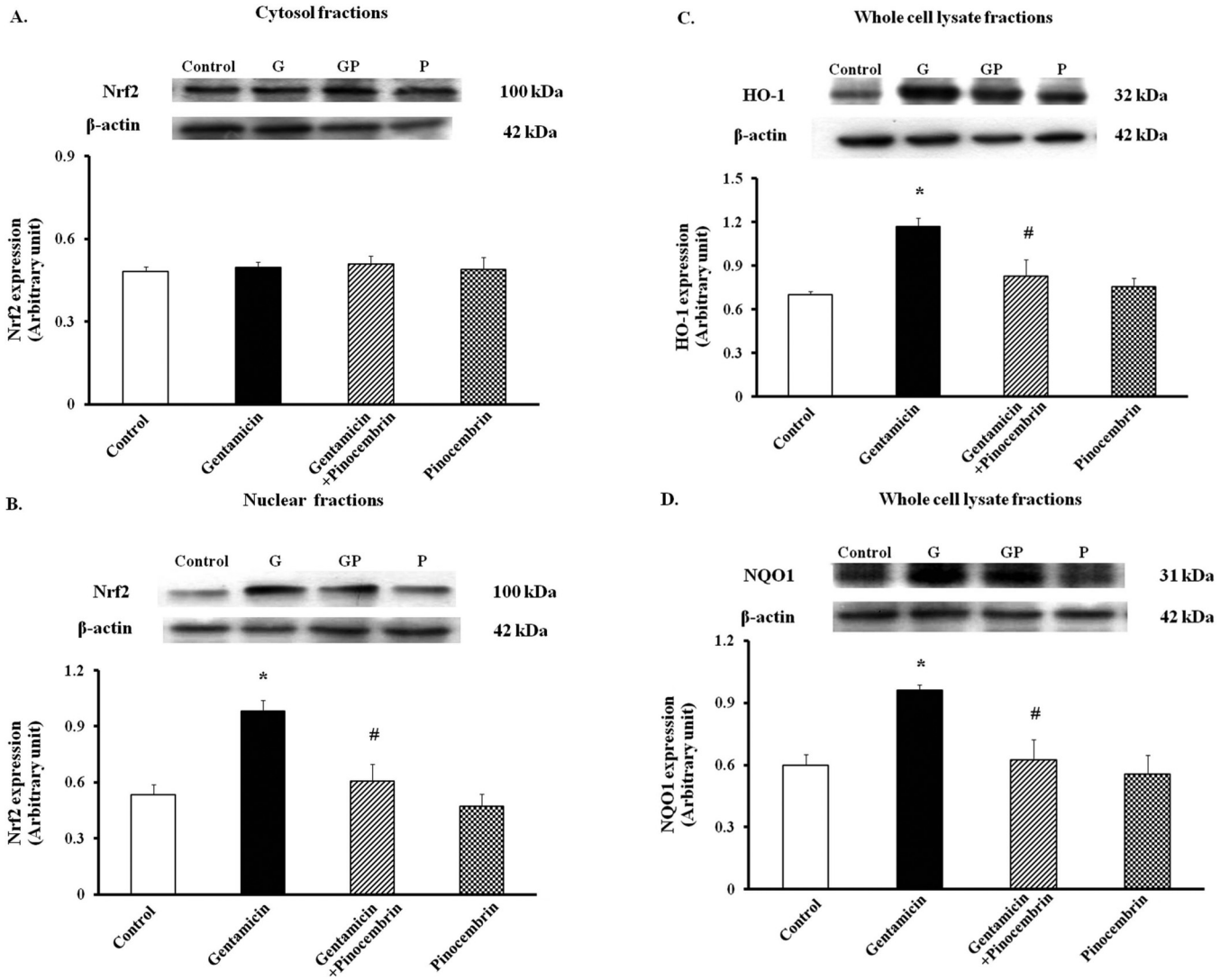

Effect of pinocembrin pretreatment on oxidative stress conditions in the gentamicin-induced nephrotoxicity

The renal cortical MDA was increased in the gentamicin-treated rats compared with the control rats ($P < 0.05$) (Fig. 3A). An apparent decrease of MDA to normal level in the pinocembrin + gentamicin group ($P < 0.05$) indicated that a marked generation of oxidative stress by gentamicin is significantly prevented by pinocembrin pretreatment. The result of SOD activity was consistent with results from the previous studies, demonstrating that gentamicin-treated rats had a significant decrease in SOD activity compared with the control rats ($P < 0.05$) (Fig. 3B). Surprisingly, pinocembrin pretreatment could not improve the activity of the SOD enzyme compared with the gentamicin-treated group.

Effect of pinocembrin pretreatment on the oxidative stress pathways in the gentamicin-induced nephrotoxicity

Based on previous findings that PKCα was activated by the overproduction of ROS, we determined whether an increased oxidative stress in the renal cortical tissue by gentamicin could activate PKCα. As shown in Fig. 4A, the gentamicin-treated rats significantly enhanced PKCα expression compared with the control rats ($P < 0.05$), and this increased PKCα expression was significantly reduced by pinocembrin pretreatment ($P < 0.05$). These findings indicate that the overproduction of ROS in gentamicin-treated rats activates PKCα signaling pathways, and pinocembrin can attenuate the production of ROS and consequently inactivate PKCα. We found that NOX4 expression was stimulated in gentamicin-treated rats ($P < 0.05$). The treatment with pinocembrin could inhibit NOX4 expression compared with the gentamicin-treated rats ($P < 0.05$) (Fig. 4B).

Nrf2, the transcription factor that promotes the antioxidant defense system or protects against oxidative stress, has been shown to protect against gentamicin-induced hair cell damage. Thus, we postulated that an increased oxidative stress in gentamicin-treated rats may activate the Nrf2 and Nrf2-mediated antioxidant enzymes. As shown in Figs. 5A and 5B, the Nrf2 expression in the nuclear fraction of the renal cortical tissue was significantly increased in the gentamicin-treated rats compared with the control rats ($P < 0.05$). However, there was no change in the Nrf2 expression in the cytosol fraction between the experimental groups. These results suggest that the activation of Nrf2 leads to an increased

Fig. 6. Effects of pinocembrin pretreatment on the expression of apoptotic proteins in the whole-cell lysate fractions of renal cortical tissues. (A, B, and D) Representative immunoblot analysis for Bax, Bcl-XL, and caspase-3 expressions in renal cortical tissues, respectively. (C) Immunostaining signal intensities of the Bax/Bcl-XL ratio. Immunostaining signal intensities of Bax, Bcl-XL, and caspase-3 expressions were normalized to β-actin. Bar graphs indicate mean ± SEM (n = 6 rats in each group). *, $P < 0.05$ compared with the control; #, $P < 0.05$ compared with the gentamicin-treated group.

translocation of Nrf2 from the cytoplasm to the nucleus in gentamicin-treated rats. Interestingly, the nuclear expression of Nrf2 was reduced ($P < 0.05$) in the pinocembrin + gentamicin treated rats compared with the gentamicin-treated rats. Additionally, the expressions of the antioxidant enzyme and the detoxification gene, HO-1 and NQO1, respectively, were apparently increased ($P < 0.05$) in the gentamicin-treated rats compared with the control rats (Figs. 5C and 5D). Importantly, the increased HO-1 and NQO1 expressions were significantly reduced by pinocembrin pretreatment ($P < 0.05$). These results suggest that pinocembrin pretreatment can lessen the oxidative stress conditions induced by gentamicin through the modulation of the antioxidant defense parameters.

Effect of pinocembrin on renal apoptosis in the gentamicin-induced nephrotoxicity

The gentamicin-treated rats demonstrated an increase in the expression of the pro-apoptotic protein Bax along with a decreased expression of the anti-apoptotic protein Bcl-XL compared with the control rats ($P < 0.05$) (Figs. 6A, 6B, and 6C). Pinocembrin pretreatment significantly reversed an altered expression of the apoptosis-related protein in the gentamicin-treated rats ($P < 0.05$). We found that caspase-3 expression was increased in the gentamicin-treated rats ($P < 0.05$). Pinocembrin treatment could reverse this effect by reducing the level of caspase-3 compared with the gentamicin-treated rats ($P < 0.05$) (Fig. 6D).

Effect of pinocembrin on renal morphology in the gentamicin-induced nephrotoxicity

The histological changes and the pathological manifestations of the kidney are presented in Fig. 7. Normal kidney morphology was observed in the control (Fig. 7A) and the pinocembrin-treated (Fig. 7D) groups. Nephrotoxicity in the gentamicin-treated rats was evidenced by tubular dilatation, tubular epithelial damage, intracellular cast formation, nuclear irregularity, karyorrhexis, and inflammation (Fig. 7B); however, these defects were ameliorated by pinocembrin pretreatment (Fig. 7C).

Discussion

The present study demonstrated that gentamicin treatment caused nephrotoxicity, which was manifested by marked increases in serum BUN and creatinine with a decrease in C_{cr}. These findings were correlated with the histopathological damages of the kidney. The impaired renal function was accompanied with the reduced renal Oat3 function, an indicator of proximal tubular transport function. The down-regulation of renal Oat3 function and expression in gentamicin-treated rats was associated with the increases in oxidative stress and apoptosis. Pinocembrin pretreatment showed marked decreases in ROS production and apoptosis leading to an improvement of renal function.

In this study, an elevation of renal cortical MDA level along with the decrease activity of SOD indicated the increased oxidative stress condition induced by gentamicin in rat kidneys. Several investigators have reported the relationship between free radical formation and gentamicin-induced acute renal injury (Karahan et al. 2005; Shin et al. 2014; Walker et al. 1999). The subsequent generation of reactive oxygen metabolites damages the protein molecules and degrades the membrane-bound phospholipids through the process of lipid peroxidation (Sahu et al. 2013), which were correlated with the inactivation of antioxidant enzymes such as GSH-Px, CAT, and SOD (Kang et al. 2013; Karahan et al. 2005). The decreased renal cortical SOD activity in gentamicin-treated rats implied the depletion of antioxidant enzymes during the combating process to oxidative stress (Kang et al. 2013). We postulated that gentamicin-induced renal injury was caused by free radical generation with an attenuation of the antioxidant enzymes. Importantly, a marked reduction of renal cortical MDA level accompanied with an improved renal function in pinocembrin + gentamicin treated rats might indicate that the ROS was scavenged and lipid peroxidation was reduced by pinocembrin. However, pinocembrin pretreatment could not restore the decreased activity of SOD enzyme in gentamicin-treated rats. We hypothesized that pinocembrin might induce other mechanisms to overdrive ROS overproduction.

The disruption of the Nrf2/Keap1 complex (Keap1 is the regulatory protein of Nrf2) has been activated by oxidative stress and electrophiles (Xing et al. 2012). PKCα was activated by the overproduction of ROS (Phatchawan et al. 2014; Lee et al. 2003). In this study, Nrf2 was activated in the gentamicin-induced nephrotocixity by the increase of oxidative stress conditions indicated by the increased renal PKCα and NOX4 expressions. The activation of Nrf2 acts as a cellular adaptive response to stimulate the expression of antioxidant enzymes at specific antioxidant response elements (ARE) within the regulatory regions of responsive genes (Itoh et al. 1997; Kobayashi and Yamamoto 2005; Li and Kong 2009) against gentamicin-induced oxidative stress. In the present study, an increased translocation of Nrf2 into the nucleus in the renal cortical tissue of the gentamicin-treated rats could lead to the activation of the expression of target genes, including NQO1 and HO-1. A study in rat kidney cells revealed a protective role of Nrf2 overexpression against triptolide-induced cytotoxicity in normal rat kidney cells (NRK-52E) through counteracting oxidative stress (Li et al. 2012). Nrf2 also protected age-related hearing injuries and gentamicin-induced ototoxicity by up-regulating antioxidant enzymes including NQO1, HO-1, SOD, and GCL and detoxifying proteins (Hoshino et al. 2011). It is noteworthy that pinocembrin pretreatment resulted in a decreased ROS production leading to the inactivation of Nrf2 as indicated by a significant reduction in the nuclear translocation of Nrf2. The attenuation of oxidative stress by pinocembrin pretreatment occurred via a decreased Nrf2-mediated transcriptional regulation, as well as NQO1 and HO-1 expressions. In rats, the cytoprotective properties of pinocembrin have been shown in chronic cerebral hypoperfusion (Guang and Du 2006) and transient global brain ischemia and reperfusion (Shi et al. 2011), which are associated with reduced oxidative stress. Pinocembrin might act as both direct and indirect antioxidants via the induction of many cytoprotective proteins, including antioxidant enzymes, and through the inactivation of Nrf2 by superimposing the overproduction of ROS, thus causing the reversal of oxidative stress conditions. Several studies have investigated the protective effects of natural compounds on gentamicin-induced nephrotoxicity. Rosmarinic acid was shown to alleviate gentamicin-induced nephrotoxicity via antioxidant activity, increases of renal GSH content, and renal antioxidant enzyme activity (Tavafi and Ahmadvand 2011). Recently, curcumin was also found to attenuate renal injuries in gentamicin-induced toxicity in rats (He et al. 2015; Manikandan et al. 2011; Negrette-Guzmán et al. 2015).

Gentamicin-induced apoptosis as shown by the elevated cellular pro-apoptotic (Bax and caspase-3) and reduced anti-apoptotic (Bcl-XL) protein expressions was consistent with the histopathological changes in gentamicin-treated rat kidneys in this study. Previously, the increased expressions of apoptotic protein Bax, cytochrome c, cleaved caspase-9, and cleaved caspase-3 with a

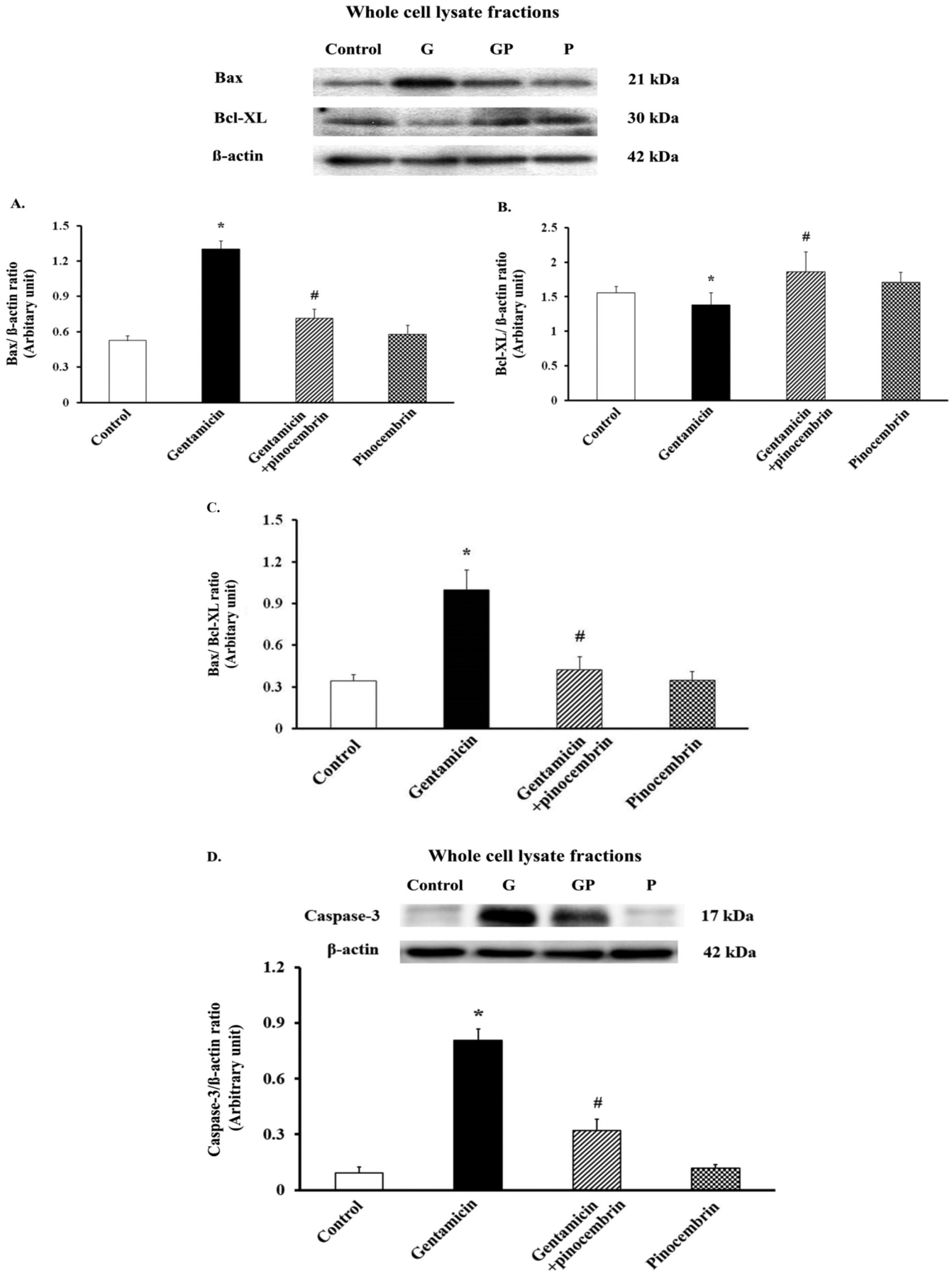

Fig. 7. Hematoxylin and eosin (H&E) staining of the kidneys (magnification, ×40). Images of glomeruli and renal tubules from (A) control, (B) gentamicin-treated, (C) gentamicin + pinocembrin treated, and (D) pinocembrin-treated rats. In the gentamicin-treated kidney (B), mitosis (arrowheads) and tubular detachment (arrow) are shown. [Colour online.]

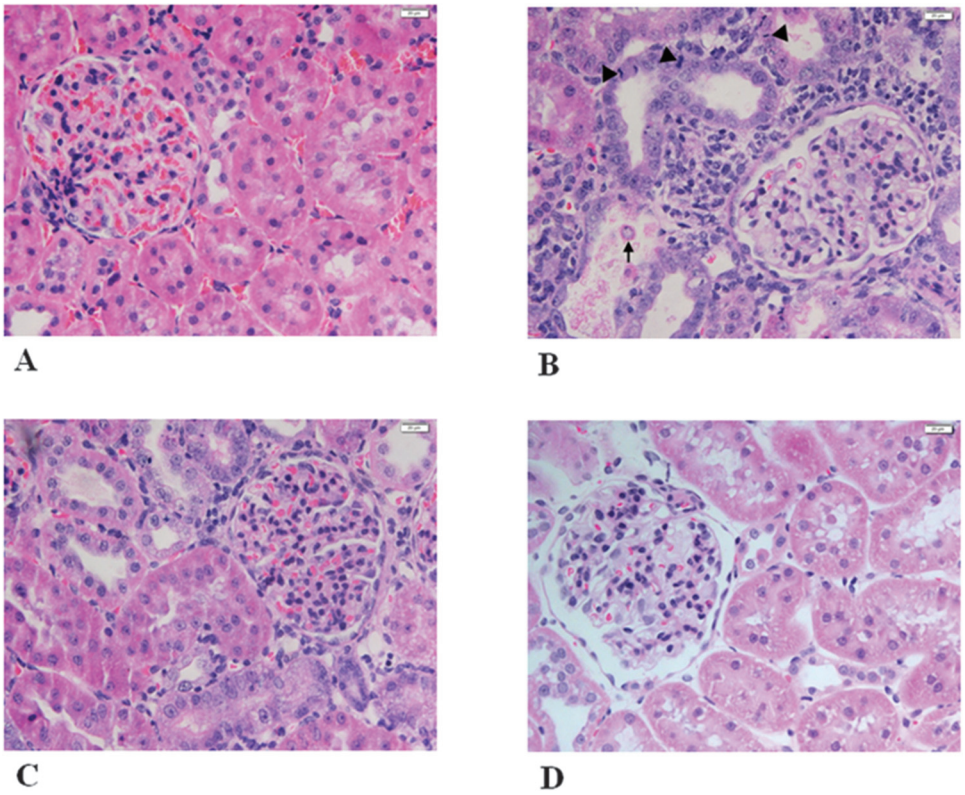

decrease in the expression of anti-apoptotic protein Bcl-2 were observed in renal tubular cells of gentamicin-induced acute kidney injury in rats (Shin et al. 2014). Excessive ROS generated in gentamicin-induced nephrotoxicity is known to cause mitochondrial dysfunction, which is an early event in the intrinsic pathway of apoptosis, resulting in morphological and functional changes (Jia et al. 2013; Morales et al. 2010). Pinocembrin provided renoprotection by inhibiting Bax and caspase-3 overexpressions induced by gentamicin with an enhancing Bcl-XL expression, leading to the alleviation of renal tubular necrosis and damage. It was reported that the anti-apoptotic Bcl-2 family protein could protect the integrity of mitochondrial membrane by binding to the outer membrane of the mitochondria and blocking the efflux of cytochrome c (Kalkan et al. 2012; Kuwana and Newmeyer 2003). The effect of antioxidant treatment on gentamicin-induced apoptosis was reported in both in vivo and in vitro studies (Kang et al. 2013; Ojano-Dirain and Antonelli 2012). Therefore, the beneficial effect of pinocembrin on gentamicin-induced apoptosis in this study could be mediated by the antioxidant effect as the altered expressions of apoptosis-related proteins were preceded by ROS production.

In the present study, gentamicin-treated rats showed decreased renal Oat3 function and membrane expression along with increased PKCα protein expression. The down-regulation of membrane expression of Oat3 was related to the PKCα activation by an increase in ROS production (Phatchawan et al. 2014). Gentamicin treatment might induce the trafficking of Oat3 from the basolateral membrane into the cytoplasm of the proximal tubular cells, resulting in decreased membrane expression of Oat3 and subsequently decreased renal Oat3 function. These actions might be associated with the activation of PKCα protein expression through an increased ROS generation by gentamicin treatment. These were supported by the correlation between the decreased membrane expressions of renal Oat1 and Oat3 and the increasing level of lipid peroxidation in nephrotoxicity rats (Ulu et al. 2012). The restored function and membrane expression of renal Oat3 in gentamicin-treated rats after pinocembrin pretreatment was consistent with the previous study, demonstrating that decreased renal Oat1 and Oat3 expressions and functions could be reversed after pretreatment with the antioxidant substance JBP485 (cyclo-trans-4-L-hydroxyprolyl-L-serine) (Guo et al. 2013). Moreover, treatment with a potent scavenger of free radicals has been reported to prevent the renal toxic effects of gentamicin via the inhibition of a PKC pathway (Parlakpinar et al. 2006). Therefore, the reduction of ROS generation in gentamicin-treated rats by pinocembrin pretreatment might inactivate PKCα, which in turn up-regulated the membrane expression of Oat3, leading to improved Oat3 function and finally reversal of renal dysfunction.

Conclusion

The present results clearly show that pinocembrin can protect gentamicin-induced kidney injury via an amelioration of oxidative stress and apoptosis of renal tissues. It attenuates the increase in oxidative stress and modulates the antioxidant enzymes via the Nrf2/HO-1, NQO1 pathways, thereby leading to reduced protein-related apoptosis resulting in improved renal Oat3 and kidney functions. Therefore, pinocembrin could be inferred as an alternative therapeutic option to prevent gentamicin-induced nephrotoxicity.

Conflict of interest

The authors declare that there is no conflict of interest associated with this work.

Acknowledgements

We thank Dr. Songkiet Suwansirikul, Department of Pathology, Faculty of Medicine, Chiang Mai University, for the valuable suggestions in renal histology. This work was supported by the Thailand Research Funds RSA5780029 (A.L.) and TRG5780019 (P.A.), Thailand, and the National Research Council of Thailand (Grant No. 164368;2558A10402068) (A.L.), CMU Mid-Career Research Fellowship program (A.L.), the Faculty of Medicine Research Fund, Chiang Mai University (A.L.), and the NSTDA Research Chair grant from the National Science and Technology Development Agency of Thailand (N.C.).

References

Abdel-Raheem, I.T., Abdel-Ghany, A.A., and Mohamed, G.A. 2009 Protective effect of quercetin against gentamicin-induced nephrotoxicity in rats. Biol. Pharm. Bull. **32**: 61–67. doi:10.1248/bpb.32.61. PMID:19122282.

Ajami, M., Eghtesadi, S., Pazoki-Toroudi, H., Habibey, R., and Ebrahimi, S.A. 2010. Effect of crocus sativus on gentamicin induced nephrotoxicity. Biol. Res. **43**(1): 83–90. PMID:21157635.

Bankova, V.S., Popov, S.S., and Marekov, N.L. 1982. High-performance liquid chromatographic analysis of flavonoids from propolis. J. Chromatogr. A, **242**(1): 135–143. doi:10.1016/S0021-9673(00)87255-6.

Cao, G., Ying, P., Yan, B., Xue, W., Li, K., Shi, A., Sun, T., Yan, J., and Hu, X. 2015. Pharmacokinetics, safety, and tolerability of single and multiple-doses of pinocembrin injection administered intravenously in healthy subjects. J. Ethnopharmacol. **168**: 31–36. doi:10.1016/j.jep.2015.03.041. PMID:25814318.

Charoensin, S., Punvittayagul, C., Pompimon, W., Mevatee, U., and Wongpoomchai, R. 2010. Toxicological and clastogenic evaluation of pinocembrin and pinostrobin isolated from *Boesenbergia pandurata* in Wistar rats. Thai J. Toxicol. **25**: 29–40.

Del Rayo Camacho, M., Sanchez, B., Quiroz, H., Contreras, J.L., and Mata, R. 1991. Pinocembrine: a bioactive flavanone from *Teloxys graveolens*. J. Ethnopharmacol. **31**(3): 383–389. doi:10.1016/0378-8741(91)90022-6. PMID:2056764.

Edson, R.S., and Terrell, C.L. 1999. The aminoglycosides. Mayo Clin. Proc. **74**(5): 519–528. doi:10.4065/74.5.519. PMID:10319086.

Gao, M., Zhang, W.C., Liu, Q.S., Hu, J.J., Liu, G.T., and Du, G.H. 2008. Pinocembrin prevents glutamate-induced apoptosis in SH-SY5Y neuronal cells via decrease of bax/bcl-2 ratio. Eur. J. Pharmacol. **591**(1–3): 73–79. doi:10.1016/j.ejphar.2008.06.071. PMID:18625218.

Guang, H.M., and Du, G.H. 2006. Protections of pinocembrin on brain mitochondria contribute to cognitive improvement in chronic cerebral hypoperfused rats. Eur. J. Pharmacol. **542**(1–3): 77–83. doi:10.1016/j.ejphar.2006.04.054. PMID:16806158.

Guo, X., Meng, Q., Liu, Q., Wang, C., Sun, H., Peng, J., Ma, X., Kaku, T., and Liu, K. 2013. JBP485 improves gentamicin-induced acute renal failure by regulating the expression and function of Oat1 and Oat3 in rats. Toxicol. Appl. Pharmacol. **271**(2): 285–295. doi:10.1016/j.taap.2013.04.029. PMID:23707770.

He, L., Peng, X., Zhu, J., Liu, G., Chen, X., Tang, C., Liu, H., Liu, F., and Peng, Y. 2015. Protective effects of curcumin on acute gentamicin-induced nephrotoxicity in rats. Can. J. Physiol. Pharmacol. **93**(4): 275–282. doi:10.1139/cjpp-2014-0459. PMID:25730179.

Hoshino, T., Tabuchi, K., Nishimura, B., Tanaka, S., Nakayama, M., Ishii, T., Warabi, E., Yanagawa, T., Shimizu, R., Yamamoto, M., and Hara, A. 2011. Protective role of Nrf2 in age-related hearing loss and gentamicin ototoxicity. Biochem. Biophys. Res. Commun. **415**(1): 94–98. doi:10.1016/j.bbrc.2011.10.019. PMID:22020098.

Itoh, K., Chiba, T., Takahashi, S., Ishii, T., Igarashi, K., Katoh, Y., Oyake, T., Hayashi, N., Satoh, K., Hatayama, I., et al. 1997. An Nrf2/small Maf heterodimer mediates the induction of phase II detoxifying enzyme genes through antioxidant response elements. Biochem. Biophys. Res. Commun. **236**(2): 313–322. doi:10.1006/bbrc.1997.6943. PMID:9240432.

Jia, P., Teng, J., Zou, J., Fang, Y., Jiang, S., Yu, X., Kriegel, A.J., Liang, M., and Ding, X. 2013. Intermittent exposure to xenon protects against gentamicin-induced nephrotoxicity. PLoS One **8**(5): e64329. doi:10.1371/journal.pone.0064329. PMID:23737979.

Kalayarasan, S., Prabhu, P.N., Sriram, N., Manikandan, R., Arumugam, M., and Sudhandiran, G. 2009. Diallyl sulfide enhances antioxidants and inhibits inflammation through the activation of Nrf2 against gentamicin-induced nephrotoxicity in Wistar rats. Eur. J. Pharmacol. **606**(1–3): 162–171. doi:10.1016/j.ejphar.2008.12.055. PMID:19374873.

Kalkan, Y., Kapakin, K.A., Kara, A., Atabay, T., Karadeniz, A., Simsek, N., Karakus, E., Can, I., Yildirim, S., Ozkanlar, S., and Sengul, E. 2012. Protective effect of Panax ginseng against serum biochemical changes and apoptosis in kidney of rats treated with gentamicin sulphate. J. Mol. Histol. **43**(5): 603–613. doi:10.1007/s10735-012-9412-4. PMID:22487736.

Kang, C., Lee, H., Hah, D.Y., Heo, J.H., Kim, C.H., Kim, E., and Kim, J.S. 2013. Protective effects of *Houttuynia cordata* Thunb. on gentamicin-induced oxidative stress and nephrotoxicity in rats. Toxicol. Res. **29**(1): 61–67. doi:10.5487/tr.2013.29.1.061. PMID:24278630.

Karahan, I., Atessahin, A., Yilmaz, S., Ceribasi, A.O., and Sakin, F. 2005. Protective effect of lycopene on gentamicin-induced oxidative stress and nephrotoxicity in rats. Toxicology, **215**(3): 198–204. doi:10.1016/j.tox.2005.07.007. PMID:16125832.

Kobayashi, M., and Yamamoto, M. 2005. Molecular mechanisms activating the Nrf2-Keap1 pathway of antioxidant gene regulation. Antioxid. Redox. Signal. **7**(3–4): 385–394. doi:10.1089/ars.2005.7.385. PMID:15706085.

Koepsell, H. 2013. The SLC22 family with transporters of organic cations, anions and zwitterions. Mol. Aspects Med. **34**(2–3): 413–435. doi:10.1016/j.mam.2012.10.010. PMID:23506881.

Kuwana, T., and Newmeyer, D.D. 2003. Bcl-2-family proteins and the role of mitochondria in apoptosis. Curr. Opin. Cell Biol. **15**(6): 691–699. doi:10.1016/j.ceb.2003.10.004. PMID:14644193.

Lee, H.B., Yu, M.R., Yang, Y., Jiang, Z., and Ha, H. 2003. Reactive oxygen species-regulated signaling pathways in diabetic nephropathy. J. Am. Soc. Nephrol. **14**(8, S3): S241–S245. doi:10.1097/01.ASN.0000077410.66390.0F. PMID:12874439.

Li, J., Jin, J., Li, M., Guan, C., Wang, W., Zhu, S., Qiu, Y., Huang, M., and Huang, Z. 2012. Role of Nrf2 in protection against triptolide-induced toxicity in rat kidney cells. Toxicol. Lett. **213**(2): 194–202. doi:10.1016/j.toxlet.2012.07.008. PMID:22820427.

Li, W., and Kong, A.N. 2009. Molecular mechanisms of Nrf2-mediated antioxidant response. Mol. Carcinog. **48**(2): 91–104. doi:10.1002/mc.20465. PMID:18618599.

Lopez-Novoa, J.M., Quiros, Y., Vicente, L., Morales, A.I., and Lopez-Hernandez, F.J. 2011. New insights into the mechanism of aminoglycoside nephrotoxicity: an integrative point of view. Kidney Int. **79**(1): 33–45. doi:10.1038/ki.2010.337. PMID:20861826.

Lungkaphin, A., Arjinajarn, P., Pongchaidecha, A., Srimaroeng, C., Chatsudthipong, L., and Chatsudthipong, V. 2014. Impaired insulin signaling affects renal organic anion transporter 3 (Oat3) function in streptozotocin-induced diabetic rats. PLoS One, **9**(5): e96236. doi:10.1371/journal.pone.0096236. PMID:24801871.

Lungkaphin, A., Pongchaidecha, A., Palee, S., Arjinajarn, P., Pompimon, W., and Chattipakorn, N. 2015. Pinocembrin reduces cardiac arrhythmia and infarct size in rats subjected to acute myocardial ischemia/reperfusion. Appl. Physiol. Nutr. Metab. **40**(10): 1031–1037. doi:10.1139/apnm-2015-0108. PMID:26319563.

Manikandan, R., Beulaja, M., Thiagarajan, R., Priyadarsini, A., Saravanan, R., and Arumugam, M. 2011. Ameliorative effects of curcumin against renal injuries mediated by inducible nitric oxide synthase and nuclear factor kappa B during gentamicin-induced toxicity in Wistar rats. Eur. J. Pharmacol. **670**(2–3): 578–585. doi:10.1016/j.ejphar.2011.08.037. PMID:21925163.

Mazzon, E., Britti, D., De Sarro, A., Caputi, A.P., and Cuzzocrea, S. 2001. Effect of *N*-acetylcysteine on gentamicin-mediated nephropathy in rats. Eur. J. Pharmacol. **424**(1): 75–83. doi:10.1016/S0014-2999(01)01130-X. PMID:11470263.

Morales, A.I., Detaille, D., Prieto, M., Puente, A., Briones, E., Arévalo, M., Leverve, X., López-Novoa, J.M., and El-Mir, M.Y. 2010. Metformin prevents experimental gentamicin-induced nephropathy by a mitochondria-dependent pathway. Kidney Int. **77**(10): 861–869. doi:10.1038/ki.2010.11. PMID:20164825.

Nagai, J., and Takano, M. 2004. Molecular aspects of renal handling of aminoglycosides and strategies for preventing the nephrotoxicity. Drug Metab. Pharmacokinet. **19**(3): 159–170. doi:10.2133/dmpk.19.159. PMID:15499183.

Nasri, H., Nematbakhsh, M., and Rafieian-Kopaei, M. 2013. Ethanolic extract of garlic for attenuation of gentamicin-induced nephrotoxicity in Wistar rats. Iran J. Kidney Dis. **7**(5): 376–382. PMID:24072150.

Negrette-Guzmán, M., Garciá-Nino, W.R., Tapia, E., Zazueta, C., Huerta-Yepez, S., León-Contreras, J.C., Hernández-Pando, R., Aparicio-Trejo, O.E., Madero, M., and Pedraza-Chaverri, J. 2015. Curcumin attenuates gentamicin-induced kidney mitochondrial alterations: possible role of a mitochondrial biogenesis mechanism. Evid. Based Complement. Alternat. Med. **2015**: 917435. doi:10.1155/2015/917435. PMID:26345660.

Noone, P., Parsons, T.M., Pattison, J.R., Slack, R.C., Garfield-Davies, D., and Hughes, K. 1974. Experience in monitoring gentamicin therapy during treatment of serious Gram-negative sepsis. Br. Med. J. **1**(5906): 477–481. doi:10.1136/bmj.1.5906.477. PMID:4206128.

Ohkawa, H., Ohishi, N., and Yagi, K. 1979. Assay for lipid peroxides in animal tissues by thiobarbituric acid reaction. Anal. Biochem. **95**(2): 351–358. doi:10.1016/0003-2697(79)90738-3. PMID:36810.

Ojano-Dirain, C.P., and Antonelli, P.J. 2012. Prevention of gentamicin-induced apoptosis with the mitochondria-targeted antioxidant mitoquinone. Laryngoscope, **122**(11): 2543–2548. doi:10.1002/lary.23593. PMID:22965463.

Parlakpinar, H., Tasdemir, S., Polat, A., Bay-Karabulut, A., Vardi, N., Ucar, M., Yanilmaz, M., Kavakli, A., and Acet, A. 2006. Protective effect of chelerythrine on gentamicin-induced nephrotoxicity. Cell Biochem. Funct. **24**(1): 41–48. doi:10.1002/cbf.1182. PMID:15584091.

Pepeljnjak, S., Jalsenjak, I., and Maysinger, D. 1985. Flavonoid content in propolis extracts and growth inhibition of *Bacillus subtilis*. Pharmazie **40**(2): 122–123. PMID:3923500.

Phatchawan, A., Chutima, S., Anusorn, L., and Varanuj, C. 2014. Decreased renal organic anion transporter 3 expression in type 1 diabetic rats. Am. J. Med. Sci. **347**(3): 221–227. doi:10.1097/MAJ.0b013e3182831740. PMID:23470271.

Punvittayagul, C., Wongpoomchai, R., Taya, S., and Pompimon, W. 2011. Effect of pinocembrin isolated from *Boesenbergia pandurata* on xenobiotic-metabolizing

enzymes in rat liver. Drug Metab. Lett. **5**(1): 1–5. doi:10.2174/187231211794455226. PMID:20942797.

Rizzi, M.D., and Hirose, K. 2007. Aminoglycoside ototoxicity. Curr. Opin. Otolaryngol. Head Neck Surg. **15**(5): 352–357. doi:10.1097/MOO.0b013e3282ef772d. PMID:17823553.

Sahu, B.D., Kuncha, M., Sindhura, G.J., and Sistla, R. 2013. Hesperidin attenuates cisplatin-induced acute renal injury by decreasing oxidative stress, inflammation and DNA damage. Phytomedicine, **20**(5): 453–460. doi:10.1016/j.phymed.2012.12.001. PMID:23353054.

Sala, A., Recio, M.C., Schinella, G.R., Máñez, S., Giner, R.M., Cerdá-Nicolás, M., and Rosí, J.L. 2003. Assessment of the anti-inflammatory activity and free radical scavenger activity of tiliroside. Eur. J. Pharmacol. **461**(1): 53–61. doi:10.1016/S0014-2999(02)02953-9. PMID:12568916.

Santos, A.C., Uyemura, S.A., Lopes, J.L., Bazon, J.N., Mingatto, F.E., and Curti, C. 1998. Effect of naturally occurring flavonoids on lipid peroxidation and membrane permeability transition in mitochondria. Free Radic. Biol. Med. **24**(9): 1455–1461. doi:10.1016/S0891-5849(98)00003-3. PMID:9641263.

Sekine, T., Cha, S.H., and Endou, H. 2000. The multispecific organic anion transporter (OAT) family. Pflugers Arch. Eur. J. Physiol. **440**(3): 337–350. doi:10.1007/s004240000297. PMID:10954321.

Shi, L.L., Chen, B.N., Gao, M., Zhang, H.A., Li, Y.J., Wang, L., and Du, G.H. 2011. The characteristics of therapeutic effect of pinocembrin in transient global brain ischemia/reperfusion rats. Life Sci. **88**(11–12): 521–528. doi:10.1016/j.lfs.2011.01.011. PMID:21262238.

Shin, H.S., Yu, M., Kim, M., Choi, H.S., and Kang, D.H. 2014. Renoprotective effect of red ginseng in gentamicin-induced acute kidney injury. Lab. Invest. **94**(10): 1147–1160. doi:10.1038/labinvest.2014.101. PMID:25111692.

Soromou, L.W., Chu, X., Jiang, L., Wei, M., Huo, M., Chen, N., Guan, S., Yang, X., Chen, C., Feng, H., and Deng, X. 2012. In vitro and in vivo protection provided by pinocembrin against lipopolysaccharide-induced inflammatory responses. Int. Immunopharmacol. **14**(1): 66–74. doi:10.1016/j.intimp.2012.06.009. PMID:22713932.

Tavafi, M., and Ahmadvand, H. 2011. Effect of rosmarinic acid on inhibition of gentamicin induced nephrotoxicity in rats. Tissue Cell, **43**(6): 392–397. doi:10.1016/j.tice.2011.09.001. PMID:22000907.

Ulu, R., Dogukan, A., Tuzcu, M., Gencoglu, H., Ulas, M., Ilhan, N., Muqbil, I., Mohammad, R.M., Kucuk, O., and Sahin, K. 2012. Regulation of renal organic anion and cation transporters by thymoquinone in cisplatin induced kidney injury. Food Chem. Toxicol. **50**(5): 1675–1679. doi:10.1016/j.fct.2012.02.082. PMID:22414646.

Walker, P.D., and Shah, S.V. 1987. Gentamicin enhanced production of hydrogen peroxide by renal cortical mitochondria. Am. J. Physiol. **253**(4 Pt 1): C495–C499. PMID:3661692.

Walker, P.D., Barri, Y., and Shah, S.V. 1999. Oxidant mechanisms in gentamicin nephrotoxicity. Ren. Fail. **21**(3–4): 433–442. doi:10.3109/08860229909085109. PMID:10416224.

Xing, X., Zhang, C., Shao, M., Tong, Q., Zhang, G., Li, C., Cheng, J., Jin, S., Ma, J., Wang, G., et al. 2012. Low-dose radiation activates Akt and Nrf2 in the kidney of diabetic mice: a potential mechanism to prevent diabetic nephropathy. Oxid. Med. Cell Longev. **2012**: 291087. doi:10.1155/2012/291087. PMID:23227273.

Yang, C.L., Du, X.H., and Han, Y.X. 1995. Renal cortical mitochondria are the source of oxygen free radicals enhanced by gentamicin. Ren. Fail. **17**(1): 21–26. doi:10.3109/08860229509036371. PMID:7770640.